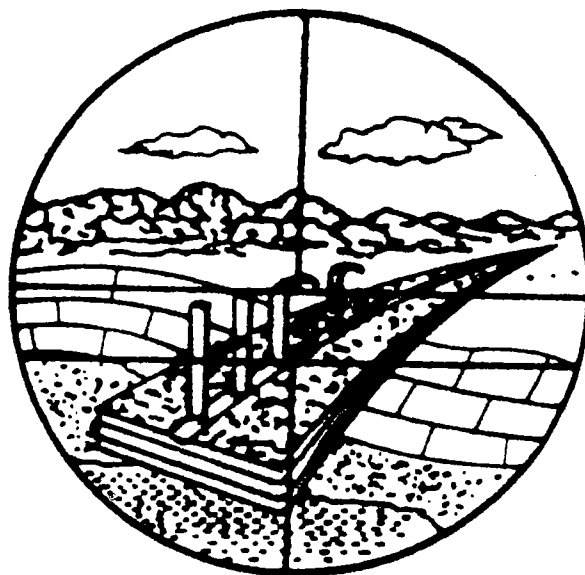


PROCEEDINGS OF THE 36TH ANNUAL HIGHWAY GEOLOGY SYMPOSIUM

BUILDING ON/WITH SEDIMENTARY BEDROCK

**CLARKSVILLE, INDIANA
May 13-15, 1985**

TERRY R. WEST, EDITOR



**CO-SPONSORED BY
Indiana Department of Highways
Kentucky Transportation Cabinet
School of Civil Engineering
Purdue University**

PROCEEDINGS OF THE 36TH ANNUAL
HIGHWAY GEOLOGY SYMPOSIUM

Building On/With
Sedimentary Bedrock

held May 13-15, 1986
CLARKSVILLE, INDIANA

Co-Sponsored by

Indiana Department of Highways, Kentucky Transportation Cabinet

and

School of Civil Engineering, Purdue University

Terry R. West, Editor

Cost \$15.00

36th Annual Highway Geology Symposium
and Field Trip
May 13-15, 1986
Clarksville, Indiana

The Planning Committee of the 36th Annual Highway Geology Symposium welcomed registrants to the Clarksville, Indiana (Greater Louisville, Kentucky) area. One and one-half days of technical sessions plus a one day field trip were included in the Symposium. Earl M. Wright and Richard T. Wilson of the Kentucky Highway Department served as field trip leaders. Construction projects along Interstates 65 and 71 in Kentucky and a stop on US 421 in Indiana were visited on the field trip. As always, the technical sessions and field trip provided opportunities to renew old friendships, establish new ones and to experience the pleasant, informal nature of the Symposium.

Dr. James F. Quinlan of the National Park Service was the speaker at the Annual banquet. His color slide presentation was entitled "Hydrology of the Mammoth Cave Kentucky Region with Emphasis on Groundwater Pollution".

C. William Lovell
Terry R. West
Symposium Co-Chairmen

36th Proceedings Volume HGS Dedicated
to David L. Royster
(1931-1985)



Mr. David L. Royster was born in Cross-Plains, Tennessee in 1931. He was educated at the University of Tennessee (BS in Geology-1958), with post graduate work through a National Institute of Public Affairs Fellowship at the University of Virginia (1967-68), and a Masters Degree in Business Administration at Middle Tennessee State University (1971). Prior to entering college Mr. Royster served in the U.S. Air Force (1950-1954).

In 1958 David Royster joined the Tennessee Department of Transportation as Assistant Soils Engineer, advancing to his most recent position (Engineering Manager of the Geotechnical and Laboratory Operations Office) through several levels of higher responsibility, including Chief Soils Engineer and Director of Soils and Geological Engineering. He served as a part time instructor at the University of Tennessee-Nashville where he taught "Geology for Engineers".

In addition to his work in Tennessee, Mr. Royster served periodically from 1979-1985 as a special consultant to the Republic of Peru concerning the correction of landslides along the Trans-Andean Highway.

David Royster was involved extensively as a leader of professional organizations, his service including: Chairman of the Section on Geology and Earth Materials of Transportation Research Board (TRB) (1976-82), Chairman Engineering Geology Committee for TRB (1971-75, 1982-85), Chairman of the Technical Advisory Committee for the Tennessee Department of Transportation, and Chairman of the National Steering Committee of the Highway Geology Symposium (1983-85). Mr. Royster was a registered Professional Engineering Geologist in California and in Georgia.

David Royster's list of awards and honors exemplified his impact on the profession of Engineering Geology. These include the Outstanding Paper Award by the Association of Engineering Geologists (AEG) in 1973 for his paper "Highway Landslide Problems Along the Cumberland Plateau in Tennessee" recognition as the only two time recipient of the best paper "Holdredge Award" presented by the AEG for his papers "Some Observations on the Use of Horizontal Drains in the Correction and Prevention of Landslides" (1978) and "Landslide Remedial Measures" (1983). Mr. Royster was also presented the Governor of Tennessee's "Outstanding Achievement Award" (1983) and the Tennessee Commissioner of the Department of Transportation's "Certificate of Merit" (1983) for his outstanding service to the transportation system of the State of Tennessee. Mr. Royster received the Medallion Award of the Highway Geology Symposium in 1982.

David Royster authored some 40 professional papers and articles in such journals as the TRB Record, AEG Bulletin, Civil Engineering Magazine, Rural Roads, World Roads, and the Highway Geology Symposium. Some of his more recent professional papers not included above are "Field Investigation", Chapter 4, Landslides: Analysis and Control co-authored with G. F. Sowers in TRB Special Report 76 (1978); Horizontal Drains and Horizontal Drilling: An Overview, 59th TRB Meeting (1980), "Analysis de los Problemas de Estabilidad de Taludes", Vol. D, Estudio de Rehabilitacion de Carreteras en el Pais (1982), and "The Use of Sinkholes for Drainage", TRB (1984).

Mr. David L. Royster passed away at his home in Hermitage, Tennessee, on April 29, 1985.

HIGHWAY GEOLOGY SYMPOSIUM

History, Organization, and Function

Established to foster a better understanding and closer cooperation between geologists and civil engineers in the highway industry, the Highway Geology Symposium was organized and held its first meeting on February 16, 1950, in Richmond, Virginia. Since then, 36 consecutive annual meetings have been held in 23 different states. Between 1950 and 1962, the meetings were held east of the Mississippi River, with Virginia, Ohio, West Virginia, Maryland, North Carolina, Pennsylvania, Georgia, Florida, and Tennessee serving as the host states.

In 1962, the Symposium moved west for the first time to Phoenix, Arizona. Since then, it has rotated, for the most part, back and forth from east to west. Following meetings in Texas and Missouri in 1963 and 1964, the Symposium moved to Lexington, Kentucky in 1965, Ames, Iowa in 1966, Lafayette, Indiana in 1967, back to West Virginia at Morgantown in 1968, and then to Urbana, Illinois in 1969. Lawrence, Kansas was the site of the 1970 meeting, Norman, Oklahoma in 1971, and Old Point Comfort, Virginia the site in 1972.

The Wyoming Highway Department hosted the 1973 meeting in Sheridan. From there it moved to Raleigh, North Carolina in 1974, back west to Coeur d'Alene, Idaho in 1975, Orlando, Florida in 1976, Rapid City, South Dakota in 1977, and then back to Maryland in 1978; this time in Annapolis. Portland, Oregon was the site of the 1979 meeting, Austin, Texas in 1980, and Gatlinburg, Tennessee in 1981. The 1982 meeting was held in Vail, Colorado, and in Stone Mountain, Georgia in 1983. The 35th meeting in 1984 was held in San Jose, California and the 36th HGS was in Clarksville, Indiana. This marked a return to Indiana for HGS after 18 years.

Unlike most groups and organizations that meet on a regular basis, the Highway Geology Symposium has no central headquarters, no annual dues, and no formal membership requirements. The governing body of the Symposium is a steering committee composed of approximately 20 engineering geologists and geotechnical engineers from state and federal agencies, colleges and universities, as well as private service companies and consulting firms throughout the country. Steering committee members are elected for three-year terms, with their elections and re-elections being determined principally by their interests and participation in and contributions to the symposium. The officers include a chairman, vice chairman, secretary, and treasurer, all of whom are elected for a two-year term. Officers except for the treasurer may only succeed themselves for one additional term.

A number of three-member standing committees conduct the affairs of the organization. Some of these committees are: By-Laws, Public Relations, Awards Selection, and Publications. The lack of rigid requirements, routine, and the relatively relaxed overall functioning of the organization is what attracts many of the participants.

Meeting sites are chosen two or four years in advance and are selected by the Steering Committee following presentations made by representatives of potential host states. These presentations are usually made at the steering committee meeting which is held during the Annual Symposium. Upon selection, the state representative becomes the state chairman and a member pro tem of the Steering Committee. Depending on interest and degree of participation, the temporary member may gain full membership to the Steering Committee.

The symposia are generally for two and one-half days, with a day-and-a-half for technical papers and a full-day for the field trip. The symposium usually begins on Wednesday morning. The field trip is usually Thursday, followed by the annual banquet that evening. The final technical session generally ends by noon on Friday.

The field trip is the focus of the meeting. In most cases, the trips cover approximately from 150 to 200 miles, provide for six to eight scheduled stops, and require about eight hours. Occasionally cultural stops are scheduled around geological and geotechnical points of interest. In Wyoming, the group viewed landslides in the Big Horn Mountains; Florida's trip included a tour of Cape Canaveral and the NASA space installation; the Idaho and South Dakota trips dealt principally with mining activities; North Carolina provided stops at a quarry site, a dam construction site, and a nuclear generating site; in Maryland the group visited the Chesapeake Bay hydraulic model and the Goddard Space Center; the Oregon trip included visits to the Columbia River Gorge and Mount Hood; the Central Mineral Region was visited in Texas; and the Tennessee trip provided stops at several repaired landslides in Appalachia. The Colorado field trip consisted of stops at geological and geotechnical problem areas along Interstate 70 in Vail Pass and Glenwood Canyon, while the Georgia trip in 1983 concentrated on highway design and construction problems in the Atlanta urban environment. The 1984 field trip had stops in the San Francisco Bay area which illustrated the interaction of fault activity, urban landslides, and coastal erosion with the planning, construction, and maintenance of transportation systems. In 1985 the one day trip illustrated new highway construction procedures in the greater Louisville area.

At the technical sessions, case histories and state-of-the-art papers are most common with highly theoretical papers the exception. The papers presented at the technical sessions are published in the annual proceedings. Some of these proceedings are out of print, but copies of most of the last fifteen proceedings may be obtained from the Treasurer of the Symposium, David Bingham, of the North Carolina Department of Transportation in Raleigh 27611. Costs generally range from \$5.00 to \$15.00, plus postage.

* MEDALLION WINNERS
HIGHWAY GEOLOGY SYMPOSIUM

Hugh Chase	- 1970
Tom Parrott	- 1970
Paul Price	- 1970
K.B. Woods	- 1971
R.J. Edmonson	- 1972
C.S. Mullin	- 1974
A.C. Dodson	- 1975
Burrell Whitlow	- 1978
William Sherman	- 1980
Virgil Burgat	- 1981
Henry Mathis	- 1982
David Royster	- 1982
Terry West	- 1983
David Bingham	- 1984

* In 1969, the Symposium instituted an awards program, and with the support of Mobile Drilling Company of Indianapolis, Indiana designed a plaque to be presented to individuals who have made significant contributions to the Highway Geology Symposium over a period of years. The award, a 3.5" medallion mounted on a walnut shield and appropriately inscribed, is presented during the banquet at the Annual Symposium.

STEERING COMMITTEE MEMBERS
1985

	<u>TERM EXPIRES</u>
David L. Royster - Chairman Engineering Administrator Geotechnical & Laboratory Operations Office Tennessee Department of Transportation 2200 Charlotte Avenue Nashville, TN 37203 Phone (615) 320-8241	1985
Henry Mathis - Vice Chairman Manager, Geotechnical Branch Division of Materials Kentucky Dept. of Transportation Frankfort, KY 40601 Phone (502) 564-3160	1986
Vernon L. Bump - Secretary Foundation Engineer Department of Transportation Division of Engineering Pierre, SD 57501 Phone (605) 773-340	1987
W.D. Bingham - Treasurer State Highway Geologist Department of Transportation Division of Highways Raleigh, NC 27611 Phone (919) 733-6911	1987
Dr. Terry R. West Associate Professor Dept. of Earth & Atmospheric Sciences Purdue University West Lafayette, IN 47907 Phone (317) 494-3296	1985
Burrell S. Whitlow President- Geotechnics, Inc. 321 Walnut Avenue (P.O. Box 217) Vinton, PA 24179 Phone (703) 344-4569; 344-0198	1986
Walter F. Fredericksen Kansas Dept. of Transportation R.R. #2, Box 13B Erie, KS 66733 Phone (316) 244-5530	1985

- John B. Gilmore 1986
Colorado Highway Department
4340 East Louisiana
Denver, CO 80222
Phone (303) 757-9275
- Joseph A. Gutierrez 1985
Mgr. Mine Planning & Development
Mideast Division
Vulcan Materials Company
P.O. Box 4195
Winton-Salem, NC 27105
Phone (919) 767-4600
- Jeffrey L. Hynes 1985
Colorado Geological Survey
1313 Sherman Street, Room 715
Denver, CO 80203
Phone (303) 866-3458
- C. William Lovell 1985
Professor of Civil Engineering
Grissom Hall
Purdue University
West Lafayette, IN 47907
Phone (317) 494-5034
- Harry Ludowise 1986
Federal Highway Administration
610 East Fifth Street
Vancouver, WA 98661
Phone (206) 696-7738
- Willard McCasland 1985
Materials Division
Oklahoma Dept. of Transportation
200 N.E. 21st Street
Oklahoma City, OK 73105
Phone (405) 521-2677
- Marvin L. McCauley 1985
California Dept. of Transportation
5900 Folsom Blvd.
Sacramento, CA 95819
Phone (916) 739-2480
- David Mitchell 1987
Chief, Geotechnical Bureau
Georgia Dept. of Transportation
Forest Park, GA 30050
Phone (404) 363-7546

- William F. Sherman 1986
Chief Geologist
Wyoming Highway Department
P.O. Box 1708
Cheyenne, WY 28001
Phone (307) 777-7450
- Mitchell D. Smith 1986
Engineer, Res. & Develop. Div.
Oklahoma Dept. of Transportation
200 N.E. 21st Street
Oklahoma City, OK 73105
Phone (405) 521-2671
- Berke Thompson 1985
Asst. Director, Materials Control,
Soil & Testing Division
West Virginia Dept. of Highways
312 Michigan Avenue
Charleston, WV 25311
Phone (304) 348-3644
- W. A. Wisner 1987
Geologist
Florida Dept. of Transportation
Office of Materials & Research
P.O. Box 1029
Gainesville, FL 32601
Phone (904) 372-5304
- Ed J. Zeigler, Associate 1986
Rummel, Klepper, and Kahl
1035 N. Calvert Street
Baltimore, MD 21202
Phone (301) 247-2260
- Mr. Joe E. Armstrong - Member Protem 1986
Chief Geologist
Montana Dept. of Highways
2701 Prospect Avenue
Helena, MT 59620
Phone (406) 449-2098

EMERITUS MEMBERS OF THE STEERING COMMITTEE FOR THE
HIGHWAY GEOLOGY SYMPOSIUM

R. F. Baker
V. E. Burgat
R. G. Charboneau
Hugh Chase
A. C. Dodson
John Lemish
George Meadors
W. T. Parrot
Paul Price
David Royster

TABLE OF CONTENTS

Welcome and Opening Remarks	Page 1
Paul L. Owens	
Outline of the Geology of the Louisville Region	2
Henry H. Gray	
Subsidence of a Highway Embankment on Karst Terrain	14
Henry Mathis, Earl Wright and Richard Wilson	
The Pellissippi Parkway Extension-Geotechnical Engineering Karst Terrain	28
Harry Moore	
Exploration and Repair of Limestone Sinkholes by Impact Densifica- tion (abs)	46
Joe C. Drumheller	
Sinkholes and Gabions: A Solution to the Solution Problem.	47
Dominick Amari and Harry Moore	
Illinois Landslide Inventory: A Tool for Geologists and Engineers. .	69
Myrna M. Killey and Paul B. Dumontelle	
Who Gets Sued When You Sink or Swim, and Why: Liability for Sinkhole Development and Flooding that Affects Homes, Roads and Other Struc- tures	73
James F. Quinlan	
Tieback Walls Stabilize Two Kentucky Landslides	75
Thomas C. Anderson and William E. Munson	
Electrical Isolation of Tieback Anchorages.	89
Ronald B. Reeves and David E. Weatherby	
Relative Durability of Shale - A Suggested Rating System.	105
David N. Richardson	
Evaluation of Geotechnical Designs for Shale Embankment Corrections .	139
William E. Munson	
Use of New Albany Shale for Subgrade and Pavement Stabilization . . .	159
Mark J. Schuhmann and Nicholas G. Schmitt	
Use of Sonic Logs in Evaluating Roof-Rock Strength for an Underground Coal Mine.	174
T.R. West and R.G. Hummeldorf	
Wick Drains (abs)	203
William Pfalzer	

The Nature of Some Glacial and Manmade Sedimentary Sequences and Their Downhole Logging by Natural Gamma Ray.	204
N.K. Bleuer	
Laboratory Testing as an Aid in the Design of Cable Anchor Systems for Rock Reinforcement	220
David A. Lienhart and Terry E. Stransky	
Predicting Settlements Within Compacted Embankments	238
S.O. Nwabukei and C.W. Lovell	
The Effects of Sample Disturbance on the Stresss-Deformation Behavior of Soft Sandstone.	257
Robert C. Bachus	
Moment-Driven Deformation in Rock Slopes.	272
Alberto S. Nieto and Peter K. Matthews	
Appendix A: 36th Annual Highway Geology Symposium Field Trip Guide .	287
Appendix B: List of Registrants, Highway Geology Symposium, May 1985	

Welcome and Opening Remarks

by Paul L. Owens

Deputy Director, Engineering and Management Services,
Indiana Department of Highways
Indianapolis, Indiana

Mr. Owens welcomed the speakers and other registrants on behalf of the Indiana Department of Highways. Following these welcoming remarks he provided examples of highway construction concerns in southern Indiana related to some specific aspects of sedimentary rocks.

OUTLINE OF THE GEOLOGY OF THE LOUISVILLE REGION

by Henry H. Gray

Indiana Geological Survey

Bloomington, IN 47405

Three physical features have been prominent in determining the location and growth of Louisville, Kentucky, and the urban cluster that surrounds it. These are 1) centrally, the Ohio River, since earliest times a principal artery of commerce; 2) the Falls of the Ohio, which early was an obstruction to this flow of commerce and which required transshipment of cargo around the Falls; and 3) the broad segment of the Ohio River valley that surrounds the Falls area and that contrasts sharply with much narrower valleys upstream and downstream.

All of these physical features are geologic in origin and were obvious to the earliest inhabitants of the region, but recognition of yet another important regional feature required the geologist's practiced eye. D. D. Owen, first State Geologist of Indiana, in 1837 noted that at Cincinnati there is, as Owen phrased it, "a kind of back-bone" from which the rocks dip away in both directions. In passage downriver from Cincinnati, Owen noted, one traverses much the same sequence of rocks that one sees enroute upstream from that town. Owen, and others of his time, had thus observed a major structural feature of this part of the continent, now known as the Cincinnati Arch, and they had contrasted the arch with subsident basins on either side, the Illinois Basin on the west and the Appalachian Basin on the east. Drill a hole at Evansville, it was observed, and you will find beneath you the entire series of rocks that you saw in passage from Cincinnati.

Owen put names on these rocks, as geologists usually do. We don't use many of his names today, but the rocks haven't changed and we still recognize most of the divisions and rock units that Owen did. Figure 1 summarizes the most important of these and

AGE	KENTUCKY	INDIANA	
MISSISSIPPIAN	Salem Ls. (100)	Sanders Gr.	Salem Ls. (60)
	Harrodsburg Ls. (30)		Harrodsburg Ls. (40)
	Borden Fm. (450)		Muldrough Fm. (70)
		Borden Gr.	Edwardsville Fm. (90)
			Spickert Knob Fm. (250)
			New Providence Sh. (200)
	Rockford Ls. (5)		
DEVONIAN	New Albany Sh. (80)	New Albany Sh. (100)	
	Sellersburg Ls. (10)	Muscatatuck Gr.	North Vernon Ls. (20)
	Jeffersonville Ls. (15)		Jeffersonville Ls. (30)
SILURIAN	Louisville Ls. (70)	Louisville Ls. (30)	
	Waldron Sh. (10)	Waldron Sh. (10)	
	Laurel Dol. (50)	Salamonie Dol. (50)	
	Osgood Fm. (15)		
	Brassfield Fm. (3)	Brassfield Ls. (5)	
ORDOVICIAN	Drakes Fm. (120)	Maquoketa Gr.	Whitewater Fm. (50)
	Bull Fork Fm. (100)		Dillsboro Fm. (450)
	Grant Lake Ls. (80)		
	Fairview Fm. (90)		
	Kope Fm. (200)		Kope Fm. (200)
	Clays Ferry Fm. (40)	Lexington Ls. (60+)	
	Lexington Ls. (40+)		

Figure 1. Chart showing principal bedrock units exposed along or near the Ohio River in the Cincinnati-Louisville region and general correlation between names used in Indiana and names used in Kentucky. Approximate thickness is given in feet.

correlates the slightly divergent nomenclatures of Indiana and Kentucky in this region. Figure 2 will serve as an areal guide.

In this discussion we will progress downriver from the Ohio-Indiana state line, and we will consider not only the stratigraphy and areal geology of the region but also some engineering aspects of the rocks and related earth materials. The dip is gentle and westerly so that we will be progressing upward in the

section, starting with the Lexington Limestone and related formations. These are important units in central Kentucky, but only their far fringes crop out along the Ohio River. Next upward is the Kope Formation, a dominantly shale unit about 200 feet thick, and above that is a sequence of limestones and calcareous shales that have been given many names; in Indiana they are called the Dillsboro and Whitewater Formations. These are about 450 and 50 feet thick, respectively.

These formations are all of Ordovician age, and they are the oldest that crop out in the Cincinnati region. They underlie a hilly area that in Indiana is called the Dearborn Upland (fig. 3); in Kentucky a similar area is part of the Outer Bluegrass Region. Where the limestones are thick, karst is well developed; where the shales dominate, slope movements such as soil slides and debris slides are common. The Lexington is quarried for aggregate in many places in Kentucky, but the younger Ordovician limestones are too shaly to pass today's requirements.

For use as embankment material, the shale and the interbedded shale and limestone of this region must be treated with care. The shale disaggregates readily and can cause excessive subsidence if it is not properly compacted, and the shale-limestone mixtures, because of their stratification, can become emplaced in stratified lifts that tend to form seepage zones.

The Kope Formation, in particular, has been so troublesome as to merit some special attention. Slopes underlain by this formation can be identified by their angle; they are somewhat less steep than slopes on the shale and limestone units above. They also tend to be without woodland cover and commonly are in pasture. Limestone rubble from the steeper slopes above, along with a thin cover or soil contribution from glacial deposits, forms a blanket a few feet thick over the shale. At the base of this blanket in many places is a thin layer of green slippery clay. This is evidently a weathering product, though its mineralogy does not seem to differ much from that of the underlying shale. Along with the underlying shale it impedes the downward flow of soil water and so creates a potentially unstable con-

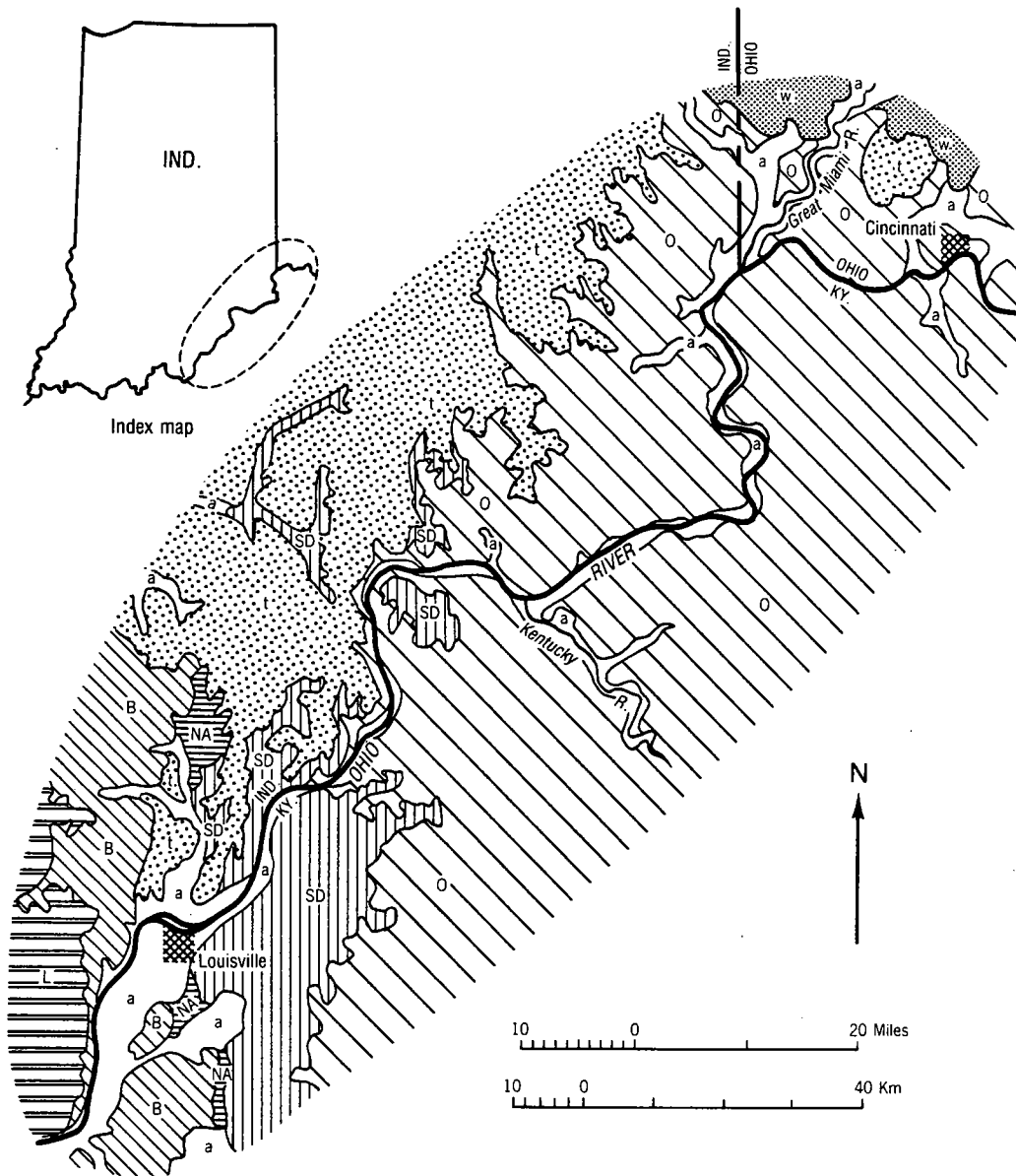


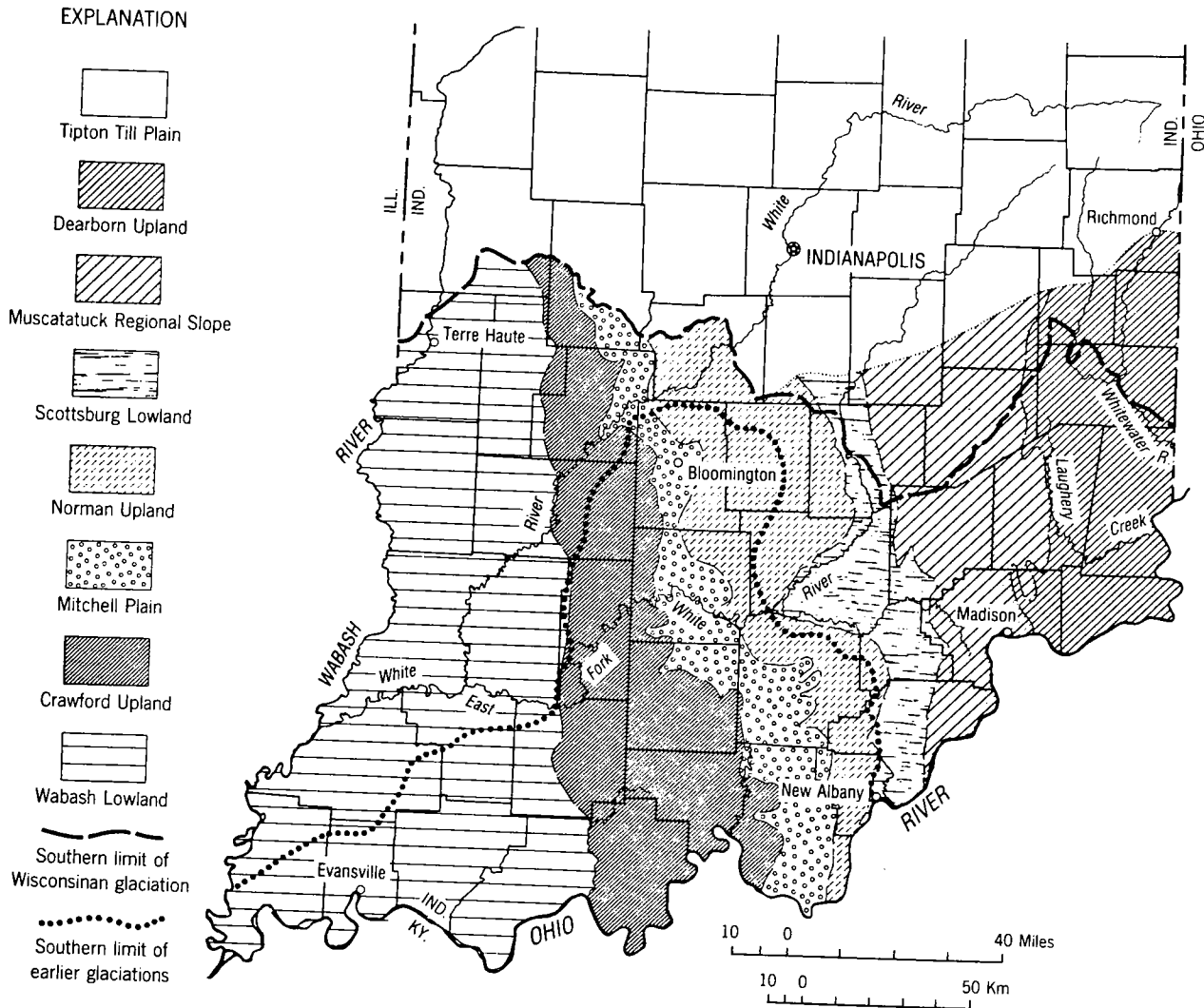
Figure 2. Geologic strip-map along the Ohio River from Cincinnati to Louisville. a, valley-fill deposits; w, Wisconsinian till; t, upland sediment complex; L, limestone of Mississippian age; B, siltstone and shale of Borden Group; NA, New Albany Shale; SD, limestone and dolomite of Silurian and Devonian age; O, shale and limestone of Ordovician age.

dition. I don't think we have ever known the rock to move; it is the soil or embankment material that slips on the rock. In some places this has happened more or less naturally, so that wrinkles can be seen in the pastureland; in other places it is the hand of man that sets off the movement.

Next westerly from the area of Ordovician rocks is a group of limestones and dolomites that are of Silurian and Devonian age (fig. 2). Although the total thickness of these rocks is barely 150 feet, they form a broad and slightly inclined limestone plateau that in Indiana is called by a jawbreaking name, the Muscatatuck Regional Slope (fig. 3); in Kentucky a similar feature is part of the Outer Bluegrass Region. Many of the streams are deeply entrenched across this region, and there is local karst development adjacent to these streams, but karst is not obvious on broad parts of the plateau in Indiana. The cover of pre-Wisconsinan till does not, however, simply mask an underlying karst topography; karst apparently is not extensive beneath this cover, which implies that in this area the karst may be a relatively recent feature, geologically speaking. The underlying Silurian and Devonian limestones are an important source of rock for aggregate and cement.

At its western edge, the limestone plateau disappears beneath a complex lowland area. This lowland is not distinguished as a physiographic feature in Kentucky, but in Indiana it is called the Scottsburg Lowland (fig. 3) and it forms an important commercial artery; highways and railroads follow it from Louisville to Indianapolis. The bedrock of this area includes the New Albany Shale (fig. 2), a crisp black organic-rich shale of Devonian and Mississippian age that holds some promise as a commercial source of hydrocarbons, and the New Providence Shale, a very soft green-gray shale of Mississippian age at the base of the Borden Group. Total thickness of these shales is about 300 feet. Glacial deposits become increasingly important northward, so that at Indianapolis the bedrock lowland is entirely concealed by drift as much as 250 feet thick.

The New Albany Shale does not degrade rapidly and when used as embankment material it commonly must be emplaced as rock, but it does not seem to create subsidence problems. The New Providence, on the other hand, degrades quickly to a plastic mass and is at best a difficult embankment material. Soils overlying the New Providence are subject to various kinds of movement, but the



- Figure 3. Physiographic regions of southern Indiana. After Malott, 1922, Handbook of Indiana geology, Pt. 2.

area underlain by this formation is relatively small. Both of these formations are difficult to revegetate in cuts and where they are used as embankment material. Usually a layer of soil has to be spread for that purpose.

At this point it is prudent to pause and consider an aspect of the geology of this region that has barely been mentioned thus far: glacial geology. The valley of the Ohio River from the mouth of the Great Miami River to a few miles above Louisville is in most places only a mile or two wide. The valley bottom widens significantly, however, where the river enters the Scottsburg Lowland, the region of the softer and more erodible shales, and

that is the second geologic reason why Louisville, New Albany, Clarksville, and Jeffersonville are here.

The floor of this valley, whether narrow or wide, is made up mostly of two kinds of materials -- glacial outwash that had as its source the Miami River, and alluvium of Holocene (recent) age. The outwash is sand and gravel that become coarser upstream toward the source of the sediment, which was the Wisconsinan ice sheet that advanced down the Miami valley almost to Cincinnati (fig. 2). The outwash stands as terraces above the Holocene valley bottom, which is more or less frequently flooded. The Holocene deposits are mostly silt at the surface but become increasingly sandy and gravelly at depth. Much of the Holocene alluvial material is outwash that has been reworked during major floods; the surficial silt is an overbank floodwater deposit. The total valley fill of sand, gravel, and silt is in many places more than 100 feet thick and is a resource of considerable value.

In only a few places in the valley are there deposits other than those just described, but the few patches of other materials are of considerable geologic interest. They include till, outwash, and other deposits associated with the earlier glaciations, just which one or ones we are not now certain, though conventionally most of the early glacial deposits in this area have been classified as Illinoian in age. These remnants of older glacial materials that once filled the entire length of the valley to some considerable depth are preserved mainly as erosion shadows on the wider bottoms and in valleys of tributary streams. There they escaped the erosion that was associated with later glacial episodes, when meltwater torrents re-excavated the valley to bedrock in most places.

Before we look at the glacial deposits of the uplands, there is one more type of valley-fill material of engineering and geologic interest to discuss. Clarksville is underlain by about 40 feet of Wisconsinan outwash sand and gravel beneath which is a limestone ledge that just to the southwest crops out in the river to form the Falls of the Ohio -- a third reason for the present location of the Falls Cities. The old bedrock channel of the

river, which is deeper and is filled with about 130 feet of outwash sand and gravel, lies to the south beneath downtown Louisville. To the north is a major tributary valley, that of Silver Creek. When the Ohio River was carrying floods of melt-water and depositing thick beds of sand and gravel, which incidentally obscured the limestone ledge and made it possible for the river to position itself over the ledge and thus to create the Falls as it cut down to its present level, the valley of Silver Creek was ponded and received only slackwater deposits. These are mainly calcareous silt and clay, and they present serious engineering problems.

The slackwater deposits stand as terraces much like those underlain by outwash along the Ohio, but because the slackwater deposits are mainly silt and clay, they drain imperfectly. Commonly they have high porosity and high saturation, but very low permeability. Their field moisture content generally is well above optimum, and so they present severe problems in many kinds of construction. Their bearing capacity is so poor that in places they exhibit negative friction, they are excessively wet for use as embankment material, and in their natural and commonly undrained condition they are subject to several kinds of slumping on the slightest provocation. We could write a book on this material and its problems, and it is common in valleys that are tributary to those major valleys, such as the Ohio, that now are partly filled with sand and gravel outwash.

A large part of the upland in southeastern Indiana is covered by material that formerly was regarded simply as till of Illinoian age. Much of the material, however, is not till but is a complex upland sedimentary deposit that incorporates not only weathered detritus from the underlying till and bedrock but also silt that probably is of windblown origin. The upland sediment (fig. 2) is crudely stratified and somewhat poorly drained and soft, and at this point that is about all we know about it. On a new map that we are preparing we are separating this unit and distinguishing it from till, but we don't yet know quite what to call it, nor do we know what age to assign it. It may be an

accretionary deposit, or it may be a product of severe frost action during part of late Pleistocene time. In any event, it is not simply till, although till commonly lies beneath it at a depth of 10 to 15 feet. Beneath the till is bedrock, in most places limestone, at depths ranging from 15 to 50 feet.

Maps of Kentucky show almost no till on the south side of the Ohio River, and indeed some regional maps draw the glacial boundary right along the river from New Albany almost to the Cincinnati area. Such a glacial boundary is, however, erroneous. There is a variety of evidence of glaciation many miles south of the Ohio in this area, but deposits of clearly recognizable till are small and isolated, so that geologists experienced in non-glacial terrain commonly find it easy to ignore such areally unimportant materials. In Indiana, however, glacial deposits are widespread and must be mapped. The apparent glacial boundary at the river, then, is more a matter of mapping philosophy than of fact.

West of and easily visible from Louisville (on a clear day) is the most prominent physiographic feature of this region, the Knobstone Escarpment. This rises as much as 500 feet above the Ohio River in the New Albany area, and though it becomes somewhat less high northward, it is prominent for a distance of about 100 miles. Farther north it becomes increasingly obscured by glacial deposits, but even as far as Lafayette it is a conspicuous feature of the buried bedrock surface. In places it is capped by limestone, but it is upheld mainly by about 350 feet of siltstone that makes up the major part of the Borden Group, a sequence of deltaic deposits of Mississippian age (fig. 2). The outcrop area of Borden rocks becomes broader northward, where the belt of hills is known as the Norman Upland (fig. 3). In Kentucky a feature similar to the Knobstone Escarpment is sometimes called the Muldraugh Escarpment, and the dissected plateau west of it is part of the Mississippian Plateaus. Except for a few soil slides on shaly substrata, this region presents relatively few serious problems for the engineering geologist.

West of the Norman Upland in Indiana is another limestone plateau that is deeply incised by major streams. This one is not glaciated except in its northernmost part. It is the Mitchell Plain, an area of classic karst features that is underlain by limestones of Mississippian age. These limestones are about 300 feet thick and are the source of most of the aggregate used in the western part of southern Indiana.

Nearly all the features characteristic of karst can be observed on the Mitchell Plain: sinkholes that open and clog, each according to its own schedule; extensive subterranean drainage; highly plastic terra rossa soils; you name it. In a single square mile on the Mitchell Plain, geomorphologist C. A. Malott counted 1,022 sinkholes. In Kentucky the same features characterize the outer part of the area called the Mississippian Plateaus. Sinkhole collapse, which in this area and within our time frame appears to involve soil subsidence rather than rock collapse, is a major engineering problem here, and it appears to be associated principally with wet seasons rather than with declining groundwater levels. Other problems, mainly involving drainage, result from the complexities and unknowns of the subterranean drainage system.

West of the Mitchell Plain in Indiana is another escarpment, often called the Chester Escarpment because it is upheld by rocks of Chesterian (Mississippian) age. In Kentucky this same feature is called the Dripping Springs Escarpment. The Chester Escarpment separates the Mitchell Plain from the Crawford Upland, another broad belt of hills that is underlain in its eastern part by about 300 feet of Mississippian shale, sandstone, and limestone; Pennsylvanian shale and sandstone about 300 feet thick are important in the western part of the Crawford Upland, which includes some of the most remote and scenic parts of southern Indiana. Here soil slides and debris slides on steep slopes that are underlain by shale are common and can be severe; rockfalls of various types from the sandstone and limestone cliffs are a less common problem.

The Crawford Upland (fig. 3) merges imperceptibly westward into the Wabash Lowland, an area in which the hills are more subdued and the valleys are broad and deeply filled with glacial and related deposits. Slackwater lake deposits and thick loess are extensive here, and the bedrock is shale and sandstone of Pennsylvanian age. These Pennsylvanian rocks reach a maximum thickness of about 1,000 feet and are the source of Indiana's coal.

The boundary of earlier glaciations reaches almost to the confluence of the Wabash and Ohio Rivers, and north of this boundary till is an important component of the upland soils. The major valleys, specifically the Wabash and the Ohio, contain as much as 150 feet of outwash, which is mainly sand and a little gravel, and tributary valleys contain slackwater silt and clay that reach an equal thickness. This region is short of good aggregate and depends to a large extent on crushed limestone brought in from areas of Mississippian rocks to the east. Engineering problems in the Wabash Lowland include bearing problems with some of the softer valley-fill materials, such as the slackwater lake deposits, and various kinds of soil slides and debris slides on shale substrata.

West of the Louisville area, Kentucky's physiographic regions are differently defined than those in Indiana. Indiana's Mitchell Plain is equivalent to the outer part of Kentucky's Mississippian Plateaus, which is broken by the Dripping Springs Escarpment so that the eastern part of Indiana's Crawford Upland is equivalent to the inner part of Kentucky's Mississippian Plateaus. Kentucky geologists also recognize a Pottsville Escarpment that bounds their Western Coal Field, but this escarpment can be traced only a short distance into Indiana, so that the Western Coal Field is equivalent to part of Indiana's Crawford Upland and all of the Wabash Lowland. These differences, however, like other so-called "state line faults," are only a matter of different perceptions and different emphases.

Having mentioned faults, however facetiously, let me close on a structural note. Broad areas in this part of the continent

are devoid of obvious tectonic features and are seismically quiet as well. There are numerous small faults in the Wabash Valley of western Indiana, however, and several zones of faults slice up Kentucky rather severely. The Rough Creek Fault Zone traverses western Kentucky from west to east, and a few splinters from this complex cross the river into southernmost Indiana. Another complex, the Kentucky River Fault Zone, lies east-west across the midsection of Kentucky. Only the Wabash Valley area shows much seismicity, and no recent movement on any of these faults has ever been perceived.

This brief discussion can provide only an introduction to the geology of this region. For further information, an excellent place to begin would be the Regional Geologic Map Series of the Indiana Geological Survey, which consists of maps that cover an area of 1° in latitude by 2° in longitude at a scale of 1:250,000, and the series of Geologic Quadrangle Maps published by the U.S. Geological Survey in cooperation with the Kentucky Geological Survey, which cover all of Kentucky at a scale of 1:24,000 on a 7 1/2-minute topographic quadrangle base.

SUBSIDENCE OF A HIGHWAY EMBANKMENT ON KARST TERRAIN

by

Henry Mathis
Geotechnical Branch Manager
Kentucky Department of Highways
Frankfort, Kentucky 40622

Earl Wright
Engineering Geology Section Head
Kentucky Department of Highways
Frankfort, Kentucky 40622

Richard Wilson
Senior Geologist
Kentucky Department of Highways
Frankfort, Kentucky 40622

Abstract. During the bituminous paving operations for a 26 million dollar rehabilitation project in Central Kentucky, a 2 to 3 foot subsidence was discovered under the northbound lane of Interstate 65. The contractor made a 30 foot deep excavation in the subsidence area to determine the cause of the problem. This operation failed to provide any answers to the problem, therefore, the Geotechnical Branch of the Kentucky Department of Highways was requested to further investigate the subsidence. The subsurface investigation which followed consisted of 73 auger borings drilled to refusal in a controlled pattern to define the rockline. The greatest depth to rock was 92 feet on a hole located beside the subsidence. Observation wells were installed in 12 holes to provide water table information and were later utilized in dye trace studies. A rock contour map was developed from the drill data to determine possible correction techniques.

The subsidence was probably caused by subsurface erosion due to large volumes of water flowing thru the voids in the soil and solution channels in the limestone rock beneath the roadway embankment.

Driving piles and bridging the deep solution features is a feasible correction technique that will provide long term stability for this area. However, due to the high cost estimate (\$1,370,000), long time delay in the completion date of this critical roadway section, and lack of an accurate method to predict a time rate of subsidence, the decision was made to backfill the excavation with rock at a cost of \$30,000.

The general opinion was the embankment and thick clay deposit would provide sufficient support to bridge the area and the subsidence would be gradual, therefore, the roadway could be maintained.

Introduction

In the middle fifties the Kentucky Turnpike was open to traffic between Louisville and Elizabethtown. This facility was incorporate into the interstate system in the early sixties. In order to upgrade the turnpike to meet current interstate standards, and rehabilitate the pavement, construction projects were let beginning in the early eighties.

The subject project (3.2 miles) located 43 miles south of Louisville, Kentucky on Interstate 65 at Elizabethtown was awarded to E. H. Hughes Company in August 1982 for \$25,981,746. This included widening the existing roadway from four lanes to six lanes, upgrading the interchanges and rehabilitating the pavement.

During the bituminous paving operations, in the late fall of 1983 a 2 to 3 foot subsidence was discovered under the northbound lane in the vicinity of mainline station 65+20. This area is located south of the I-65/Western Kentucky Parkway Interchange (Figure 1).

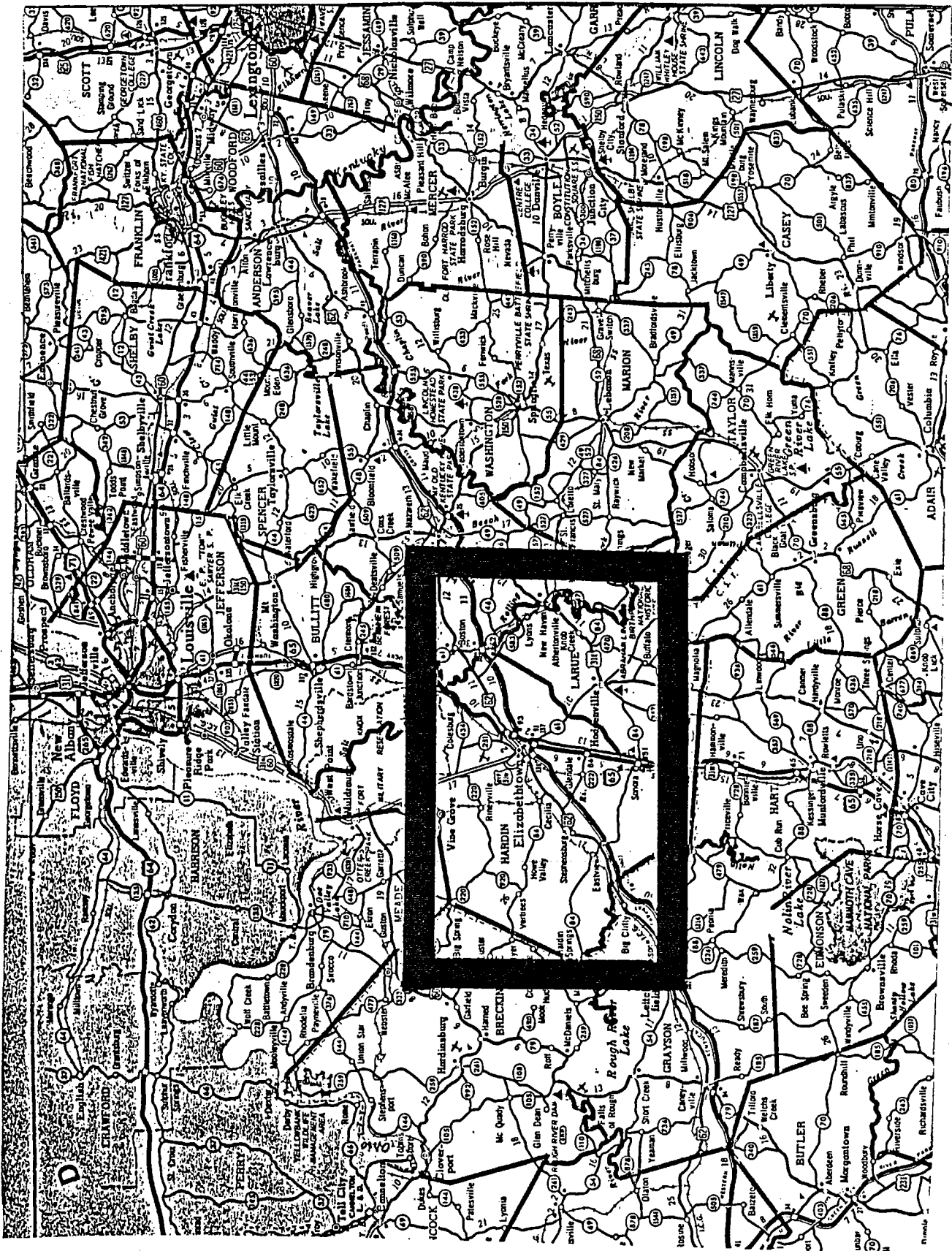


Figure 1. Location Map.

As part of the original construction of the turnpike in the early fifties an embankment, approximately 28 feet in height, was constructed over a solution feature. During this construction a 24 inch cross drain pipe was placed a few feet above the original ground to drain the median drop inlet at station 65+20 (Figure 4).

The new construction plans specified removal of the 24 inch cross drain pipe beneath the roadway, removal of the median drain inlet, and filling in the old depressed median (approximately 3 feet). According to the resident engineer this was accomplished during the earlier construction phases on the project.

In order to investigate the cause of the subsidence and correct the problem, the contractor excavated a large hole approximately 30 feet deep without encountering bedrock. The Geotechnical Branch of the Division of Materials was then requested to investigate the problem.

Geology

The project is situated on typical karst terrain and geologically underlain by the St. Louis Limestone Member of Mississippian age. The limestone is characteristically thick bedded with chert bands and some thin shale partings. Residual soil in this area consists of stiff red clays, silts, and some scattered chert fragments. Thickness of the soil vary according to locations related to sink holes and other solution features.

Subsurface Drainage

Subsurface drainage conditions are controlled by dip of the underlying stratigraphic units, faulting and solution features which developed along the joint systems in the limestone. The rock formation dips to the southwest approximately 1/2 degree and 2 sets of vertical joints trend northwest and northeast. Piping also occurs in the red clay and provides escape channels for water to reach the joint systems. A trellis drainage pattern in this immediate subsurface area is confined between two northwest trending faults with displacements of 60 feet and 100 feet until it reaches outlets along Valley Creek at approximately elevation 670.

Hydrostatic head is high due to the differences in high water ponding elevations and the outlet elevation of the Elizabethtown Spring. The low water level contour map, (Figure 2) developed by USGS in report 84-4057, indicates a steep water gradient in the immediate vicinity of the subsidence problem. Since the water level in hole 23-B changes 20 feet within a 24 hour period, it is assumed that water flowing under the embankment area is subjecting the soil to erosion after every heavy rainfall. The Elizabethtown water plant has recorded a 74 percent increase in the spring discharge rate from the period of 1972 - 1983. This increase maybe due to changes in surface drainage by new construction and may explain why the old embankment was stable but the new embankment subsided.

Subsurface Exploration

A total of seventy-three holes were drilled in a controlled pattern in order to define the subsurface conditions and establish a reliable rockline. Refer to Figure 3, for the Subsurface Exploration Plan. Fifty holes were drilled to refusal with 4 inch and 6 inch augers and twenty-three holes were drilled using a roller bit. Twelve observation wells (1 inch PVC pipe) were installed in select holes to provide water level information and were later utilized in the dye trace studies.

The deepest hole was augered 92 feet and the bottom of the hole elevation of 667 corresponds to the elevation of the Elizabethtown Spring outlet which is part of the city water supply. Numerous voids and cavities were encountered in the soil and nineteen drill holes contained zones described as "very soft and soupy". In four holes the driller was able to "push augers" in several zones between depths of 45 feet and 80 feet. Hole 14B, located approximately 20 feet left of the subsidence beside the southbound lane, penetrated 4 feet of limestone and encountered a 5 1/2 foot cave with running water.

The drilling and water level data is illustrated on profile sheets, (Figures 4 and 5), and cross section sheets, (Figures 6, 7, and 8). A two foot rock contour map (Figure 9) was made to define the size and trend of the sink. This map was used for determining possible correction techniques.

Figure 2. Water Level Contour Map.

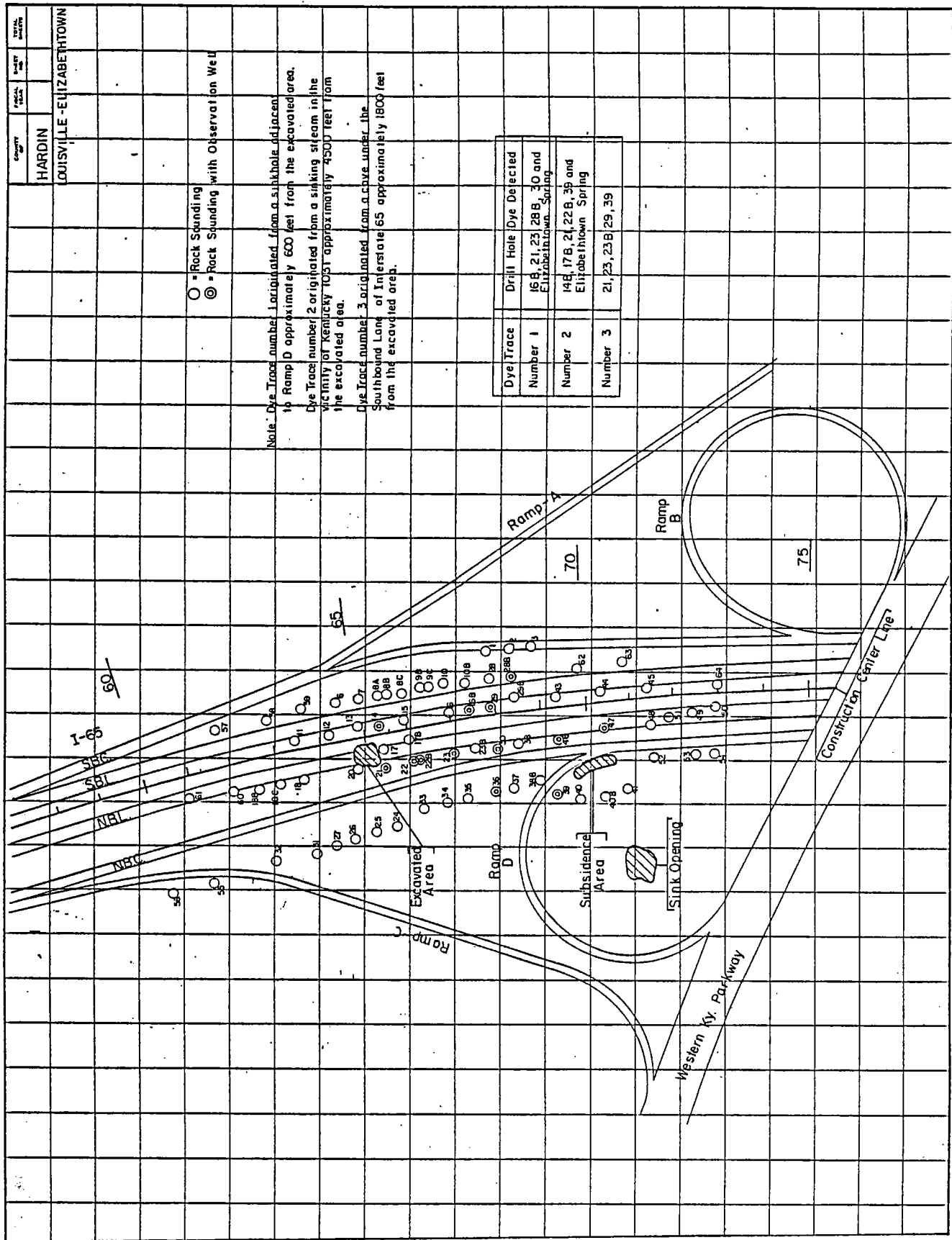


Figure 3. Subsurface Exploration Plan.

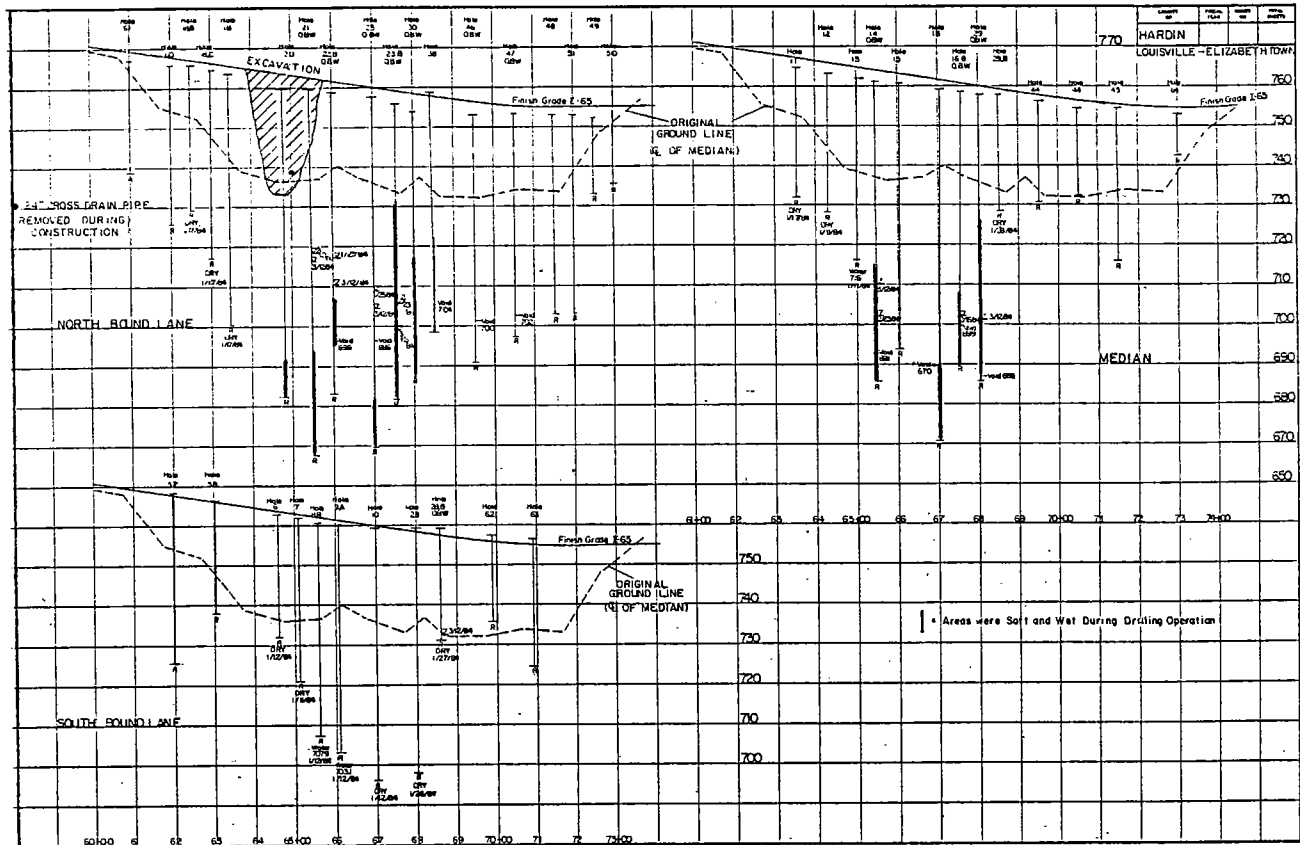


Figure 4. Subsurface Data For Mainline
Plotted on Profiles.

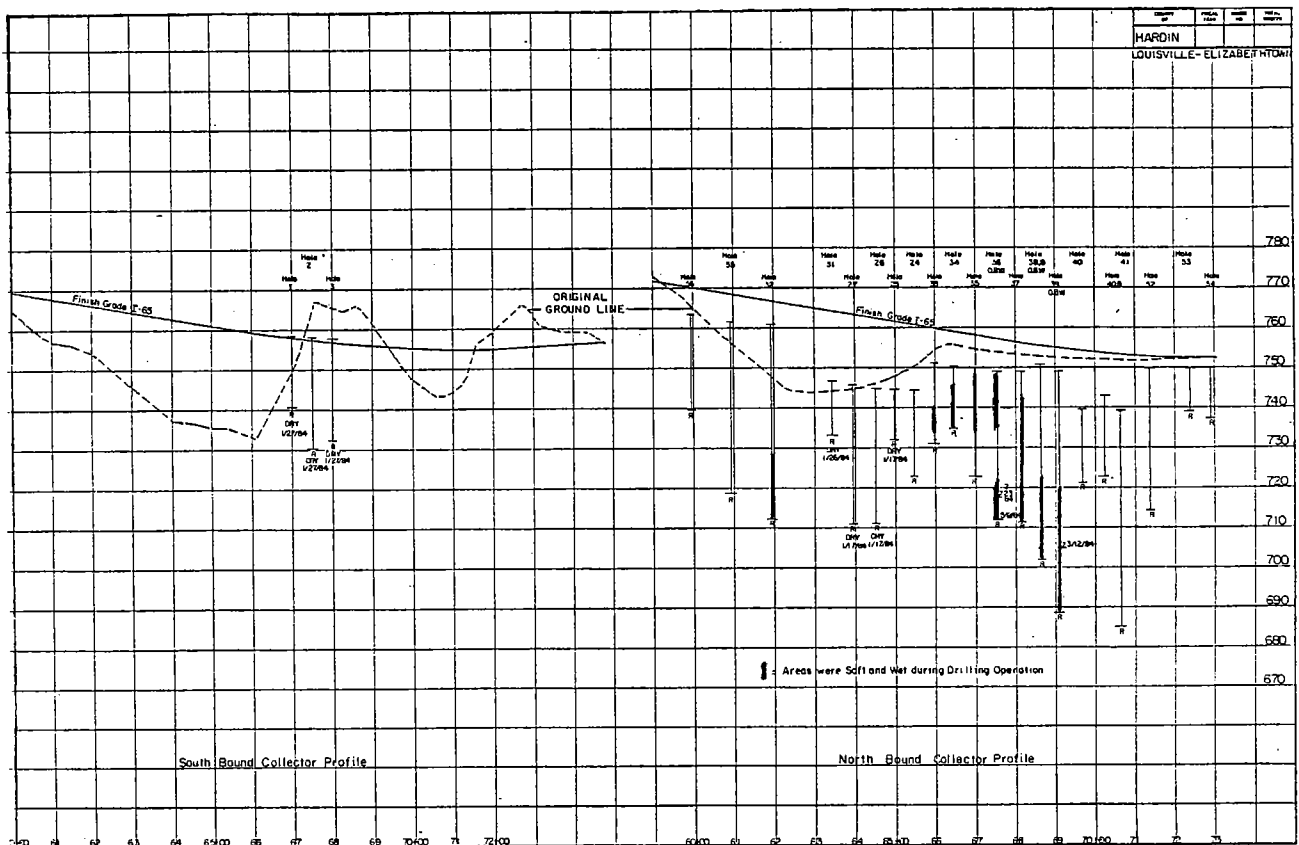


Figure 5. Subsurface Data For Collectors
Plotted on Profiles.

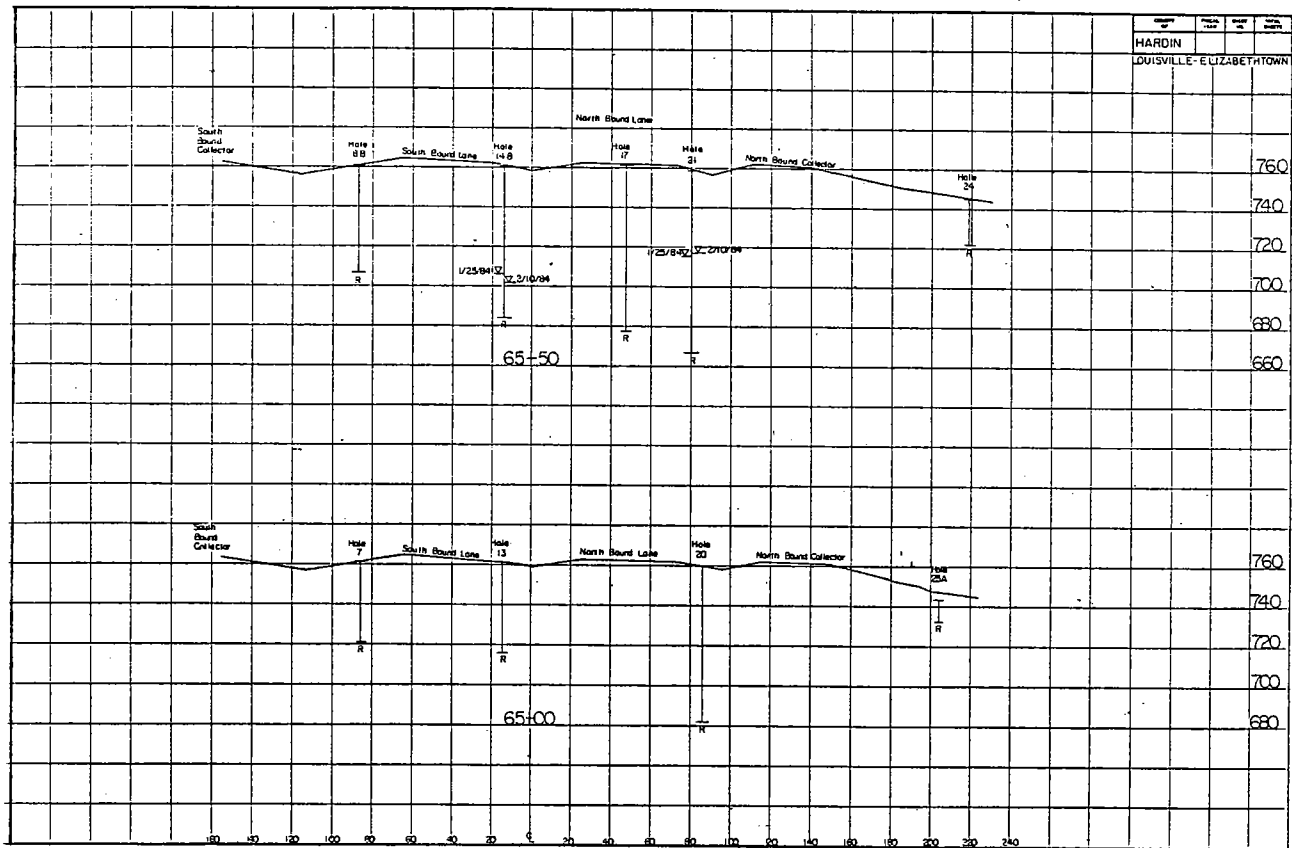


Figure 6. Subsurface Data For Roadway Plotted on Cross-Sections at Stations 65+00 & 65+50.

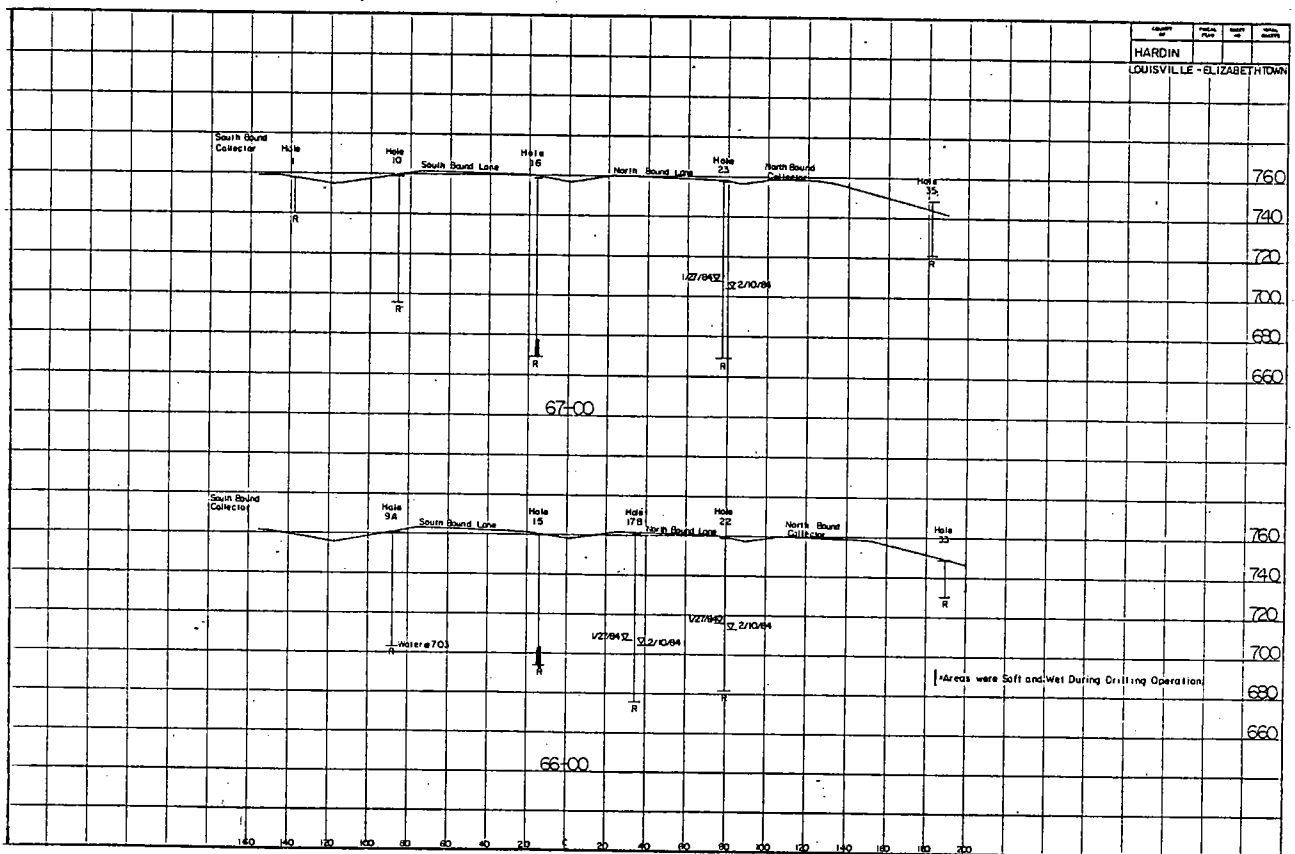


Figure 7. Subsurface Data For Roadway Plotted on Cross-Sections at Stations 66+00 & 67+00.

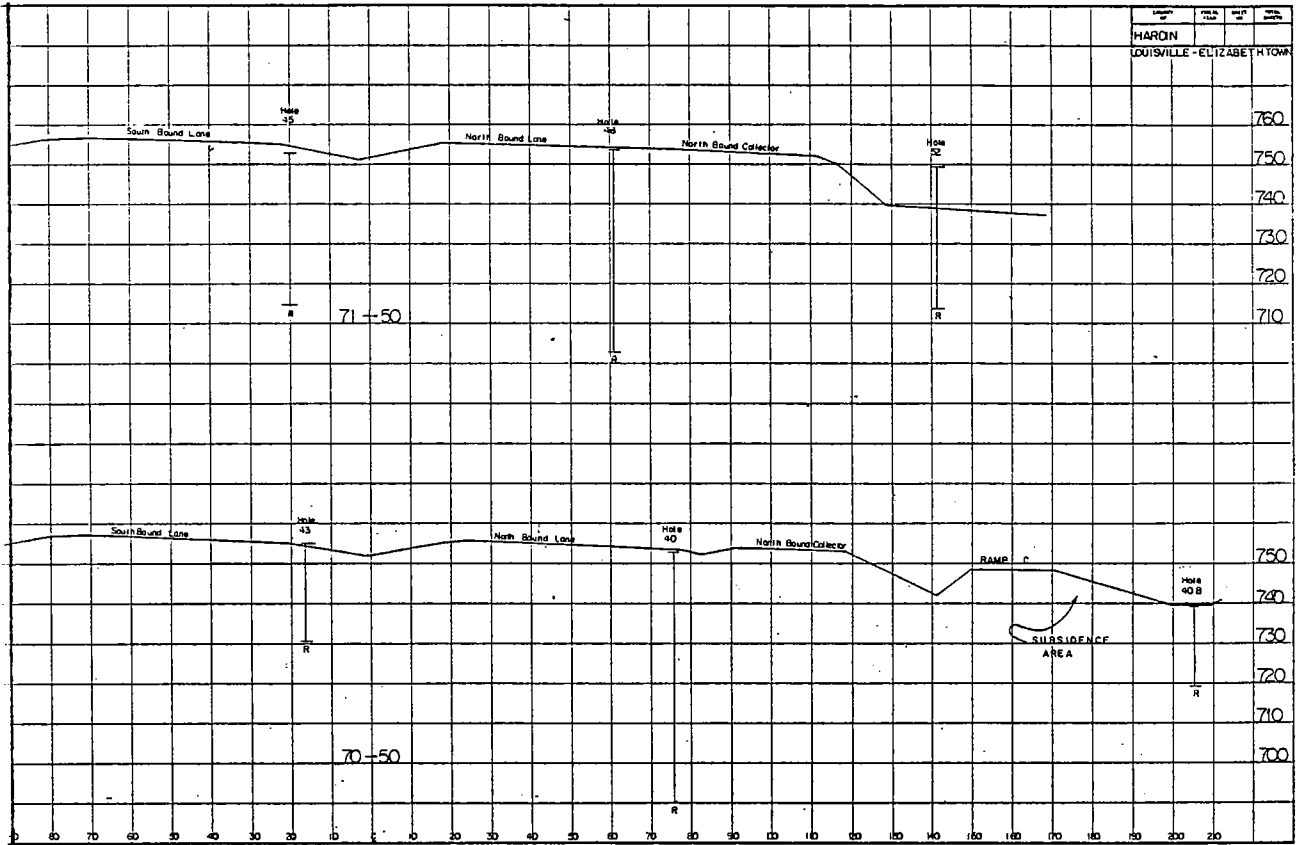


Figure 8. Subsurface Data For Roadway Plotted on Cross-Sections at Stations 70+50 & 71+50.

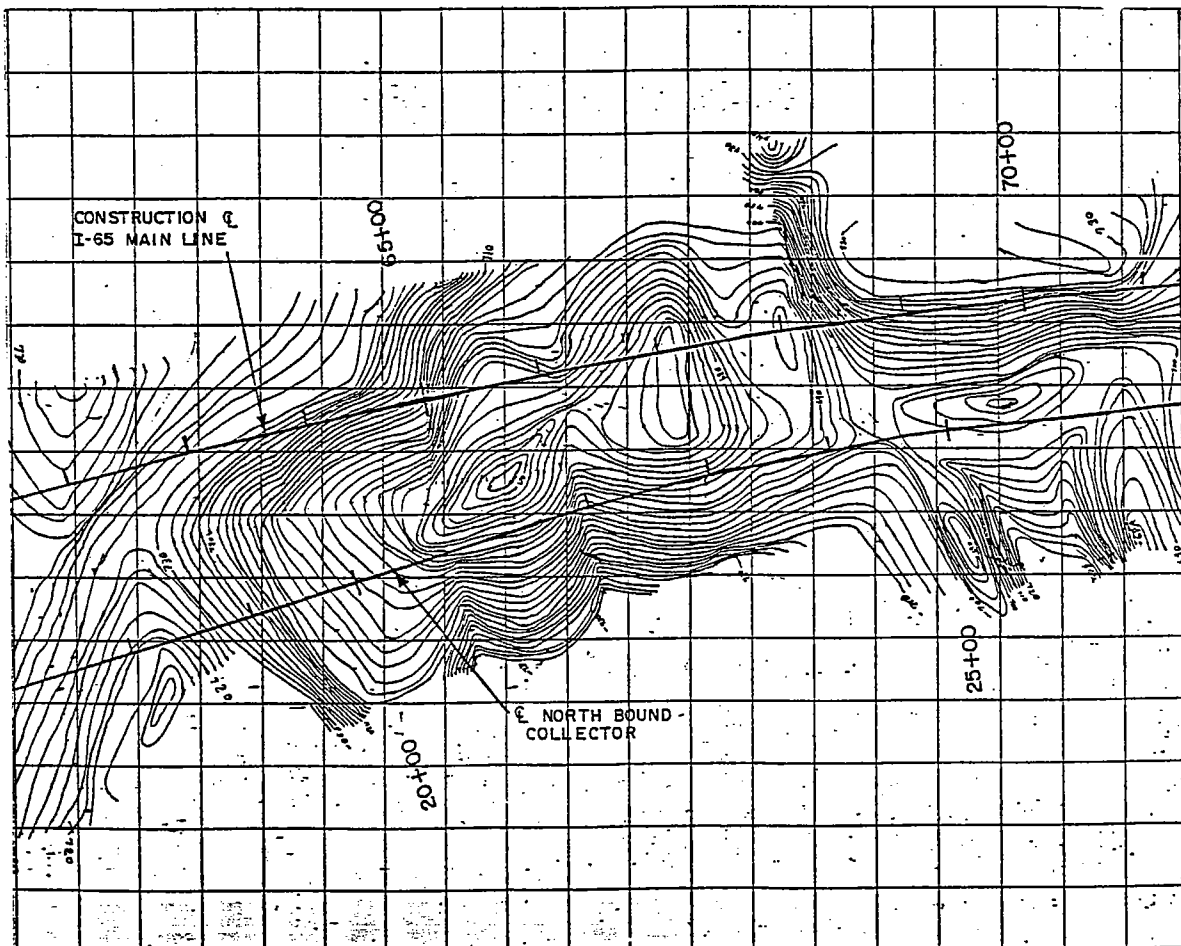


Figure 9. Rock Contour Map.

Dye Tracing

Three Fluorescein dye traces (Figure 3) were utilized to identify recharge areas effecting the subsidence, trace water movements, and locate a point of discharge. Dye trace number 1 was injected into the sink hole inside Ramp D and was detected in holes 16B, 21, 23, 28B, 30 and also in the excavation where the subsidence occurred. The dye reached the Elizabethtown Spring, which is one source of the town's drinking water, and was noticed by water plant personnel. This dye, diluted with 2,000 gallons of water, traveled approximately 1 1/2 miles in 22 hours during a relatively dry period. Dye trace number 2 was placed in a sinking stream near Ky. 1031 and was detected in holes 14B, 17B, 21, 22B, 28B, 39 and at the Elizabethtown Spring within 24 hours. Dye trace number 3 was placed during a rain storm into the surface runoff which entered the cave under the southbound lane of I-65. The third dye trace was detected in holes 21, 23, 23B, 29 and 39, however, it was undetected at the Elizabethtown Spring site. This probably was because the water was very muddy and the water plant had stopped pumping operations and switched to an alternate water source.

The fact that dye from all three dye trace locations was detected in drill hole number 21 is very significant. This hole, located in the immediate vicinity of the excavated area, indicates the water effecting the subsidence is coming from three separate drainage areas.

As a result of the dye tests, we are of the opinion that approximately 28 square miles of surface and subsurface water is being funneled under the embankment area and discharges into the Elizabethtown Spring. The surface area includes drainage along I-65, Ky. 61, Ky. 1031, US 31W and from a newly constructed retention basin.

Conclusions and Recommendations

The subsidence was probably caused by subsurface erosion due to the large volumes of water flowing thru the voids in the soil and solution channels in the limestone rock beneath the roadway embankment. Since the rock line was relatively shallow under the southbound lane the risk of subsidence is much less, therefore further considerations were not deemed necessary for this lane.

Driving piles and bridging the deep solution features is a feasible correction technique that would provide long term stability for this area. However, due to the high cost estimate for this method of correction, and since there is no way to predict an accurate time rate of subsidence due to the subsurface erosion caused by the drainage, two alternate recommendations were proposed for consideration.

Alternate I

Bridge the area under the northbound lane from station 62+50 to 72+50 using 50' simple span units bearing on steel piling driven to rock. Refer to Figure 10 for the bridging locations. Estimated cost \$1,370,000.

Alternate IA and IB

Bridging the northbound collector and Ramp D was considered but since traffic could be diverted in case of a total collapse, this proposal was not further considered.

Alternate II

- (1) Pump water out of the excavation and refill with quarry run stone. Place geotextile fabric between the rock backfill and soil subgrade.
- (2) Develop emergency traffic plan in case of additional subsidence.
- (3) Continue to monitor area with surface measurements every month.

Estimated cost \$30,000.

Considering the costs involved in bridging, and the serious time delay in the completion date of this critical roadway section, the Department decided to use Alternate II. In a meeting of highway personnel, the general opinion was that the embankment and thick clay deposits would provide sufficient support to bridge the area and subsidence would be gradual and could be maintained. As a precaution, District personnel will develop and emergency traffic plan in case the northbound lane and/or northbound collector should be closed due to subsidence. Survey methods will be utilized to monitor the roadway area to detect early indications of any possible subsidence problems.

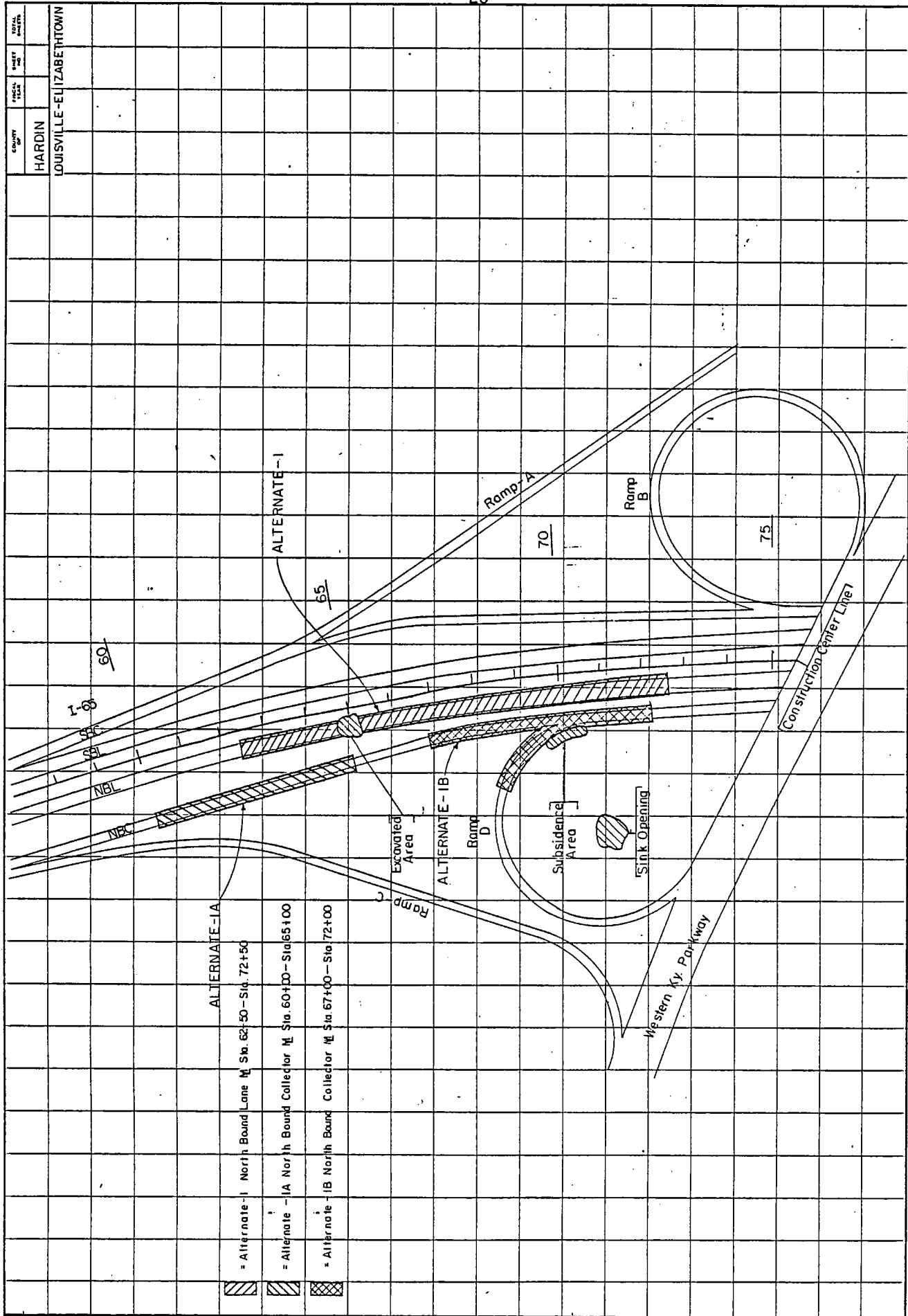


Figure 10. Alternate Correction By Bridging.

Acknowledgements

Special recognition is extended to T. Steller and G. Raymer, District Construction Personnel, and C. Bryant and D. Pedigo employees of the City of Elizabethtown for their records and other assistance. Also our appreciation is expressed to Geotechnical Branch Employees: D. Molen and M. Johnson for drilling, T. Gash for graphics, and K. Sheets for secretarial work.

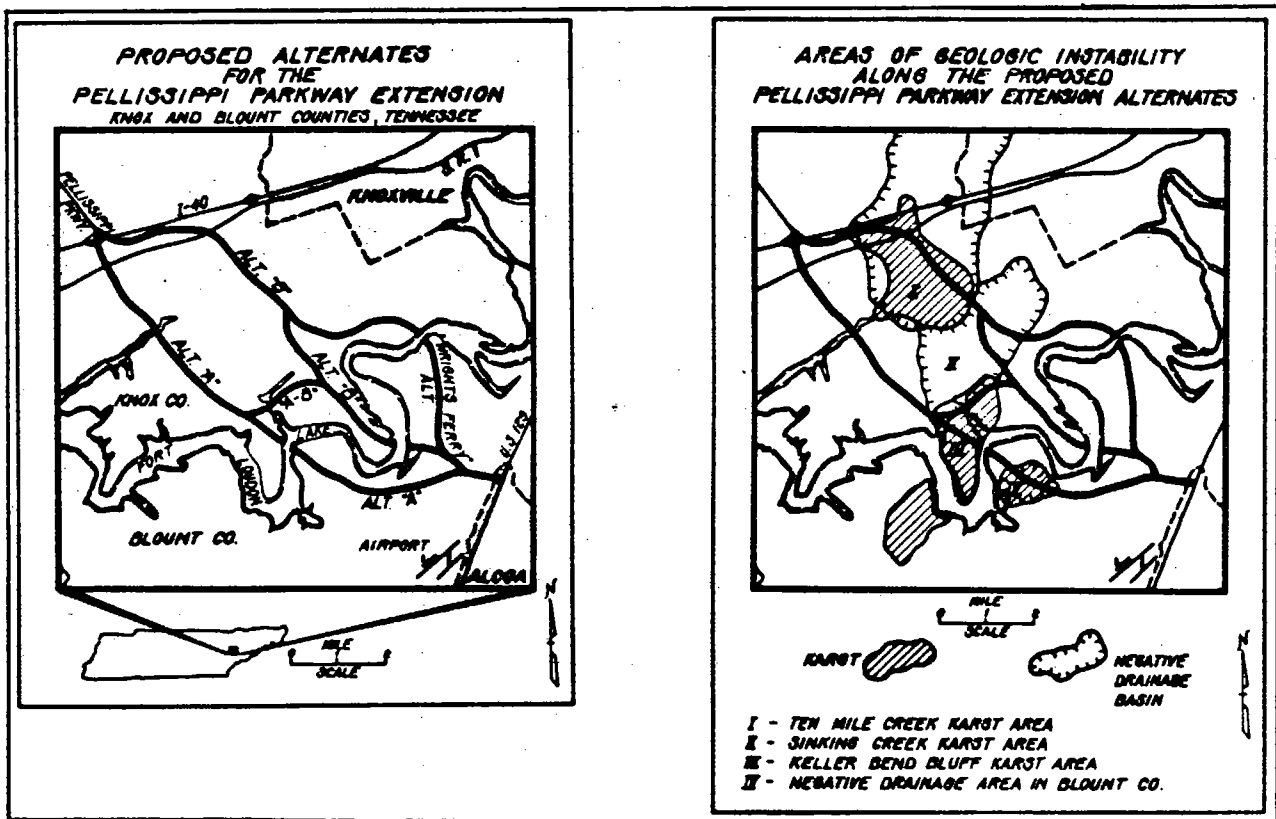
References

1. D.S. Mull and M.A. Lyverse, "Ground Water Hydrology of the Elizabethtown Area, Kentucky", U.S. Geological Survey Water-Resources Investigations Report 84-4057.

"THE PELLISSIPPI PARKWAY EXTENSION -
 GEOTECHNICAL ENGINEERING
 IN KARST TERRAIN"

BY

HARRY MOORE
 GEOLOGIC ENGINEERING SUPERVISOR I
 GEOLOGIC SECTION
 TENNESSEE DEPARTMENT OF TRANSPORTATION



GEOTECHNICAL CONSIDERATIONS IN THE
LOCATION, DESIGN, AND CONSTRUCTION OF
HIGHWAYS IN KARST TERRAIN

"THE PELLISSIPPI PARKWAY EXTENSION,"

KNOX-BLOUNT COUNTIES, TENNESSEE

Harry L. Moore, Tennessee Department of Transportation, Geotechnical
Section, P. O. Box 58, Knoxville, TN 37901

ABSTRACT

The extension of a limited access, four-lane highway facility, "The Pellissippi Parkway", involves the possible location of corridors in active karst areas of Knox and Blount Counties in East Tennessee. Geotechnical involvement in the location and design phases of this highway development process has resulted in the recognition of several unstable areas of karst and has led to the adoption of remedial and preventive design measures which are to be incorporated in the construction plans.

Karst problems identified along the proposed "Pellissippi Corridors" include induced subsidence and collapse, bridging of existing caves and flooding and siltation of existing swallets and ponors. Innovative design concepts and construction methods used in the Pellissippi Parkway Project include rock pads and rock fills, rock backfill, paved ditches, curbs and flumes, overflow channels, and swallet improvement/protection.

Introduction

The construction of highway facilities in karst areas is becoming more common due to urban development. As the spread of construction projects encroaches on karst areas the resulting geotechnical problems will require varied and innovative remedial concepts.

The continued development and expansion along East Tennessee's high technology corridor - - - The Pellissippi Parkway - - - has required the need for it's extension. Located in the western part of Knox County, the Parkway extension is designed to connect the high-tech areas of Oak Ridge and west Knox County to the Knoxville Airport

in neighboring Blount County. (Figure 1).

The peculiarity of karst areas with characteristic sinkholes, depressions, swallets, and cave systems have intrigued the earth scientist for years. The technical understanding of the development of karst is still a fresh science with new information and understanding continually being developed. However, the treatment of karst areas with respect to man's impact (i. e. highways, commercial and residential development) has been approached with uncertainty in years past. Very little information seems to have been published with regard to the treatment of karst in relation to construction projects. Newton, 1976, Moore, 1981, and Royster, 1984, are technical papers related to highway engineering in karst terrain. Additionally, Sowers, 1976, Newton, 1981, and Foote & Humphreys, 1979, detail specific engineering problems related to karst and karst terrain.

Experience has shown that the treatment of karst problems can be tenuous at best. Often the treatment of one kind of karst problem can lead directly to the cause of another kind of karst problem (i. e. treating sinkhole flooding problems can lead to induced collapse problems).

Karst problems are usually dealt with in an after-the-fact maintenance approach. Involvement of geotechnical expertise in the location, design, and construction phases of highway development in karst areas can and often does reduce the incidence of karst related problems. The recognition of potential karst problems before the fact can and often does lead to better engineered projects. Combined with refined karst related

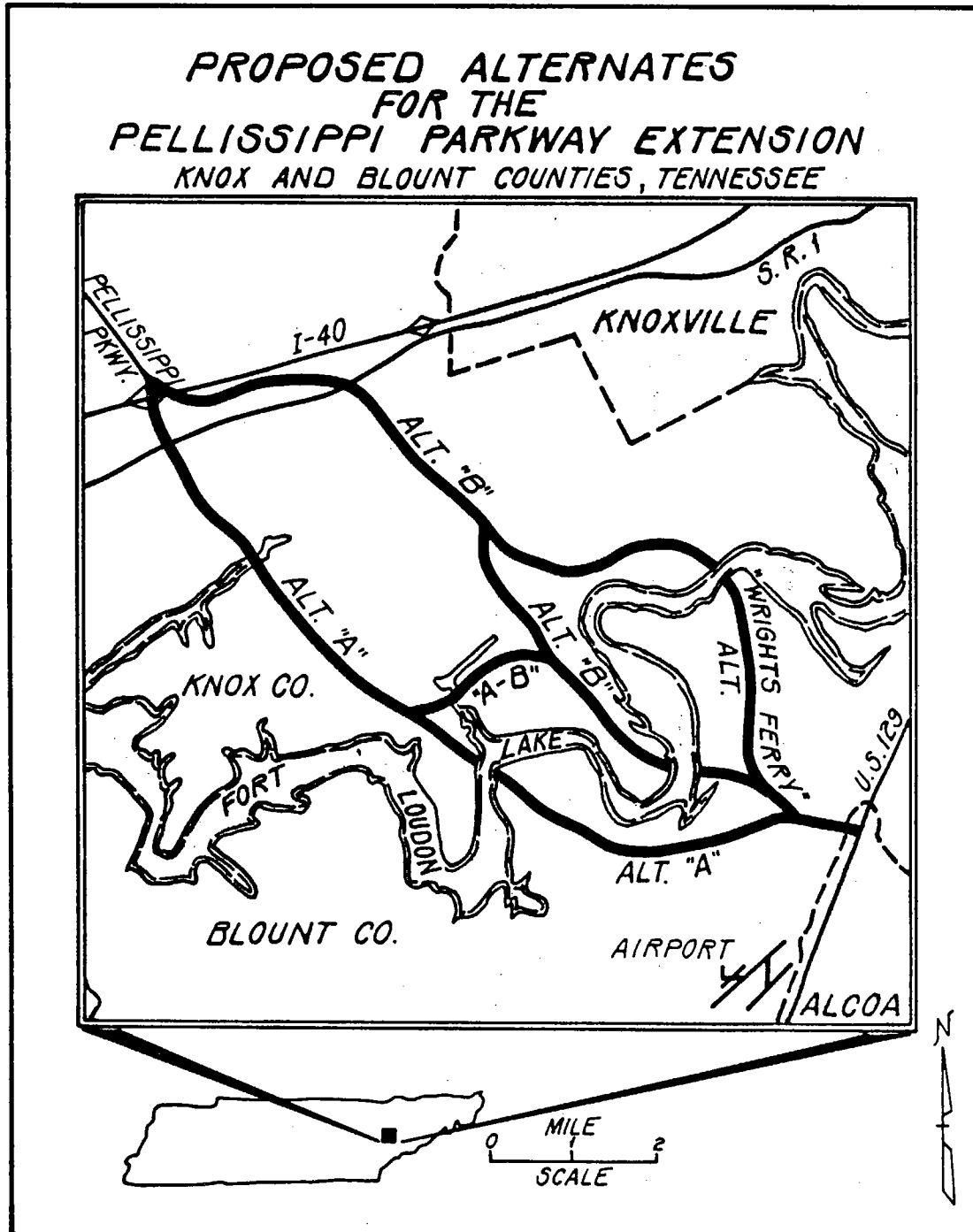


Figure 1 - Location Map for Study Area

remedial concepts the effect of geotechnical expertise can result in a more environmentally compatible facility.

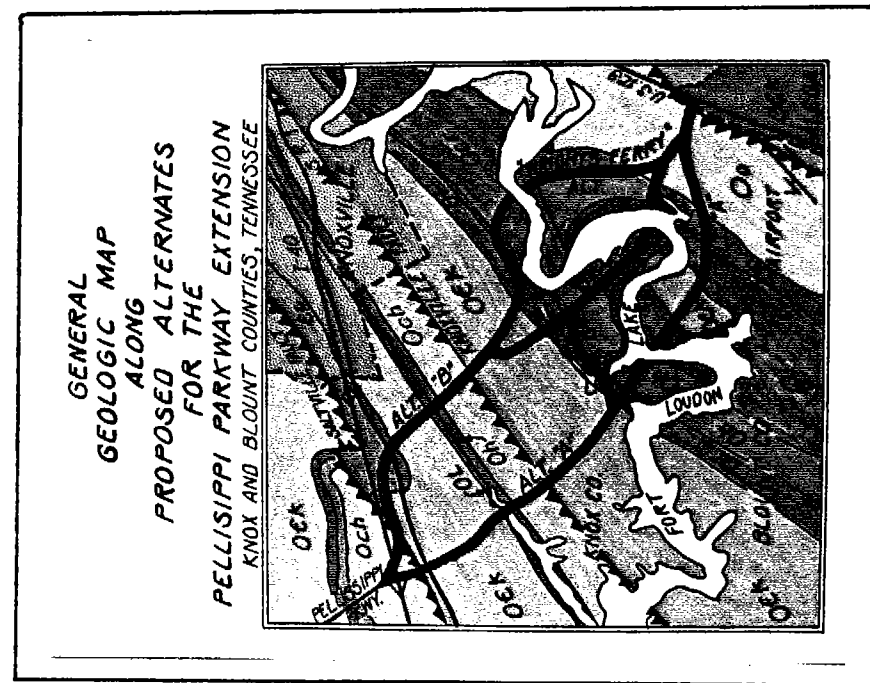
This paper describes the geotechnical aspects of several karst areas that may be impacted by the extension of the Pellissippi Parkway. In addition, proposed remedial design concepts are discussed.

General Geology

Geotechnical involvement during the location phase of the highway project development resulted in the compilation of geologic data detailing karst areas. The locations of four alternates were studied with respect to geologically unstable conditions.

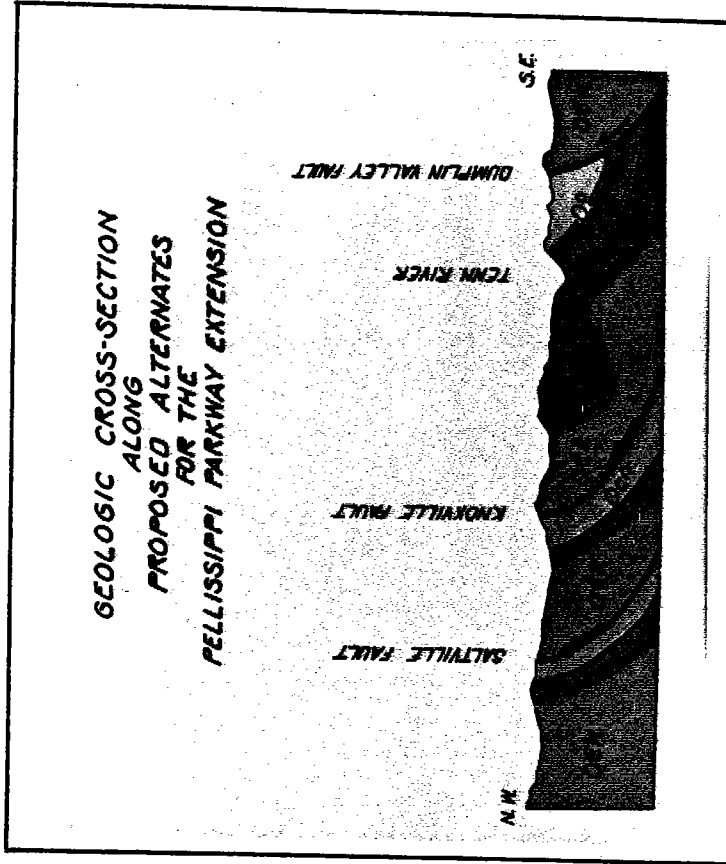
All of the proposed alternates are located in a topographic area composed of alternating ridges and valleys underlain by tilted sedimentary rock strata. Most of the area is underlain by carbonate rock strata containing limestone and dolostone lithologies of Cambrian and Ordovician age (Figure 2). Thick residual clay soils are found along some sections of the alternates while numerous outcrops of bedrock can be found along other sections.

There are three geologic formations composed of carbonate strata that are crossed by the proposed alternates and exhibit characteristic karst conditions. These rock units strike in a NE-SW direction with average dips of 30° to the southeast. The three formations are the Knox Group (Cambrian/Ordovician) and the Holston and the Lenoir formations (Ordovician).



Cambrian/Ordovician-Knox Gp.
O&K (Limestone & Dolostone)

Cambrian-Conasauga Gp.
C&C (Limestone & Shale)



Ordovician —

- Ottossee Shale Oo (Shale)
- Chapman Ridge Sandstone Ocr (Sandstone)
- Holston Formation Oh (Massive Limestone)
- Lenoir Formation Ol (Limestone)

Chickamauga Gp. Och

Figure 2 - Geologic Map and Cross Section of Study Area.

Karst

The characteristic karst conditions found along the proposed alternates include depressions, sinkholes, ponors, caves, uvalas, springs and underground drainage systems. The Holston Formation and the Knox Group are very prone to solution activity and contain characteristic karst along the alternates. Existing karst features, induced subsidence and collapse, and flooding were determined to be the main karst problems found along the project.

Four main areas of karst were identified within the project limits (Figure 3). These are as follows:

- I. Ten Mile Creek negative drainage basin and associated cave system (Knox Co.)
- II. Sinking Creek drainage basin (Knox Co.)
- III. Keller Bend cave system (Knox Co.)
- IV. Negative drainage area on Alternate "A" in Blount County.

In addition to existing karst features, there are two main problems associated with karst. These are stability problems (subsidence/collapse features) and flooding.

Typically, active karst areas experience subsidence and collapse features which are usually associated with cave systems. Very often, these days, collapse and subsidence features are man-induced, triggered by 1) altering the natural flow of surface and subsurface drainage, 2) increasing soil moisture seepage pressures, and 3) increasing subsurface erosion. However, natural fluctuation in groundwater tables and subsurface erosion can and often do lead to the occurrence of continued subsidence, new collapse features, and flooding.

In some areas along the proposed extension alternates negative drainage basins have been created due to the formation

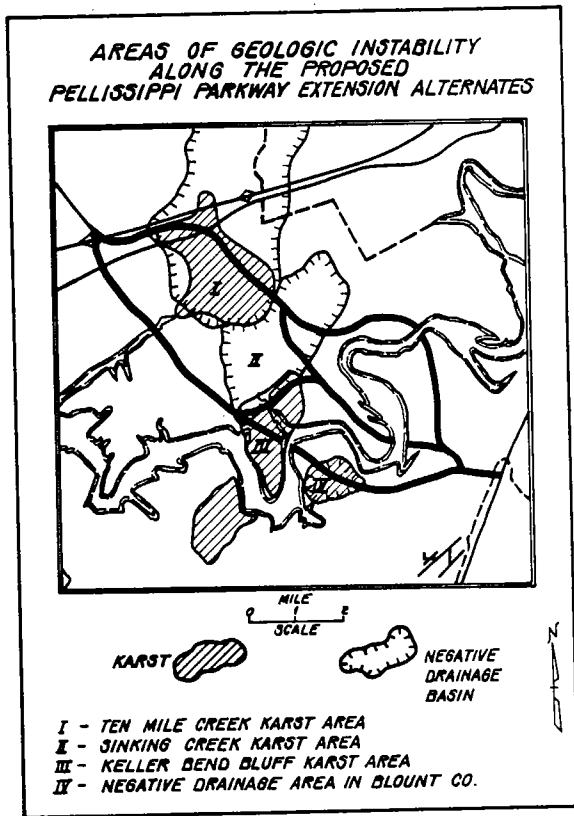
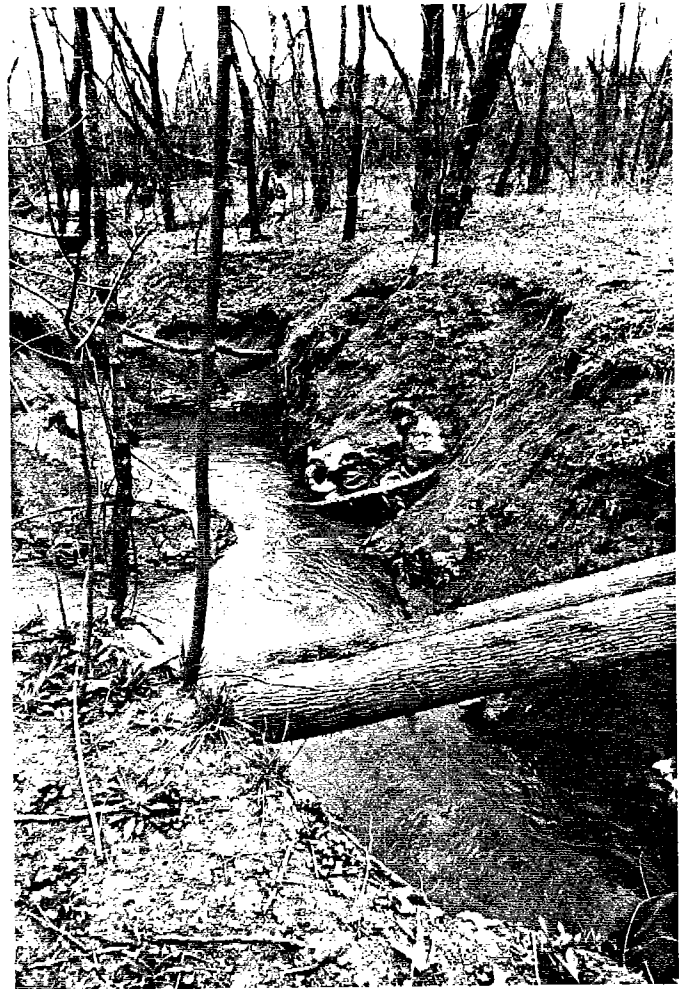


Figure 3 - Location of Karst Areas and Negative Drainage Basins in Study Area.

Figure 4 - Point at which Ten Mile Creek enters subsurface (ponor) in Holston Formation.



of depressions and sinkholes which have coalesced into very large areas of negative flow. Three such large scale negative drainage basins are located within the project limits. The Ten Mile Creek and Sinking Creek drainage basins are two such areas of negative flow (see Figure 2). The third smaller negative drainage basin is located along Rankin Ferry Road in Blount County (Alternate "A").

Alternate "B" crosses the Ten Mile Creek and Sinking Creek drainage basins while Alternate "A-B" crosses the Sinking Creek drainage basin. The largest negative drainage basin within the study area is the Ten Mile Creek drainage basin composed of an area approximately 42 sq. kilometers (15.8 square miles) in size and characterized by sinkholes, depressions and cave systems. An extensive cave system (composed of over 4.8 kilometers (3 miles) of mapped passageways) carries Ten Mile Creek underground (Figure 4) in a SW direction from the south end of the basin to nearby Fort Loudon Lake where Ten Mile Creek reemerges as a large spring (Figure 5). During periods of heavy precipitation the basin often floods covering existing roads and property with as much as 15 feet of water (Figures 6, 7).

The Keller Bend Bluff area along Alternate "A" (at the north side of Fort Loudon Lake) is underlain by the Holston Formation and contains numerous interconnected caves. The caves are developed along joints that are both parallel and normal to the bedding strike. The Keller Bend Bluff area is subject to continued cavern enlargement and subsequent sinkhole enlargement as evidenced by at least three different levels of past solution activity.



Figure 5 - Resurgence of Ten Mile Creek from Ten Mile Creek Cave System (photo made during May, 1984 flood.



Figure 6 - Flooded Road in Ten Mile Creek Negative Drainage Basin, Knox County.



Figure 7 - Flooding Conditions at the Ponor Location of Ten Mile Creek, Knox County (water is 10-15 feet deep-May, 1984 flood).



Figure 8 - Collapse Structures such as this along S. R. 72 in Loudon County, TN, usually occur along unpaved ditches in karst areas.

Figure 9 - The Prevention of Karst Related Subsidence and Collapse of Highways is centered around controlling the Drainage; I-40, Loudon County, TN.



Geotechnically related stability problems and related karst features (negative drainage basins, cave systems, and sinkhole development) which will impact the Parkway project might include one or all of the following:

- *The increased likelihood of flooding due to the unpredictable nature of negative drainage systems.
- *Stability problems concerning induced collapses and sinkhole enlargement.
- *Stability problems concerning toe saturation of embankments due to flooding within sinkholes and depressions.
- *Alteration of groundwater conditions by induced siltation or runoff contaminants entering the subsurface via sinkholes, caves, etc.

Karst and Highway Construction - Conceptual Design

The construction of highway facilities across karst areas usually result in the development of collapse features and flooding. The collapse features along with subsidence usually occur along unpaved ditches where a freshly excavated cut interval has approached the soil/rock interface (Figure 8). Occasionally, a collapse will occur beneath the roadway driving surface where subsurface erosion has enlarged a cavity in the soil (Figure 9).

The purpose of the geotechnical investigation for the Pellissippi Parkway extension was not only to locate and identify specific karst problems but to develop remedial concepts for these problems. Experience with these kinds of karst problems in East Tennessee has led to the development of geotechnical concepts with which to treat karst areas effectively.

Controlling the drainage is of primary importance in coping with karst problems. Providing the appropriate

drainage treatment for a karst condition during design and construction can result in reducing the impact a new highway will have on a karst regime (i. e. channeling runoff into depressions and sinkholes without appropriate design measures can and usually does result in the formation of collapse features and serious flooding).

A number of innovative and "tried and proven" concepts were applied to the preliminary design of the Pellissippi Parkway Extension alternates. Some of the more effective concepts utilized include:

- *Paved ditches - The use of paved ditching for all ditches and channels with a karst area is recommended to prevent or greatly reduce the build-up of groundwater seepage pressures and subsurface erosion which can lead to collapse problems (Figure 10).
- *Rock pads - The use of rock pads for bridging depressions and sinkholes and preventing fill-toe saturation during flooding involves constructing the lower lifts of an embankment out of rock fill material. This concept works best when the soil cover is removed down to bedrock before placing the rock fill material (Figure 11).
- *Rock backfill - The use of the rock backfill concept is designed to bridge collapse features with a "chunk" rock backfill plug (Figure 12).
- *Curbs for fill sections - The use of asphalt curbs will provide for better control of runoff through karst areas assuring that water will flow along established courses reducing seepage pressures and erosion (Figure 13).
- *Overflow channels - Overflow channels are a method which provides a positive flow for runoff in a negative drainage basin. This concept involves the construction of a lined channel or pipe from a negative drainage area to a positive draining system (Figure 14).
- *Swallet improvement/protection - This concept involves improving the runoff flow into subsurface cavities by removing debris and trees from around the throat of a swallet and protection of the cavity opening from siltation or clogging by debris laden runoff. Protection methods may involve the use of siltation barriers, debris catchment fences, rip-rap, gabion barriers and concrete structures (Figure 15).

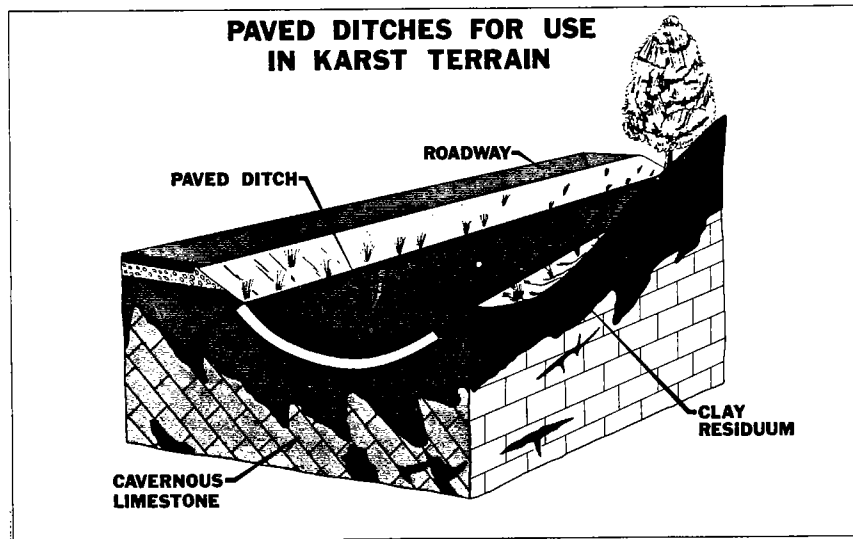


Figure 10 - Schematic Diagram Illustrating the use of Paved Ditches in Karst Areas.

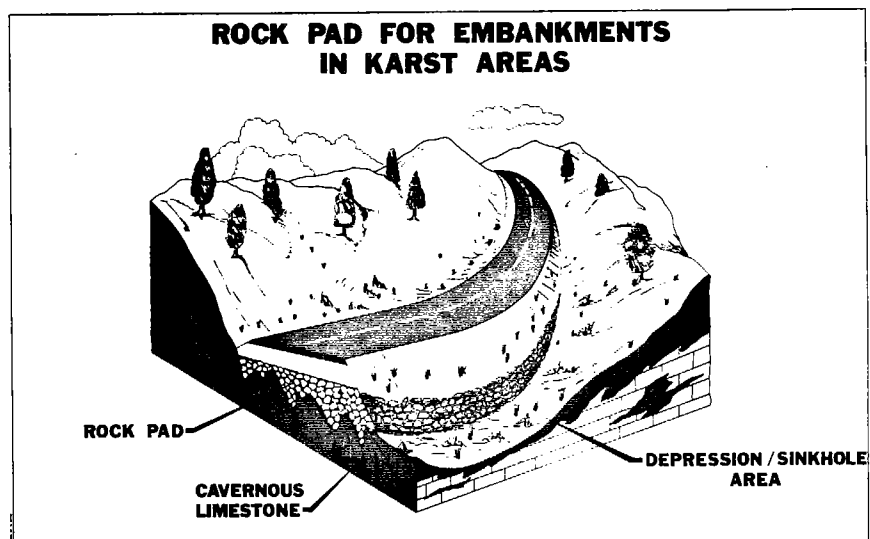


Figure 11 - Schematic Diagram Illustrating the use of Rock Pads for Embankments in Karst Terrain.

CHUNK ROCK BACKFILL FOR KARST AREAS

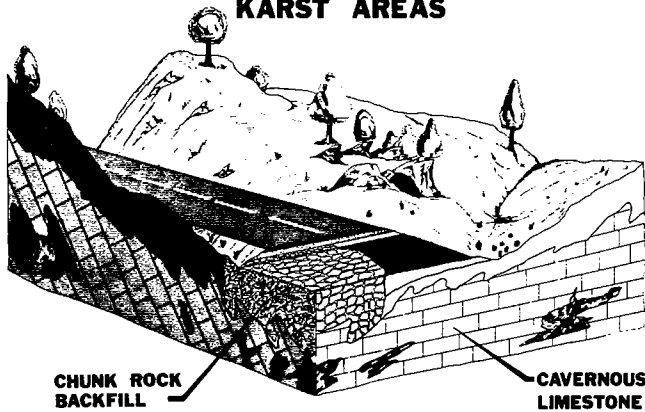
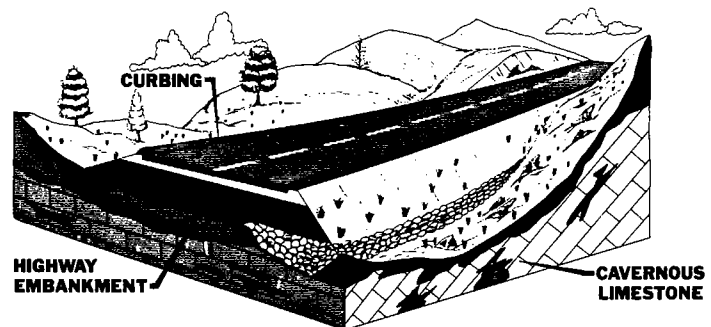


Figure 12 - Schematic Diagram Illustrating how Chunk Rock Backfill is Utilized for Collapse Features in Karst Areas.

Figure 13 - The Use of Curbing for Embankments helps to control drainage run-off in sinkholes as illustrated in this schematic diagram.

CURBING FOR EMBANKMENTS IN KARST AREAS



OVERFLOW CHANNEL FOR KARST AREAS

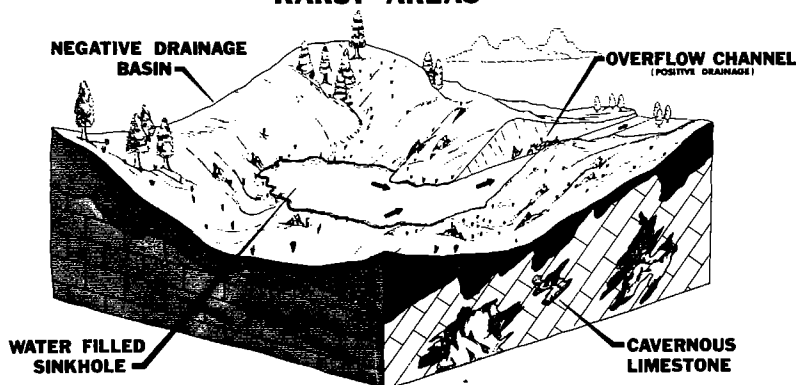


Figure 14 - Schematic diagram illustrating the use of an overflow channel to relieve negative drainage basins.

In addition, relocation and the alteration of grades were considered. However, the avoidance of the karst and negative drainage areas located within the proposed corridor limits was not possible without altering the integrity of the Parkway project.

Closing Remarks

The selected route for the Pellissippi Parkway Extension was made after considerable study of all influencing factors along each route. Factors such as right-of-way costs, number of displacements, construction costs, geotechnical conditions, and environmental impact were all considered. The route chosen consists of portions of the "A" route and "B" route (Figure 16). Referred to as the "A-B" route, this corridor misses the severe karst areas connected with Ten Mile Creek Drainage Basin and cave system and the Keller Bend karst area.

The majority of the "A-B" route is located in very stable geologic terrain. Only the connector between the "A" and "B" routes is located in a karst area. This portion of "A-B" route skirts the edge of the Sinking Creek negative drainage basin and karst area. Minimal impact to surrounding depressions and sinkholes will be made and runoff from the highway will be purposely diverted from several sinkholes and depressions.

It is significant to note that the route selected was in the most favorable geologic environment of the four proposed routes. Significant consideration was given to the geologic evaluation of the project by administrative officials . . . a positive indication of progress in the scientific-engineering communities.

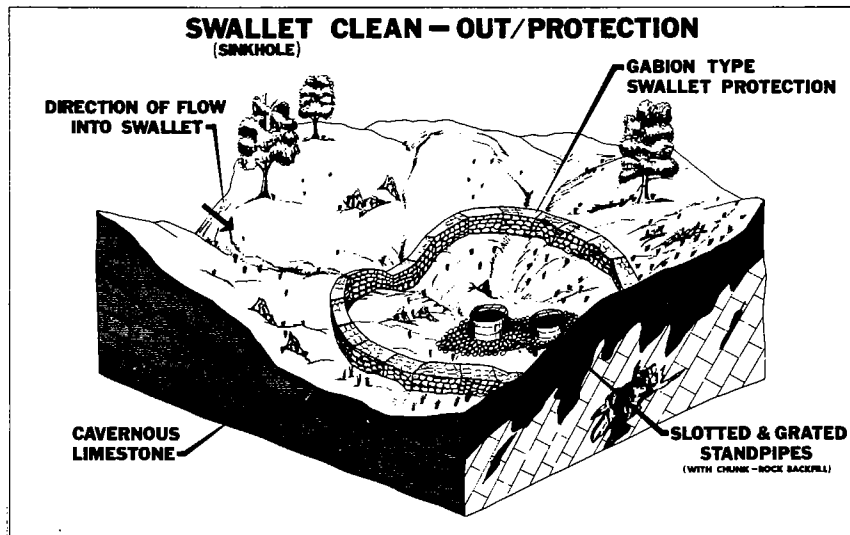


Figure 15 - Schematic diagram illustrating the concept of swallet clean-out and protection.

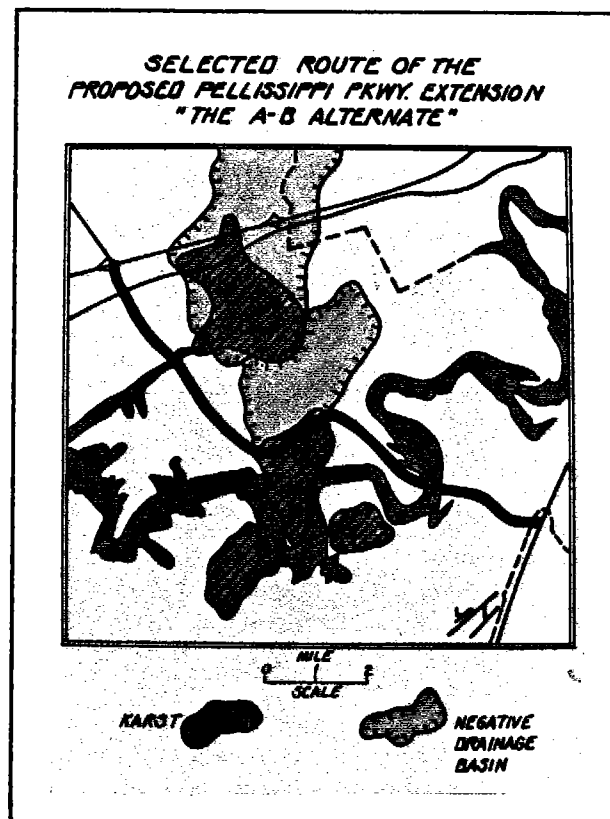


Figure 16 - Location of route selected for the proposed Pellissippi Parkway Extension in Knox and Blount Counties, TN.

Innovative and cost effective remedial concepts for solving karst related geotechnical problems will require modifications and refinement to insure proper results. Stringent land use and building codes for the karst areas outlined in this study will be required to insure the success of the karst related remedial design concepts proposed for the extension of the Pellissippi Parkway in Knox and Blount Counties, Tennessee.

Acknowledgements

The writer wishes to acknowledge the Tennessee Department of Transportation and specifically the Geotechnical Section and the Region I Design Office for their assistance and support in the development of this paper.

References

- Foose, Richard M., and Humphreville, James A., 1979, Engineering Geological Approaches to Foundations in the Karst Terrain of the Hershey Valley: Bull. of the Association of Engineering Geologists, Volume XVI, Number 3, Summer, 1979, pp. 355-381.
- Moore, Harry L., 1981, Karst Problems Along Tennessee Highways: An Overview. Proceedings of the 31st Annual Highway Geology Symposium, Austin, Texas, August, pp. 1-28.
- Newton, J. G., 1976, Induced and Natural Sinkholes in Alabama -- A Continuing Problem Along Highway Corridors. Transportation Research Record 612, pp. 9-16.
- Newton, J. G., 1981, Induced Sinkholes: An Engineering Problem: ASCE Journal of the Irrigation and Drainage Division, Volume IR2, June, pp. 175-185.
- Royster, D. L., 1984, The Use of Sinkholes for Drainage: Proceedings of the 63rd Annual Transportation Research Board Meeting, Washington, D. C., January, pp. 1-26.
- Sowers, George F., 1976, Mechanisms of Subsidence Due to Underground Openings: Transportation Research Record 612, pp. 2-8.

EXPLORATION AND REPAIR OF LIMESTONE SINKHOLES BY IMPACT DENSIFICATION

Joe C. Drumheller, P.G.

Senior Geologist, GeoSystems, Inc., Sterling, Virginia

Impact Densification, an exploration and remedial tool that involves dropping a heavy weight (8-15 tons) repeatedly from heights up to 70 feet, has been used successfully in locating and repairing soft zones and soil voids formed in residual soils overlying dipping and jointed limestone.

The technique utilizes a heavy weight dropped on a close grid pattern over the entire building or highway area to locate and/or collapse existing soil domes. The weight produces large craters which are backfilled with either compacted granular fill or crushed stone. Depth measurements are obtained for each crater, and are used in detecting domed or soft areas. These soft areas are evidenced by noticeably deeper craters.

Once a dome is located, additional high energy drops are used to collapse the void or cavity. The craters are backfilled, and are repounded until an acceptable weight penetration response is achieved.

Open sinkholes encountered in conjunction with this treatment are generally repaired by alternating layers of filter fabric and select compacted fill material overlying a concrete plug in the throat of the sinkhole.

This paper presents two case histories where impact densification has been used, Valley Forge, PA and Knoxville, TN.

SINKHOLES & GABIONS

A SOLUTION TO THE SOLUTION PROBLEM

BY

DOMINICK AMARI, MACCAFERRI GABIONS, INC., NASHVILLE, TN 37210

HARRY MOORE, TENNESSEE D.O.T., KNOXVILLE, TN 37901

ABSTRACT

Karst features such as sinkholes, depressions, swallets, and ponors present a unique problem to engineering projects. Rapid and unplanned commercial and residential expansion into active karst areas usually results in a number of geologically related stability problems including flooding, subsidence, and collapse.

The control of surface drainage is a key factor in developing geotechnical remedial design for karst areas.

For karst problems involving the control of surface drainage features and siltation, the use of gabion structures should be considered. The principal advantage in utilizing gabion structures for some karst problems is the gabion's unique characteristics of permeability and flexibility. The control of surface run-off into karst structures, such as depressions and sinkholes, can be effectively achieved with gabion check dams and "gabion trash racks".

The cleanout of swallets to provide adequate drainage into the subsurface requires the protection of the swallets and depressions. This can be adequately achieved with the use of small gabion barriers.

Although the use of gabion structures to correct or improve the stability of depressions and swallets is not a panacea, it, nevertheless, deserves appropriate consideration.

INTRODUCTION

Down through time engineers have sought to identify, recognize, and isolate the perils of nature in order to develop systems that would compensate for and modify natural processes. In terrain underlain by soluble limestone and dolostone, karst topography evolves. Sinkholes form and are manifest as the primary means of drainage. Generally, urbanization increases the frequency of sinkhole collapse and associated flooding problems. Development of sinkholes in urban environments usually result in major economic loss for all parties affected. Planning bridges, roadways and other public works projects in karst areas challenges geologists and engineers alike and should be treated with utmost respect.

This paper will introduce methods for the use of gabions (wire baskets filled with rocks) as one construction practice for attempting to diminish the hazardous results of urban sinkhole collapse. The flexible, porous nature of a gabion structure makes it ideal for the unique circumstance of urban sinkhole development. Whether in residential, commercial, or industrial applications, gabions have demonstrated their ability to adjust to a variety of karst environments. They have been successfully used for retaining walls to keep soil slopes from failing, stormwater control structures, culvert headwalls, and aprons where rigid structures would most often fail, and a range of other innovative applications where the control of soil erosion is paramount.

However, until recent years little has been published about remedial concepts surrounding engineering projects in karst terrain. Often, nothing is done to compensate for the karst instability until after the fact. The utilization of gabion structures in the remedial concepts required to compensate for karst problems is a relatively recent development. In this paper two case histories involving karst problems that were corrected with gabions are discussed. The use of gabions is not intended (in the context of this paper) to be a panacea but a viable tool to be utilized in appropriate situations.

DEFINITIONS

I. SINKHOLES

"Sinkholes can be broadly defined as closed topographic depressions, generally elliptical-to-circular in landscape view, resulting from the settlement or collapse of soil or rock into solution openings beneath the ground surface, such as caves or enlarged rock fractures. Sinkhole terrains, formally called karst topography, are a geologically delicate landscape category characterized by sinkholes, caves, springs, streams that

disappear underground, and well-developed subsurface drainage" (Kemmerly 1981). Within the framework of this paper, sinkholes and their display will be defined as localized subsidence or collapse induced through natural processes.

Sinkholes in most temperate-climate karst regions are displayed as small bowl- or funnel-shaped depressions called dolines, topographically described as areas of internal drainage. They may have narrow steep sides or exhibit shallow pan-like cross sections. Often in tropical-climate karst regions, these depressions can be measured in tens of meters. In both regions sinkholes can be open drainage holes where surface run-off is discharged directly to the water table, usually with limestone or dolostone exposed at the bottom, or soil-filled depressions with surface drainage filtering through the soil to the water table below. Morphology, distribution, and frequency of occurrence are common topics of investigation. Frequency and distribution studies have been successfully completed over a wide range of karst areas. All of these studies conclude that sink depressions are unique geomorphological expressions requiring individual attention.

II. GABIONS

Gabions have been used world wide in controlling erosion. They have gained rejuvenated popularity due to their high efficiency rate and economic (cost efficient) nature.

"Gabions are prefabricated 'baskets' of heavily galvanized steel wire woven into a flexible, double-twist, hexagonal mesh. These compartmentalized, rectangular containers or 'baskets' are assembled and filled at the job site with locally acquired crushed stone. (Summers and Johnson, 1982) They vary in size and shape and are most often laced together to form very competent erosion control structures." (Amari 1984)

Gabions can be used for a variety of difficult construction situations. For erosion control and retaining structures, gabions offer the user a number of advantages.

A) Permeability

A hydrostatic head will not develop behind a gabion structure. The structure is pervious to water and stabilizes a slope by the combined action of draining and retaining. Drainage is accomplished by gravity, and there is almost unlimited porosity.

B) Flexibility

Its double-twist hexagonal mesh construction permits it to

tolerate differential settlement without fracture. This property is especially important when a structure is on unstable ground. It lends itself well to use in diverse geological environments.

C) Durability

The wire mesh used in gabions is heavily galvanized. It may be safely used in fresh water and in areas where an acid situation will not develop. For highly corrosive conditions, a PVC (polyvinyl chloride) coating is applied over the galvanizing. PVC-coated gabions are used in corrosive environments such as polluted urban discharge areas, polluted streams, areas adjacent to salted highways, and in acid soils such as muck, peat, or cinders.

D) Strength

Steel wire hexagonal mesh has the strength and flexibility to withstand forces generated by water and earth mass movement. The nature of a gabion structure allows it to absorb and dissipate much energy. Compact gabion structures often remain effective long after a massive rigid structure fails, when failure is due to earth movement.

E) Economy and Low Maintenance

Gabion installations are more economical than rigid or semi-rigid structures. Gabion construction is simple and does not require skilled labor. Preliminary foundation preparation is unnecessary and the surface needs to be only reasonably level and smooth. No costly drainage provision is required since gabions remain porous even after years of use.

METHODOLOGY

It is difficult to analyze sinkhole collapse from a purely quantitative approach. The unique circumstances involved with this phenomenon preclude the utilization of a standardized methodology for design criteria. Early in the designing of remedial structures, one should consider whether to direct surface run-off into a doline depression or to circumvent the drainage in an attempt to prevent further hydraulic percolation. This is clearly a complex process and should be comprehensively evaluated using every available resource. Once the decision is made, however, the following approaches may assist the planner in rectifying an otherwise challenging problem through the use of gabions.

GABION PROTECTION FOR OPEN SWALLETS

When preparing a sinkhole to allow the draining of surface run-off in order to prevent flooding, the goal one should strive for is preventing the obstruction of the primary areas of infiltration. For large open sinkholes, such as cave entrances in urban environments, the major problem seems to be litter. Cave openings clog rapidly with an influx of brush, grass clippings, plastic milk jugs, and styrofoam cups. Maintenance becomes a nightmare.

Consideration should be given to protecting the throat of the open swallet with a gabion trash rack built in a star-shaped configuration. This design will increase the gabion surface and, therefore, its permeability. The average surge of debris-laden run-off can be calculated, and a wall can then be designed high enough to retain the debris and prevent clogging. Maintenance then becomes a routine litter pickup. (Figure 1) Drainage channels and streams supplying run-off to sinkholes can be treated for debris and sediment with a series of weirs and check dams. (Figure 2) A gabion weir allows surface run-off to permeate it at a slow rate. The "mini retention pond" created efficiently traps trash, leaves and debris which would otherwise reach the throat of the sinkhole threatening closure. As a weir, it slows the velocity of the surface discharge permitting increased infiltration as well as allowing deposition of silt and clay. Since gabions are permeable, low flows are allowed to completely drain through toward a natural drainage course. (Figure 3)

I. CASE 1 WESTWOOD APARTMENT COMPLEX, KNOX COUNTY, TENNESSEE

In 1979 the design and construction of a stormwater detention system and sinkhole drainage was proposed for the Westwood Apartment Complex in Knox County, Tennessee. This was an almost total urbanization of the natural watershed which drained into an open swallet sinkhole. This was designed in accordance with Knox County Stormwater Ordinance # 6191.

A. Geologic Description

The site is underlain by the Newala Formation of the Knox group. The rock type can best be described as a light grey, fine-grained dolostone. It weathers to a buff-grey or cream-white color. The rock units trend to the northeast but are overridden to the south by the Saltville Fault. The soil/rock interface is often irregular with rock pinnacles at isolated locations.

The formation is a thick soil former in East Tennessee, so

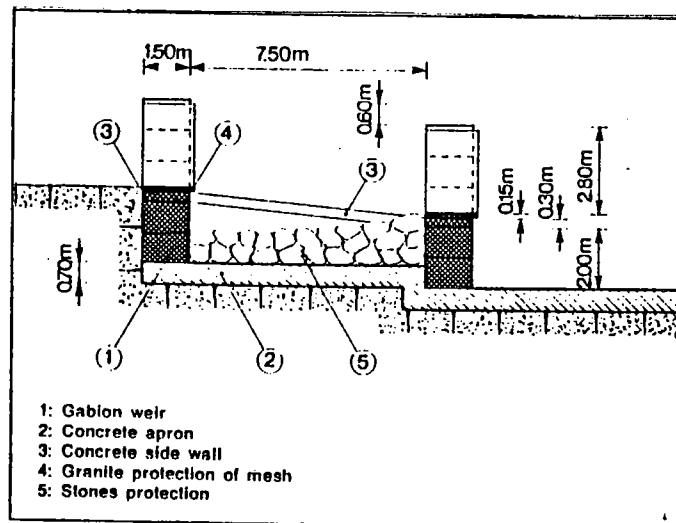


FIGURE 1
TYPICAL GABION DROP STRUCTURE

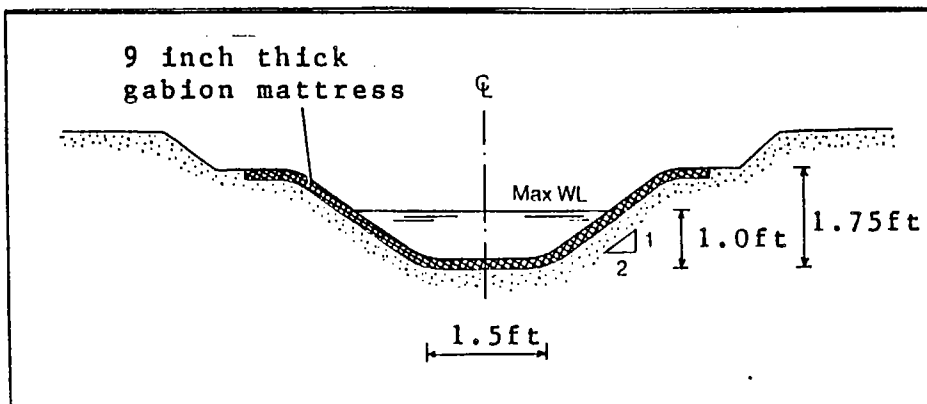


FIGURE 2

TYPICAL CHANNELIZED WATER COURSE

SCHEMATIC OF GABION WEIRS AND DROP STRUCTURES

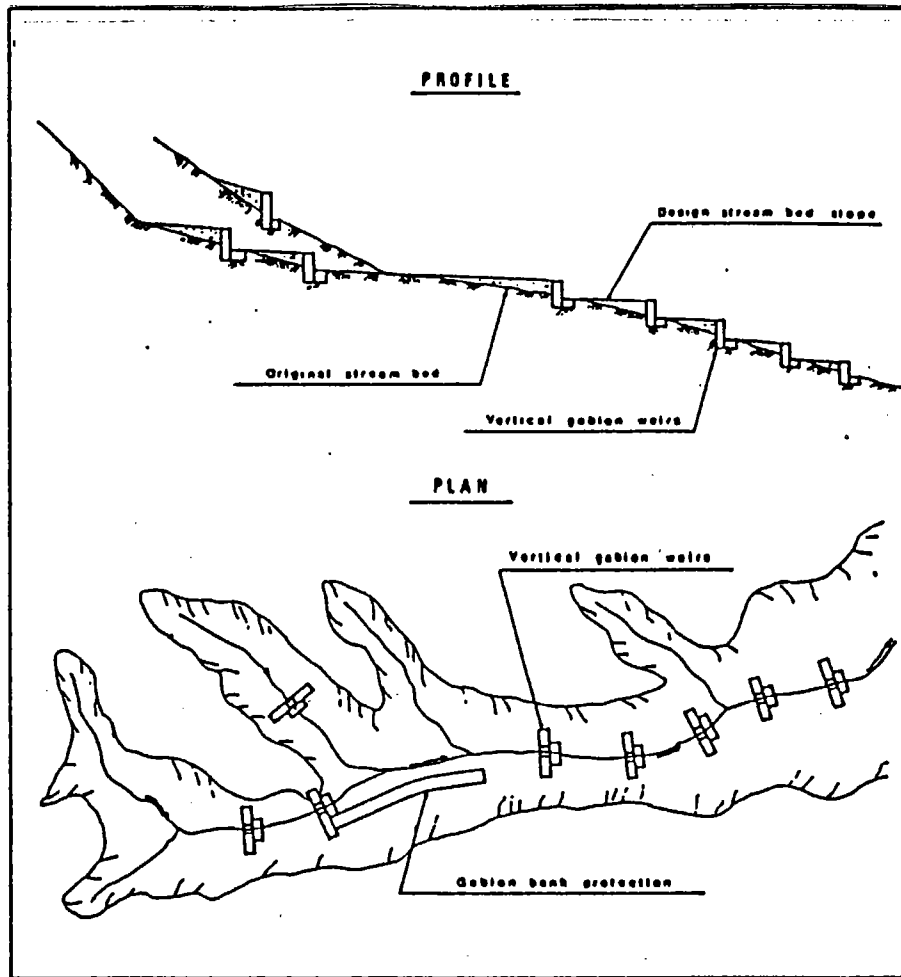


FIGURE 3

Plan and profile of gabion training works along Mountclair Gully.
(Ciarla, 1985)

it was doubtful that bed rock would be encountered during excavation. However, there was a possibility of encountering rock pinnacles which are more common in the proximity of the sinkhole structures. The residuum is characteristically a red plastic clay with moisture content increasing with depth. The U.S. Department of Agriculture classifies and labels the soil as Fullerton series, and Dewey silty clay loam (in the proximity of the sinkhole). The site falls within the "rolling-to-hilly phase" and is described as a "red, cherty clay having patchy clay films and sub-angular, blocky structure". The soil units are very strongly acid, with a moderate-to-slow permeability in the clay phases and moderate permeability in the sandy loam phase. This soil has a moderate-to-great erosional characteristic. Great care was taken during the construction phase not to expose the sink hole drainage discharge system to excessive soil infiltration.

B. Drainage Evaluation

The building site was partially drained by a normal dendritic, intermittent stream and partially by subsurface means. There were two forms of subsurface drainage present, percolation through the soil to the water table, and direct drainage through a sinkhole located adjacent to an old barn on the site. This was an active sinkhole with evidence of open subsurface cavities existing at depth. It was apparent that at one time the sinkhole had drained a much larger acreage than it does today. Due to stream piracy in that area, it had not been draining the volume it was capable of handling.

It was possible to increase the infiltration of the existing sinkhole with a variety of techniques which would enhance the drainage of the building site. Using a combined design program for discharge, catchment basin and settling ponds, storage areas and proper construction procedures, the existing sink hole would be able to drain the run-off of the housing project to the extent needed.

All hydrology work will be referenced by "Urban Hydrology for Small Watersheds", technical release number 55, USDA Soil Conservation Service as recommended by the Knox County hydrologist.

C. Overall Methodology for Drainage Stabilization

The following are some considerations which were adhered to for normalization and stabilization of hydrologic parameters during and after construction of the project. The methods for controlling surface run-off and peak discharge into the existing drainage patterns were two-fold. First, it was expected that planned run-off delay for sediment entrapment would aid in keeping stream loading to a minimum during construction. Some of these procedures would also reduce peak discharge after project completion. Second, these devices would incorporate a design that would also reduce the volume of water entering the present watershed. This was done by physically increasing the subsurface

drainage rate through the active sinkhole existing on the property and by increasing the infiltration rate of the run-off.

The above were accomplished through the development of gabion drop structures, to entrap run-off, and contoured gabion-lined ditches. This rapidly retarded down-slope water migration. The peak discharge was channeled into a detention basin for sediment settling, prior to flowing into the sinkhole, and was disposed of by subsurface means. The volume of water drained into this natural subsurface drainage system considerably lessened the hydrologic discharge that was plaguing the area.

D. Sinkhole Drainage and Detention Basin

The sinkhole located at elevation 1004 had to be prepared prior to the introduction of any run-off from its planned watershed. This meant that, prior to any land disturbance, the sinkhole had to be protected from silt and debris which might seal the opening and clog the hole. It was imperative that during construction mud-laden water not be allowed to run freely into it. In order to assure that the sinkhole was protected from siltation, these precautions were taken. (Figure 4)

- 1) The active part of the sinkhole was cleaned out until it was empty and clear of all trash. Heavy equipment operation was restricted so as to preserve as much of the vegetative cover as possible around the sinkhole.
- 2) An eight-foot-high chain link cyclone fence, with barbed wire on top, was built around the circumference of the opening. This was placed just outside the tree line. A gate was included in the fence for access.
- 3) At the base of the fence bales of straw were tied to the fence and staked to the ground. These bales acted as a filter during construction for sediment and trash and, therefore, had to form a continuous barrier around the fence. (Figure 5)
- 4) A gabion berm with coarse stone riprap was placed a minimum of ten (10) feet from the fence. The berm was three (3) feet high and connected to contour. This slowed the speed of the run-off and "strained" the water of particulates.
- 5) Enlargement of the semi-circular depression to the north of the sinkhole acted as an impoundment area and settlement basin for the run-off. This detention basin now has a capacity of 90,000 cubic feet, with the approximate dimensions of 120 feet x 150 feet x 5 feet deep. It opens to the south by a berm of gabions and riprap stone. This berm had to be one foot higher in elevation than the sinkhole berm and had to drain into

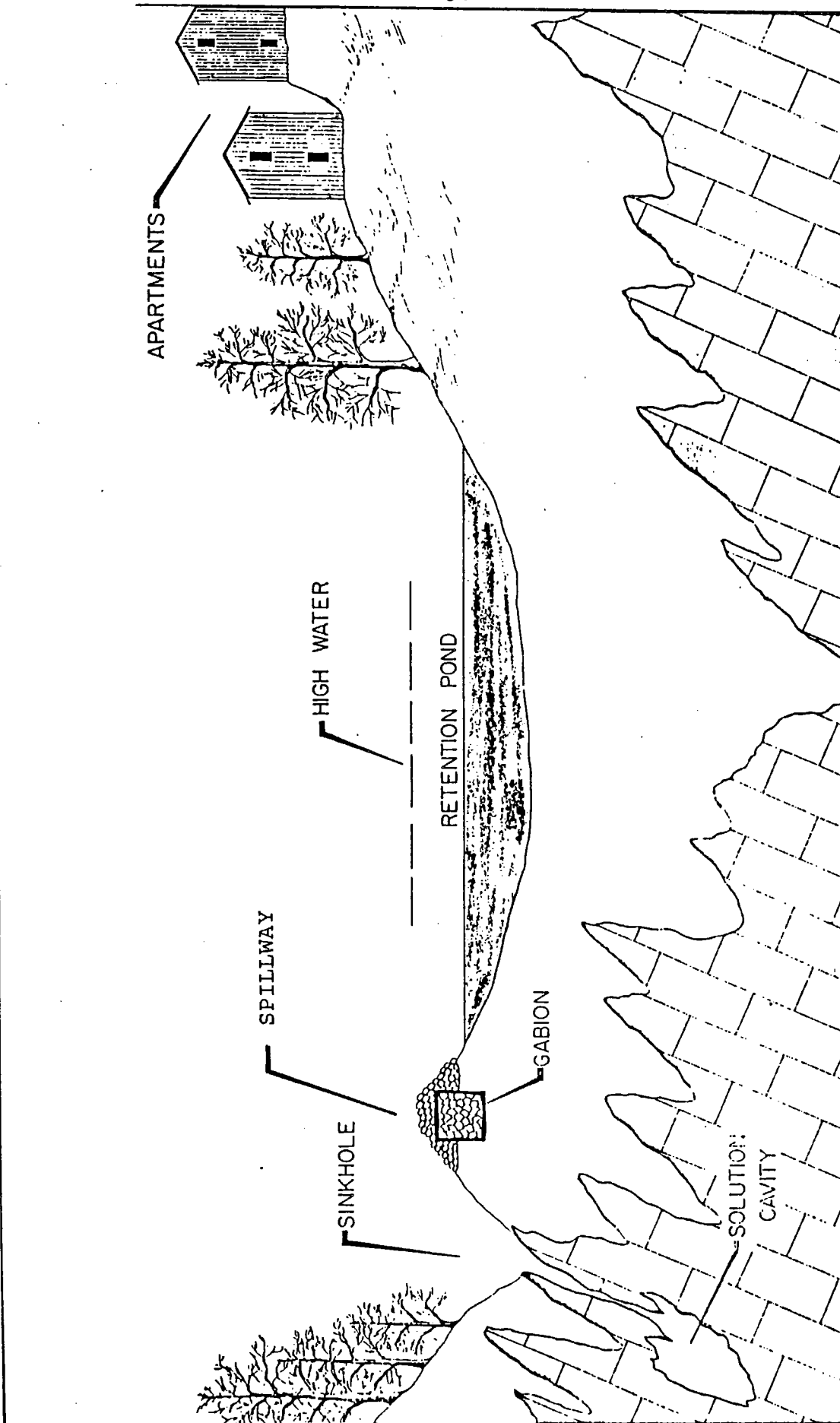


FIGURE 4

SCHEMATIC CROSS SECTION OF CASE HISTORY II

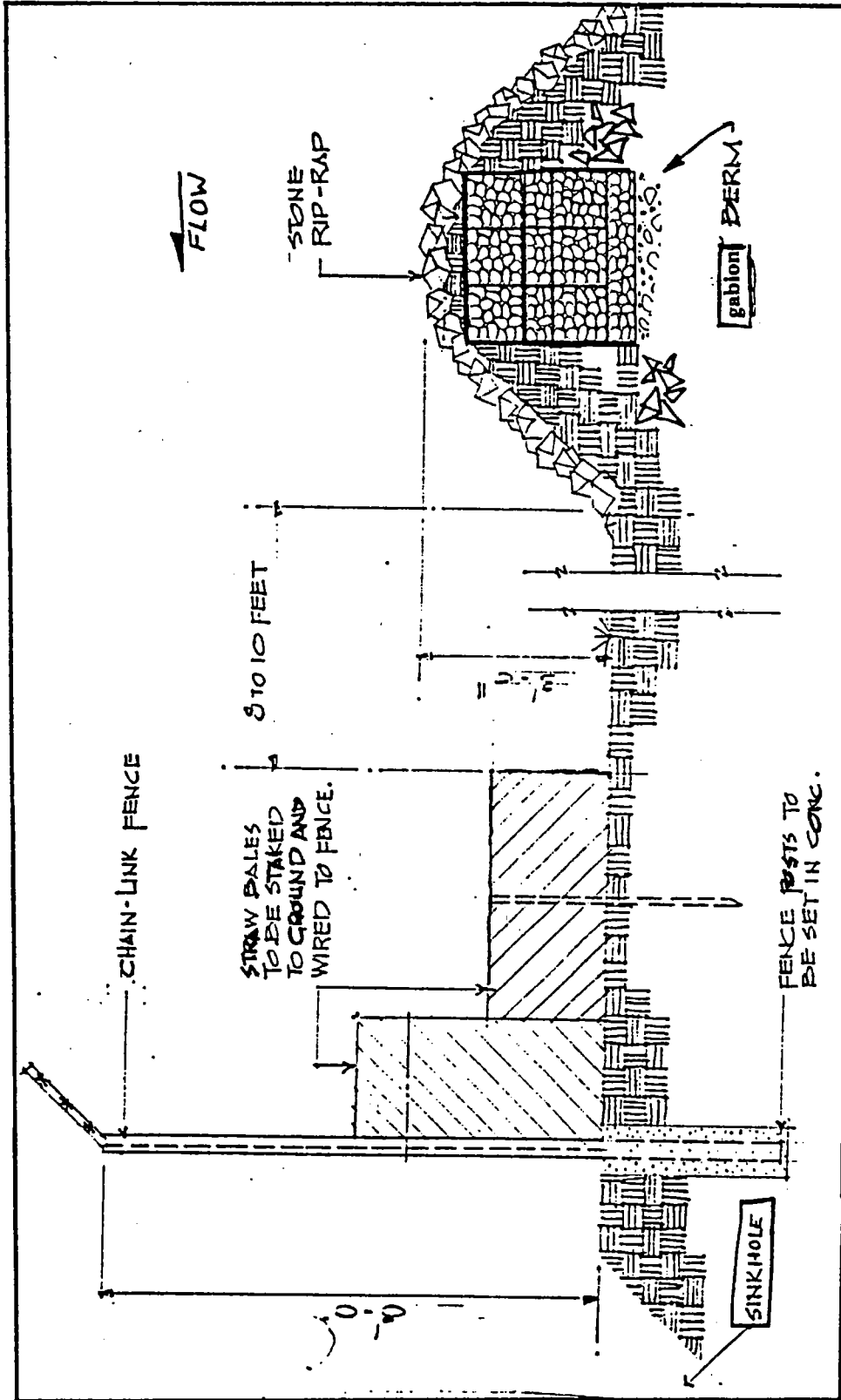


FIGURE 5 - GABION BERM

the area protected by it.

The retention basin embankment to the east was kept at elevation 1012 making it impossible for water to rise above this contour and endanger the structures. In case of temporary sinkhole stoppage, or an unprecedented rainfall over 6 inches, the intermittent stream to the east below the level of the retention basin will carry off the overflow water into the natural drainage. This watercourse was channelized with 9 inch thick gabion mattresses to slow water velocity. A vegetative cover will eventually overgrow these watercourses.

II. CASE 2 I-640/I-40 INTERCHANGE, KNOXVILLE, TENNESSEE

The location of the project covered by case history II centers along the I-640/I-40 interchange on the east side of Knoxville, Tennessee. The subject interchange, originally constructed over 20 years ago and reconstructed in 1981-82, has a drainage area of just over 16 acres which is funneled into a sinkhole along the eastern side of the interchange. (Figure 6)

Prior to the reconstruction in 1981, siltation and debris-laden run-off had sufficiently clogged the sinkhole receiving the run-off to cause flooding on adjacent private property. The flooding was also damaging an adjacent roadway embankment and becoming a very serious maintenance problem.

During the reconstruction of the interchange, it was decided to try to alleviate the drainage problem that existed at the subject site. At that point, a geotechnical investigation was requested.

The results of the investigation indicated that all of the run-off within the 64,752 square meters (16 acres) of the interchange was being directed into a very small swallet about 1 meter in diameter. Twenty-four-hour precipitation rates of 1 inch or more caused considerable flooding around the subject sinkhole. The flood waters then moved onto adjacent private property and entered another much larger swallet some 6.5 meters (20 feet) in diameter. (Figure 7)

It was disclosed from the field investigation that a lineament of 5 sinkholes had developed along the strike of the Holston Formation (with the first sinkhole being the subject, silt-clogged swallet). Some 300 meters east of the subject swallet the groundwater re-emerged as a spring which fed into near-by Love's Creek.

The Holston Formation, which is exposed in the larger swallet, is Middle Ordovician, bryozoan reef complex and consists of massive beds of coarse-grained bio-sparite with cross-bedded reef-flanks of fine-grained sparite. In the Knoxville area the

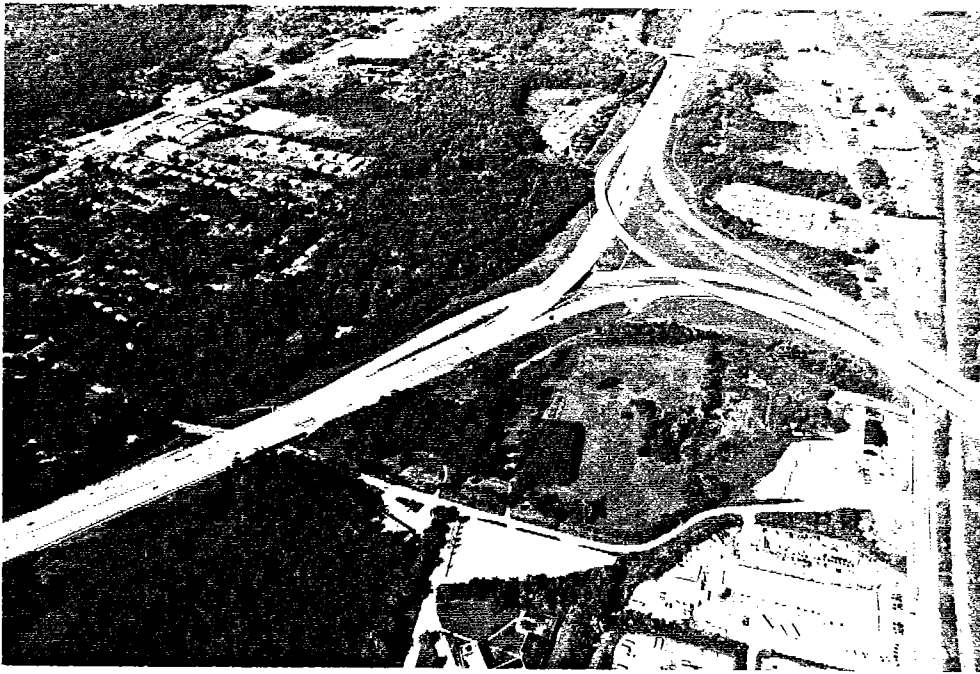


FIGURE 6

Run-off from this interchange is being funneled into a series of sinkholes present in the Holston formation.



FIGURE 7

This photograph shows heavy run-off flowing into the larger of the swallets being used as drainage facilities for the I-640/I-40 interchange in east Knoxville.

Holston Formation has undergone intense solution producing numerous cave systems and typical surface karst features. A number of the karst problems associated with engineering projects in the Knoxville area are found within the bounds of the Holston Formation.

It was decided to utilize the concept of 'swallet cleanout and protection' as a remedial measure for correcting the subject problem. In addition a paved riprap ditch, a small retention pond, and a gabion protection wall were added.

The project began with the removal of silt and debris from the subject sinkhole. This procedure enlarged the sinkhole's dimensions to about 5 meters in diameter and about 3.5 meters deep. (Figure 8) This enlarged sinkhole was to act as a retention pond and siltation basin for heavy run-off situations. Lighter amounts of precipitation were to flow into the swallet opening.

An overflow channel was constructed from the subject sinkhole to the large adjacent sinkhole. This feature enabled heavy run-off to flow freely into the large sinkhole which could adequately handle the flow.

The gabion protection wall was constructed between the initial swallet and the 'overflow' swallet. (Figure 9) The purpose of the gabion wall was to protect the swallet from debris and excessive siltation generated during flooding conditions. The permeability of the gabion wall permits trash and other debris to be filtered out while transmitting the water through the gabion wall and into the swallet. (Figure 10)

The initial swallet was cleaned out and enlarged to provide both a siltation and retention pond. The ditch leading into the swallet was concrete riprapped providing for energy dissipation and erosion resistance. (Figure 11)

At present run-off is channeled into the retention pond where most of the debris and silt are deposited. From there the runoff flows down a riprapped channel into the larger sinkhole. During flood conditions, high water is impeded by the gabion wall which acts as a filter for the debris-laden run-off protecting the sinkhole drainage facility. (Figure 12)

It is important to note that periodic maintenance of this facility is mandatory for the drainage system to function properly and to prevent flood damage to adjacent private properties.



FIGURE B

The initial swallet, as discussed in Case II, was enlarged to create a combination sedimentation/retention pond. The gabion wall was later constructed in the lower portion of the area shown in this photograph.



FIGURE 9

Construction of the gabion wall was performed by Region I maintenance personnel.

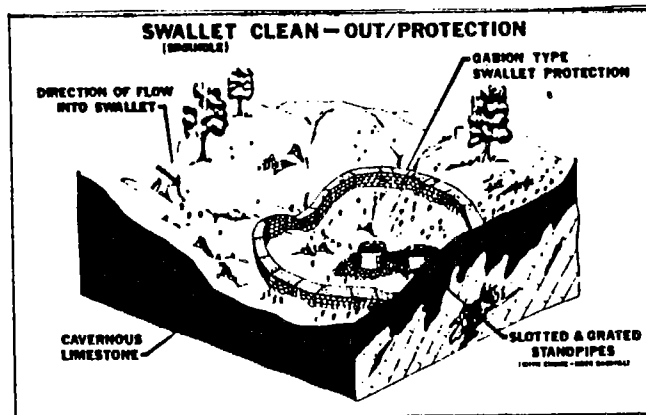


FIGURE 10

Schematic diagram illustrating the concept of swallet clean-out and protection. (Moore, 1984)



FIGURE 11

The riprapped concrete ditch is shown leading to the newly-constructed pond (in background).



FIGURE 12

The completed gabion wall provides erosion-free energy dissipation between the retention basin(to left) and the free-draining sinkhole to the right.

CLOSING REMARKS

In studying sinkhole case histories it is evident that no two sinkhole situations are the same. This requires creative thinking in the development of remedial design.

The utilization of existing karst features such as sinkholes and cave openings should be considered only after all other possibilities have been investigated. The effects of sinkhole use can be very detrimental if not adequately researched and designed (Royster, 1984 and Moore, 1980).

It is fundamental to the success of using karst features (as drainage facilities) that erosion, siltation, and blockage by debris do not occur. The cleanout of a swallet to provide adequate drainage into the subsurface requires the protection of the sinkholes and depressions from further blockage or damage.

It has been demonstrated that this can be adequately achieved through the use of small gabion barriers. Their permeability and flexibility provide gabions with a unique ability to adapt to varying karst conditions. However, it is not intended that the use of gabion structures will prevent the development of sinkholes and subsidence features, but that their use will assist in better utilization of these features as drainage facilities.

Finally, it is important to emphasize that a very accurate and complete geotechnical study of each sinkhole system (to be utilized) be considered a mandatory process. As commercial, industrial, and residential urban development continue to expand into karst areas, sensitivity to the resulting negative impact must be mandated by both the public/political process and the scientific community.

REFERENCES

- Amari, Dominick J., and Crowhurst, Alan D., 1984, Controlling Erosion with Gabions: Tennessee Public Works, v.1, no.6, pp.20, 21, & 28, March 1984.
- Ciarla, Massimo, 1985, Gabion Weirs in Water Erosion Control Projects Design and Construction Criteria: Conference XVI, International Erosion Control Association, February 21-22, 1985, San Francisco, California.
- Crawford, Nicholas C., 1984, Sinkhole Flooding Associated with Urban Development upon Karst Terrain: Bowling Green, Kentucky: First Multidisciplinary Conference on Sinkholes, Orlando, Florida, October 15-17, 1984.
- Kemmerly, Phillip R., 1981, Spatial Analysis of a Karst Depression Population: Clues to Genesis: Geological Society of America Bulletin, v.93, pp.1078-1086, November 1982.
- 1976, Definitive Doline Characteristics of the Clarksville Quadrangle, Tennessee: Geological Society of America Bulletin, v.87, pp.42-46.
- 1980, Sinkhole Collapse in Montgomery County, Tennessee: An Overview for the Planning Process: Environmental Geology Series No.6: Nashville, Tennessee, Tennessee Division of Geology.
- Moore, Harry L., 1984, Geotechnical Considerations in the Location, Design, and Construction of Highways in Karst Terrain... "The Pellissippi Parkway Extension", Knox-Blount Counties, Tennessee: First Multidisciplinary Conference on Sinkholes, Orlando, Florida, October 15-17, 1984.
- 1980, Karst Problems Along Tennessee Highways: An Overview.
- Royster, David L., 1984, The Use of Sinkholes for Drainage: 63rd Annual Transportation Research Board Meeting, Washington, D.C., January 16-20, 1984.
- Summers, Rebecca M., and Johnson, Robert E., 1982, Rock Durability Evaluation Procedure for Riprap and Diversion Channel Construction in Coal Mining Areas: Symposium on Surface Mining Hydrology, Sedimentology and Reclamation (University of Kentucky, Lexington, Kentucky, December 5 - 10, 1982).

ILLINOIS LANDSLIDE INVENTORY:
A TOOL FOR GEOLOGISTS AND ENGINEERS

MYRNA M. KILLEY, Associate Geologist
Environmental Studies and Assessment Unit

PAUL. B. DUMONTELLE, Geologist and Head
Earth Hazards and Engineering Geology Section

Illinois State Geological Survey
615 E. Peabody Drive, Champaign IL 61820

In 1982 the Illinois State Geological Survey undertook a project to inventory all known landslides in the state in order to better understand the hazard as it now occurs in Illinois. The project was partially funded by the U. S. Geological Survey and had three goals: (1) to produce a 1:500,000-scale map of the state showing the locations and types of known landslides in the state, (2) to compile a list of references of known publications on landslides in Illinois, and (3) to collect information on all known costs of damage and repair due to landslides in Illinois.

Because landslides in the Midwest are not spectacularly high or large compared with those in western states, they rarely result in loss of life. Only two types have resulted in or have the potential for loss of life: rock falls, and earth flows which occur at the toes of major slumps. The other types of landslides classified in Illinois generally do not have this potential.

Three Survey geologists--the two authors of this paper and Jennifer Hines--spent varying amounts of time over a one-year period to (1) search the literature and compile a bibliography; (2) categorize landslide types on the basis of available information, using a modified classification based on that of David Varnes (1978) of the U. S. Geological Survey; (3) create a landslide report form with supporting diagrams; (4) contact various agencies, including the Illinois Department of Transportation and the Soil Conservation Service (both of whom we acknowledge with gratitude for their generous assistance), for additional information; and (5) write a BASIC computer program facilitating storage and retrieval of landslide records by location or other criteria. Our present effort is to transfer the data set to the Survey's Prime 750 computer because of the availability of ARC/INFO, a relational data-base and Geographic Information System (GIS).

As a result of the information we compiled, Illinois landslides have been classified (Killey, Hines, DuMontelle, and Brabb, 1984; Killey, Hines, and DuMontelle, 1985) into the following six types: rock creep, rock falls, rock slumps, earth slumps on bedrock, earth slumps, and earth flows. These six types are described briefly below, along with explanations of some examples which are of more direct interest to highway geologists and engineers.

Rock creep is the least common type of landslide found in Illinois. Only one has been mapped to date, and it is in northwestern Illinois. It involves blocks of dolomite sliding very slowly down a gentle slope of shale. Downslope movement is so slow

that it is usually detectable only over a number of years. Obviously, this type of landslide poses little hazard to lives or property.

A rock fall involves free-falling rock from a steep bedrock bluff. Although the potential for loss of life is high, the frequency of occurrence is low, and its geographical distribution is limited primarily to the Mississippi River bluffs. A rock fall occurred in July 1972 along the river bluff road in southwestern Illinois. Large limestone boulders fell from the bluff to the county road below, knocking down some power lines and completely blocking the road. This landslide had both natural and man-made causes. Repeated cycles of freezing and thawing, which cause frost crystal growth to expand microcracks in the jointed limestone of the bluff over many years, resulted in gradual detachment of blocks of rock from the bluff face, which then toppled. Root growth in the joints also helped to force the blocks apart and allowed water and debris to infiltrate. However, borrowing for roadway construction removed some of the underlying support for the bluff and was probably the precipitating factor in this rock fall. An examination of this same site 11 years later revealed that there had been little change in the bluff face, although there had been a great deal of vegetation growth below. Rock-fall type landslides tend to stay in their new state of equilibrium for a long time.

Information on cost of damages and repairs due to landslides in Illinois was available for 25 out of the total of 145 landslides mapped in the inventory. The total damage figure for all 25 landslides is about \$8.25 million; damage information was available for only 1 rock fall, and it came to \$30,000 in 1982 dollars.

An earth flow type of landslide refers to any flow of sand or other poorly consolidated earth material, regardless of the rate of movement. Earth flows occur fairly commonly as extensions at the toes of slumps. The other common occurrence of earth flows is as "skin slides," because they involve only the uppermost soil layer. They are particularly common along many of the major highways in Illinois where saturated surface soils seem to turn to a viscous liquid and flow downslope. Earth flows pose no hazard to life but are a great nuisance to roadway maintenance crews. It is our understanding that PAVER, a computer data-base management system, is being developed by civil engineers at the University of Illinois; this system will be used to monitor this and other kinds of problems and expense associated with highway construction and maintenance.

Damage information was available for only 4 earth flows, totaling nearly \$200,000 in 1982 dollars. Many more have been observed across the state for which we have no cost information.

The rock slump category refers generally to bedrock but can include overlying thin glacial material that moves with the rock unit. Again, because of the limited bedrock outcrop area in the state, this is not a common type of landslide, and the hazard to life is very low. Most of the rock slumps mapped were induced by removing the toe of the slope, and they are found mostly in roadcuts along the Illinois and Mississippi Rivers.

Available cost of damage information was available for 4 rock slumps, totaling more than \$600,000 in 1982 dollars.

The second most common type of landslide mapped is glacial material sliding on a bedrock surface, a type we called earth slump

on bedrock. This condition is found primarily along the Mississippi and Illinois Rivers but also may occur in any locality where the bedrock surface intercepts a slope on the land surface. This kind of slump usually occurs when water percolates through somewhat more permeable glacial material until it reaches a less permeable bedrock material such as shale. The accumulation of water at the interface increases the pore-water pressure and lubricates the contact, inducing slumping. The threat to life posed by this type of landslide is quite low. A large earth slump on bedrock along the Illinois River in central Illinois occurred in 1982. Its primary cause was probably clearcutting along the bluff for power lines to descend into the Illinois River valley. This allowed greater water infiltration and greater saturation of the glacial material. At the toe of this slump is an earth flow, in which the soil layer has curled over on itself, taking with it some young trees. A highway is located near the base of the bluff here. The highway in this region has experienced continual problems since its construction. An aerial view shows a stretch of highway along the Illinois River bluffs in north central Illinois. Most of the slumping in this area is glacial material sliding on underlying shale, and it is a natural phenomenon of the region. A bridge constructed in the same locality has shown evidence of continued activity.

Two-thirds of the landslides mapped in the earth slump on bedrock category were man-induced, and damage costs were available for 8 such slumps. Costs ranged from \$60,000 to \$2,220,000 in 1982 dollars.

Earth slumps--where glacial deposits are thick and failure planes occur within the glacial material--are the most common type of landslide found in Illinois. A common geologic situation implicated in earth slumps is one in which lenses of noncohesive sand contained in glacial till are exposed and flow outward, causing the overlying glacial material to lose support and collapse. Although the hazard to life is generally low, loss of life has occurred rarely in this situation. For example, at a site in southwestern Illinois, excavation for construction intercepted loose sand underlying thick loess. A young child playing at the site was killed when the sand flowed outward and the overlying loess collapsed. Another commonly occurring earth slump is that typified by a situation in west-central Illinois, in which a county road has been built into the side of a slope above the outside of a creek meander--the part of a creek bank most susceptible to removal of the toe by natural stream erosion. Two visits to the site three weeks apart revealed that the slumping in the creek bank had, in the space of these three weeks, extended into the roadway and considerably damaged it. This situation is probably rather typical of many roadways throughout the state, and road maintenance is probably the greatest loss from landslides in terms of money.

Cost of damage information was available for 9 earth slumps and accounted for over \$2,000,000 (in 1982 dollars) in damage and repair costs.

A site in western Illinois offers a good example of the necessity for combining the expertise of geologists and engineers in viable roadway design and maintenance. When we visited the site, we found that a county road had been built near the top of a hill occupied by a cemetery; a stream flowing at the base of the slope was

continually eroding the toe of the slope. The area had slumped several times over the years, as could easily be seen by the hummocky surface of the wooded hillside below the roadway. A local resident told us that the hillside had slumped 7 years ago; a scarp close to 10 feet high was still unvegetated from that episode. The current episode of slumping came to the outside edge of the county road skirting the cemetery. In order to bring the shoulder of the road back to road level, about 300 tons of limestone blocks were dumped at the top of the slump. Within 24 hours, the slope failed again, this time taking part of the road with it.

If engineers and geologists combining their expertise had examined this site together, they could have arrived at the understanding that slumping is a natural hazard of long standing at the site due to natural stream erosion. Had that been understood, the roadway might originally have been built in a less vulnerable position, or at least mitigation measures could have been undertaken to prevent the continual slumping and damage inflicted on the road. If such measures are not undertaken fairly soon at this site, the next such slump will not only damage the road again but will also start incorporating part of the land inside the cemetery.

We believe that the Illinois Landslide Inventory can serve as a tool to promote both better communication between the two professions in order to help prevent this kind of situation, and greater understanding of the landslide hazard itself and measures available to mitigate it in Illinois.

LIST OF REFERENCES

- Killey, M. M., J. K. Hines, P. B. DuMontelle, and Earl Brabb. 1984. Illinois Landslide Inventory Map: Miscellaneous Field Studies Map MF-1691, U. S. Geological Survey. Scale 1:500,000.
- Killey, Myrna M., Jennifer K. Hines, and Paul B. DuMontelle. 1985. Landslide Inventory of Illinois: Illinois State Geological Survey Circular. In press.
- Varnes, David J. 1978. Slope Movement Types and Processes: in Krizek, R. J. and Schuster, R. L., eds., Landslides, Analysis and Control: National Academy of Sciences, Transportation Research Board, Special Report 176, p. 11-33.

WHO GETS SUED WHEN YOU SINK OR SWIM, AND WHY: LIABILITY FOR
SINKHOLE DEVELOPMENT AND FLOODING THAT AFFECTS HOMES, ROADS, AND
OTHER STRUCTURES

James F. Quinlan
National Park Service
Box 8
Mammoth Cave, Kentucky 42259

Structures built within the area of influence of a sinkhole can be affected by collapse, subsidence, or flooding. Unanticipated property losses may be involved; litigation commonly ensues. Insurance compensation for damages which are a result of sinkhole collapse or subsidence in a karst terrane are covered by statute only in Florida. Voluntary agreement of companies operating in Tennessee provides such coverage in homeowner policies. Liability or insurance compensation for damages which are a result of sinkhole flooding is not specifically covered by any state or federal statute, but several cities in Kentucky, Missouri, and Texas have adopted ordinances to regulate the causes of such flooding.

Claims for damages as a consequence of sinkhole development and flooding have been based on allegations of: negligence, breach of various water law doctrines, nuisance, loss of support, breach of contract, and implied warranty of habitability. Defenses against these allegations have been based on the merits of each of them and on caveat emptor. Alternative rationales are proposed and discussed by Quinlan (1986, p. 53-54).

Concepts of liability of the consulting professional are

evolving (Quinlan, 1986, p. 55; Walsh, 1985; Hughes, 1981). The courts are holding design professionals liable for negligent design, even when there is no privity of contract. Given both a foreseeable risk and a foreseeable victim, engineers have been held liable for flooding damages associated with bridges. I predict that the consulting geologist or engineer will have an increasing number of claims made against him or her which allege responsibility for sinkhole-related damages. Such damages can often be prevented by sound engineering, creative zoning, and better husbandry of land.

The extensive text of this paper has been published elsewhere (Quinlan, 1986). A relevant paper concerning liability of professionals, published after submission of the text, was written by Walsh (1985).

References Cited

- Hughes, L.N., 1981. The legal implications of the consulting relationship: Professional liability of consulting geologists in the urban environmental context, in Etter, R.M., ed., Houston Area Environmental Geology: Surface Faulting, Ground Subsidence, Hazard Liability. Houston Geological Society, Houston. p. 114-125.
- Quinlan, J.F., 1986. Legal aspects of sinkhole development and flooding in karst terranes: 1. Review and Synthesis: Environmental Geology and Water Sciences, v. 8, p. 41-61.
- Walsh, P., 1985. Consultant and regulator liability for landfill design failures: Madison Waste Conference (8th, Madison, Wisconsin, 1985), Proceedings, p. 160-172.

TIEDBACK WALLS STABILIZE TWO KENTUCKY LANDSLIDES

Thomas C. Anderson, P.E.
Design and Construction Manager
Schnabel Foundation Company
Cary, Illinois

and

William E. Munson, P.E.
Chief Civil Engineer
Kentucky Department of Highways
Frankfort, Kentucky

ABSTRACT

Two tiedback walls were built to stabilize landslides on Kentucky Highways. Both of these landslides were overburden/fill slides on the downhill side of the roadways. Driven H-piles with pile points, pressure-treated wood lagging with a drainage system behind, and corrosion-protected rock tiebacks anchored in the interbedded shales and limestones of the Kope/Eden Formation were utilized for both slide control walls.

This paper deals with the nature of the landslides, design, and construction of the tiedback walls, corrosion protection, tieback testing methods, performance monitoring results, and performance specification method.

INTRODUCTION

Tiedback walls were selected to stabilize two existing landslides along Kentucky highways. Both tiedback walls were constructed from the top down which enabled the support to be provided throughout construction without significantly disturbing the slide mass. As a result, highway traffic was not disrupted to any further extent while the walls were under construction.

An unstable landslide area was located on Kentucky Route 227 (Carrollton-Worthville Road in Carroll County) approximately eight miles southeast of Carrollton, Kentucky. The slide affected approximately 1000 feet of roadway and embankment between Station 234+25 and Station 244+25. A railroad track is located on the same hillside just below the roadway and must be periodically realigned due to the slide. Figures 1 and 2 respectively, show a photo of the slide area prior to stabilization and a plan for the section of KY 227 under consideration. Horizontal drains and relocation of the highway were also considered as corrective measures, but the 1000-foot-long by 14-foot-high tiedback wall was chosen as the most cost-effective solution.



Figure 1. KY 227 Slide Area Prior to Stabilization

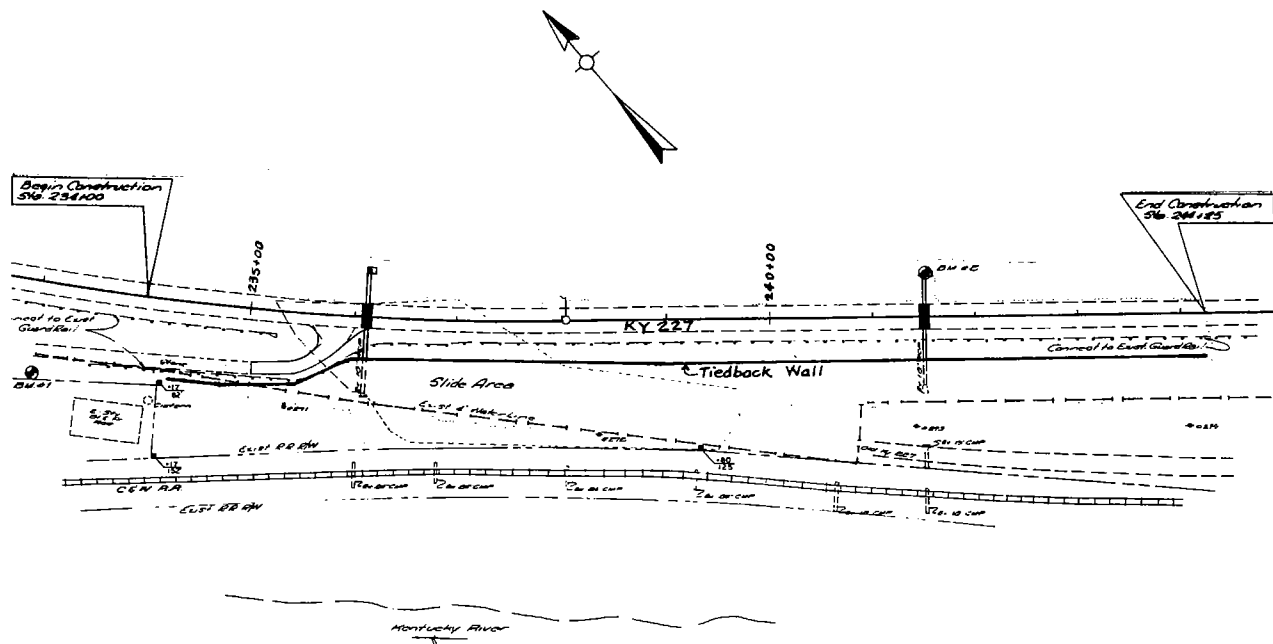


Figure 2. Plan for KY 227 Tiedback Wall

Originally, a berm with a shear key was considered, but had the disadvantage of having to wait for the summer dry season for construction along with the risk of losing the remaining two traffic lanes as the toe excavation was undertaken. As a result, a 360-foot-long by 20-foot-high tiedback wall was selected for the landslide stabilization.

GEOLOGY

The two slide areas are both located in the northern part of the outer Bluegrass topographic region of Kentucky. The rocks encountered in the area are predominately interbedded limestone and shales of Ordovician Age. The main rock formation in the region is the Kope Formation, a problem maker, well documented in engineering and geological literature. The shale is a clay shale subject to rapid disintegration when exposed to air and water. This shale is locally known as Kope or Eden Shale.

At both sites, the surface soils consist of clay fill resulting from the roadway cut/fill operations. The thickness of the fill varies from five to ten feet on the KY 227 slide to 20 to 30 feet on the U.S. 27 slide. The fill is underlain by moderately plastic residual overburden, developed from the underlying bedrock. Both the fill and overburden typically consist of brown clay with fragments and floater slabs of limestone. The underlying bedrock consists of horizontally bedded, layered shale with intermittent thin fossiliferous limestone layers. Brown-weathered shale predominates within the upper five feet of the rock, then transitions to essentially unweathered gray shale below. At the KY 227 site, the bedrock contained approximately 25 percent limestone, whereas at the U.S. 27 site, the limestone percentage was in the 30- to 35-percent range.

DESIGN

For the KY 227 slide, the slide depth varied between 15 to 25 feet. The design lateral pressure on the tiedback wall was developed utilizing the following soil strength parameters: $\bar{c} = 0$, $\phi = 18^\circ$ (residual friction angle), which resulted from back-analyzing the existing slide. Once the required stabilizing force was developed, it was divided by the slide depth and distributed on the back of the wall as either a uniform or trapezoidal pressure diagram. Figure 5 shows a cross section of the wall at Station 236+00 with the indicated design pressure diagram. The resulting tiedback wall design consisted of HP10x42 and HP12x53 piles at roughly eight-foot-on-center supported by two levels of rock tiebacks with design loads in the 90- to 175-kip range.

On the U.S. 27 project, the maximum slide depth was 35 feet. At this location, the design wall pressure was based on strength parameters of $\bar{c} = 0$ and $\phi = 16^\circ$ and on the fact that the final berm in front of the wall was stable and thus, provided passive resistance to the portion of wall below the 20-foot depth. As a result, HP12x53 and HP12x74 piles at approximately 7.5 feet-on-center supported by two tiers of rock tiebacks having design loads of 120 to 155 kips was utilized. A section of the wall at Station 246+50 is shown in Figure 6.

In December 1983, a landslide took out two of the four lanes of U.S. 27 south of Cold Springs in Campbell County, Kentucky. An approximate 360-foot length of roadway was affected between Stations 244+44 and 248+04. A photo of the slide area along with a plan of this section of U.S. 27 are contained in Figures 3 and 4.

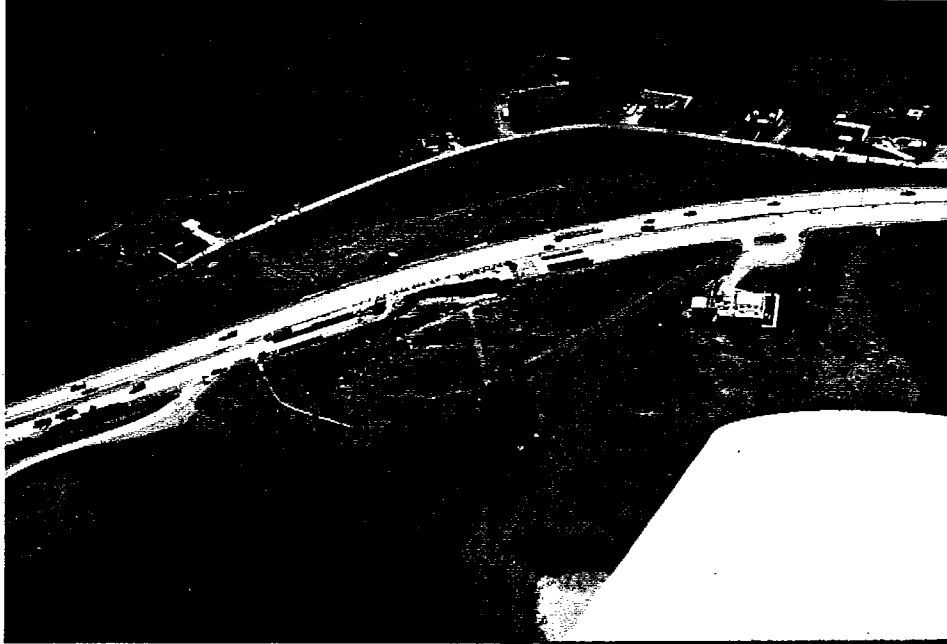


Figure 3. U.S. 27 Slide Area Prior to Stabilization

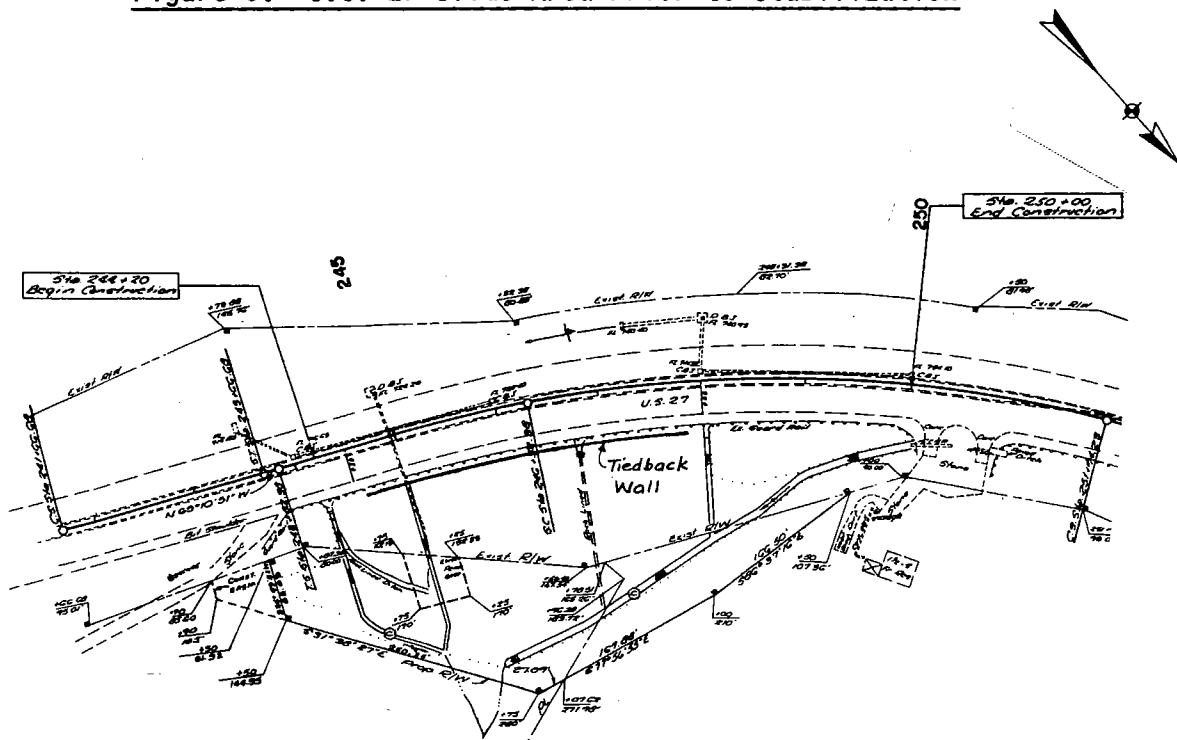


Figure 4. Plan for U.S. 27 Tiedback Wall

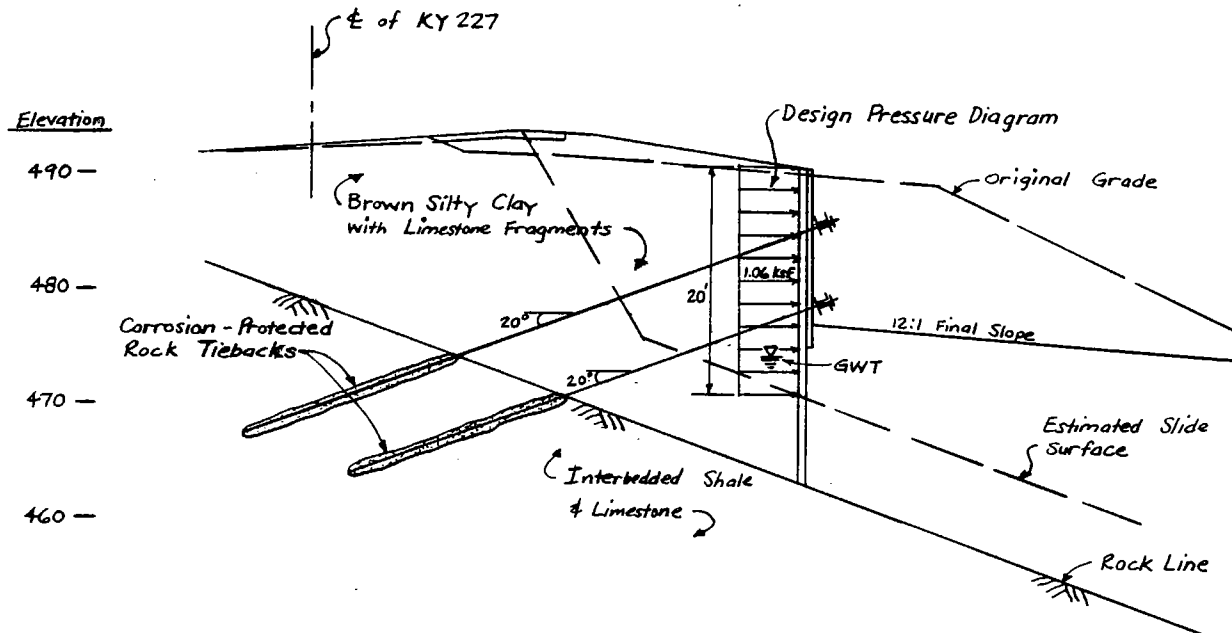


Figure 5. KY 227 Section at Station 236+00

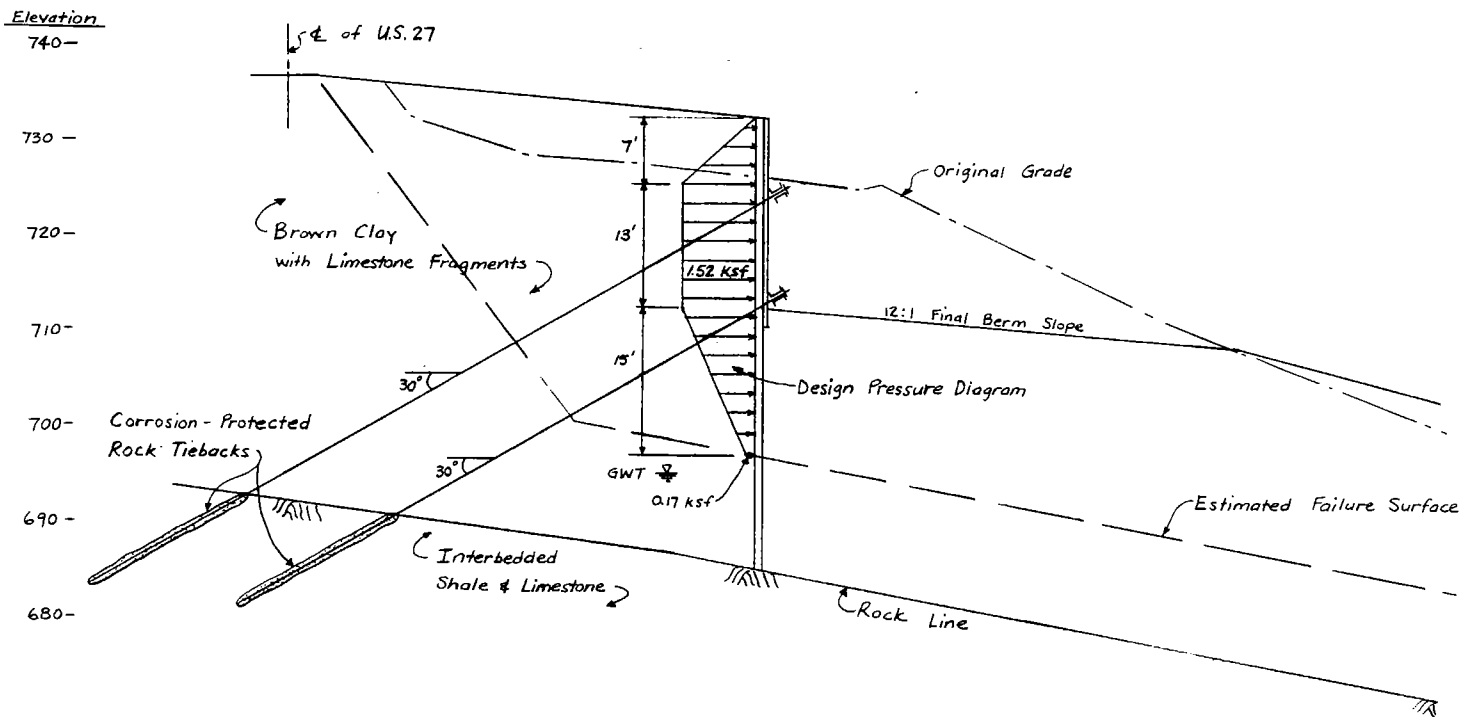


Figure 6. U.S. 27 Section at Station 246+50

A typical wall section for both projects is shown in Figure 7. As can be seen, the earth between the vertical H-piles was temporarily and permanently supported by four-inch-thick pressure-treated wood lagging fastened to the piles with threaded studs, nuts, and plates. CCA preservative treatment was used and the lagging consisted of Southern Pine, Dense Select Structural grade. Behind the wood lagging against the soil cut face, a prefabricated drainage material was installed. This drainage material consisted of an Amoco filter fabric against the soil surface which allowed water to pass while filtering and retaining the soil particles. Against the filter fabric, a Tensar drainage mesh was placed so that water would flow vertically behind the lagging into an eight-inch diameter perforated, corrugated plastic pipe collector drain at the base of the wall. Outlet drains running perpendicular to the wall were provided to direct the water collected at the base outward away from the wall to a point where the outlet drains daylighted on the final slope.

External walers, consisting of two channel sections placed back-to-back with spacers in between, transferred the load from the tiebacks to the soldier beams. For long-term protection of the exposed steel, the face of the H-piles, wales, brackets, lagging plates, studs, and nuts were covered with a Tapecoat TC Mastic protectant applied in the field.

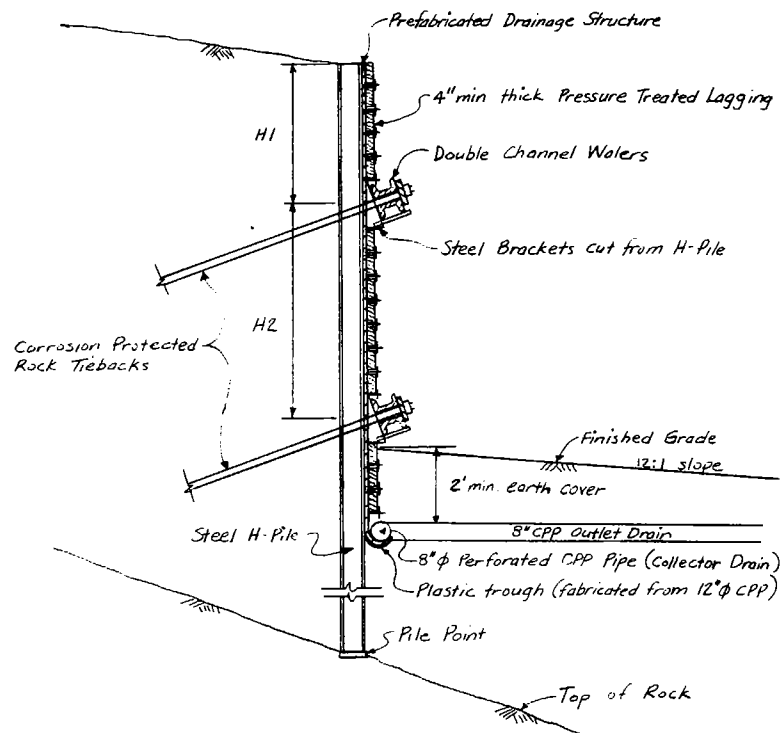


Figure 7. Typical Wall Section

TIEBACK CORROSION PROTECTION

Based on the results of chemical tests on the rock and groundwater, simple corrosion-protected strand tiebacks were utilized as shown in Figure 8. For this purpose, PIC Polystand Tendons were employed, consisting of seven-wire, 270-ksi-grade, high-tensile steel strand coated with a corrosion inhibitor and

an extruded polypropylene sheath over the unbonded length of the tendons. In the anchor length, protection was provided by the cement grout around the tendon. Combination spacer-centralizers spaced at five-foot-on-center were utilized in the anchor length to maintain a minimum 0.5-of-an-inch grout cover.

The critical area of the tendon below the bearing plate was protected by a steel trumpet filled with an anti-corrosive grease as illustrated in Figure 8. In order to interrupt potential long-line differential aeration and stray-current corrosion systems, electrical isolation was provided by an insulation pad below the bearing plate.

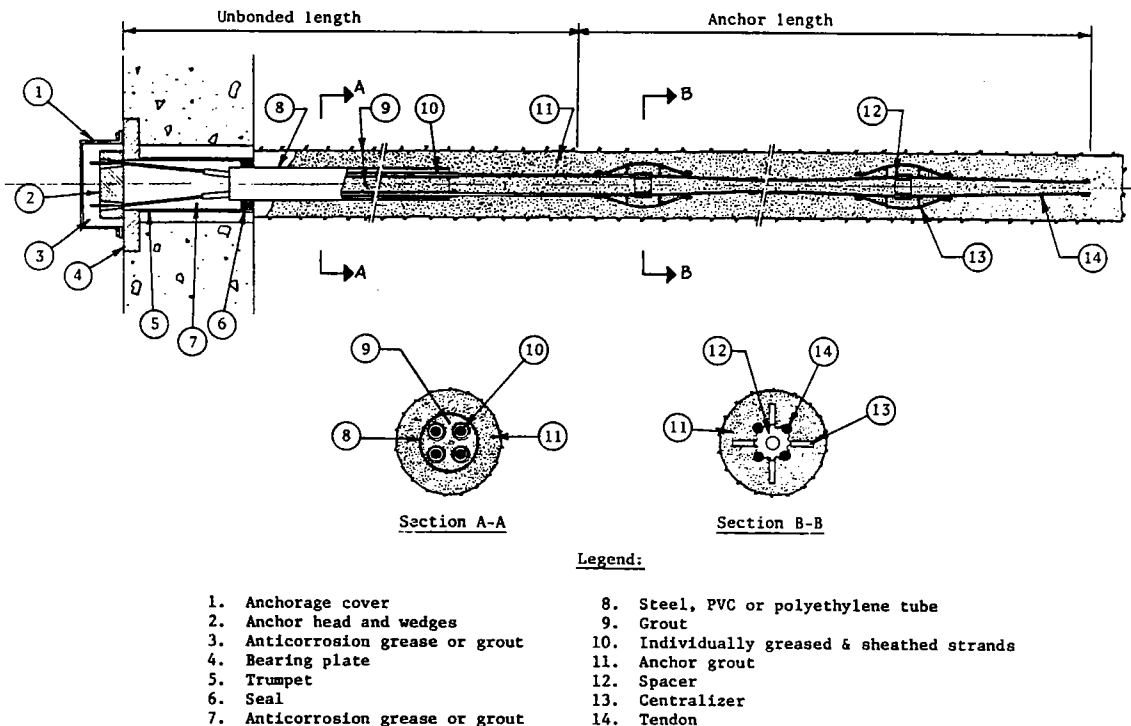


Figure 8. Simple Corrosion-protected Strand Tieback

CONSTRUCTION

The soldier piles for both walls were driven with pile points using a diesel pile hammer. In order to penetrate the overburden and to seat the piles on hard rock, a final driving resistance of 100 tons by the Engineering News Record formula was specified.

A large Gardner-Denver air-track drill was employed to percussive-drill uncased tieback holes. After a five-inch diameter hole was advanced to the intended depth, a grout tube was used to tremie-grout the hole from the bottom until clean grout emerged at the surface. Finally, the tendon was inserted into the grout-filled hole.

On the U.S. 27 project in Campbell County, the slide was very active and continued to move during the winter and spring of 1984. By the time the H-piles were driven in May 1984, the height of the scarp had increased to ten feet or more. No detectable movement occurred during or immediately after the pile driving. However, following three straight days of rain over Memorial Day weekend, the slide started moving again and displaced the central section of the wall H-piles 1.2 to 1.8 feet downslope before the upper tier of tiebacks could be installed and stressed. As a result of the continued slide movements, the upper tiebacks had to be stressed in stages as compacted fill was placed behind the wall.

During drilling of one of the upper tiebacks in the eastern portion of the U.S. 27 wall, a buried pipe was hit at a depth of 25 feet and a considerable flow of water resulted. This pipe was apparently part of a drainage system for the original two-lane highway, which was covered over by the embankment fill on the north side of the road when it was widened to four lanes. It appears that no outlet was provided at that time for the drainage system. Once the water pressure was relieved by the above-tieback drill hole, it was noted that the project observation walls showed a ten- to 15-foot drop in the water table. As a result, three horizontal drains were installed to provide an outlet for this buried drainage system.

Figures 9 and 10, respectively, show photographs of the completed tiedback walls for the KY 227 and U.S. 27 projects.

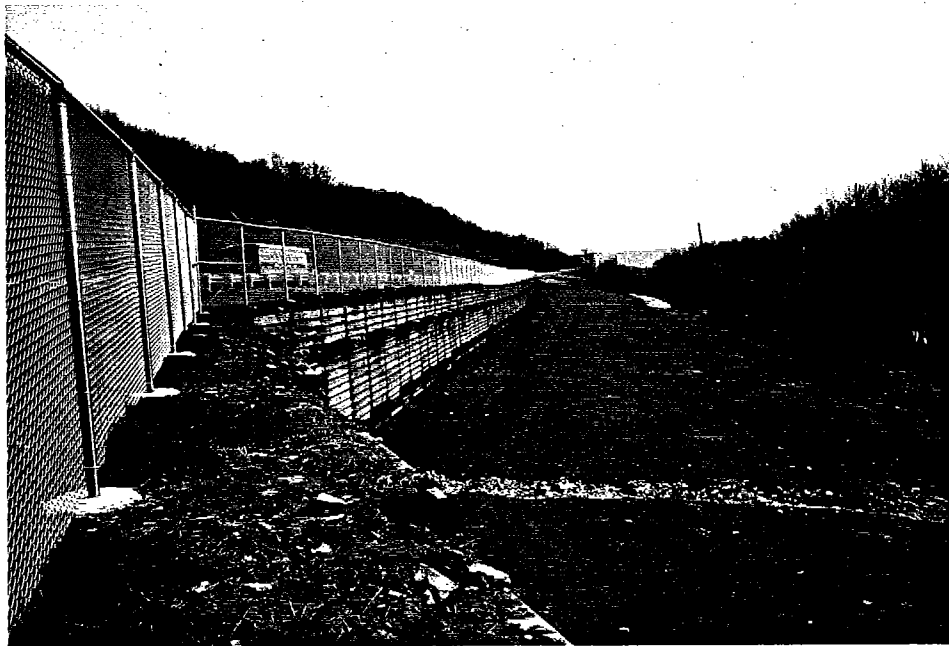


Figure 9. KY 227 Completed Tiedback Wall

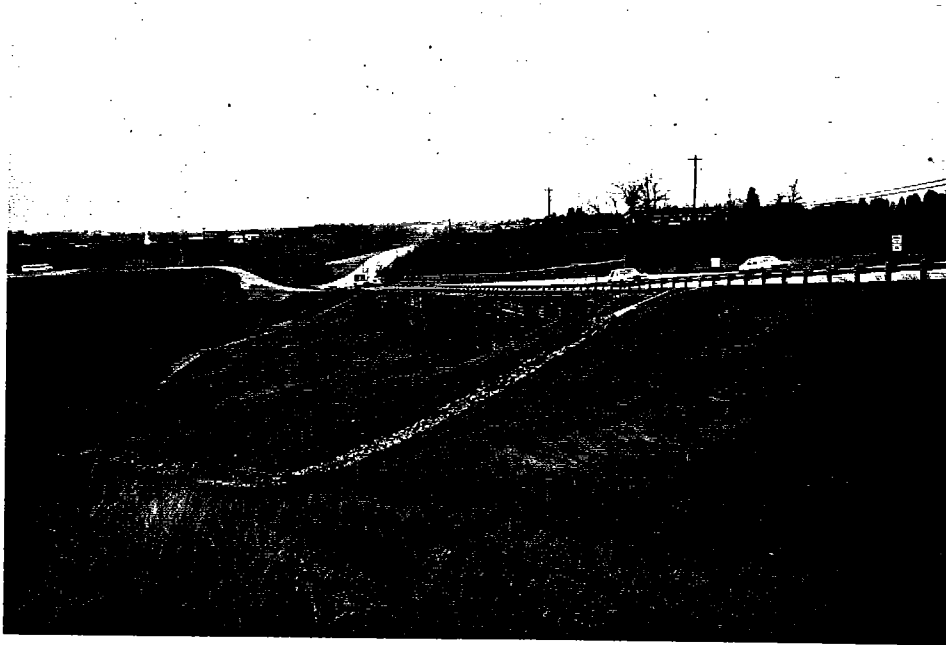


Figure 10. U.S. 27 Completed Tiedback Wall

TIEBACK TESTING

All of the tiebacks were tested to verify that they would carry the design load without excessive movement. Three types of tests were performed: performance, proof, and creep. For each of these tests, a calibrated hydraulic jack and pump were used to apply the load and an Ames Dial gauge mounted on an independent tripod was utilized to measure the movement of the tendon to the nearest 0.001-of-an-inch.

At least four tiebacks on each wall were creep tested. During the creep performance test, the tieback was incrementally loaded and unloaded up to a maximum of 133 percent of the design load. Each load increment was held constant using an electrical resistance load cell for ten to 60 minutes, with the exception of the final load which was held for 300 minutes, and the elongations recorded. Figure 11 shows the plot of one of the creep performance tests. The upper graph in this Figure shows the total tieback movement as a function of load, while the lower graph shows the residual movement of the anchor as a function of load. The residual movement (permanent set) of the anchor is the nonelastic or unrecoverable movement of the anchor which is measured when the load is released after each loading increment.

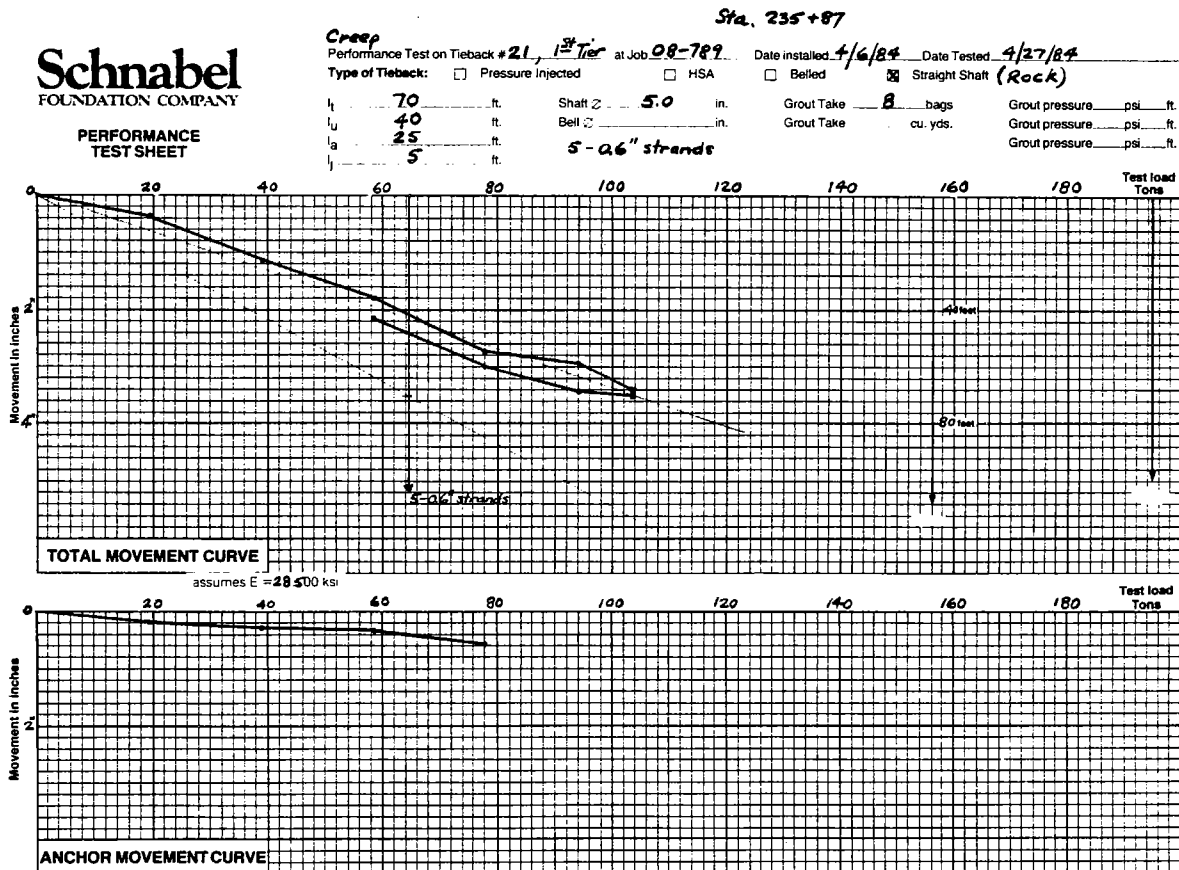


Figure 11. KY 227 Creep Performance Test

The graph in Figure 12 shows the plot of creep movement versus time on a semi-logarithmic graph, with each curve representing the creep movement at each load increment. The criteria for acceptance was that the creep movement plots had to be approximately straight lines or concave downward with a creep rate less than 0.08-of-an-inch per log cycle of time. This creep rate would produce a creep movement of approximately 0.5-of-an-inch over a period of fifty years.

Five to ten percent of the remaining tiebacks were performance tested. The performance test used the same incremental loading and unloading procedure as the creep test, except that only the maximum load was held constant. The tieback was considered acceptable if the movement during the ten-minute load-hold was less than 0.04-of-an-inch, otherwise the load had to be maintained for 60 minutes so that a creep curve could be plotted.

The remaining tiebacks were proof tested by measuring the load applied to the tieback and its movement during incremental loading to a maximum of 120 percent of the design load. The maximum load applied during the proof test was held constant for five minutes and the tieback movement recorded. If the movement during the five minute observation period was less than 0.03-of-an-inch, the test was discontinued. If the movement exceeded 0.03-of-an-inch, the load was maintained until a creep rate could be determined and compared to the creep tests.

The tiebacks on both projects which failed to meet the above-testing procedure indicated an ultimate bond stress between the grout and rock of 23 to 42 psi.

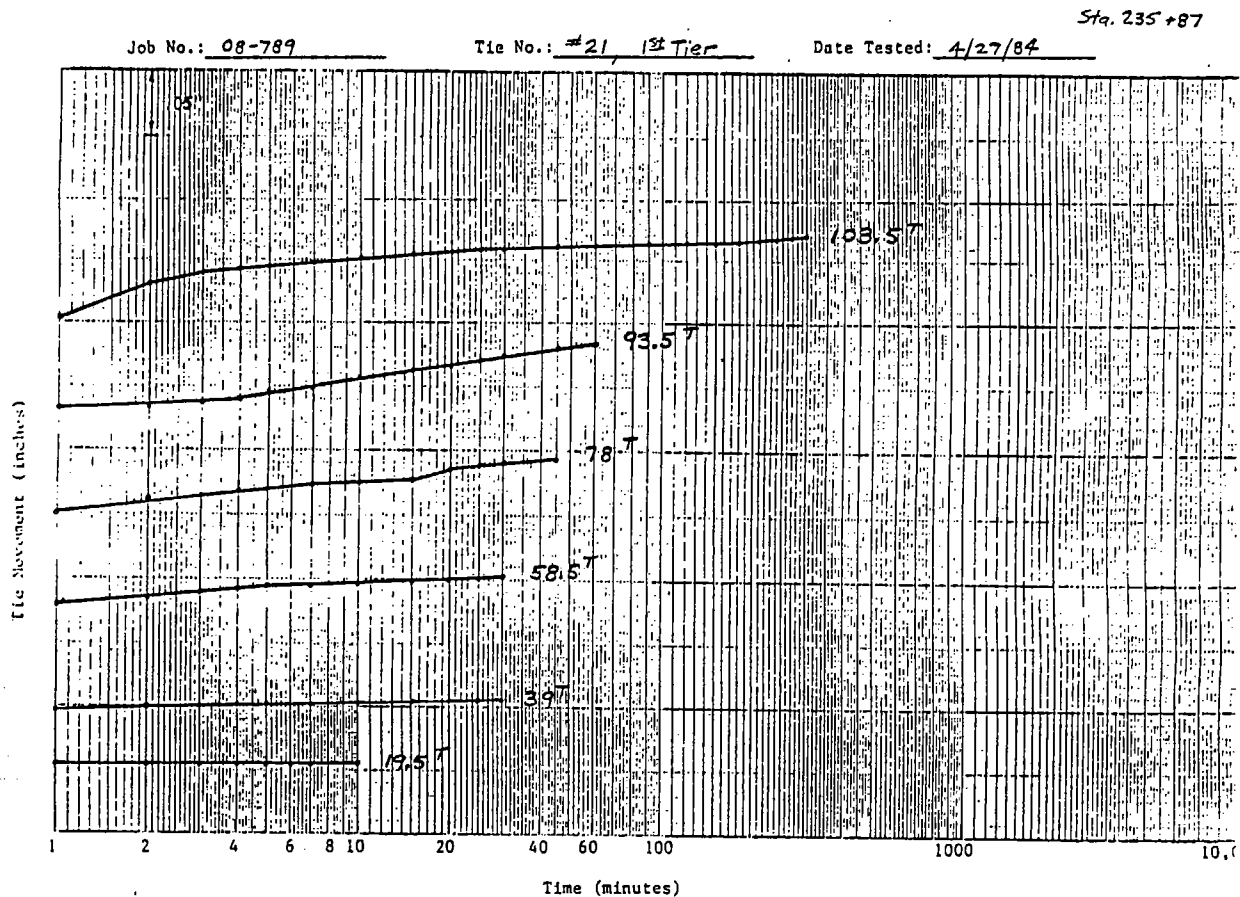


Figure 12. KY 227 Creep Test Movements

MONITORING

The short-term and long-term performance of the tiedback walls has been monitored through the use of load cells and slope inclinometers. A total of four IRAD GAGE load cells were installed on first and second tier tiebacks on each wall. Figures 13 and 14 show the results of the load cell readings for the KY 227 and U.S. 27 walls, respectively.

The load cells on the first tier of tiebacks of the KY 227 project showed a significant drop-off in load immediately following lock-off. This drop-off resulted from the soldier piles being pulled back into the soft and wet overburden/fill as stressing occurred during the spring rainy season. Following the initial time period, all four load cells have shown stable tieback loads over a ten- to 11-month period.

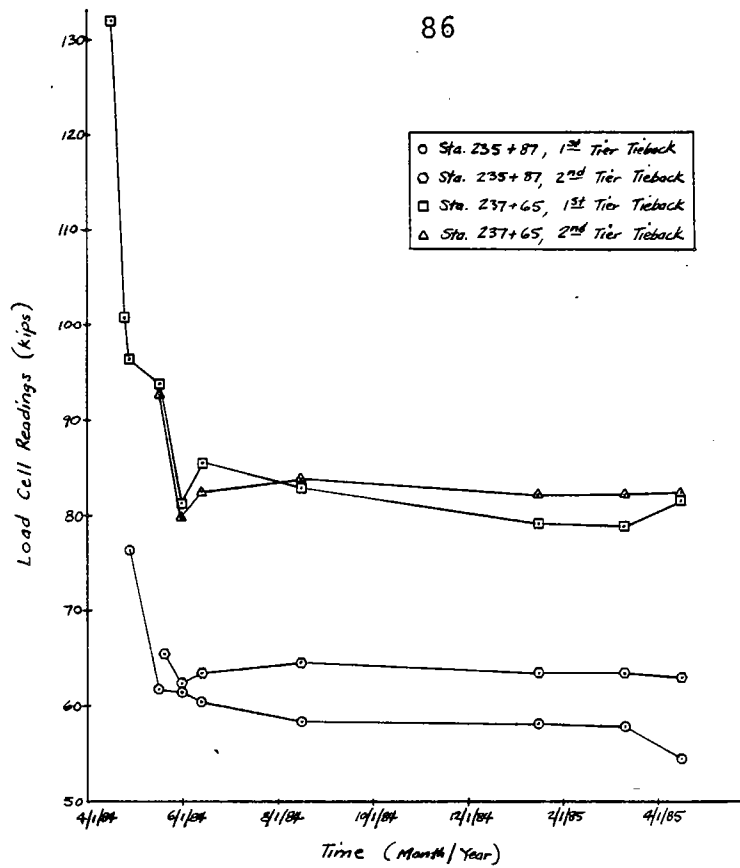


Figure 13. KY 227 Load Cell Readings

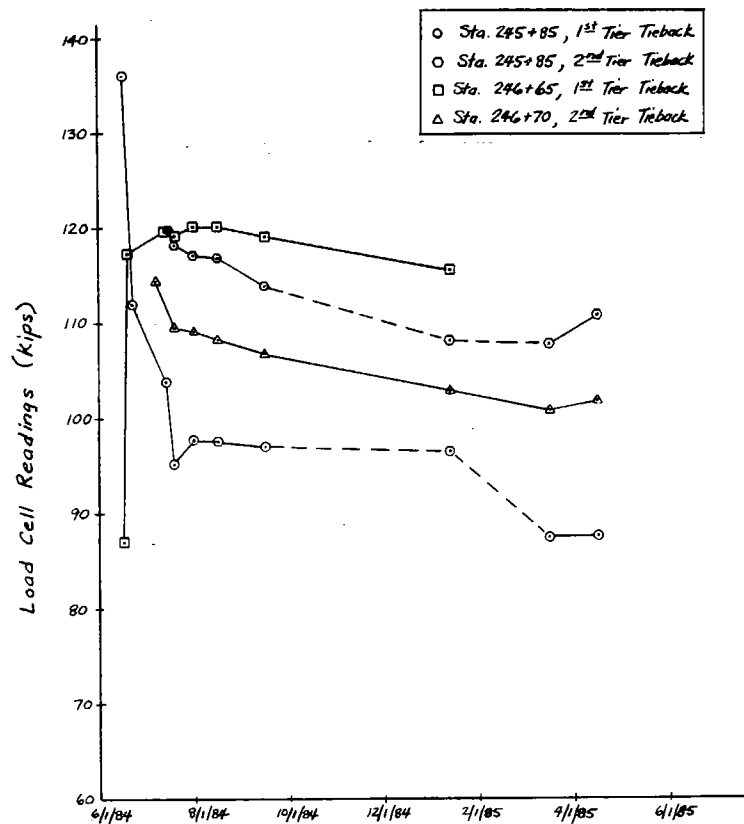


Figure 14. U.S. 27 Load Cell Readings

On the U.S. 27 project, placement of compacted backfill behind the wall near Station 246+65 resulted in a significant increase in the upper tieback load in the first week or two after lock-off of the tiebacks. In contrast to this behavior, the first tier tieback at Station 245+85 showed a sizable loss in load in the first two to three weeks following lock-off, which was the result of excavation around the wall and the backfill being loosely placed so as to allow the piles in this area to move back towards their original driven position. After the first couple of weeks, all four load cell readings have been relatively stable for an eight- to nine-month period.

Vertical slope inclinometer casings were installed at seven locations behind the KY 227 wall just prior to installation of the first tier of tiebacks and at two locations behind the U.S. 27 wall in early 1985. Figure 15 shows the results of the inclinometer readings for the KY 227 wall for two representative locations. These readings indicate that the tiedback wall has only moved downslope roughly 1/8-of-an-inch in the nearly one-year period since the tiebacks were locked off. The inclinometer casings on the U.S. 27 wall have been only recently installed and thus, no meaningful data is available yet.

The KY 227 wall was designated a FHWA demonstration project and was also instrumented with earth-pressure cells and tiltmeter plates. The results of this instrumentation will be available in a report by the Kentucky Transportation Research Program.

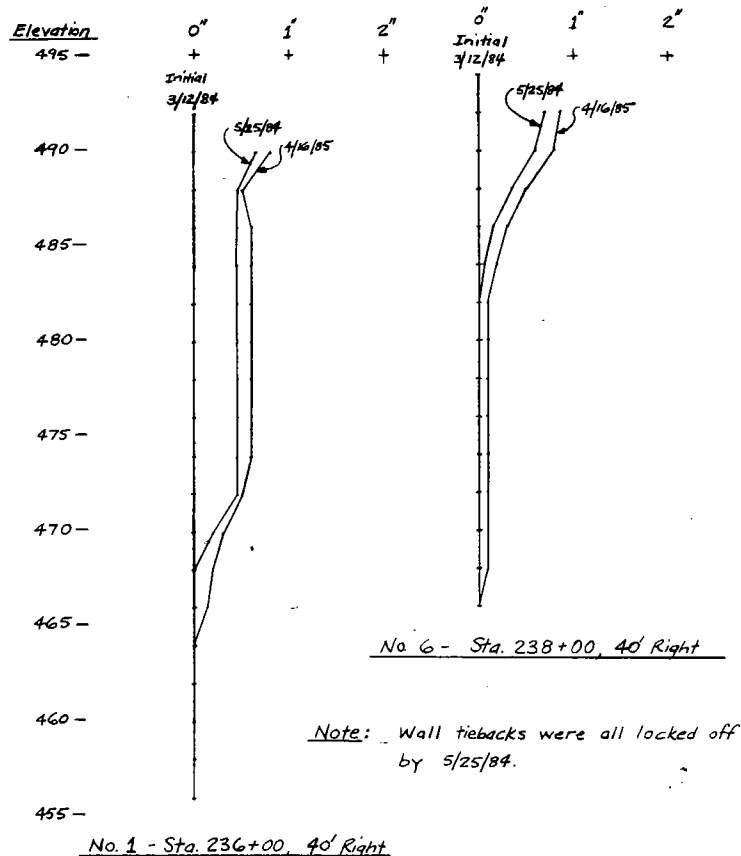


Figure 15. KY 227 Inclinometer Readings

PERFORMANCE SPECIFICATION METHOD

The Kentucky Department of Highways used a unique specification procedure for these tiedback walls. A performance specification was prepared which spelled out the following critical design requirements:

- o location and profile of the walls;
- o lateral pressure to be used in the wall design;
- o minimum unbonded length of the tiebacks;
- o required tieback corrosion protection; and
- o tieback testing and monitoring requirements.

Prequalified tiedback wall specialty contractors were then invited to submit wall designs based on these specifications about one month prior to the bid date. These wall designs were then reviewed and either approved or rejected. A bulletin or addendum was then issued about a week before the bid indicating the names of the specialty contractors with approved designs who could bid the tiedback walls.

This specification procedure is believed to have resulted in the most cost-effective, efficient wall designs in accordance with the performance specifications.

CONCLUSIONS

Tiedback walls were selected for the stabilization of two Kentucky highway landslides. These walls were constructed from the top down on the downhill side of the roadways and thus, existing highway traffic was not disrupted while the walls were under construction. The results of the testing during construction and performance monitoring has indicated that the tiedback walls have performed consistent with the design expectations and has affirmed the reliability of tiedback walls being a permanent solution to highway landslide problems. In addition, an effective specification method has been developed for the design and construction of tiedback walls.

ELECTRICAL ISOLATION, A CORROSION PROTECTION METHOD FOR PERMANENT TIEBACKS

by

Ronald B. Reeves

Lang Tendons, Inc.

and

David E. Weatherby

Schnabel Foundation Company

INTRODUCTION

Permanent tiebacks have given satisfactory service under a wide variety of ground conditions for the past 25 years. Corrosion failures have occurred at the tieback anchorages and along the unbonded length in the vicinity of the anchorage. Corrosion failures along the bond length of simple corrosion-protected and encapsulated tieback tendons have not been reported. Corrosion failures of post-tensioned, unbonded tendons in prestressed concrete have been reported, and these reports suggest a corrosion process which could cause corrosion to the bond lengths of simple corrosion-protected permanent tiebacks. For tiebacks, such failures may occur after years of service because the rate of corrosion may be very low due to high soil resistance and low current density¹.

Electrical isolation interrupts, at the tieback anchorage, the metallic path

for electron flow from the bond length of the tieback to the structure. This prevents formation of a galvanic cell that has widely separated electrodes in contact with a common electrolyte provided by groundwater. This cell, called a long-line concentration cell, and could be the cause of yet to be reported, long-term corrosion damage to the bond length of simple corrosion-protected tendons.

U.S. Patent No. 4,348,844, "Electrically Isolated Tendon Assembly and Method" covers electrical isolation. The details suggested in this paper are not proprietary, but application warrants consideration of the rights of the owners of the patent. Patent owners may be contacted through Schupack Suarez Engineers, Inc., South Norwalk, CT.

Electrical isolation will cause an negligible increase in the price of an installed simple corrosion-protected tieback. The estimated increase is from 0.6% to 1.2%. Electrical isolation details are similar to those required for permanent corrosion protection of tieback anchorages except for electrical insulation between the anchorage bearing plate and the structure. The increased corrosion protection given by electrical isolation justifies the slight increase in price.

CORROSION

Prestressing steel that is covered by portland cement concrete or grout corrodes when an agent depassivates the steel in the presence of oxygen and an electrolyte. For tiebacks, groundwater becomes the electrolyte, and the

atmosphere provides the oxygen. Galvanic corrosion of prestressing steel is often accompanied by embrittlement corrosion. Both types of corrosion can usually be traced to poor details and workmanship. Embrittlement corrosion may be prevented by details that prevent galvanic corrosion.

Galvanic Corrosion

Galvanic corrosion occurs when steel rusts or corrodes. The differential aeration cell, cathode, and anode connected by steel and immersed in an electrolyte (See Figure 1) causes galvanic corrosion. A potential difference between the electrodes caused by free oxygen at the cathode provides the energy to oxidize iron at the anode and disassociate the electrolyte into hydrogen ions (H^+) and hydroxyl ions (OH^-). Iron ions (Fe^{++}) enter the electrolyte, create a pit in the metal surface, react with the hydroxyl ions and become rust. Free electrons (e^-) move through the body of the metal to the cathode where hydrogen ions capture the electrons and form atomic hydrogen, hydrogen gas and water. This corrosion will continue unless the metallic path is interrupted.

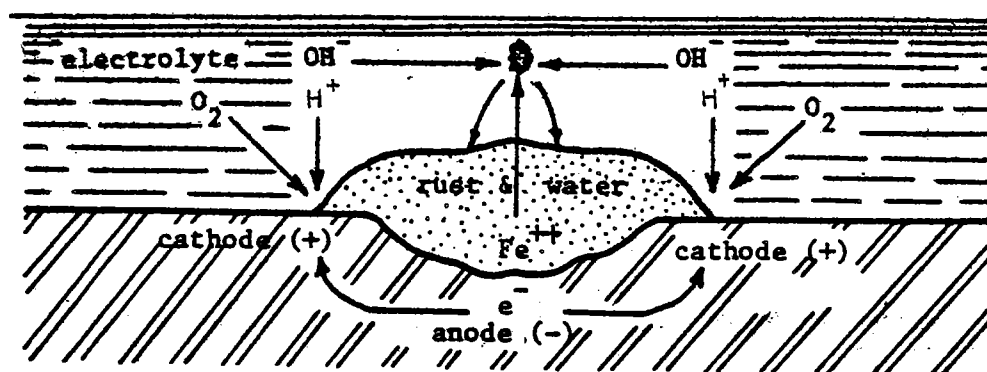


Figure 1. Galvanic corrosion by a local differential aeration cell.

Long-Line Corrosion Cell

The local differential aeration cell shown by Figure 1 becomes a long-line corrosion cell when corrosion-free metal separates the anode and cathode. The long-line cell shown by Figure 2 may develop on a simple corrosion-protected tieback. The ground conditions depassivate the prestressing steel in the bond-length. Oxygen at the structure supplied by the atmosphere makes the steel in the structure cathodic with respect to the prestressing steel in the bond length. A continuous metallic path exists between the anode and the cathode. Groundwater disassociates and supplies hydroxyl ions to the anode and hydrogen ions to the cathode. The conditions necessary for galvanic corrosion exist, and the rate of metal loss at the anode (bond length prestressing steel) will depend on the strength of the electrolyte (ground resistivity) and the potential difference between the cathode and the anode. This cell could cause severe pitting because the exposed surface at the structure (cathode) is usually much greater than the anodic area.

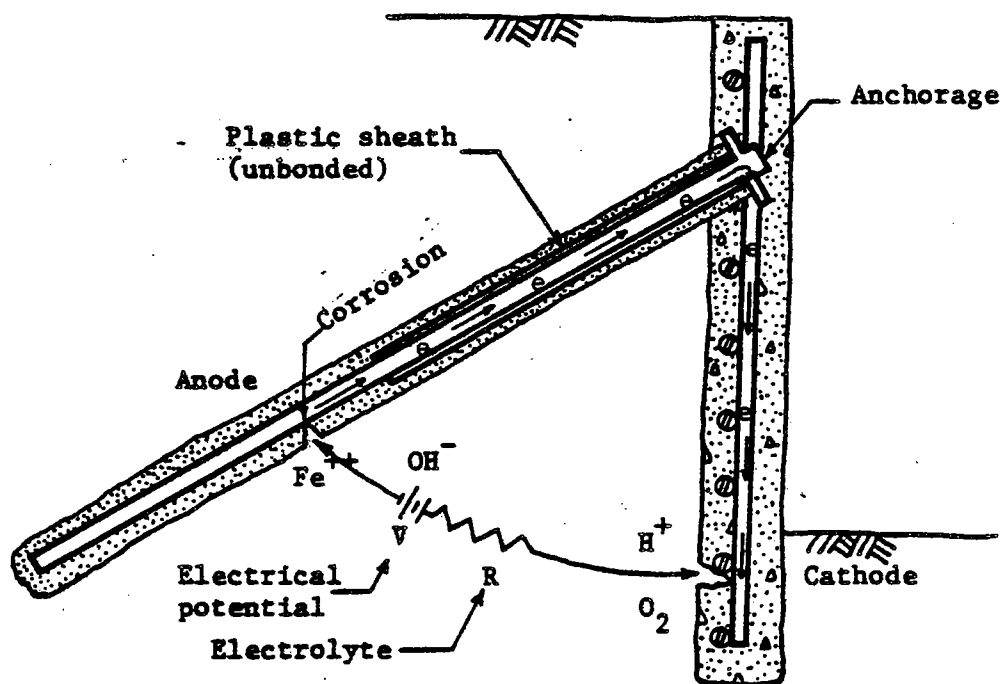


Figure 2. A long-line corrosion cell.

Corrosion Failures

At present (1985) corrosion failures of simple corrosion-protected tiebacks by long-line corrosion cells have not been reported; however corrosion failures of bonded and unbonded post-tensioned tendons used in prestressed concrete structures have been reported by Schupack and Suarez². These failures suggest existence of long-line cells caused by depassivation of the steel with electrical potential difference between failures and the end anchorages. All failures can be traced to ill-conceived details and poor workmanship that exposed the steel to corrosive conditions³. Corrosion failures at tieback anchorages have been reported⁴. These reports indicate that failures were caused by unsatisfactory details that allowed oxygen and water to reach depassivated steel. Electrical isolation details and good workmanship will prevent corrosion at the anchorages.

The absence of tieback corrosion failures which indicate the presence of long-line corrosion cells may be explained by the following:

- * The frequency of occurrence is low because the occurrence of corrosion failures in prestressed concrete structures is low⁵.
- * The average age of all installed simple corrosion-protected tiebacks is less than the time required for weak corrosion currents with weak electrolytes to cause corrosion failures.
- * The quantity of simple corrosion-protected tiebacks that are ten years old is small compared to the quantity currently being installed.

Possible corrosive environment, passage of time and increased tieback usage strongly indicate the need to protect simple corrosion-protected tiebacks from long-line corrosion cells. Lack of oxygen in the bond length makes formation of local aeration cells unlikely, however, long-line corrosion cells may form because the atmosphere provides oxygen at the structure.

QUALITY

Price

Tieback construction has become competitive; hence, suppliers and contractors tend to offer the least costly installation which does not create any visible problems during construction. This philosophy has been applied to post-tensioned unbonded tendons for prestressed concrete and has produced failures which could have been prevented by proper detailing⁶. Since electrical isolation will increase the price for an installed simple corrosion-protected tieback by 0.6% to 1.2%, this detail will not be provided unless specified by the Engineer.

Investigation of failures of prestressing steel indicate that these failures occurred as a result of unsatisfactory details and/or poor workmanship rather than from properties of the prestressing steel. Engineers should specify quality levels and details which satisfy corrosion protection needs generated by the site conditions, and quality control must assure satisfying of the Engineer's requirements. Competition drives price; however, the force must be improved productivity that achieves specified quality. Unless the Engineer injects this force, the quality will decrease.

Quality Assurance

An inspector cannot visualize the work done for installation of a tieback to assure that the work satisfies all of the design requirements. Nonuniform ground conditions produce changes in quality; hence uniform procedures do not necessarily produce uniform results. The practice to field load test each production tieback has been developed to verify design load capacity which would otherwise be uncertain due to nonuniform ground conditions. Latent tieback installation defects which increase susceptibility to corrosion (See Figure 3) are as follows:

- * Grout cover over prestressing steel in the bond length may be less than 0.5 inches (13 mm).
- * Cracks that develop in the bond length by strain due to transfer of tension force from the steel may allow depassivation of the steel.
- * A void in the bond length grout may expose steel to ground conditions. (A local corrosion cell is unlikely because of the absence of oxygen in this region.)
- * Shrinkage of grout in the anchorage trumpet may create a passageway for water to reach the bottom of the anchorage.
- * Grout bleed may create voids under the anchorage that expose bare steel to water and oxygen.

- * Electrical contact between the anchorage and the steel in the structure may provide the electron path necessary for formation of a long-line corrosion cell.
- o Portland cement concrete or grout cover of the anchorage may not prevent corrosion by carbonation.

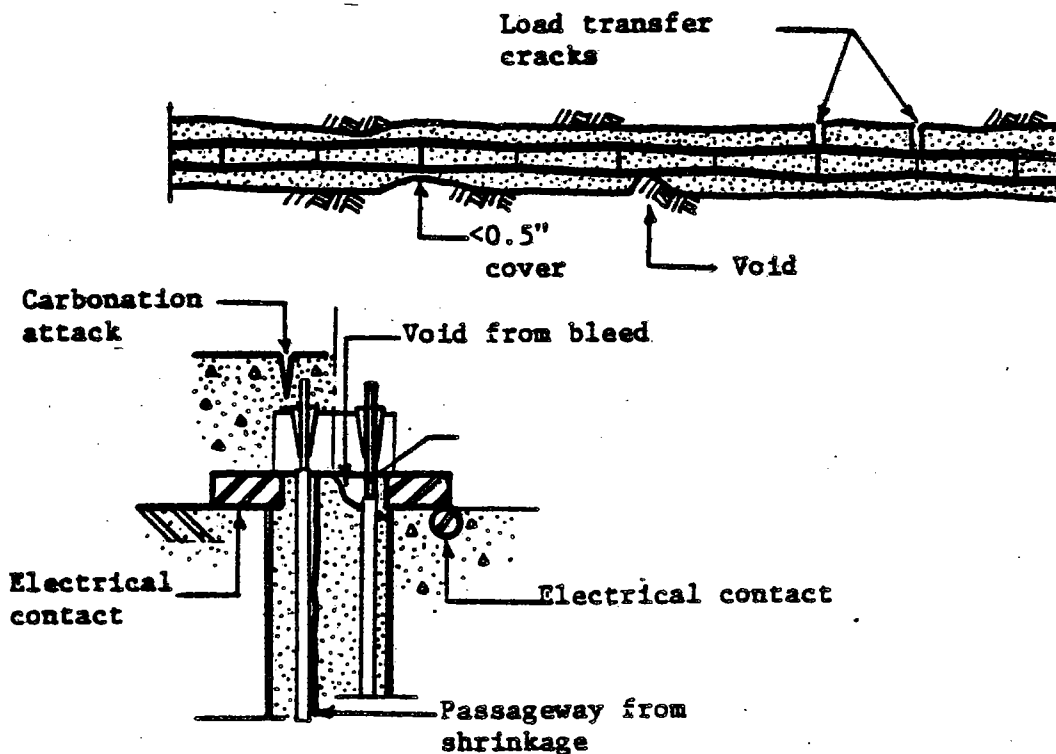


Figure 3. Defects in installation of simple corrosion-protected tendons that could cause failures.

CRITERIA FOR CORROSION PROTECTION

Corrosion protection for the bond lengths of permanent tiebacks has been classified as simple corrosion protection or encapsulated corrosion

protection⁷. Simple corrosion-protected tiebacks have prestressing steel covered by a minimum of 0.5 inches (13 mm) of portland cement grout. Encapsulated corrosion-protected tiebacks have prestressing steel grouted into a corrugated plastic or steel pipe which in turn is grouted in the soil or rock. Simple corrosion protection is used in nonaggressive environments, and encapsulated corrosion protection is used in aggressive environments.

The effect of the environment on the passivator, the inhibitor, or the coating determines the corrosion protection system. These effects have been classified as nonaggressive and aggressive depending on the hydrogen activity, pH; the ability of the electrolyte to dissociate, resistivity; presence of sulfides and the performance of nearby buried portland cement concrete structures. Steel is depassivated when the pH drops below 4.5. Soils with resistivities less than 2,000 ohm-cm are corrosive toward metals. Sulfides prevent formation of hydrogen gas from atomic hydrogen at the cathode and create conditions necessary for hydrogen cracking. Ground conditions have been classified as shown in Table 1.

Table 1. Aggressive and Nonaggressive Ground Conditions⁸

NONAGGRESSIVE	CONDITION	AGGRESSIVE
greater than 4.5	pH	less than 4.5
greater than 2,000 ohm-cm	resistivity	less than 2,000 ohm-cm
not present	sulfides	present
no record	damage to buried concrete structures	record
not present	stray current	present

The subsurface exploration program should include tests to determine pH, resistivity, and presence of sulfides.

Electrical insulation between the anchorage and the structure breaks the metallic path for electron flow between the anode and cathode. Without a continuous supply of electrons at the cathode, corrosion cannot occur. Tiebacks with bond lengths encapsulated in corrugated plastic or steel pipe do not require electric isolation because iron ions from the tendon cannot enter the electrolyte; hence they do not form, which eliminates the supply of electrons to the cathode.

Encapsulated corrosion-protected tiebacks do not require electrical isolation; however, encapsulation increases the price for the tieback 40 percent to 100 percent over the price for a simple corrosion-protected tieback. Encapsulation should be used where indicated by the ground conditions, and simple corrosion protection should include electrical isolation⁹.

DETAILS FOR ELECTRICAL ISOLATION

Electrical isolation insulates the anchorage from the structure and protects the anchorage from corrosion. The detail includes six features shown by Figure 4 and described below:

- * Watertight seal between the bottom of the anchor device and the sheath that encapsulates the unbonded length.
- * Electrical insulator between the anchorage and the structure.

- * Trumpet to allow movement of the tendon relative to the structure during stressing operations.
- * Mastic coating over the exposed portion of the anchorage.
- * Expansive, nonshrink grout to fill the trumpet after lock-off of post-tension force.
- * Metal, plastic, or portland cement cover over the anchor device.

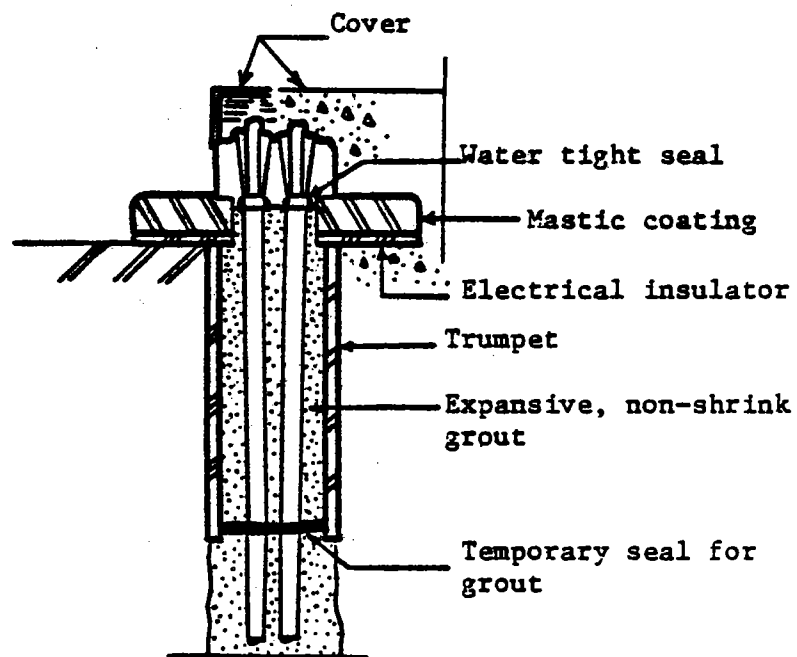


Figure 4. Functional features of electrical isolation.

The details for these features depend on the structure, the tendon and the method of tieback installation. Electrical isolation should be specified by quality and performance, and final details and design should be submitted on shop drawings for approval by the Engineer.

Watertight Seal

A watertight seal between the underside of the anchor device and the corrosion protection system for the unbonded length of the tieback prevents corrosion under and in the anchorage. Expansive grout or corrosion inhibitor grease provides this seal (See Expansive, Nonshrink Grout).

Electrical Insulator

A plastic sheet placed between the bearing plate and the support surface of the structure electrically isolates the tieback from the structure by interrupting the path for electron travel from the anode to the cathode (See Figure 2). This plastic sheet should have the compressive strength to support the design load during the service life of the structure without failure from deformation. The dielectric strength of the sheet should be 200 volts or greater. Korolath, manufactured by the Koro Corporation, Hudson, MA, has given satisfactory service.

Mastic Coating

The exposed surface of the locked-off anchorage should be coated with a mastic designed for corrosion protection of steel for the expected service conditions

(sunlight or buried). Mastic coating insulates the anchorage from the structure if the anchorage is embedded in portland cement concrete. Further, portland cement concrete or grout cover of anchorages should be augmented by mastic coatings in order to protect against corrosion by carbonation. Corrosion failures of portland cement grout covered anchorages have been reported by Schupack and Suarez¹⁰. Mastic coatings, manufactured by the Tapecoat Company, Evanston, IL, have given satisfactory service for protection of buried steel pipelines.

Trumpet

A trumpet made from a steel or plastic pipe, 2 to 3 feet long (0.6 m to 1 m), maintains correct alignment of the strands through the anchor head and provided a transition for corrosion protection between the unbonded length and the bottom of the anchorage of the tieback. Plastic pipe is preferred to steel because of lower cost and better corrosion resistance. Steel pipe is indicated when movement of the structure during stressing operations may damage a plastic trumpet.

Expansive, Nonshrink Grout

After lock-off of the post-tension force, the trumpet should be completely filled with an expansive, nonshrink grout. This grout forms a watertight seal around the plastic sheath encapsulating the unbonded length and permanently excludes water from the bottom of the anchor device. The grout should be made from portland cement and an admixture such as Conbex 209X, manufactured by Celitite, Inc., Cleveland, OH¹¹.

Cover

The mastic coated anchorhead should be covered by portland cement concrete/grout, or a plastic or metal cover. This gives protection from ultraviolet light deterioration and from mechanical damage. Plastic covers, manufactured by RayChem Corp., West Chester, PA, product designation CPSM/87, will give satisfactory service. These are heat-shrink sleeves lined with a mastic coating designed for corrosion protection. Metal covers should be filled with corrosion inhibitor grease or expansive grout.

Coatings

Organic coatings (mastics) are recommended for corrosion protection of metal surfaces of trumpets, bearing plates, and anchor devices. Metallic coatings (zinc and cadmium) are sacrificial; hence, corrosion is not prevented; its effects are only delayed. Under certain conditions free hydrogen atoms produced by oxidation of the sacrificial metal could cause hydrogen embrittlement of the tieback tendon.

SUMMARY

- * Long-line corrosion cells are potentially, the most likely source of corrosion damage to the bond lengths of simple corrosion-protected tiebacks.
- * Reported corrosion failures of post-tensioned unbonded tendons in prestressed concrete indicate that electrical isolation may have prevented the corrosion.

- * Electrical isolation will prevent development of long-line corrosion cells between the bond length of simple corrosion-protected tiebacks and the structure supported by the tiebacks.
- * The price increase for electric isolation is negligible, 0.6% to 1.2% increase in the price for a simple corrosion-protected tieback.
- * Electrical isolation enhances the corrosion protection of simple corrosion-protected tiebacks, and it encourages their use where field tests indicate that encapsulation would be unnecessary.
- * Performance and quality level details for electrical isolation should be specified and the details should be submitted on shop drawings for approval by the Engineer.

REFERENCES

1. Weatherby, D. E., Tiebacks, FHWA/RD-82/047, Federal Highway Administration, Washington, DC, pp. 84-85, July 1982.
2. Schupack, M., Suarez, M., "Some Recent Corrosion Embrittlement Failures of Prestressing Systems in the United States", Journal of the Prestressed Concrete Institute, v. 27, no. 2, March-April 1982, pp. 6-16.
3. Schupack, M., A Survey of the Durability Performance of Post-Tensioning Tendons, Post-Tensioning Institute, Phoenix, AZ, p. 1, 1978.
4. Weatherby, op. cit. p. 61.
5. Schupack, Suarez, op. cit. p. 3.
6. Schupack, M., "Protecting Post-Tensioning Tendons in Concrete Structures", Civil Engineering, ASCE, NY, December 1982, pp. 43-45.
7. Weatherby, op. cit. p. 71.
8. Weatherby, op. cit. p. 91.
9. Weatherby, op. cit. p. 95.
10. Schupack, Suarez, loc. cit
11. Schupack, M., "Admixture for Controlling Bleed in Cement Grout Used in Post-Tensioning", Journal of the Prestressed Concrete Institute, v. 19, no. 6, pp. 28-37.

RELATIVE DURABILITY OF SHALE-
A SUGGESTED RATING SYSTEM

by

David N. Richardson
Assistant Professor
University of Missouri-Rolla

Submitted for Presentation at
the 36th Annual Highway Geology Symposium

Clarksville, Indiana

May 1985

ABSTRACT

The inability to predict the degradation tendencies of shale has resulted in numerous failures of projects where shale was used as a construction material. Because shale does not fit neatly into either a soil category or a rock category, the tests that are commonly used to classify soil or rock are in many instances not totally suitable for classifying shale as to its long-term behavior properties. Thus, special classification tests of shale types has become necessary. The durability of shale relates to how well it can withstand its changing environment and still retain its initial properties. Strength, expansion characteristics, and permeability play a part in the durability of a shale. A good classification system would incorporate in some manner these parameters to reflect the short-term and long-term durability of the shale. A new method of predicting shale durability has been developed based upon an analysis of a battery of index tests. Using multiple regression techniques, six tests have been shown to reflect the overall durability of shale. One of these tests is a new modification of the slake durability index test. These tests have been incorporated into a simple linear equation which can be used to obtain a durability rating on a scale of 0 to 100 for a particular shale.

INTRODUCTION

Shale is a variably indurated geological material which exhibits behavior ranging from that of an overconsolidated clay to that of a hard, durable, cemented rock. Various researchers and practitioners define shale in different ways, from very narrow definitions to quite broad ones. In this paper the term shale will be used to describe any geologic material which is a indurated, nonmetamorphosed sediment composed mainly of clay or silt. Shale will thus include siltstones, mudstones, mudshales, claystones, clayshales, arenaceous shales, siliceous shales, bituminous shales, and gypsiferous shales.

Shale can degrade to a certain extent with time when it is removed from its natural condition and is subjected to stress relief and an altered environment or to weathering processes. Thus, the engineering properties can change with time. Some shales may be reduced from a rock-like state to a soil-like material of silt or clay sized particles. The rate and magnitude of degradation varies among shale types. Some durable shales degrade very little during the life span of engineering projects. Such shales may be considered as durable rocks with long-term rock-like properties. Less durable shales undergo different modes of degradation which ultimately result in degraded materials of greatly varying properties. Thus it may be said that both weathered and unweathered shales encompass a wide range of materials with quite different engineering properties.

In order to estimate the long-term engineering properties of a shale, one must first predict the long-term degradation tendencies. This information may be obtained from a durability rating system.

Shale durability could be broadly defined as a shale's resistance to change from its in situ condition. A more narrow definition would confine durability to a resistance to slaking. The current trend seems to be toward embracing the wider scope of conditions related to durability. For example, the Franklin system (Franklin, 1981) includes the point load index, a measure of tensile strength which is related to degradation occurring during construction of embankments. The Franklin ratings are correlated to such field behavior as rippability, permeability, and embankment slope stability parameters.

If durability is a resistance to change from the in situ condition, then durability should be proportional to the factors that would enhance resistance to the intrusion and effects of water, to the forces applied to shale during excavation, dumping, spreading, and compacting, to repeated wheel loads, and to the dead weight of the embankment itself. Thus durability should be in some manner related to permeability, swelling, dispersion, air breakage, tensile strength and toughness, abrasion resistance, and compressibility.

Unfortunately, for the overall life of the shale from excavation through service, it is not known at this time which of these factors predominate. Indeed, the predominance may vary from shale to shale.

Of course, if one wanted to accurately measure such properties as the shear strength of a compacted shale, one would conduct shear strength tests. But sometimes it is useful to be able to quickly estimate a variety of parameters on a graduated scale by performing simple index tests. Then, if necessary and if time and money permit, the more arduous testing can be accomplished.

The need for a numerical gradational shale durability classification

system is apparent. Although there are numerous shale classification systems reported in the literature, very few are numerical and gradational. Preliminary evaluation (Richardson, 1984) of several of these systems indicated the need for creating and evaluating a different system. This paper presents the status of this new system. The system is presently being evaluated and the results will be the subject of upcoming reports.

A classification system can be useful in several ways. As a first-order material quality indicator, the system could be used to delineate potential uses for various shales, such as in embankment zoning. The classification of shales also can provide a method for determining which shales require further testing by the more traditional geotechnical analyses. Another use would be the correlation of shale durability with other parameters, such as changes in subgrade bearing value, estimates of vertical strain, and estimates of slope stability parameters.

The purpose of this study was to develop a shale durability classification system which would serve as a first order predictor of shale behavior from excavation through service life.

Many of the existing shale durability systems are primarily concerned with delineating potential durability-related problems in regard to large scale settlement and slope stability of compacted shale embankments. One aspect of the research at the University of Missouri-Rolla was to develop a system which could also include durability of shales used in highway subgrades. For a classification system to be useful, several criteria would have to be satisfied:

- (1) the test methods should be simple, quick, and inexpensive to perform,
- (2) the system should be able to differentiate between shales of differing durabilities,

- (3) the system should provide a gradational ranking, and
- (4) the system should be able to rank shales in accordance with observed behavior.

DEGRADATION MECHANISMS

Shales will slake because of one of two reasons. Either the force causing the shale to fail has increased above a threshold value, or the material properties of the shale have changed such that the resistance threshold value has been lowered to the level of the applied force. Slaking mechanisms involve the migration of water either into or out of the shale. Usually the presence of water can either increase the slaking force or decrease the slaking resistance. Moisture migration can be caused by capillarity or by the condensation from water vapor onto adsorbing surfaces (Dunn and Hudec, 1965, 1972; Augenbaugh, 1974; Harper et al., 1979).

Shale slakes because internal cracks propagate, which eventually leads to complete isolation of a shale particle. Exceptions to this model include particle dispersion and dissolution of cementing agents.

Increased force criteria take the general forms of either air breakage (increased pore air pressure resulting from capillary suction of water) or increased differential straining which includes shrinking or expanding. Shrinking can be caused by drying. Expansion of shale can be brought about by one or more mechanisms, including hydration swelling, capillary suction, secondary mineral growth, elastic rebound, and freezing (Dunn and Hudec, 1965; Terzaghi and Peck, 1967; Moriwaki, 1966; Taylor and Spears, 1970; Van Eeckhout, 1976; Bjerrum, 1967; Brooker, 1967). Slaking can also occur as a result of a reduction in the resistance of the shale to the slaking forces. This resistance loss is again due to the intrusion and its result. Reduced resistance

can take the form of capillary tension decrease, fracture surface energy reduction, or chemical deterioration. There are several types of chemical deterioration phenomena. These include the dissolution of cementing agents, a change in slaking fluid chemistry, and mineralogical weathering (Dunn and Hudec, 1965; Moriwaki, 1966; Van Eeckhout, 1976; Rehbinder and Lichtman, 1957; Colback and Wiid, 1965; Russell, 1982).

In addition to disintegration by slaking, a shale can undergo fragmentation during excavation, loading, hauling, dumping, spreading, and compacting. It has been reported that the initial gradation of the shale to be compacted is a function of the geology and the excavation methods (Strohm et al., 1978). It is desirable to obtain as much degradation during construction procedures so as to minimize the magnitude of settlement of the embankment during its service life.

The durability of a shale relates to how well it can withstand its changing environment and still retain its initial properties. As strength, toughness, swelling characteristics, physio-chemical behavior, and permeability play a part in the durability of a shale, a classification system must incorporate in some manner these parameters to reflect the short-and long-term durability of the shale.

CLASSIFICATION SYSTEM TESTS

A number of tests have been utilized in the past in attempts to determine the relative durability of shale. These can be divided into two broad groups: characterization tests and durability tests. Characterization tests provide fundamental characteristic background information about the material

to assist in classification and explanation of durability-related behavior. The durability tests are a direct measurement of slaking, or degradation during construction procedures.

In Table I are listed the tests used in this study. These tests reflect a range of effort and expense from simple index tests to more complex methods.

LABORATORY INVESTIGATIVE PROCEDURE

The purpose of the laboratory portion of the study was to narrow the number of tests to a few that, if incorporated into a system, would take into account the range of predominant degradation mechanisms, and be able to describe durability behavior over a broad range in magnitude.

The shale samples used in the study were sampled from different shale formations at sites located in Missouri and Arkansas. The shales were of Pennsylvanian and Mississippian ages.

In each case, the material was obtained by excavating into the exposed formation to procure a relatively unweathered sample. The sampling was performed with hand tools such as a rock hammer, mattock, and shovel, and the sample was placed in a canvas bag lined with plastic. Upon delivery to the laboratory, a thorough mixing of each shale sample was performed to increase the likelihood of obtaining representative samples from each bag. The bags were then sealed and stored at room temperature and ambient humidity.

It was decided that a gradational quantitative scale of durability would be more useful in regard to correlation with other engineering property behavior than assignment of shales into three or four categories of durability. Certainly the gradational scale could also be separated into stepwise

Table I. Characterization and Durability Tests

Characterization	Durability
specific gravity (G_s)	2-cycle slake durability (I_{D2})
grain size analysis (PCS, PMS, PSS)*	sieved slake durability (I_{SD2})
exchange capacity (EC)	jar slake (I_J)
carbonate content (CO_3)	ultrasonic cavitation (DI)*
moisture adsorption (MI_{RH})	compaction-degradation (IC)
moisture-density relationship ($OMC, \gamma_{d(max)}$)	
free-swelling (PSW)	
liquid limit (LL)	
plastic limit (PL)	
plasticity index (PI)	
dispersion (PD)	
natural moisture content (NMC)	
shale-water pH	
chemical analysis	
x-ray diffraction	
petrographic examination	
point-load strength index ($I_{S(50)}$)	
air breakage (ABR)	
insitu dry unit weight (γ_{id})	

*PCS = percent clay size

PMS = percent silt size

PSS = percent sand size

OMC = optimum moisture content

 $\gamma_{d(max)}$ = maximum dry density

DI = disaggregation index

IC = index of crushing

descriptive groupings of durability. In order to achieve a gradational quantitative scale, durability values would have to be empirically assigned to a number of shales representing a wide range in durability-related behavior. Then, using multiple regression techniques, various combinations of tests could be used to predict these assigned durabilities. It was anticipated that the list could be narrowed to a few tests that would meet the criteria mentioned previously.

The method by which durabilities were assigned was to combine several existing shale durability classification systems which rendered numerical gradational ratings but utilized differing methods of durability determination. The three systems or methods used were those of Franklin (1981), Annamalai (1974), and Bailey (1976)/Hale (1979). Franklin's system includes the point load strength index, plasticity index, and the slake durability test which is a cyclic wetting/drying type of durability test. The method of Annamalai employs an ultrasonic cavitation degradation to classify shales as to durability behavior, while the Bailey-Hale method is concerned with the particle breakdown during compaction.

Modified Franklin Rating

The Franklin system was changed by substituting a modification of the slake durability method. Although the slake durability method is a widely used test (Russell, 1982; Strohm et al., 1978; Deere and Gamble, 1971; Deo, 1972; Aufmuth, 1974; Chapman, 1975; Lutton, 1977; Noble, 1977; Hudec, 1978; Strohm, 1978; Franklin, 1981; Oakland and Lovell, 1982; Hopkins and Deen, 1984; Richardson, 1984; Andrews et al., 1980; Chandra, 1970; Franklin and Chandra, 1972; Franklin, Broch, and Walton, 1970; International Society of Rock Mechanics, 1979), there has been some criticism of it resulting in

several modifications to the method (Andrews, 1980; Aughenbaugh and Bruzewski, 1976; Sickler, 1981; Deere and Gamble, 1971; Deo, 1972; Franklin and Chandra, 1972; Hopkins and Deen, 1984; Hudec, 1978; Noble, 1977; Richardson, 1984). A major criticism of the original test is that it is insensitive to shales which slake into chips which are, for the most part, larger than the #10 sieve. Thus two different shales could possess the same slake durability index (I_D) but one could be completely intact after the test while the other shale type could break down into small chips all larger than the #10 sieve. Another criticism is that during testing, some of the more plastic shales may form mudballs thus rendering falsely high I_D values. A third criticism is that if several soft soil-like shales of different durabilities are subjected to a large slaking energy via additional cycles or revolutions, these shales may be given almost equally low ratings. Conversely if several hard rock-like shales of different durabilities are subjected to a reduced slaking energy these shales may also be rated as having almost the same durability.

Richardson (1984) introduced a method to quantitatively determine the effect of the retention of small chips in the drum by performing a sieve analysis of the retained material after the second cycle of drying. The modified test was called the "sieved slake durability" test, and the resulting index was called the "sieved slake durability index, ISD_2 ".

A study was performed to determine the optimum method for performing the slake durability test in terms of precision, testing ease, length of testing time, ability to discriminate between shales, and ability to rank shales in order of observed durability (Richardson and Long, 1985). The study included the effects of changing the testing variables of initial moisture content, duration of slaking, and number of slaking cycles. Comparisons were made

between the sieved slake durability tests and 11 other versions of the slake durability test. The results of this study showed that the 2-cycle 200-revolution sieved slake durability test was the modification of choice in terms of the above criteria.

During the sieved slake durability test, the shale specimens are subjected to soaking. The permeability of the shale is manifested in the volume and rate of water entering the specimens, setting the stage for the slaking mechanisms to occur. These mechanisms include the previously discussed swelling, air breakage, and dispersion. Also, because the specimens are tumbling in the rotating mesh drum, some abrasion is taking place. Thus the sieved slake durability test is in effect testing these various factors of durability.

The plasticity index has been traditionally related to swelling potential. In a previous study (Richardson, 1984) involving many of the shales utilized in this paper, the plasticity indices were shown to correlate well ($r = 0.848$) with free swelling. Several researchers have found a general relationship between increasing plasticity indices and decreasing durabilities (Deere and Gamble, 1971; Franklin, 1981; Richardson, 1984).

As an alternative to other types of strength testing, Broch and Franklin (1972) developed the "point-load" strength test. The point-load test is an indirect tensile strength test. A concentrated vertical load is applied which produces a horizontal tensile stress within the specimen. Failure eventually occurs by splitting along a vertical plane. The critically stressed region is in the interior of the specimen. Within certain limits, specimen geometry has little effect upon results. Testing large numbers of specimens is feasible because of the quickness and simplicity of the test. The influence of

specimen size and shape is compensated by correction factors which relate the results to a standard size specimen. The test has received wide acceptance in the rock mechanics field (Beiniawski, 1975; Goodman, 1980; Hoek and Brown, 1980; Oakland and Lovell, 1982; Richardson, 1984; Strohm, et al., 1978). The test has been accepted as a standard procedure by the International Society of Rock Mechanics, (International Society of Rock Mechanics, 1979).

The results of the plasticity index, point load index, and sieved slake durability testing were used to enter Franklin's chart (Franklin, 1981) to determine the modified Franklin shale ratings.

Annamalai Disaggregation Index

Ultrasonic cavitation disaggregation as used by Annamalai (1974) was utilized to obtain "disaggregation index" values for the shales. This test method imparts ultrasonic wave energy to the shales, breaking them down. The resulting increase in the number of clay size particles is quantified. The greater the change, the less durable is the shale and the results are deemed to be an indication of interparticle bond strength. For a more detailed description of the test method, the reader is referred to Richardson (1984).

Because of the increased degradation energy applied to the shale, it would seem that this test would provide more useful information than the sieved slake durability test in predicting long-term behavior of an embankment subject to water infiltration.

Index of Crushing

A portion of durability involves the resistance to breakdown during compaction. A more durable rock-like shale exhibits higher strength than a less durable shale, and hence should break down to a lesser degree under compaction loads. Bailey (1976) and later Hale (1979) presented a method of

quantifying the amount of breakdown (degradation) during compaction. This method was an adaptation of one developed by Aughenbaugh and others (1962) for use with carbonate rocks. The index of crushing (IC) is calculated based on the results of a before-and-after sieve analysis of shale that is compacted in the laboratory. It is a percentage change in mean aggregate size during compaction. The test method is well documented in the literature cited. Specific testing parameters used in this study are listed in the appendix.

Durability Rating Equation

The results of the classification by the above three methods were combined into a single set of durability ratings for 13 shales. All three methods were given equal weight. The tests involved in rendering these assigned ratings represented most of the durability-related factors previously discussed:

permeability	ISD2
swelling	PI
dispersion	ISD2
air breakage	ISD2,PI
tensile strength and toughness.....	IS(50),IC,DI
abrasion resistance	ISD2

The assigned durability ratings are listed in Table II along with the raw data used for predicting these ratings.

The next task was to approximate the assigned durabilities by a combination of some of the parameters listed in Table I. It was desirable that the number of tests should be reduced to a few which exhibited the characteristics previously discussed. Several of the tests were eliminated from further consideration for one or more reasons. Some tests were not truly quantifiable. Others were shown by bivariate correlation analysis to have no

Table II. Raw Data Used in Regression Analysis.

Shale Units	DR _A	I _{SD2}	PI %	NMC %	γ_{id} pcf	IC %	OMC %	$\gamma_{d(max)}$ pcf	LL %	PCS %	DI %	I _{S(50)} psi
Boundary	0	0	50	27.2	107.0	94	26.6	80.8	88.0	82.0	40	0
Galesburg	33	2	29	14.6	119.3	57	21.7	102.8	54.0	39.0	25	0
Carbonaceous Hushpuckney	35	13	26	16.4	107.0	67	24.7	95.2	52.1	43.0	21	0
Pleasanton "A"	37	17	25	12.9	116.8	51	20.2	102.1	52.6	47.0	26	0
Mound City	44	20	19	12.5	122.4	38	16.6	114.8	35.0	30.0	26	0
Crosby	51	15	9	3.6	153.1	18	10.7	121.9	26.4	14.0	27	435
East Rosebud	57	49	12	5.8	129.8	27	15.4	116.8	33.8	22.0	21	0
Stark	60	82	19	15.1	110.9	51	22.2	80.8	45.0	27.5	19	0
Critzer	67	74	17	9.4	125.4	25	15.8	116.2	40.0	37.5	16	0
Riverton	68	87	2	6.2	126.5	47	16.6	111.2	22.7	11.0	11	0
Romance	75	90	4	3.2	146.3	18	9.8	117.4	23.4	9.0	16	0
Northview	78	86	9	6.9	134.7	32	12.4	122.8	26.8	21.0	6	94
Lagonda	78	90	0	5.4	127.8	32	14.8	115.7	22.5	12.0	6	0
Letona	83	86	2	1.1	151.4	26	13.2	121.7	19.7	12.0	9	537
Boundary	100	100	0	0.3	170.0	0	9.8	127.6	17.8	9.0	0	1450

* DR_A = assigned durabilities

significant relationship to durability in a quantifiable way. Several tests are used marginally and insufficient data were available for establishing the ranges of values necessary for the data normalization procedure used in the multiple regression portion of the study.

The number of tests which were deemed to be related to durability was reduced to 11. The test data, shown in Table II, were normalized prior to further use.

At this point, multiple regression analysis were used to determine the most efficient combination of the remaining 11 parameters. The result was an equation of the form:

$$DR = \sum_{i=1}^n A_i P_i$$

where DR = durability rating

A_i = weighting coefficient

P_i = parameter result.

n = number of tests

Numerous combinations of parameters were tried. The input was the test data for 13 shales resulting from the 11 parameters being evaluated. These parameters were sieved slake durability, plasticity index, optimum moisture content, maximum dry density, ultrasonic cavitation "disaggregation index", natural moisture content, in situ dry density, index of crushing, point load index, liquid limit, and the percent claysize particles. Also included were two fictitious shales, one representing zero durability and one representing a durability of 100 to give boundary values to the model. All of the test data

were normalized to give relative results on a scale of 0 to 1.0.

Each attempted combination produced a set of coefficients, A_i , and also predicted the durability of each shale based upon these coefficients. The mean squared error of each set of predictions was tabulated as a measure of accuracy.

The final set of parameters was chosen based upon a low mean squared error and the ease of testing. A few of the various trials are ranked in order of mean squared error in Table III. The combination of six parameters (sieved slake durability, plasticity index, natural moisture content, in situ dry density, liquid limit, and point load index) gave almost as close agreement with assigned durabilities as did the combination of the previously mentioned 11 parameters. These six parameters are all easily obtained by simple laboratory testing methods. The relative error introduced by deleting the other five tests is not very significant in regard to prediction of the assigned durabilities, and the system becomes quite manageable by the exclusion of these five.

The resulting equation for predicting durability of shale on a gradational scale of 0 to 100 using the six test parameters is shown in Table IV.

For the shales upon which the equation is based, inclusion of the liquid limit is marginally helpful in terms of accuracy. However, because the liquid limit data would already be available from determining the plasticity index, it is included.

Durability of shale has been shown to be proportional to dry unit weight (Deere and Gamble, 1971) and inversely proportional to natural moisture content (Deere and Gamble, 1971; Richardson, 1984) in a general way. Their inclusion in the equation seems to be compensating for those shales that are

Table III. Regression Parameters Ranked According to Mean Squared Error (MSE)

I _{SD2}	PI	LL	PCS	DI	OMC	IC	γ_{id}	NMC	$\gamma d_{(max)}$	I _{S(50)}	MSE	
											X10 ⁻³	
X											31.25	
X	X										22.60	
X	X	X									13.54	
X	X	X	X								13.16	
X	X	X	X	X							10.50	
X	X	X	X	X							10.21	
X	X	X	X	X		X					9.98	
X	X						X	X			8.03	
X	X	X					X	X			6.30	
X	X	X					X	X		X	6.10	
X	X	X	X				X	X		X	6.08	
X	X	X				X	X	X			5.54	
X	X	X				X	X	X		X	5.54	
X	X	X	X	X		X	X				2.76	
X	X	X	X	X		X	X	X			2.77	
X	X	X	X		X	X	X	X	X		0.71	
X	X	X	X	X	X	X	X	X	X		0.69	
X	X	X	X	X	X	X	X	X	X	X	0.58	

Table IV. Durability Equation:

$$DR = A_1P_1 + A_2P_2 + A_3P_3 + A_4P_4 + A_5P_5 + A_6P_6$$

Term	A	P	Description	Unit
1	0.55274	I _{SD2}	Sieved Slake Durability	%
2	1.40282	PI	Plasticity Index	%
3	1.72581	NMC-0.3	Natural Moisture Content	%
4	0.84561	γ _{id} -107.0	<u>In situ</u> Dry Unit Weight	pcf
5	-1.42813	LL-17.8	Liquid Limit	%
6	-0.00608	I _S (50)	Point Load Index	psi

not as durable as the sieved slake durability test would indicate.

Dissolution Problem Determination

Based on work by Noble (1977), Strohm and others (1978) recommended that hard shales that are classified as durable should be given a final check for susceptibility to chemical breakdown. The test water from the slake durability test should have the pH determined. If the pH is less than six, an acid condition is indicated, and the shale mineralogy should be checked for minerals that can cause chemical deterioration. Dark colored shales should be checked for iron sulfide and chlorite. This combination is highly conducive to rapid weathering; shales with iron sulfide that will oxidize and have access to water can produce sulfuric acid, which could dissolve the chlorite.

On the other hand, some western shales are dispersive, and may react adversely with alkaline water.

COMPARISON TO EXISTING SYSTEMS

A comparison of the shale ratings obtained in this study to four other shale classification systems is presented in Table V. In general there is good agreement between all systems including cutoff points between changes in descriptive ratings. The most pronounced exception is the Stark shale. The four existing systems rely heavily on the two or three cycle slake durability test. Stark is a low density, soft, fissile, nondurable organic shale that can be easily crumbled by hand, yet results of the slake durability test indicate that it is quite durable. The visual description portion of the Strohm and others (1978) method allows for this phenomenon; the unit weight portion of the "DR" rating system does also.

Table V. Comparison of Shale Classifications.

Shale	Deere And Gamble (1971)	Strohm et al. (1978)	Hudec (1978)	Franklin (1981)	DR
Carbonaceous Hushpuckney	very low	soil-like, nondurable	high loss	1.95	22
Galesburg	very low	soil-like, nondurable	high loss	1.45	25
Pleasanton "A"	very low	soil-like, nondurable	high loss	2.10	25
Mound City	very low	soil-like, nondurable	high loss	2.35	47
Crosby	very low	soil-like, nondurable	high loss	2.80	50
East Rosebud	medium	soil-like, nondurable	intermediate loss	4.00	50
Stark	medium high	soil-like, nondurable	low loss	5.60	62
Critzer	medium	soil-like, nondurable	low loss	4.45	64
Riverton	medium high	intermediate hard, nondurable	low loss	5.35	70
Lagonda	medium high	rock-like, durable	low loss	5.40	70
Northview	medium high	intermediate hard, nondurable	low loss	5.45	82
Letona	medium high	intermediate hard, nondurable	low loss	7.25	83
Romance	medium high	rock-like, durable	low loss	5.50	86
--	high	rock-like, durable	rock-like	--	90
--	very high	rock-like, durable	rock-like	9.0	100

It appears that for DR ratings of below 50, shales can be considered soil like, and should be broken down and compacted into thin lifts to minimize settlement and stability problems. Shales with DR ratings of between 50 and 70 are of intermediate behavior. More difficulty in excavation and breakdown during compaction should be expected, but again these should be broken down and compacted into thinner lifts. Shales with DR ratings between 70 and 90 tend to be hard and more durable, and will present even more difficulty in excavation and compaction. These should not be considered rock like. The upper limit for this group (90) is not well defined at present. Further research examining truly rock like shales will be necessary.

Upcoming research in the usage of DR ratings should include correlation of ratings with estimates of design and construction parameters such as lift thickness and rippability. Some of these relationships may very well have to be specific to a particular region, and thus would have to be developed locally.

CORRELATION WITH FIELD EXPERIENCE

In order for a shale durability classification system to be useful, the results of its application must correlate significantly well with field behavior. Field behavior of interest includes cut slope stability, compacted embankment stability, and compacted embankment or subgrade pavement distress.

The problem with evaluating the classification system developed in this study is that for any given shale, two basic sets of information must be known: (1) field behavior in terms of failure or success, and (2) the results of the six classification indices which are used in the durability equation.

A survey of state and federal agencies, along with an extensive literature search, was conducted in an attempt to correlate the system with observed field performance and to update knowledge as to the laboratory tests and classification systems currently being used to predict durability.

The survey was conducted by means of a mailed questionnaire. These were sent to state highway departments, U. S. Army Corps of Engineers district offices, Federal Highway Administration regional offices, Federal Aviation Administration regional offices, Bureau of Reclamation regional offices, and Bureau of Mines regional offices. Of the 51 questionnaires returned, 22 were from state highway departments. Only 21 of the 51 respondents indicated that they dealt with shale to any significant degree. Fourteen of these were state highway departments.

Of the 21 respondents that have experience with shale, it appeared that five conducted specific tests in order to classify the shale in terms of durability. Only two of these five performed some form of the slake durability test and only one agency performed all six of the tests that are required by the equation developed in this study. However, this agency could not supply us with any field-related distress or nondistress behavior. Thus, the results of the questionnaire could not assist in evaluation of the durability equation.

Five of the 13 shales used in this study were being used in the construction of a dam embankment at the time of sampling. The durability ratings of these ranged from 22 to 64, indicating soil-like natures and that they should be broken down and compacted in thin lifts. This indeed was what was specified. Lift thickness were limited to eight inches.

Lutton and others (1978) and Franklin (1981) have correlated durability

with lift thickness. These relationships are depicted in Figures 1 and 2, respectively. The durability ratings presented in this paper correlate well with the Franklin ratings. In Figure 2 the horizontal axis is scaled with DR ratings as well as their corresponding Franklin ratings. The Stark shale has been identified in this study as a troublesome shale. Its two-cycle slake durability index (I_{D2}) is 92, indicating a more competent material. Its Franklin rating is 5.6. Use of an I_{D2} of 92 in Figure 1 indicates that Stark could be placed in lifts of over 20 inches with few minor and no major settlement problems projected. Use of Figure 2 indicates a similar result. Yet in practice the Stark shale is rather weak. The DR value of Stark is 62, indicating that it is soil like. Use of Figure 2 with this value indicates a 14 inch maximum lift thickness, which is a more realistic value to be specified for this material.

Franklin related his ratings to recommended excavation equipment. Again using the correlation between the two classification systems, the ratings developed in this paper are compared to recommended excavation equipment in Table VI. Further work in both lift thickness and excavation correlation needs to be done to verify the above estimates. It is hoped that in the future, more field data will become available so that field verification of the equation can occur.

CONCLUSIONS

A new method of predicting shale durability was developed from an analysis of the data developed from a battery of tests. By determining the sieved slake durability index, the natural moisture content, the in situ dry density, the point load index, the liquid limit, and the plasticity index, the durability rating of shale can be calculated by use of the following equation:

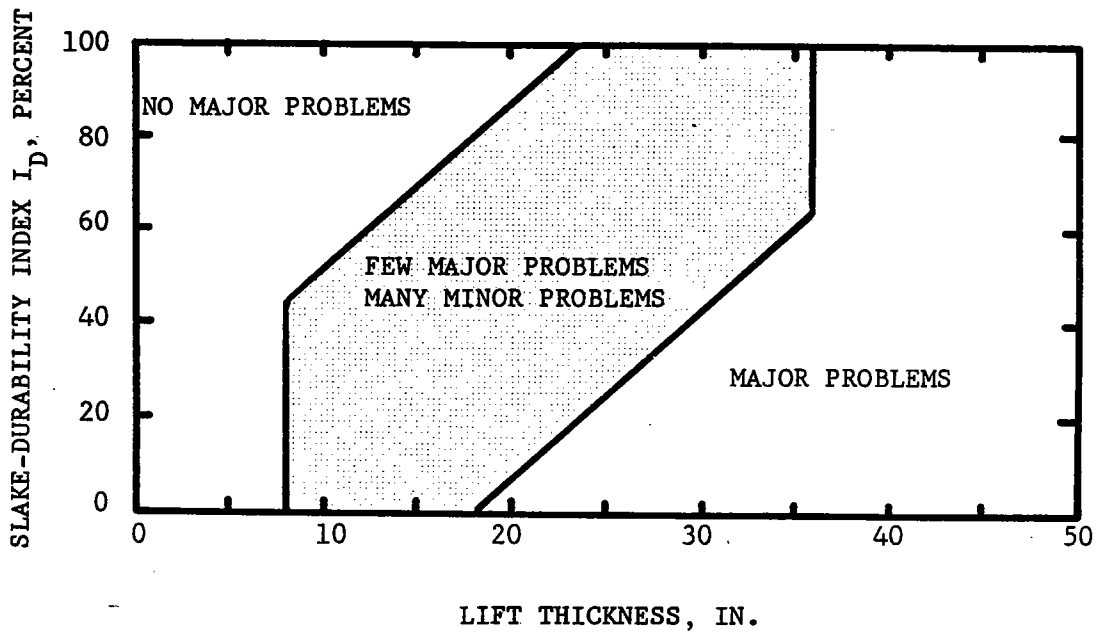


Figure 1. Preliminary criterion for evaluating embankment construction on the basis of slaking behavior.
(after Strohm et al., 1978)

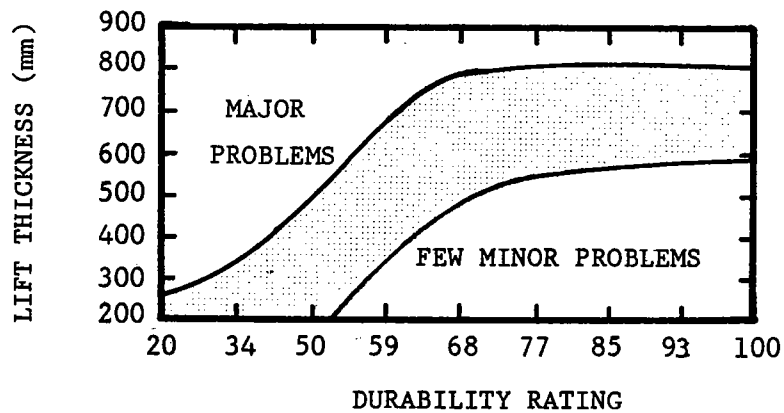


Figure 2. Lift thickness as a function of durability rating. (after Franklin, 1981)

Table VI.

Excavation Equipment Recommendations

Method or Equipment	Durability Rating
Backhoe	0-70
Shovel	0-70
Medium ripper	40-80
Heavy ripper	40-90
Blasting	80-100

$$DR = 0.55274 (I_{SD2}) + 1.40282 (PI) + 1.72581 (NMC-0.3) + 0.84561$$

$$(\gamma_{id}-107.0) - 1.42813 (LL-17.8) - 0.00608 (I_s(50))$$

Durability ratings range from zero (least durable) to 100 (most durable).

It is recommended that the pH of the slaking water should be checked for a pH of less than six. If this is the case, dark colored shales should be analyzed for the presence of iron sulfide and chlorite---a dangerous combination in terms of slaking by dissolution of chlorite.

The ability to classify shale enables an estimation of durability behavior. This facilitates the classification of construction materials and material usage for the practitioner. For the researcher, useful correlations of durability ratings with other parameters may be possible.

The data upon which these equations are based represents a wide range in durability behavior. However, shales representing the most rock like behavior ($DR = 90^+$) were not included in the study. Secondly, the test shales were restricted to Pennsylvanian and Mississippian ages. Finally, the data were obtained from only 13 formations. Thus additional testing of other shales would help verify the above conclusions. Likewise, the durability rating system needs to be correlated with such parameters as resilient modulus, rippability, permeability, shear strength parameters, and volumetric strain.

REFERENCES

- Andrews, D.E.; Withiam, J.L., Perry, E.F; and Crouse, H.L., 1980, Environmental Effects of Slaking of Surface Mine Spoils-Eastern and Central United States: Report No. 78-275, Bureau of Mines, Denver, CO, 247 p.
- Annamalai, M., 1974, Engineering Properties of Raw and Ultrasonic Treated Oklahoma Shale: Unpublished Ph.D. Dissertation, University of Oklahoma, Norman, OK, 159 p.
- Aufmuth, R.E., 1974, A Systematic Determination of Engineering Criteria for Rock: Bulletin of the Association of Engineering Geologists, Vol. 11, No. 3, pp. 235-245.
- Aughenbaugh, N.B., Johnson, R.B., and Yoder, E.J., 1962, Factors Influencing the Breakdown of Carbonate Aggregates During Field Compaction: Transactions of the Society of Mining Engineers, pp. 402 - 406.
- Aughenbaugh, N.B., 1974, Effect of Moisture on Shale, 23rd Annual Soil Mechanics and Foundation Conference: University of Kansas, Lawrence, KS, pp. 1-14.
- Aughenbaugh, N.B. and Bruzewski, R.F., 1976, Humidity Effects of Coal Mine Roof Stability: Report No. Bumines OFR 5-78, Department of Interior, Washington, DC, 160 p.
- Bailey, M.J., 1976, Degradation and Other Parameters Relating to the Use of Shale in Compacted Embankments: MS Thesis and Joint Highway Research Project Report 76-23, Purdue University, West Lafayette, IN, 208 p.

- Bjerrum, L., 1967, Progressive Failure in Slopes of Overconsolidated Plastic Clay and Clay Shales: Journal of Soil Mechanics and Foundations Division, American Society of Civil Engineers, Vol. 93, No. SM5, pp. 1-19.
- Brooker, E.W., 1967, Strain Energy and Behaviour of Overconsolidated Soils: Canadian Geotechnical Journal, Vol. 4, No. 3, pp. 326-333.
- Chandra, R., 1970, Slake-Durability Test for Rocks: Unpublished MS Thesis, Department of Mining, Imperial College, England, 54 p.
- Chapman, D.R., 1975, Shale Classification Tests and Systems: A Comparative Study: Joint Highway Research Project, Project No. C-36-SL, Purdue University, West Lafayette, IN, 86 p.
- Colback, P.S.B. and Wiid, B.L., 1965, The Influence of Moisture Content on the Compressive Strength of Rocks: Proceedings of Rock Mechanics Symposium, Toronto, Canada, pp. 65-72.
- Deere, D.U. and Gamble, J.C., 1971, Durability-Plasticity Classification of Shales and Indurated Clay: Proceedings of the 22nd Annual Highway Geological Symposium, University of Oklahoma, Norman, OK, pp. 37-52.
- Deo, P., 1972, Shales as Embankment Material: Joint Highway Research Project, Project No. C-36-5J, Purdue University, West Lafayette, IN, 202 p.
- Dunn, J.R. and Hudec, P.P., 1965, The Influence of Clays on Water and Ice in Rock Pores, Part Two, Physical Research Project 4: New York State Department of Public Works, 138 p.

- Dunn, J.R. and Hudec, P.P., 1972, Frost and Sorption Effects in Argillaceous Rocks: Highway Research Record, No. 393, pp. 65-78.
- Franklin, J.A.,; Broch, E.; and Walton, G., 1970, Logging the Mechanical Character of Rock: Rock Mechanics Research Report D-14, Imperial College, London, England
- Franklin, J.A. and Chandra, R., 1972, The Slake Durability Test: International Journal of Rock Mechanics and Mining Science, Vol. 9, pp. 325-341.
- Franklin, J.A., 1981, A Shale Rating System and Tentative Applications to Shale Performance: Transportation Research Record, No. 790, pp. 2-12.
- Hale, B.C., 1979, The Development and Application of a Standard Compaction-Degradation Test for Shales: Unpublished MS Thesis, Purdue University, West Lafayette, IN, 180p.
- Harper, T.R.; Appel, G.; Pendleton, M.W.; Szymanski, J.S.; and Taylor, R.K., 1979, Swelling Strain Development in Sedimentary Rock in Northern New York: International Journal of Rock Mechanics and Mining Science and Geomechanics Abstracts, Vol. 16, pp. 271-292.
- Hopkins, T.C. and Deen, R.C., 1984, Identification of Shales: Geotechnical Testing Journal, American Society of Testing and Materials, Vol. 7, No. 1, pp. 10-18.
- Hudec, P.P., 1978, Development of Durability Tests for Shales in Embankments and Swamp Backfills: Project 1313, Ontario Joint Transportation and Communications Research Program, Report R12 216, Ontario, Canada, pp. 1-51.

- International Society of Rock Mechanics, Commission on
Standardization of Laboratory and Field Test, Committee on
Laboratory Tests, 1979, Suggested Methods for Determining
Water Content, Porosity, Density, Absorption and Related
Properties and Swelling and Slake-Durability Index
Properties: International Journal of Rock Mechanics and
Mining Science and Geomechanics Abstracts, Vol. 16, No. 2,
pp. 148-156.
- Lutton, R.J., 1977, Design and Construction of Compacted Shale
Embankments, Vol. 3, Slaking Indexes for Design: Report No.
FHWA-RD-77-1, FHA, Washington, DC, 87 p.
- Moriwaki, Y., 1966, Causes of Slaking in Argillaceous
Materials: Unpublished PhD Dissertation, University of
California-Berkeley, Berkeley, CA, 290 p.
- Noble, D.F., 1977, Accelerated Weathering of Tough Shales, Final
Report: Virginia Highway and Transportation Research Council,
Charlottesville, VA, No. VHTRC 78-R20, 38 p.
- Oakland, M.W. and Lovell, C.W., 1982, Classification and Other
Standard Tests of Shale Embankments: Joint Highway Research
Project Report 82-4, Purdue University, West Lafayette, IN,
171 p.
- Rehbinder, P. and Lichtman, V., 1957, Effect of Surface Active
Media on Strains and Rupture in Solids: Proceedings of the 2nd
International Congress on Surface Activity, Vol. 3,
pp. 563-582.

Richardson, D.N., 1984, Relative Durability of Shale, Unpublished PhD Dissertation, Civil Engineering Department, University of Missouri-Rolla, Rolla, MO, 315 p.

Richardson, D.N. and Long, J.D., 1985, The Sieve Slake Durability Test: publication pending.

Russell, D.J., 1982, Controls on Shale Durability: The Response of Two Ordovician Shales in the Slake Durability Test: Canadian Geotechnical Journal, Vol. 19, No. 1, pp. 1-13.

Sickler, R.A., 1981, Testing and Rock Classification of Fine-Grained Earth Material: Unpublished MS Thesis, Geological Engineering Department, University of Missouri-Rolla, Rolla, MO, 158 p.

Strohm, W.E., 1978, Design and Construction of Compacted Shale Embankments, Vol. 4: Field and Laboratory Investigations, Phase III, Report No. FHWA-RD-78-140: FHA, Washington, D.C., 146 p.

Strohm, W.E.; Bragg, G.H.; and Ziegler, T.W., 1978, Design and Construction of Compacted Shale Embankments, Vol. 5: Technical Guidelines, Report No. FHWA-RE-78-141: FHA, Washington, D.C., 207 p.

Taylor, R.K. and Spears, D.A., 1970, The Breakdown of British Coal Measure Rocks: International Journal of Rock Mechanics and Mining Science, Vol. 7, pp. 481-501.

Terzaghi, K. and Peck, R.B., 1967, Soil Mechanics in Engineering Practice, 2nd Edition, John Wiley and Sons, Inc., New York, NY, 729 p.

Van Eeckhout, E.M., 1976, Mechanisms of Strength Reduction Due to
Moisture in Coal Mine Shales: International Journal of Rock
Mechanics and Mining Science and Geomechanics Abstracts,
Vol. 13, pp. 61-67.

APPENDIX
INDEX OF CRUSHING

Testing Parameters:

1. Gradation prepared according to:

$$P = 100 (d/D)$$

where P = percent passing a given sieve

d = size of sieve opening

D = largest size sieve opening in gradation

2. Compactive effort:

5.5 lb. hammer

12 in. drop

25 blows/layer

3 layers

4 in. diameter mold

3. Maximum particle size = 3/4 in.

4. Moisture content = natural

5. Sieves: 1-1/2", 3/4", 3/8", #4, #10, #20, #50, #100

EVALUATIONS OF GEOTECHNICAL DESIGNS
FOR SHALE EMBANKMENT CORRECTIONS

BY

WILLIAM E. MUNSON, P.E.

TRANSPORTATION ENGINEER

KY DEPARTMENT OF TRANSPORTATION

Beginning shortly after its construction in the late 1950's, I-75 in north central Kentucky has been plagued with embankment landslides, large fill settlement and splitting pavements. In response to these problems the Geotechnical Branch became involved in extensive investigations of forty-nine miles of the Interstate.

The geology of the problem area has been well documented through the years. The materials used to construct the embankments come from the Bull Fork, Fairview and Kope Formations which can be described as interbedded shale and limestones. The percentages of shale ranges from about 40 to 80. The limestone beds are generally one foot or less in thickness.

During the construction of the embankments there were difficulties in breaking down the shales because of the flaggy limestone slabs. The slabs caused the compaction equipment to bridge over the softer materials, leaving voids to be filled with water. This in turn caused the shales to become soft and change in volume. During construction it was close to the edges of the slopes and around drainage structures. This problem may have also led to shallow failures on the slopes later on.

In the mid 1970's the Division of Materials began an engineering study of the problems for the purpose of diagnosing the problems and designing to correct them. In addition the knowledge gained would be used in future projects to eliminate many of these same problems. The subsurface exploration and field investigation provided a bounty of data for use in determining the soils conditions. One of the first points which became apparent is that embankments over thirty feet high with 2:1 side slopes and tend to become unstable in the long term. The nature of the shales themselves in combination with compaction and drainage problems made a 2:1 slope overly steep for embankments above this height.

A typical example of the drainage problem is an embankment with a sizeable quantity of water flowing out of it about halfway up the slope. When seen from the roadway, the median ditch is very wet. Water does not make its way to drainage boxes to be piped away. Settlement of the embankment and erosion around the median drainage structures has left many opportunities for water to stand or flow down beside the structures. In most all cases 3 to 6 inch gaps have developed at the upstream edges of the inlet structures leaving them dry.

Calculating the degree of saturation of the samples taken from the slopes and center of the embankment, we found a "zone of saturation" corresponding rather closely to the location of seepage on the fill slopes. The zone was typically 15 to 25 feet higher than the groundwater measured in observation wells. Refer to Figure 1.

The data obtained from Consolidation Undrained Triaxial Tests was used for the analyses of the existing (failing) conditions and for the design of corrections. The average triaxial strength parameters based on 336 stress paths for the I-75 Embankment Study were $\phi = 24.7^\circ$, $c = 5.3$ and $C = 368$ psf, $\sigma = 252$ psf. Existing condition analyses using average strength parameters and observed water tables did not adequately model the known failing conditions. Our analyses produced safety factors of 1.7 to 2.0 using these parameters. When the strength parameters were reduced by one standard deviation and the zone of saturation was used as the water table, safety factors of 0.85 to 1.0 were obtained. The strength parameters of $\phi = 19$ and $C = 100$ to 150 psf closely match the assumed strength parameters for soil-like shale based on Slake Durability Index Tests, $\phi = 20$, $C = 200$ psf.

The reason for designing corrective measures using the "elevated" water table was the probability that the saturation zone would produce pore pressures periodically. In this way the corrective designs would have to adequately counteract the detrimental effects of higher water pressures within the slopes.

The purpose of the drainage blankets under the berms is to prevent a water table or saturation zone from building up in them.

The first corrective designs were made with some rather severe constraints. Right of way acquisition was to be avoided as well as disturbing the pavement guardrail, and traffic. Also, economics constrained us to a 30 percent increase in safety factor ($F.S. = 1.3$) for the corrected slope. With the use of tighter controls on construction and internal drainage, we thought that we could produce a design to satisfy these limitations.

The original concept was to construct embankment benching with a one foot natural sand drainage blanket wrapped in geotextile. The benching was designed on an effective 1:1 slope. Typically the benching was to run about halfway up the slope. By this measure 10 to 20 feet of the toe was excavated with the drainage blanket to force the saturation zone farther back from the proposed berm. Berm widths ranged from a 15 foot minimum on smaller embankments up to 30 feet on larger ones. See Figure 2.

Construction of the slide corrections began in the fall of 1982. The embankments undergoing repair ranged in height from 40 to 80 feet. Problems and contractor complaints arose quickly over the construction of the embankment benching and drainage blankets. The rubbly shale fill material of which the embankments were constructed was extremely difficult to excavate for drainage benches. The large limestone slabs tended to rip out irregular backslopes on the benches.

Heavy seepage also caused the soil to slump, making the benches fail. During the construction operations it was noticed that the front six to ten feet of the embankment bench cracked vertically, causing some benches to fail. The main cause of this was attributed to heavy equipment passing back and forth over the benches during excavation.

In the early spring of 1983 twelve inches or more of rain fell in less than two weeks. The partially completed drainage blankets were overloaded by the heavy runoff, raising much concern about the capability of the natural sand and geotextile to carry water. The natural sand is not capable of carrying quantities of water beyond that seen in normal seepage, so the heavy runoff caused problems.

Shortly after their completion two of the larger embankments began to fail. Soil samples were taken and slope inclinometers were installed to determine the failure mechanisms taking place. Sliding was detected to four to six feet below the reported bench elevation. This led us to believe that the benching may have weakened the existing slope. A sliding surface apparently formed in this disturbed zone around the benching. Observation wells indicated that water levels stayed below the drainage blankets on the benches as well.

Another cause for concern was the wet material observed going into the construction of the berms. Several slide corrections were subsequently sampled and instrumented. Numerous samples were tested for in-place density, unconfined compressive strength and optimum moisture and density.

A total of 45 undisturbed samples were tested in this way. In general the densities were expressed as a percentage of the average maximum dry density from various standard compaction tests. Similarly the moisture contents were expressed as percentages above or below the average optimum moisture content. The unconfined compressive strength were converted to cohesion ($\phi = 0$ assumption, $C = 1/2 q_u$). Statistical analyses were performed with the SAS (Statistical Analysis System) fitting three-dimensional surfaces with the General Linear Model procedure. The axes for the plot were moisture, density and cohesion. Cohesion was modeled as a surface based on a complete quadratic fit of the form:

$$C = A_0 + A_1M + A_2D + A_3M^2 + A_4D^2 + A_5MD$$

where:

C = cohesion (psf)

M = moisture above/below optimum (%)

D = density as percent of standard compaction

A_i = coefficients fit by SAS

The fitted values were plotted as a contour plot using the SAS plot procedures with contour option. See Figure 4 for the contour plot. Note that the contour plot was based entirely on fitting of lab test data from field samples, not on theoretical considerations. The actual contour relationships may be another form other than quadratic, however, the graph shows that soil strength is controlled by a combination of compactive effort and moisture content. The plot simply shows the potential for higher soil strengths is contingent on soils being compacted very near optimum moisture and receiving full compactive effort.

Although the contour plot in Figure 4 shows the general trends, it is not completely realistic because of the unrealistically high densities at low and high moisture contents.

A composite moisture-density curve was superimposed on the contour plot to eliminate unrealistic densities. Figure 5 represents the strengths which may be expected on the moisture-density curve for full compaction. The curve is significant also because it illustrates the drop in strength that can be expected for moisture contents above or below optimum at any amount of compactive effort. An example is seen at 4 percent below optimum moisture at 95 percent maximum, acceptable by current standards. The resulting loss of 20 percent of strength compared to the optimum conditions shows how dangerously low safety factors can become when designing for safety factors assumed to be 1.3. A 20 percent drop on a 1.3 safety factor means failure.

A Special Note for Shale Embankments was developed for soil-like and intermediate shale materials used to construct embankments. Refer to the Special Note at the end of this paper. The Special Note requires that all soil-like and intermediate shales be compacted with a vibratory-foot roller. The weight of the roller, embankment lift dimensions, and moisture content control are specified in the note.

In addition new designs were made for an increasing safety factor of 1.5. Still using our "average typical" strength parameters, design charts were made for berm widths to vary proportionally to embankment heights. The designed berm slopes were also flattened to 3:1 from 2:1. See Figure 6.

Our engineering design assumptions were, in most instances, confirmed by our experiences on construction of slide corrections on I-75. In other cases we had to change them in order to meet the realities of conditions on construction.

Our assumptions were apparently verified in the use of our strength parameters. For example, the results of soil strength testing, when applied in slope analyses with saturated zones, gave some very close approximations to actual field conditions. We also saw that our assumptions about maximum fill heights born out with a couple of large berms failing on construction.

We were forced to change other details of the designs and some of our assumptions based on what did not work in the field. We found that embankment benching was not easily constructed due to the rocky material in the fills and may have actually caused new problems by damaging existing slopes. Random boulders caused large voids or cracks in the benches when they were pulled out by excavating equipment. The damage seems to be part of the reason for slope failures after the slide corrections were complete. Later experience proved to us that a 2 foot natural sand drainage blanket laid on the existing slope caused fewer problems on construction.

The bottom portion of the drainage blanket was also altered to use one foot of crushed rock wrapped in geotextile. This helps water to drain more quickly once it reaches the base of the berm. Rock toe drains were also added to replace perforated pipe which are hard to locate for proper drainage and prone to be crushed during construction.

Controlling the moisture and density of the shale being placed in the embankments may have been almost as much as a problem as it was on the original construction. Moisture-density-soil strength relationships indicated a very narrow band of moisture contents which a slope design must have to operate properly. Our experiences led us to change the specifications for embankment construction to include moisture contents as well as dry densities for controlling acceptability.

In order to cover the unavoidable moisture-density control problems which must surely occur undetected on any projects, the minimum safety factor for corrected slopes had to be raised to 1.5. Appreciable costs for the added safety factor do not really add up until embankments exceed 50 feet in height. At this point the costs could be justified by the amount of inconvenience and safety for the public if such an embankment failed.

SPECIAL NOTE FOR COMPACTION OF SHALE EMBANKMENTS

I. DESCRIPTION

This work shall consist of constructing and compacting embankments composed predominately of soil-like shale and/or intermediate shale (SDI less than 95 by KM 64-513) when designated on the plans, utilizing the construction techniques specified herein. These requirements are in addition to Sections 207 and 208 of the current Standard Specifications for Road and Bridge Construction.

II. CONSTRUCTION REQUIREMENTS

Soil-like shale, intermediate shale, and/or these materials interbedded with thin seams (less than 4 inches thick) of harder rock shall be compacted utilizing an approved static tamping-foot roller in conjunction with a vibratory tamping-foot roller. The minimum weight for the static tamping-foot roller shall be 60,000 pounds. The minimum total compactive effort for the vibratory tamping-foot roller shall be 55,000 pounds. Total compactive effort is defined as that portion of the static weight acting upon the unsprung compaction drum added to the "Centrifugal Force" provided by that drum. If the manufacturer's charts do not list the static weight acting upon the compaction drum, the Contractor will be required to have the roller weighed to the satisfaction of the Engineer, and that weight shall be added to the Centrifugal Force, rated in accordance with the Construction Industry Manufacturer's Association (CIMA). Each tamping-foot on the static roller shall project from the drum a minimum of 6 inches. Each tamping-foot on the vibratory tamping-foot roller shall project from the drum a minimum of 4 inches. The surface area of the end of each foot on each roller shall be no less than 5 1/2 square inches.

Shale shall be placed in 8 inch maximum loose lifts to the full width of the cross section. Excavation and blasting procedures shall accommodate the selective placement of the material. Each lift shall be bladed as required prior to compaction to ensure uniform layer thickness. Large rock fragments or limestone slabs having thickness greater than 4 inches and/or any dimension greater than 1 1/2 feet shall be removed from the layer to be compacted, or broken down and then incorporated into the lift.

If the shale is dry, the Contractor shall apply water to accelerate the slaking action (breakdown) and to facilitate compaction. The water shall be distributed by an approved method which provides uniform application of the required quantity of water. The water shall be uniformly incorporated throughout the entire lift by a multiple gang disk with a minimum disk wheel diameter of 24 inches. The amount of water shall be that required to achieve a moisture content of optimum ± 2.0 percent as determined by KM 64-511. This moisture content requirement shall have equal weight with the density requirements specified herein when determining the acceptability of a layer. Moisture content tests will be conducted at such a frequency as deemed necessary to assure that the entire layer conforms to the specified moisture content.

SPECIAL NOTE FOR
COMPACTION OF SHALE EMBANKMENTS

Unless otherwise approved in writing by the Engineer, each embankment lift shall receive a minimum of 3 passes with the static roller followed by blading and a minimum of 2 passes with the vibratory roller. The rollers shall not exceed 3 mph during these passes. Each embankment layer shall be compacted to a minimum of 95 percent of maximum dry density as determined by KM 64-511. The number of passes will, at the direction of the Engineer, be adjusted upward if necessary to obtain 95 percent of maximum dry density.

The in-place density will be determined by KM 64-512 or by using nuclear gages. Tests will be conducted at such a frequency as deemed necessary to assure that the entire layer is compacted to the specified density.

II. METHOD OF MEASUREMENT

No separate measurement or payment will be made for compaction, as specified herein. Payment for all labor, machinery, materials, and other costs associated with the compaction of shale embankments to the specified density, except water, is considered incidental to earthwork items in the contract.

Water used as directed for providing the specified moisture will be measured by weight or volume (tank capacity or meter) and converted to 1,000 gallon units.

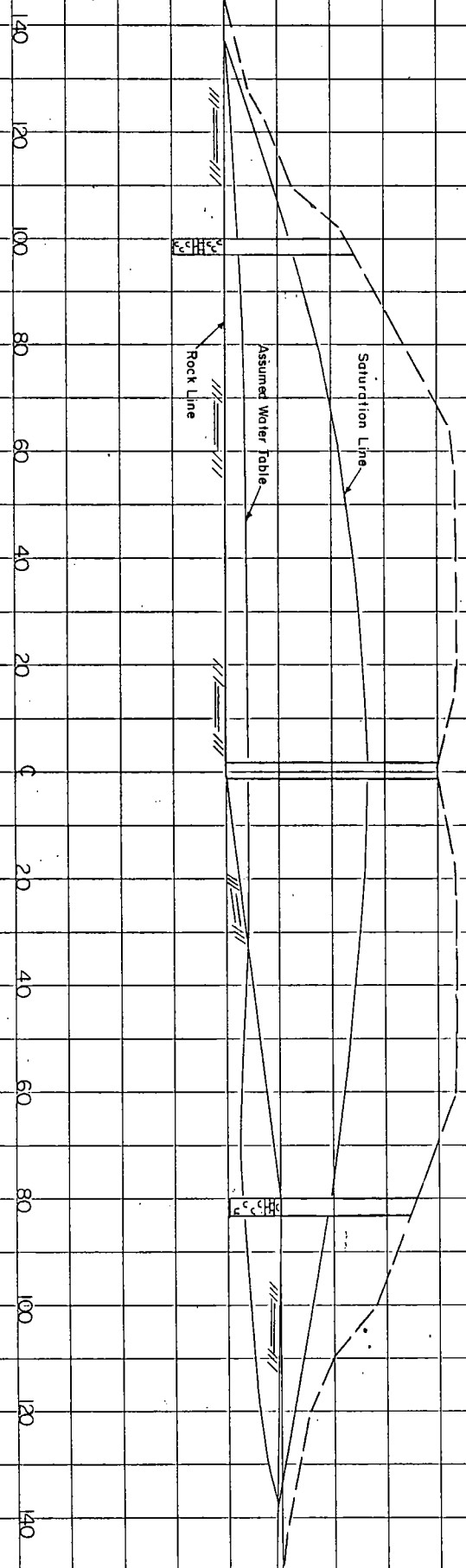
IV. BASIS OF PAYMENT

The accepted quantity of water will be paid for at the contract unit price per 1,000 gallon unit, which shall be full compensation for all work necessary to furnish and properly apply and incorporate the water.

March 27, 1985

FIGURE 1
TYPICAL SATURATION CONDITION

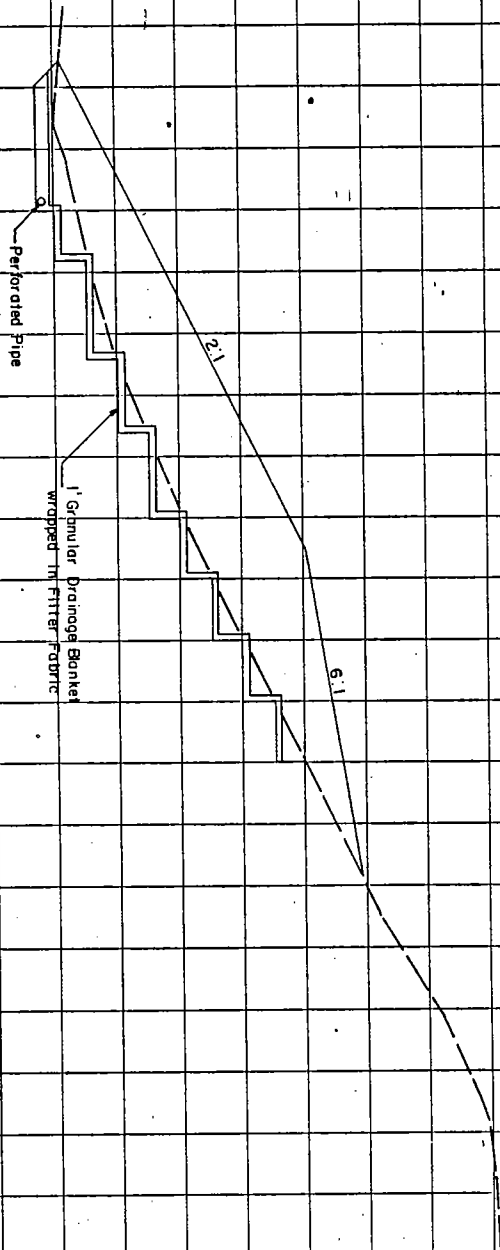
TYPICAL SATURATION CONDITION



COUNT OF	WATER TABLE	WATER LEVEL	TOTAL WATER

FIGURE 2
TYPICAL CORRECTION ON
ORIGINAL DESIGN PROJECT

TYPICAL CORRECTION ON ORIGINAL DESIGN PROJECT



890
880
870
860
850

200

150

100

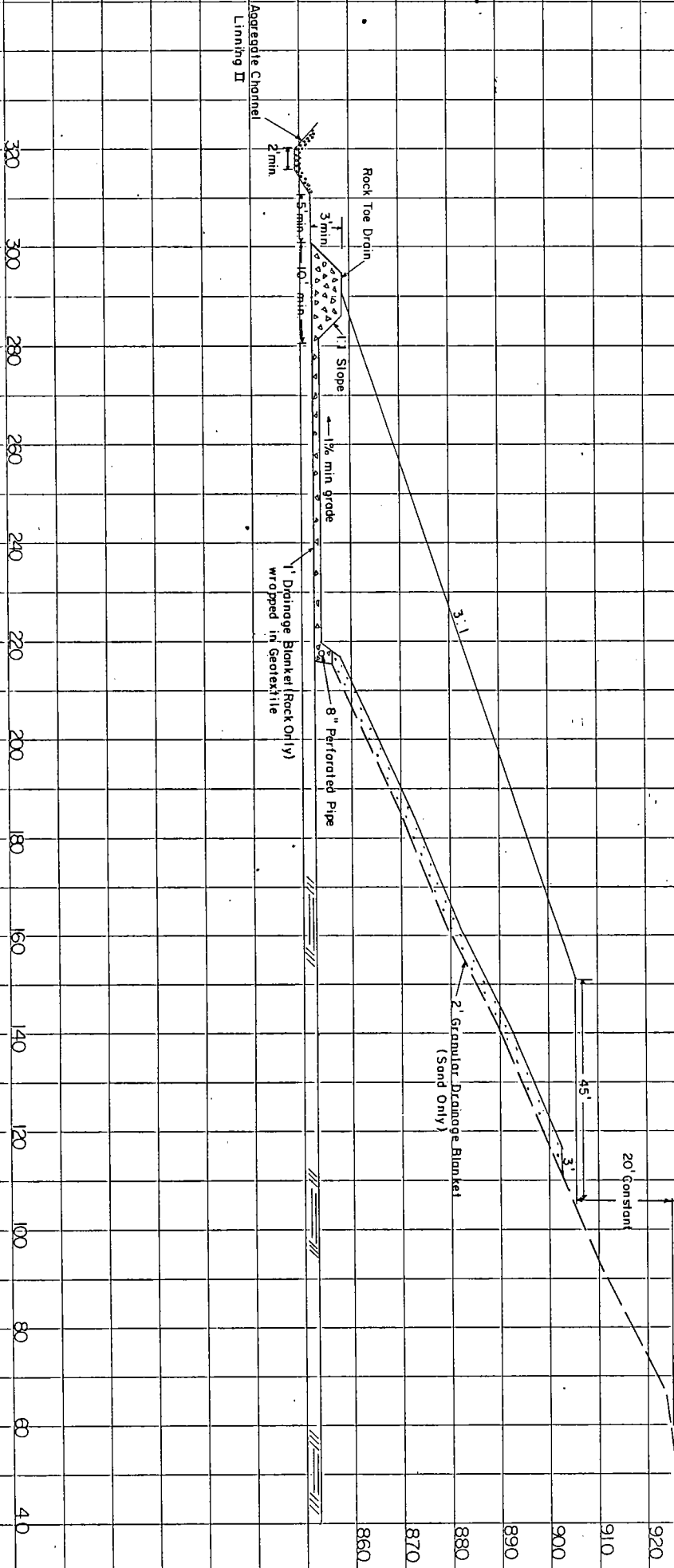
50

0

DATE	BY	CHKD	APP'D

FIGURE 3
TYPICAL REVISED CORRECTION DESIGN

TYPICAL REVISED DESIGN



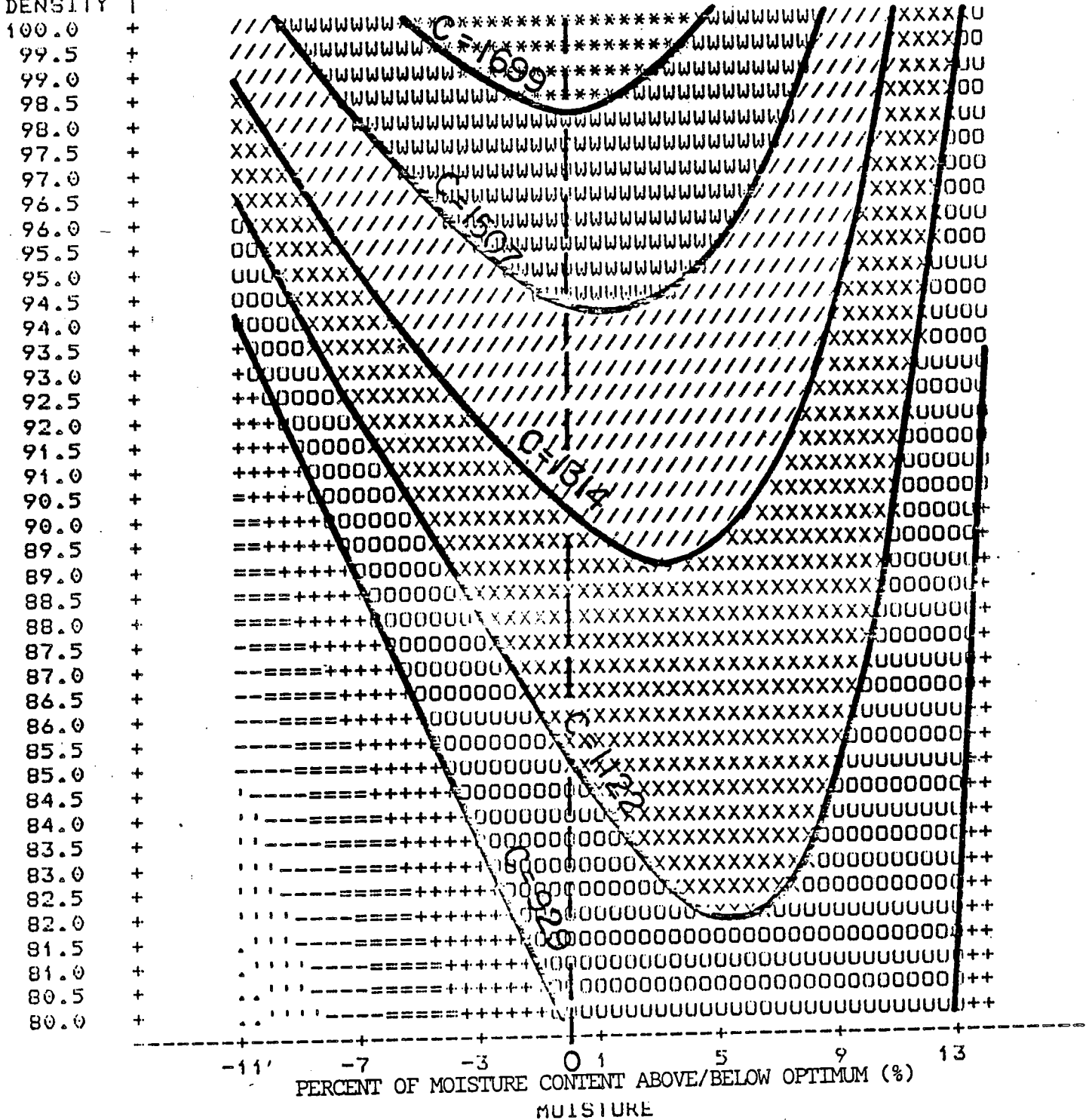
COORDINATE	FEET	INCHES	FEET	INCHES

FIGURE 4
PLOT OF MOISTURE-DENSITY
VS.
COHESION

MOISTURE-DENSITY VS. COHESION

PERCENT OF
STANDARD
COMPACTION
DENSITY 1

CONTOUR PLOT OF DENSITY*MOISTURE
CONTOURS ARE COHESION = $Q_u/2$ (PSF)



SYMBOL	COHESION	SYMBOL	COHESION
.....	63.73809 - 159.93005	UUUUUU	929.46573 - 1121.84965
	159.93005 - 352.31397	XXXXXX	1121.84965 - 1314.23357
-----	352.31397 - 544.69789	//////	1314.23357 - 1506.61749
=====	544.69789 - 737.03181	WWWWW	1506.61749 - 1699.00141
	737.03181 - 929.46573	UUUUUU	1699.00141 - 1795.19537

FIGURE 5
PLOT OF SOIL STRENGTH
CONTOURS ON MOISTURE-DENSITY
CURVE

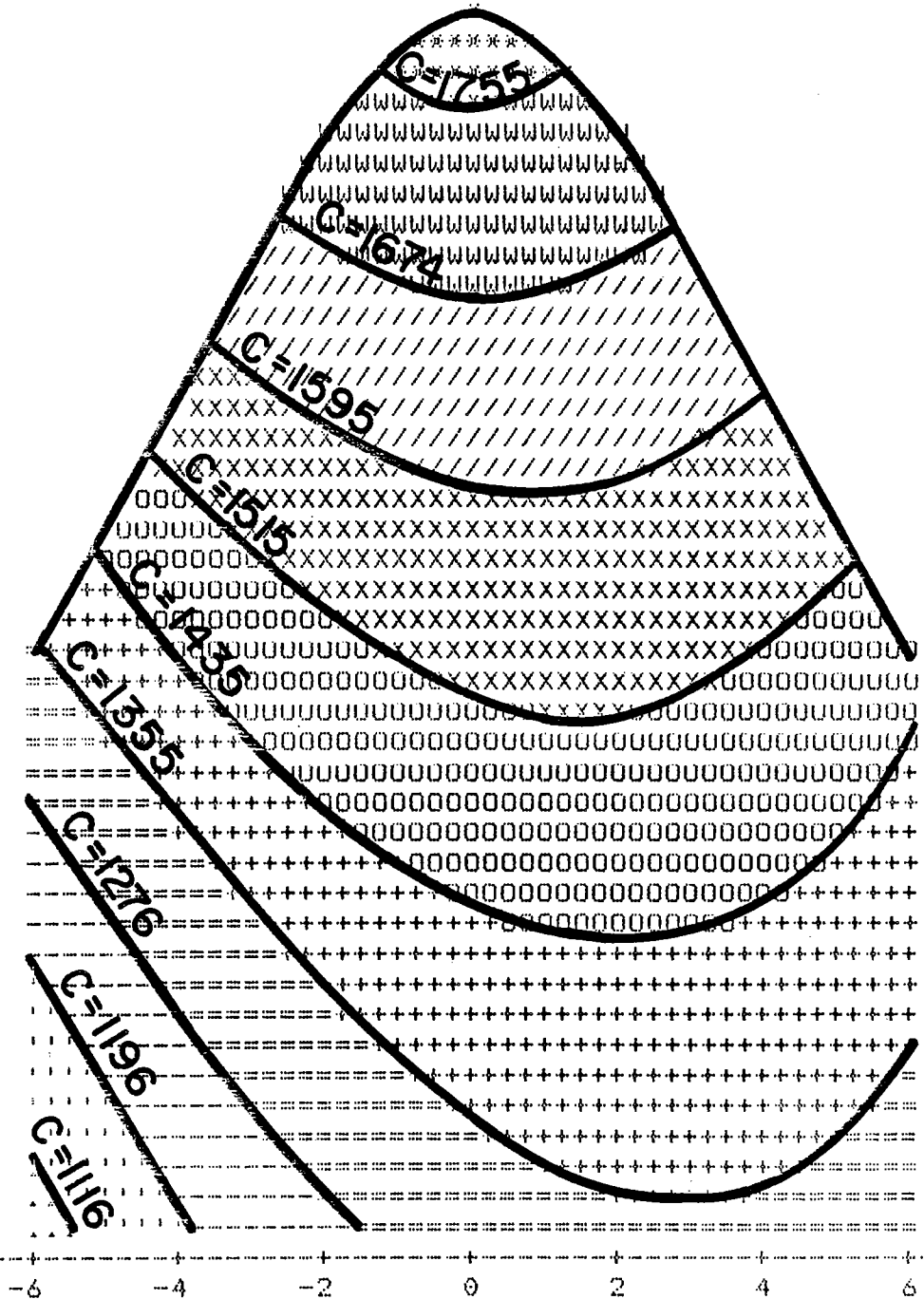
MOISTURE-DENSITY VS. COHESION

PERCENT OF
STANDARD
COMPACTION

DENSITY |

100.00 +
99.75 +
99.50 +
99.25 +
99.00 +
98.75 +
98.50 +
98.25 +
98.00 +
97.75 +
97.50 +
97.25 +
97.00 +
96.75 +
96.50 +
96.25 +
96.00 +
95.75 +
95.50 +
95.25 +
95.00 +
94.75 +
94.50 +
94.25 +
94.00 +
93.75 +
93.50 +
93.25 +
93.00 +
92.75 +
92.50 +
92.25 +
92.00 +
91.75 +
91.50 +
91.25 +
91.00 +
90.75 +
90.50 +
90.25 +
90.00 +

CONTOUR PLOT OF DENSITY*MOISTURE
CONTOURS ARE COHESION = $\frac{1}{2} Q_u$ (PSF)

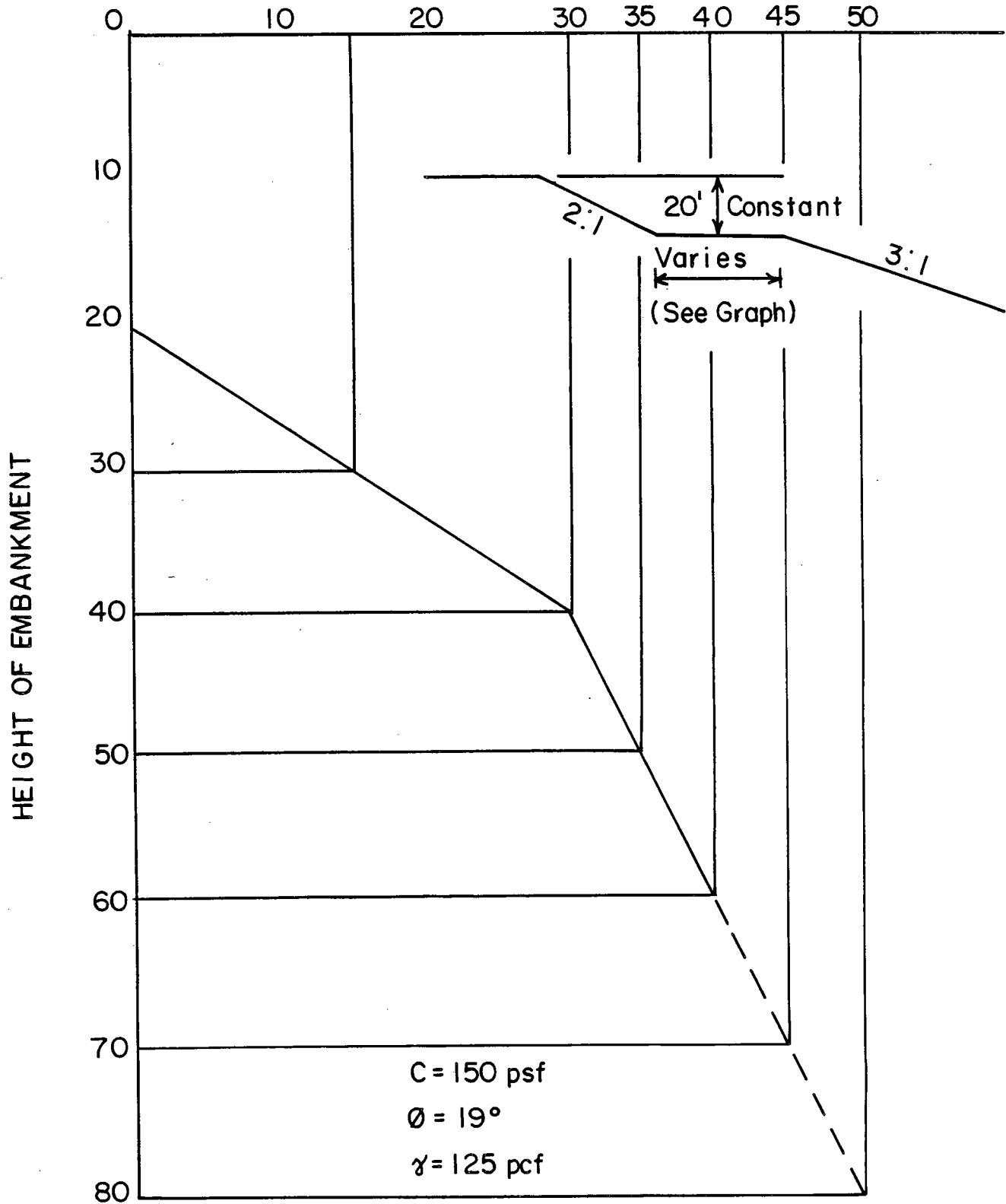


PERCENT OF MOISTURE CONTENT ABOVE/BELOW OPTIMUM
MOISTURE

SYMBOL	COHESION	SYMBOL	COHESION
.....	1075.904 - 1115.833	000000	1435.264 - 1515.121
.....	1115.833 - 1195.691	XXXXXX	1515.121 - 1594.979
-----	1195.691 - 1275.548	////////	1594.979 - 1674.837
-----	1275.548 - 1355.406	WWWWW	1674.837 - 1754.695
+++++	1355.406 - 1435.264	*****	1754.695 - 1794.623

FIGURE 6
GRAPH OF BERM WIDTH
VS. EMBANKMENT HEIGHT

WIDTH OF BERM



ASSUMING WATER TABLE AT TOP
OF DRAINAGE BLANKET.

USE OF NEW ALBANY SHALE FOR SUBGRADE AND PAVEMENT STABILIZATION

By
Mark J. Schuhmann¹, P.E.
and
Nicholas G. Schmitt², P.E.

Many sites in the Louisville area, particularly in south-central and southwestern Jefferson County, are poorly drained with seasonally high water levels at or near the ground surface. Site trafficability is very difficult for even track-mounted equipment. Many of these sites are poor to marginal from a geotechnical viewpoint, particularly for the construction of pavement systems. Typical flexible pavement designs, based on saturated California Bearing Ratio test results of remolded samples, indicate that parking areas with light traffic may require only a pavement system of 8 to 10 inches of crushed stone base overlain by 2 to 3 inches of asphalt. More heavily-loaded pavement systems such as, distribution centers, Class B connector roads, and main traffic lanes result in pavement designs of 10 to 18 inches of crushed stone overlain by 3 to 4 inches of asphalt paving. The site trafficability problems during construction make the installation of such flexible pavement systems nearly impossible using normal construction practices. In addition, severe construction traffic loading (concrete trucks, loads of building supplies, and even pavement materials) are excluded from the typical flexible pavement design. Because of these problems and other design and site development requirements, "shot" New Albany shale has been used as part of the flexible pavement design and as a site improvement and stabilization media.

New Albany shale is described in published geologic literature as a silty carbonaceous, olive to grayish-black, massive shale that weathers to thin brittle chips. The formation is of the Devonian

¹Office and Engineering Manager, Law Engineering Testing Company, Louisville, KY

²Chief Engineer, Law Engineering Testing Company, Nashville/
Louisville Branch

system. Normal quarrying operations produce a well graded stone with particle dimensions varying from about 1 to 36 inches. The material breaks down into "platelets" with lengths and widths much greater than its thickness. Due to its brittle nature, it can be further "broken-down" during placement by construction traffic. Experience indicates the material is somewhat resistant to solution weathering, especially after the surface is covered with paving or a structure.

The random nature of the materials particle distribution, its large particle size (maximum dimension about 36 inches), and the variability of subsurface conditions, makes creating a standard for design, evaluation, and application of "shot" shale fill very difficult and problematical. In addition, the subsurface conditions vary dramatically from site to site and the difference in construction considerations and planned site usages make it difficult to correlate experiences from one site to the next. Therefore, an engineer must rely on experimentation, previous experience, engineering judgement, and engineering intuition in order to outline a design criteria and placement program which will address his particular needs on a particular project site.

This report presents our findings and experience on two particular sites in Jefferson County. These two sites were chosen to show different applications in the use of crushed shale for pavement and site subgrade stabilization.

Site I

Site I consists of a two-story, multi-unit housing development and a Class B county connector road. The subsurface conditions consist of an upper veneer of organic laden clayey silt underlain by firm to stiff, tan and gray, silty clay and clayey silt. Standard penetration resistances within the overburden soils varied from about 5 to 10 blows per foot with an average of about 9 blows per foot. Unified Soil Classification of these materials

varied from ML to CL; clayey silts and silty clays of low plasticity. Moisture contents were typically at or above the plastic limit and oftentimes approached the liquid limit. The site was nearly level with poor surface drainage characteristics. Groundwater levels at the time of our studies were at or near the ground surface.

The materials provided sufficient supported for soil supported foundations for the apartment dwellings, however, site trafficability problems and excessive construction traffic loading of the Class B interceptor road during the construction of these units required the use of shot shale for pavement stabilization. We recommended that a shale haul road consisting of a loose 4 foot thickness of shale be placed along the centerline of the Class B roadway and construction traffic was to use this haul road throughout the construction process. Once the apartment units were completed, the shale haul road could be thinned to the planned 2 foot thickness with the extra material used to stabilize the parking areas and the pavement section constructed.

The contractor, however, chose not to create a haul road and placed up to 3 feet of no. 3 stone along the connector road route. The stone placed was of insufficient thickness to withstand severe construction equipment loading, the area deteriorated with usage, and the stone base became contaminated with silty clay. In addition, other areas adjacent to the road deteriorated with traffic and by the time the apartment units were constructed, the Class B connector road route had been rutted severely and had deteriorated to very very poor conditions. The local fire marshall threatened to shut down the project because fire fighting equipment could not traverse the site.

Two alternatives for remediation seem reasonable: excavate and remove the deteriorated material, dry it, and replaced and compacted in thin lifts; or remove the material and replace with sufficient shale thickness to support the paving operations. Due to approaching inclement weather, time, and monetary constraints it was decided to excavate the poor materials to a depth of approximately 2 to 4 feet, place the shale, and construct the pavement system.

It was decided to use the shale subgrade system. At a depth of about 2 feet, the subgrade soils were of insufficient strength to support other than track-mounted, construction equipment, therefore, the undercutting was done in two fashions: in excessively poor quality areas, the undercutting was done by gradall or large track-mounted backhoe which excavated an adjacent strip; in areas of marginal quality, the excavation was performed by track-mounted dozers and front end loaders. However, in both applications, the shale was end-dumped and pushed in place with the dozer. Once in place, the ensuing truck loads of shale could use the 4 foot shale paved road as a haul road, but the materials were always end-dumped and pushed in place.

Site II

Site II consists of a large warehouse style retail center in southwestern Jefferson County. The eastern portions of the site were paved with the western portions covered with debris and some ponded water. Surface drainage was excessively poor and even our all-terrain drill could not reach the planned boring locations. Surface drainage could not be enhanced during the construction process, because storm water systems owned by the county would not be completed until late in the construction phase of the project.

Subsurface conditions consisted of miscellaneous saturated fills to a depth of about of 5 to 7 feet. The subsurface conditions

are described in more detail on the attached boring logs. Site conditions were too poor for structural support within the debris fill, and based on extensive discussions with our client, it was decided to remove the debris from within the building area. However, a flexible pavement system consisting of geotextile, 22 inches of crushed stone, and 2-1/2 inches of asphalt paving was selected for the site.

The building area was excavated using a large, track-mounted backhoe excavating the site in strips. All the debris-laden material was removed and a sump was dug in one corner of the building area to allow for control of groundwater infiltration into the excavation. The excavation exposed a firm, tan and gray, silty clay which would pump and rut and deteriorate by passage of rubber-tired construction equipment. The material also pumped excessively due to the passage of track-mounted high-lifts or dozers.

To stabilize the subgrade in the building area and allow for the placement of engineered fill, shot New Albany shale was placed by end-dumping and spreading operations. The average thickness of the placed shale was on the order of 12 inches. The next step was to place the engineered fill with the first lift of fill consisting of bankrun sand and gravel, end-dumped, and spread in place by a dozer and compacted with a vibratory, steel-wheeled roller, however, the vibrating activator was not used. After placement of 1 to 2 lifts of sand fill, the vibrating equipment was used and the fill was brought to floor slab subgrade elevation. The building was supported on shallow, soil-supported footings supported in the sand and gravel fill.

The pavement system presented a completely different assortment of geotechnical problems. In addition, the large (approximately 3.5 acres) pavement area would require considerable construction traffic for hauling of debris and paving materials. A test strip was constructed in an area thought to be representative of the

overall site conditions. In this area, the existing site grades were about 6 inches above planned pavement subgrade elevations. Therefore, an area approximately 20 feet wide and 50 feet long was excavated to a depth of 30 inches, filter fabric placed, and 18 inches of crushed stone placed by end-dumping and spreading. The crushed stone was compacted by using the vibratory steel-wheeled roller without using the vibrating activator. During compaction, the rubber-tired drive wheels of the steel-wheeled roller rutted the crushed stone severely. A moderately-loaded dump truck was placed on the area and it too rutted severely.

At that time, a meeting was held between the designer, contractor, and construction managers to develop a new project approach. It was decided that crushed shale would be used to stabilize the subgrade, that with planned thicknesses of crushed shale to vary from 24 to 48 inches. The construction sequence would consist of excavating narrow strips, approximately 10 feet wide, using a large track-mounted backhoe, constructing a temporary haul road using crushed shale for the dump trucks to haul the excavated material off site, and to backfill the excavations with lifts of crushed shale. Originally, it was thought that the initial lift of shot shale would be on the order of 18 inches thick and pushed in place with track-mounted equipment. The ensuing lifts would be about 12 inches thick, pushed in place with track mounted equipment, and then rolled with construction traffic.

The subsurface conditions were so poor that it was very difficult for our project engineer to evaluate when the exposed subgrade, which exhibited a consistency of pea soup, was of sufficient strength for the shale placement system to work. The initial areas were undercut to a depth of 5 to 6 feet; an initial 18 to 24 inch thick lift of shale placed and an additional 12 inch lift of shale placed. When the second strip was excavated, the first strip comprising of a 5 to 6 foot thickness of crushed shot shale backfill began to deteriorate with passage of construction

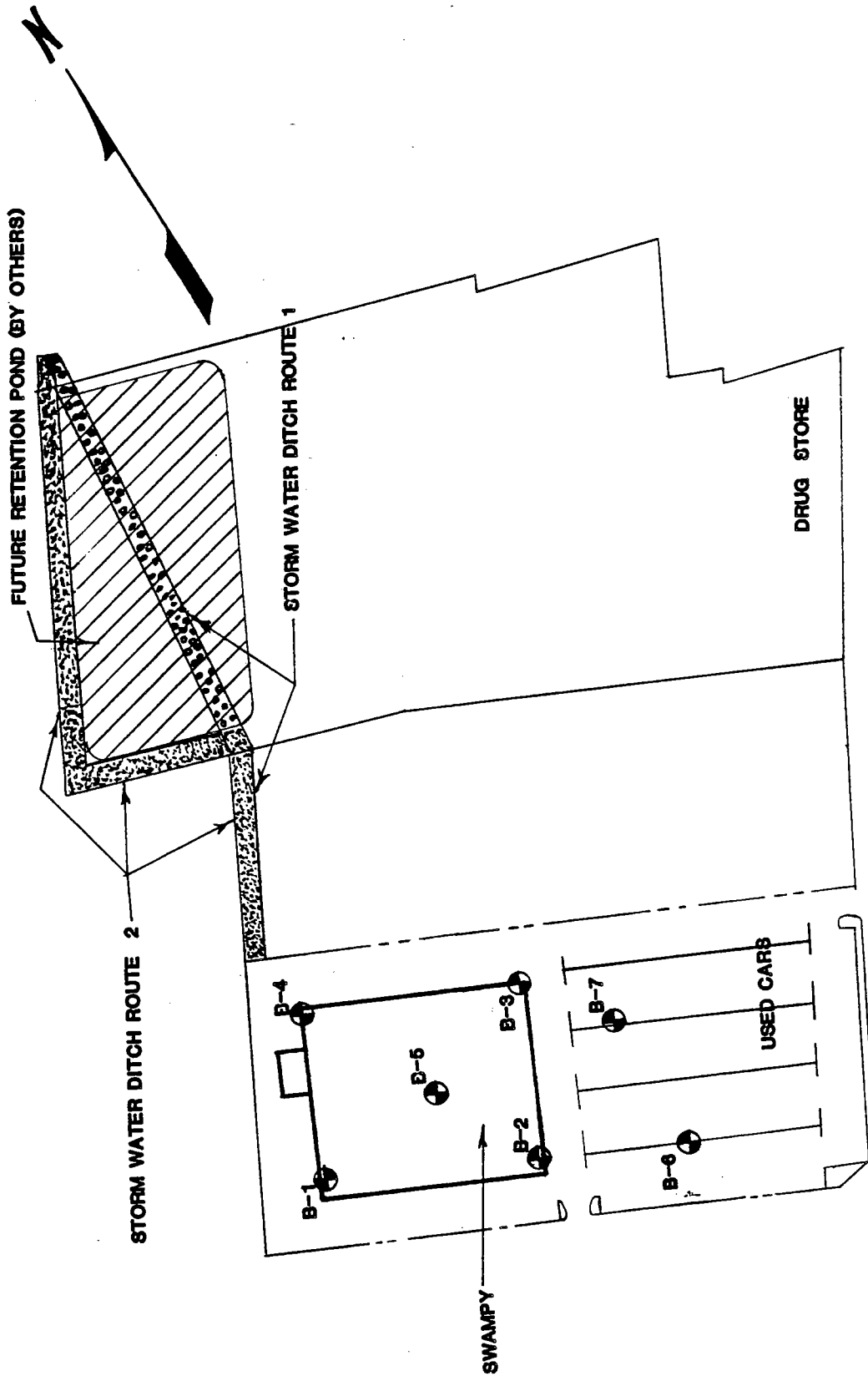
equipment. In the initial areas, the contractor had minimal leeway for varying the path of construction traffic and the deterioration in this area continued.

As additional strips were excavated, it was apparent that soupy conditions would be encountered to depths of at least 7 feet, and that if all the material was removed the owner would be financially unable to continue the construction. Therefore, the first lift thickness was increased to 48 inches thick, placed on the subgrade regardless of the subgrades condition. Strip undercutting was continued, shale was end-dumped and pushed in place using the dozer and a single 48 inch thick lift. Immediately after being pushed in place by the dozer, fully loaded dump-trucks were allowed to traverse the area. Very few, if any, soft spots or areas of deterioration were noted using this placement criteria. As the project continued towards the east, subsurface conditions became somewhat better and the shale thickness was diminished to as little as 24 inches. However, in all cases, the shale was end-dumped and pushed in place by a dozer in a single lift.

CONCLUSION

Based on our experience using "shot" New Albany shale as pavement and subgrade stabilization media, the following conclusions can be made:

- 1) "Shot" New Albany shale can be used effectively for pavement and subgrade stabilization regardless of site conditions.
- 2) Second, no hard and fast rules concerning lift thickness or design thickness can be established at this time. The engineer must base his decisions on previous experience and intuition. The project should be set up to allow for experimentation and flexibility in design.
- 3) Third, no detrimental effects were noticed using a single lift placement criteria with lifts as thick as 4 feet.



SITE & BORING PLAN
DISTRIBUTION CENTER

SCALE NTS
DATE

APPROVED BY

DRAWN BY

REVISED

DIXIE HIGHWAY AREA

Law Engineering Testing Company

DRAWING NUMBER

167
TEST BORING RECORD

DEPTH FEET	DESCRIPTION	ELEVATION	N	W.T. & CORE DATA	PENETRATION RESISTANCE, "N" BLOWS PER FOOT										SCALE- FEET	LABORATORY RESULTS AND REMARKS
0.0	TOPSOIL				0	10	20	30	40	50	60	70	80			
1.0			3	*												
4.0	SOFT Brownish-Gray Silty CLAY with Organics															*
7.5	VERY STIFF Grayish-Brown SILT with Small Roots		27													
10.0	HARD Brownish-Gray Silty CLAY w/ Small Roots		53													
			29												10	
15.5	VERY FIRM Brownish-Black Fine SAND With about 1" Gray-Brown Silt Lense near 14'		25													
	BORING TERMINATED AT 15.5 FEET															
															20	
															30	
															40	

DATE DRILLED 4-18-84
 DRILLING METHOD Hollow Stem
 BORING AND SAMPLING MEETS Auger
 ASTM D 1586
 UNDISTURBED SAMPLING MEETS
 ASTM D 1587
 CORE DRILLING MEETS
 ASTM D 2113

CORE SIZE NQ
 CASING LENGTH -
 WATER TABLE 24 HR.
 WATER TABLE 1 HR.
 BULK (BAG SAMPLE)
 LABORATORY TEST LOCATION,
 SEE LABORATORY TEST RESULTS
 UNDISTURBED SAMPLE

BORING NUMBER B-1
 PAGE 1 OF 1
 JOB NUMBER _____
 CORE DATA:
 LENGTH OF RUN _____
 CORE RECOVERY, % _____
 ROCK QUALITY DESIGNATION, % _____
 LOSS OF DRILLING FLUID _____

168
TEST BORING RECORD



DEPTH FEET	DESCRIPTION	ELEVATION	N	W.T. & CORE DATA	PENETRATION RESISTANCE, "N" BLOWS PER FOOT	SCALE-FT.	LABORATORY RESULTS AND REMARKS
0.0					0 10 20 30 40 50 60 70 80		
1.0	TOPSOIL		10				
5.0	STIFF Brownish-Tan Silty CLAY w/ Wood Fragments near 4.0 feet		12				
	VERY STIFF Mottled Grayish-Tan Silty CLAY with Trace Organics		30				
			31			10	
15.0			21				
	VERY FIRM Orange-Brown Fine SAND With Gray Silty Lense near 19.0 feet		18			20	
20.5	BORING TERMINATED AT 20.5 FEET					30	
						40	

DATE DRILLED 4-17-84
 DRILLING METHOD Hollow Stem
Aguer
 BORING AND SAMPLING MEETS
 ASTM D 1586
 UNDISTURBED SAMPLING MEETS
 ASTM D 1587
 CORE DRILLING MEETS
 ASTM D 2113

CORE SIZE NQ
 CASING LENGTH -
 WATER TABLE 24 HR.
 WATER TABLE 1 HR.
 BULK (BAG SAMPLE)
 LABORATORY TEST LOCATION,
 SEE LABORATORY TEST RESULTS
 UNDISTURBED SAMPLE

BORING NUMBER B-2
 PAGE 1 OF 1
 JOB NUMBER -
 CORE DATA:
 LENGTH OF RUN
 CORE RECOVERY, %
 ROCK QUALITY DESIGNATION, %
 LOSS OF DRILLING FLUID

TEST BORING RECORD

DEPTH FEET	DESCRIPTION	ELEVATION	N	W.T. & CORE DATA	PENETRATION RESISTANCE, "N" BLOWS PER FOOT							SCALE-FT.	LABORATORY RESULTS AND REMARKS
0.0					0	10	20	30	40	60	80		
3.5	VERY STIFF Black SILT with White Silty Debris * near 1.5 Feet		26										
7.0	LOOSE Black SILT with Small Gravel		3										
10.0	HARD Grayish-Brown Tan Silty CLAY		34										
15.5	VERY STIFF Brownish-Gray SILT with Very Fine Sand		21									10	
	BORING TERMINATED AT 15.5 FEET		17										
												20	
												30	
												40	

* - Apparent
Drywall
Fragments

DATE DRILLED 4-18-84
DRILLING METHOD Hollow Stem

BORING AND SAMPLING MEETS Auger
ASTM D 1586
UNDISTURBED SAMPLING MEETS
ASTM D 1587
CORE DRILLING MEETS
ASTM D 2113

CORE SIZE NQ
CASING LENGTH -
WATER TABLE 24 HR.
WATER TABLE 1 HR.
BULK (BAG SAMPLE
LABORATORY TEST LOCATION,
SEE LABORATORY TEST RESULTS
UNDISTURBED SAMPLE

BORING NUMBER B-3
PAGE 1 OF 1
JOB NUMBER -

CORE DATA:
LENGTH OF RUN
CORE RECOVERY, %
ROCK QUALITY DESIGNATION, %
LOSS OF DRILLING FLUID

TEST BORING RECORD

DEPTH FEET 0.0	DESCRIPTION	ELEVATION	N	W.T. & CORE DATA	PENETRATION RESISTANCE, "N" BLOWS PER FOOT	SCALE-FT.	LABORATORY RESULTS AND REMARKS
2.5	LOOSE Black Silt Fill with Organics		3		0 10 20 30 40 50 60 70 80		
5.0	STIFF Gray Slightly Silty CLAY		21				
7.5	VERY STIFF Gray Slightly Silty CLAY With Trace Organics		23				
10.0	STIFF Grayish-Brown Slightly Silty CLAY		12			10	
	FIRM Greyish-Orange Fine SAND with Brown Silt Lense near 15.0 feet		24				
20.0			27			20	
	VERY FIRM Brown Medium SAND						
25.0			34				
	DENSE Coarse Brown SAND With Small Gravel						
29.0							
30.5	FIRM COARSE SAND With Small Gravel		15			30	
	BORING TERMINATED AT 30.5 FEET						
						40	

DATE DRILLED 4-18-84
 DRILLING METHOD Hollow Stem
Auger
 BORING AND SAMPLING MEETS
 ASTM D 1586
 UNDISTURBED SAMPLING MEETS
 ASTM D 1587
 CORE DRILLING MEETS
 ASTM D 2113

CORE SIZE NO
 CASING LENGTH -
 WATER TABLE 24 HR.
 WATER TABLE 1 HR.
 BULK (BAG SAMPLE)
 LABORATORY TEST LOCATION,
 SEE LABORATORY TEST RESULTS
 UNDISTURBED SAMPLE

BORING NUMBER B-4
 PAGE 1 OF 1
 JOB NUMBER 7
 CORE DATA:
 LENGTH OF RUN
 CORE RECOVERY, %
 ROCK QUALITY DESIGNATION, %
 LOSS OF DRILLING FLUID

DATE DRILLED <u>4-17-84</u>	CORE SIZE <u>NQ</u>	BORING NUMBER <u>B-5</u>
DRILLING METHOD <u>Hollow Stem</u>	CASING LENGTH <u>-</u>	PAGE <u>1</u> OF <u>1</u>
BORING AND SAMPLING MEETS	WATER TABLE 24 HR.	JOB NUMBER <u> </u>
ASTM D 1586	WATER TABLE 1 HR.	CORE DATA
UNDISTURBED SAMPLING MEETS	BULK (BAG SAMPLE	LENGTH OF RUN
ASTM D 1587	LABORATORY TEST LOCATION.	CORE RECOVERY, %
CORE DRILLING MEETS	SEE LABORATORY TEST RESULTS	ROCK QUALITY DESIGNATION, %
ASTM D 2113	UNDISTURBED SAMPLE	LOSS OF DRILLING FLUID

*Collected bulk sample from auger cuttings.

**Dry at time of Boring.

BORING NUMBER B-6
PAGE 1 OF 1
JOB NUMBER _____
CORE DATA: _____
LENGTH OF RUN _____
CORE RECOVERY, % _____
ROCK QUALITY DESIGNATION, % _____
LOSS OF DRILLING FLUID _____

TEST BORING RECORD

DEPTH FEET	DESCRIPTION	ELEVATION	N	W.T. & CORE DATA	PENETRATION RESISTANCE, "N" BLOWS PER FOOT								SCALE-FT.	LABORATORY RESULTS AND REMARKS
					0	10	20	30	40	50	60	80		
0.0														
0.4	Asphalt & Sand stone base													
	Brown to Dark Gray Silty Fine SAND			*										
5.0	BORING TERMINATED AT 5.0 FEET			**										
													10	
														*Collected bulk sample from auger cuttings
														**Dry at time of boring.
													20	
													30	
													40	

DATE DRILLED 4-17-84DRILLING METHOD Hollow Stem
AugerBORING AND SAMPLING MEETS
ASTM D 1586
UNDISTURBED SAMPLING MEETS
ASTM D 1587
CORE DRILLING MEETS
ASTM D 2113CORE SIZE NQCASING LENGTH -

WATER TABLE 24 HR.

WATER TABLE 1 HR.

BULK (BAG SAMPLE)

LABORATORY TEST LOCATION,
SEE LABORATORY TEST RESULTS

UNDISTURBED SAMPLE

BORING NUMBER B-7PAGE 1 OF 1JOB NUMBER -CORE DATA:
LENGTH OF RUNCORE RECOVERY, %
ROCK QUALITY DESIGNATION, %
LOSS OF DRILLING FLUID

USE OF SONIC LOGS IN EVALUATING ROOF-ROCK
STRENGTH FOR AN UNDERGROUND COAL MINE

T.R. West and R.G. Hummeldorf
Department of Geosciences, Purdue University
and Batelle Institute, respectively

Abstract

Strength of the roof rock is a major concern for underground coal mines in the Illinois Basin. Because of the expense of rock coring and laboratory testing to evaluate roof strength, sonic logging is being considered as a means for strength prediction. Also if the borehole technique proves useful in coal mine work it can be applied to exploration programs for other engineering projects including highways.

The sonic log is a continuous record of depth versus the time for the compressional wave to traverse a given vertical distance in the immediate vicinity of the bore hole. It is obtained using conventional bore hole geophysical methods.

In this study, strength of roof rock was determined by unconfined compression, point load, pulse velocity, and Brazilian tests. The RQD classification and fracture interval aspects were also utilized. Point load results proved not to be useful as they failed to correlate with the unconfined compression strength.

Sonic logging used in the study involved a dual receiver sonde which had some inherent problems affecting sonic log response. Transit time values were assigned to the sample core intervals that had been tested for strength and to the core intervals classified using the RQD method. The value assigned to a given core interval was determined by averaging the transit times measured for the length of the core interval involved.

Scatter diagrams were prepared relating rock strength and RQD values to the sonic log responses. Based on standard deviation, mean deviation, and scatter diagrams, Young's modulus values determined in uniaxial compression, and unconfined compressive strengths were compared statistically with sonic log response.

Using data from this study along with some from previous studies, a straight line approximation of Young's modulus versus sonic log response was computed using a least squares method for regression analysis.

Unconfined compressive strength values showed a trend with a reverse slope as that shown for published data so no further statistical comparison with sonic log response was made.

However, a plot of RQD versus unconfined compression strength showed reasonably good correlation.

Results of this study indicate that the sonic log was not a good predictor of roof strength as measured by the unconfined compression test or RQD. Young's modulus may be used indirectly as a roof strength indication and sonic log data predicted this modulus to some extent. RQD values do correlate with the unconfined compression strength.

INTRODUCTION

Considerable variation in roof character of underground coal mines occurs in the Illinois Basin. The coal is typically overlain by shales of various thickness and character with localized sandstone units present as well. This variability of roof conditions leads to support problems in the coal mine and possible roof falls.

In an attempt to forecast roof conditions in advance of mining, rock coring and laboratory testing are performed. As this procedure is both expensive and time-consuming, it was proposed that sonic logs from the bore holes be used in place of testing to predict rock strength. To accomplish this, sonic log responses were compared to the corresponding rock strengths for a particular core section. Rock strength tests included uniaxial compression, tensile strength and point load tests. Rock quality designation (RQD) was utilized in addition to rock strength values for the comparison.

The underground coal mine utilized in this study is located in southern Illinois in the Illinois Basin Region. The Springfield-Harrisburg No.5 coal member of the Pennsylvanian Carbondale Formation is mined.

The coal is mined at a depth of approximately 930 feet at the study site. The roof rock consists of the Dykersburg Shale, a gray silty shale containing an occasional sandstone unit.

The research was supported in part by the U.S. Department of Interior, Bureau of Mines, Office of Mineral Institute, Indiana Mining and Minerals Resources Research Institute.

LABORATORY TESTING OF ROCK

Rock strength values were obtained on cores from five boreholes in areas scheduled to be mined. The cores were 3 inches in diameter (or more precisely, 2.96").

The portions of core chosen for testing were obtained in the immediate vicinity of the top of the coal bed (from a few feet to a few tens of feet above it) as this is where fall problems have occurred. Where the core was too badly broken for this zone immediately above the coal and hence lab testing was not possible, samples were obtained from somewhat higher elevations.

As previously stated the strength parameters measured included RQD, unconfined compression strength, tensile strength and point load strength. Unconfined compression strength was determined according to ASTM D-2938-71a and D-3148-72 (ASTM Annual Book of Standards).

Young's modulus of elasticity was determined during the unconfined compression testing and by pulse velocity testing, the latter according to ASTM D-2845-69. Tensile strength was determined by use of the Brazilian Test as per ASTM C-496-71.

ROCK QUALITY DESIGNATION

Classification of the rock core using Deere's RQD System (Rock Quality Designation) had a threefold advantage in this study. Firstly, it is non-destructive, easy to apply to rock core and hence fast and inexpensive. Secondly, RQD is widely used both as a parameter in other rock mass evaluations but also as an indicator of rock mass quality involving RQD values alone. Thirdly, RQD can be compared directly to sonic log responses for a specific core interval.

The RQD is computed by the following equation:

$$\text{RQD}(\%) = 100 \times \frac{\text{Summation of Length of Core Pieces} > 4 \text{ inches}}{\text{Length of Core Interval}}$$

Commonly the length of core interval used in the determination is two meters, five feet or ten feet, typically based on the length of the core barrel used in the coring process. In this study three lengths of core interval were selected for computing RQD. This was based on the fact that the core had been placed in the core boxes in eight foot sections which made it simplest to use 8 feet as the primary length. Two other lengths were chosen, 2 and 4 feet, corresponding to the resolution of the sonic logs. Geologic detail of the cores also suggested that 4 feet was a good length to include for the evaluation.

Rock quality ratings have been developed to coincide with RQD values. These are presented in Table 1.

Table 1. Numerical Value for RQD and Corresponding Rock Quality Rating (Hoek and Brown, 1980).

RQD (%)	Rock Quality
0-25	Very Poor
25-50	Poor
50-75	Fair
75-90	Good
90-100	Very Good

The results of the RQD evaluation for the cores included in this study are presented in Table 2. These RQD values were obtained some time after the rock had been cored and placed in the core boxes. The cores were stored in plastic which is a common procedure for cores associated with coal exploration. This helped to preserve the natural moisture conditions to some extent. However, it is preferred that the RQD be determined as the coring program proceeds, but this was not possible during the present study. The core boxes were also

Table 2. Results of RQD classification.

Borehole Number	Core Interval (Feet)	RQD (%) Short Length	Core Interval (Feet)	RQD (%) Medium Length	Core Interval (Feet)	RQD (%) Long Length
C3-104	945.0 -947.0	22.9	945.0 -949.0	30.2	945.0 -953.0	19.3
	947.0 -949.0	37.5	947.0 -951.0	27.1	947.0 -955.0	18.2
	949.0 -951.0	16.7	949.0 -953.0	8.3	949.0 -957.0	8.9
	951.0 -953.0	0.0	951.0 -955.0	9.4	951.0 -959.0	4.7
	953.0 -955.0	18.0	953.0 -957.0	9.4	953.0 -960.5	5.0
	955.0 -957.0	0.0	955.0 -959.0	0.0		
	957.0 -959.0	0.0	957.0 -960.5	0.0		
	959.0 -960.5	0.0			945.0 -951.0*	25.7*
C3-116	889.0 -891.0	0.0	889.0 -893.0	0.0	889.0 -897.0	30.2
	891.0 -893.0	0.0	891.0 -895.0	23.4	891.0 -899.0	34.9
	893.0 -895.0	46.9	893.0 -897.0	60.4	893.0 -901.0	34.9
	895.0 -897.0	74.0	895.0 -899.0	46.4	895.0 -903.0	23.2
	897.0 -899.0	18.8	897.0 -901.0	9.4	897.0 -904.0	4.7
	899.0 -901.0	0.0	899.0 -903.0	0.0		
	901.0 -903.0	0.0	901.0 -904.0	0.0		
	903.0 -904.0	0.0			893.0 -899.0*	46.5*
C3-118	898.5 -900.5	88.5	898.5 -902.5	72.1	898.5 -905.0	44.4
	900.5 -902.5	55.7	900.5 -904.5	27.9	900.5 -907.0	13.9
	902.5 -904.5	0.0	902.5 -905.0	0.0	902.5 -909.0	0.0
	904.5 -905.0	0.0	904.5 -907.0	0.0	904.5 -911.0	0.0
	905.0 -907.0	0.0	905.0 -909.0	0.0	905.0 -912.25	5.1
	907.0 -909.0	0.0	907.0 -911.0	0.0	907.0 -914.0	5.4
	909.0 -911.0	0.0	909.0 -912.25	9.4	909.0 -915.25	5.8
	911.0 -912.25	28.1	911.0 -914.0	9.4		
	912.25 -914.0	0.0	912.25 -915.25	0.0		
	914.0 -915.25	0.0				
C3-120	747.0 -749.0	0.0	747.0 -751.0	40.6	747.0 -755.0	56.8
	749.0 -751.0	81.3	749.0 -753.0	75.0	749.0 -757.0	68.7
	751.0 -753.0	68.8	751.0 -755.0	72.9	751.0 -759.0	69.1
	753.0 -755.0	77.1	753.0 -757.0	62.2	753.0 -761.0	52.0
	755.0 -757.0	47.4	755.0 -759.0	65.4	755.0 -763.0	32.7
	757.0 -759.0	83.3	757.0 -761.0	41.7		
	759.0 -761.0	0.0	759.0 -763.0	0.0		
	761.0 -763.0	0.0				
C3-125	903.0 -905.0	0.0	903.0 -907.0	21.6	903.0 -911.0	19.8
	905.0 -907.0	43.2	905.0 -909.0	39.6	905.0 -913.0	25.3
	907.0 -909.0	35.9	907.0 -911.0	18.0	907.0 -915.0	18.6
	909.0 -911.0	0.0	909.0 -913.0	10.9	909.0 -917.0	14.3
	911.0 -913.0	21.9	911.0 -915.0	19.3		
	913.0 -915.0	16.7	913.0 -917.0	17.7		
	915.0 -917.0	18.8				
	925.0 -927.0	37.0	925.0 -929.0	18.5	925.0 -933.0	13.4
	927.0 -929.0	0.0	927.0 -931.0	8.3	927.0 -935.0	4.2
	929.0 -931.0	16.7	929.0 -933.0	8.3	929.0 -937.0	4.2
	931.0 -933.0	0.0	931.0 -935.0	0.0	931.0 -939.0	0.0
	933.0 -935.0	0.0	933.0 -937.0	0.0	933.0 -940.5	0.0
	935.0 -937.0	0.0	935.0 -939.0	0.0		
	937.0 -939.0	0.0	937.0 -940.5	0.0		
	939.0 -940.5	0.0				
	940.5 -942.5	17.7	940.5 -944.5	26.6	940.5 -947.4	20.6
	942.5 -944.5	35.4	942.5 -946.5	32.3		
	944.5 -946.5	29.2	944.5 -947.4	14.6		
	946.5 -947.4	0.0				

* 6 foot length interval.

transported from the field to the laboratory, a distance of about 300 miles, before the RQD was determined.

ROCK SAMPLE PREPARATION

For strength tests other than the RQD, rock sample preparation was required. The samples were cut and ground smooth according to ASTM specifications or other controlling procedures.

The samples were cut with a water-cooled continuous rim diamond saw, model 11-B manufactured by Felker Dresser. Grinding was accomplished using a water lubricated, 70 micron diamond disc polisher manufactured by AB Buehler, Ltd.

Because of the water spraying action of the saw and polisher, the original moisture content of the rock samples was not necessarily maintained. With the concern for slaking of saturated shale, the samples were all tested in the dry state. It was recognized that the strength of dry shale can be as high as twice that of specimens tested under fully saturated conditions (Hoek and Brown, 1980), but under the circumstances involved, it was concluded that testing the shale samples when dry provided the best results for purposes of comparison.

UNCONFINED AND UNIAXIAL COMPRESSION TESTING

Unconfined compression testing, which consists of loading the sample to failure with a compressive load along the core axis, was conducted on six samples, according to ASTM D-2938-71a. Uniaxial compression testing, this involving the measurement of axial and lateral strain as the axial load is increased to failure, was conducted on eight samples, in accordance with ASTM D-3148-72.

For the unconfined compression tests, when the length to diameter ratio of the sample was less than two, a corrected compressive strength was computed using the following empirical relationship (ASTM D-2938-71a).

$$q_u = q_a / [0.88 + .24(b/h)]$$

where

q_u = computed compressive strength for a sample with an equivalent length to diameter ratio of two

q_a = measured compressive strength,

b = test core diameter, and

h = test core height.

Both measured and corrected values (shown in parentheses) for the unconfined compression samples are provided in Table 3. The six values have no Young's modulus or Poisson's ratio values associated with them.

Test equipment utilized in unconfined compression testing consisted of a hand pumped compression tester with a 300,000 pound capacity. The loading rate to failure was 10,000 pounds per minute.

In the uniaxial compression testing, Young's modulus of elasticity and Poisson's ratio were determined at three stress levels: 1000, 3000 and 5000 psi using both the tangent and secant methods. The 1000 psi stress level corresponds to the state of stress in the mine assuming a vertical stress gradient of 1 psi per foot and approximately 1000 feet of overburden. The 3000 and 5000 psi levels were selected to better understand how the moduli behave under increasing stress as the coal is extracted.

Data for the eight samples tested in unconfined compression which includes Young's modulus and Poisson's ratio are given in Table 3. Where no values are included for Poisson's ratio technical difficulties developed during that test and lateral strains were not obtained.

Table 3. Unconfined compressive strength, Young's Modulus, and Poisson's Ratio for samples tested.

Borehole Number	Core Interval (feet)	Unconfined Compressive Strength q_u (psi)	Young's Modulus Tangent Method			Young's Modulus Secant Method			Poisson's Ratio Tangent Method			Poisson's Ratio Secant Method				
			E_{tan} (psi) @ stresses	$\times 10^6$ (psi)	$\times 10^6$ (psi)	E_{sec} (psi) @ stresses	$\times 10^6$ (psi)	$\times 10^6$ (psi)	ν_{tan} stresses (psi)	1000	3000	5000	ν_{sec} stresses (psi)	1000	3000	5000
C3-104	952.5 - 952.92	11731(11464)*														
C3-116	893.0 - 893.42	7343(7116)*														
C3-118	898.5 - 899.0	7583	1.9	1.6	1.4	1.9	1.8	1.7	0.11	0.12	0.23		0.11	0.10	0.14	
	899.0 - 899.5	6680	2.2	1.6	1.4	2.2	1.8	1.7	0.11	0.25	0.31		0.17	0.22	0.26	
	899.5 - 900.0	7835	1.8	1.6	1.3	1.7	1.7	1.6	0.11	0.21	0.28		0.09	0.14	0.18	
	900.5 - 901.0	4313(3374)*														
	901.83-902.33	8094	1.0	1.0	1.3	1.0	1.2	1.3	-	0.15	0.22		-	0.09	0.13	
C3-120	750.08-750.58	11460(8931)*														
	751.92-752.42	10755(8444)*	1.6	1.4	1.3	1.7	1.5	1.5	-	-	-		-	-	-	
	753.25-753.83	8499	1.4	1.5	1.4	1.2	1.4	1.4	-	-	-		-	-	-	
	754.5 - 755.0	9075(7304)*	1.7	1.5	1.3	1.7	1.6	1.5	0.23	0.19	0.26		0.10	0.13	0.17	
	756.0 - 756.67	10876(8572)*														
C3-125	758.25-758.83	8696	1.6	1.4	1.3	1.4	1.5	1.4	0.12	0.20	0.29		0.07	0.15	0.17	
	945.5 - 946.08	6113														

* Values in parentheses are standardized. See text.

The equipment utilized in uniaxial compression testing consisted of the same hand-pumped compression tester used in unconfined compression testing, a Budd multi-channel strain indicator (Model P-350) and a Budd strain bridge. The strain gages were constantan grids completely encapsulated in polyimide, self temperature compensating and had large integral, copper-coated terminals.

Four strain gages were used for each sample and placed 90 degrees apart around the circumference of the core. The two vertical gages were 180 degrees apart as were the two horizontal gages.

The strain gages were attached to the rock samples after sanding the attachment area with 220 and 400 grit sandpaper. Next the area was wet sanded using a solution of weak acid and 400 grit sandpaper. The acid was neutralized with a weak base solution. Finally, the samples were cleaned with an isopropyl alcohol solution and the gages attached at mid-height of the sample with a cyanocrylate ester adhesive.

The Budd strain bridge measured resistance changes in the gages with the gage factor set at 2.045 percent. Strain was read directly in microinches per inch.

POINT LOAD TESTING

Point load tests were conducted on core samples in keeping with procedures set forth by Broch and Franklin (1972).

The equation for the point load test is

$$I_s = \frac{P}{L^2}$$

where

I_s = the point load index in psi

P = the failure compressive load in pounds

L = the thickness of the sample parallel to the load axis.

A conversion from the point load index to an equivalent unconfined compression strength is indicated by Broch and Franklin (1972). This is based on the relationship

$$q_{up1} = KI_s$$

where K increases with increasing sample size. For a core diameter of 2.96 inches (75.2 millimeters) the factor K must be extrapolated beyond the plot provided by Broch and Franklin. A value of 28 is obtained for K when this is done.

Samples were tested parallel to the axis of the core. For the longer core pieces of the shale, most failures occurred along bedding planes, that is, perpendicular to the load axis rather than parallel to it as was expected. Using these failure load values to calculate q_{up1} gave considerably larger values than those obtained in unconfined compression testing. The values for q_{up1} from the point load tests are given in Table 4 and a comparison with Table 3 shows just how much greater the q_{up1} values are than those for q_u .

Smaller core lengths were selected and for these, failure parallel to the load axis was obtained. These values were orders of magnitude higher than strength values directly from unconfined compression testing. Based on these very high values or the high values shown for the longer core samples (Table 4) it was concluded that the point load value for the shale samples in this study were inconsistent and totally unreliable. No attempt was made to correlate point load data to the sonic log response.

PULSE VELOCITY TESTING

The pulse velocity tests were conducted in accordance with ASTM D-2845-69 (Annual Book of ASTM Standards, 1979). Shear wave velocity measurements, were not made, but only that of the compression wave, and the tests were run on dry samples.

Table 4. Results of point load tests.

Borehole Number	Core Interval (Feet)	Unconfined Compressive Strength, Point Load Test
		q _{upl} (psi)
C3-116	898.0 -898.03	179200
	898.17-898.33	23972
	898.62-898.7	113932
	898.83-898.94	43353
C3-120	749.17-749.25	66901
	749.33-749.5	22866
	751.0 -751.25	11211
	754.0 -754.25	16151
	754.25-754.5	17719
	761.17-761.42	1161
C3-125	942.92-943.25	10117

Young's modulus calculated from pulse velocity is determined from the following equation:

$$E = \frac{(1-2\nu)(1+\nu)\gamma V_p^2}{g(1-\nu)}$$

where:

E = Young's modulus

ν = Poisson's ratio = 0.17

γ = Unit Weight = 162 pounds per cubic foot,

V_p = Velocity of compression wave, and

g = acceleration due to gravity. (Myung and Helander, 1972)

Poisson's ratio was obtained as an average value determined from the uniaxial compression tests. Unit weight used in the calculations was the dry unit weight determined by weighing three samples of known volume and dividing the weight by the volume. An average value for γ was used.

Table 5 presents the Young's modulus values determined by the pulse velocity test for the listed core intervals. Values are generally higher than those determined using uniaxial compression testing (see Table 3).

Poor contact between the transmitter and/or the receiver and the rock sample could account for the variations, as could the anisotropy of the rock samples. As noted in ASTM D-2845-69 (Annual Book of ASTM Standards, 1979), the greater the anisotropy, the larger the percent error that occurs.

The equipment used was a pulse velocity meter, Model C-4899, produced by James Electronics, Inc.. Castrol water pump grease was utilized for maximizing contact between the transmitter and receiver with the rock samples.

Table 5. Young's Modulus determined by pulse velocity testing.

Borehole Number	Core Interval (Feet)	Young's Modulus Pulse Velocity Test E_{pv} (psi) $\times 10^6$
C3-104	946.33-946.62	3.32
	947.67-948.0	3.45
	948.5-948.75	3.20
	949.08-949.25	3.25
	949.33-949.5	3.25
	950.08-950.42	3.79
	950.5-950.67	3.72
	950.67-950.83	3.72
	951.08-951.33	3.58
	952.17-952.5	2.69
	952.5-952.92	3.58
	953.0-953.25	1.34
	955.17-955.42	3.32
	955.42-955.67	3.24
	960.17-960.33	3.01
	960.33-960.5	3.01
C3-116	893.42-893.75	3.38
	894.5-894.75	2.35
	895.25-895.42	2.73
	895.42-895.58	2.73
	895.67-895.83	3.72
	896.0-896.17	3.72
	896.17-896.42	2.73
	896.42-896.75	2.49
C3-118	898.33-898.62	1.88
	899.0-899.5	2.86
	899.5-900.0	3.58
	900.5-901.0	1.70
C3-120	901.83-902.33	0.71
	749.67-749.92	3.45
	749.92-750.08	3.45
	750.08-750.58	3.45
C3-120	750.58-750.83	3.58
	750.83-751.0	3.58
	751.0-751.25	3.13
	751.42-751.67	2.82
	751.67-751.83	2.82
	751.92-752.42	3.38
	753.25-753.83	3.25
	754.5-755.0	3.25
	756.0-756.67	3.52
	756.67-757.0	3.45
	757.0-757.42	2.95
	757.42-757.75	3.05
	757.75-757.92	3.45
	758.0-758.17	3.45
	758.25-758.83	2.95
	759.17-759.5	3.19
	761.17-761.42	1.98
	762.33-762.58	1.84
C3-125	942.92-943.25	1.45
	945.5-946.08	1.93

RESULTS OF THE BRAZILIAN TEST

Tensile strength was determined indirectly for 36 samples by use of the Brazilian test, per ASTM C-496-71 (Annual Book of ASTM Standards, 1979). The loading rate used to fail the specimens was 5000 pounds per minute, yielding failure at three to six minutes after loading of the samples was initiated.

Most of the specimens failed along the line of loading as anticipated. According to the Griffith Failure Criterion in unconfined compression, tensile strength in 2-D analysis is approximately one-eighth the unconfined compressive strength and one-twelfth of the unconfined compressive strength in 3-D analysis (Jaeger and Cook, 1976).

The tensile strength values obtained, shown in Table 6, agree reasonably well with these criteria (see Table 3). Equipment used for the Brazilian test was the same as that utilized for unconfined compression testing.

SONIC LOG INTERPRETATION

THE SONIC LOG

A brief overview concerning sonic logging and corresponding response times is necessary to understand the interpretation and limitations of sonic logs used in this study. The correlation between rock strength and sonic log response was examined using this relationship.

The sonic log is a continuous record of depth versus the time required for the compressional wave component of an acoustic wave to traverse a given vertical distance of the formation in the immediate vicinity of a borehole. The given vertical distance utilized by the logging company in this study was one foot.

The travel time of the compressional wave component of the acoustic wave is a function of the density and modulus of elasticity of the medium traversed. The unit travel time is determined by the following equation:

Table 6. Results of Brazilian tests.

Borehole Number	Core Interval (Feet)	Tensile Strength σ_t (psi)
C3-104	946.33-946.22	655
	947.67-948.0	1071
	948.5 -948.75	1066
	949.08-949.25	1295
	949.33-949.5	937
	950.08-950.42	1100
	950.5 -950.67	1369
	950.67-950.83	921
	951.08-951.33	1184
	952.17-952.5	864
	953.0 -953.25	1269
	955.17-955.42	1337
	955.42-955.67	785
	960.17-960.33	1147
	960.33-960.5	1182
C3-116	893.42-893.75	1252
	894.5 -894.75	1079
	895.25-895.42	1195
	895.42-895.58	932
	895.67-895.83	983
	896.0 -896.17	1177
	896.17-896.42	1217
	896.42-896.75	708
	898.33-898.62	928
C3-120	749.67-749.92	1113
	749.92-750.08	976
	750.58-750.83	844
	750.83-751.0	1269
	751.42-751.67	1155
	751.67-751.83	1061
	756.67-757.0	1319
	757.0 -757.42	978
	757.75-757.92	1108
	758.0 -758.17	1013
	759.17-759.5	732
	762.33-762.58	747

$$T_c = \frac{\rho}{gM_b}$$

where T_c = unit travel time for the compressional wave component

ρ = density of the medium traversed

M_b = bulk modulus of elasticity of the medium

g = acceleration due to gravity (Wichmann, 1974).

The time T_c is the total time for the sound wave to travel through the one foot interval of formation.

The acoustic wave utilized in sonic logging is produced by a transmitting transducer. The wave propagates as a compressional wave and as a shear wave, with compressional wave component traveling about twice the velocity of the shear wave component (Wichmann, 1974). The transit time of the compressional wave component is measured by sonic logging.

The compressional wave component travels through the borehole at the characteristic velocity of the borehole fluid. As it reaches the face of the formation in the borehole, the compressional wave component refracts according to Snell's Law and traverses the formation at a velocity characteristic of the formation (Pirson, 1963).

The electronic recording circuits are triggered by the compressional wave component as it reaches the receiving transducer. For a dual receiver system, as was used by the logging company, the wave also triggers an electronic timing device in the first receiver which is shut off as the wave reaches the second receiver. The time is measured in microseconds per foot of formation.

The sonic log sonde utilized in this study has dual receivers placed below the transmitter T. The first receiver R_1 is three feet below T. R_1 and R_2 are spaced one foot apart (Pirson, 1963).

Table 7 presents borehole data for the boring C3-118. These borehole data are similar for all borings examined in this study.

Table 7. Borehole Data for Boring C3-118.

Total Depth - Driller:	925 ft.
Total Depth - Logger:	933 ft.
Total Footage Logged:	133 ft.
Logging Speed:	20 ft/min.
Reference Level:	Surface Elevation
Bit Size:	5.1"
Casing-Type & Size:	5"/steel
Casing Depth:	23 ft.
Borehole Fluid:	Water

Several problems may occur in the dual receiver sonic logging system. In normal operation, the two receivers are triggered by the first movement of sound energy. Under less than ideal conditions, however, the first movement or compressional wave component may be too weak to trigger the receivers. The receivers are consequently triggered by later arriving waves.

If the same wave feature triggers both receivers, the true transit time is recorded. However, if the two receivers are triggered by two different wave events a false transit time measurement is recorded. This phenomenon is known as cycle skipping.

Cycle skipping can be recognized on the log record by sharp spikes toward large transit time. These cycles indicate zones of large attenuation that may result from substantial fracturing or vug formation (Pirson, 1963).

In addition to cycle skipping, false transit times may be recorded when the time intervals from the two receivers to the formation are unequal. This condition may occur when the sonde is tilted in the borehole, the walls of the borehole are very irregular, or by a combination of these two situations (Wichmann, 1974). Shale zones especially tend to cave and enlarge in boreholes as indicated by caliper curves, thus yielding questionable transit times (Dresser Atlas, 1975).

The sonic log also behaves questionably where the rocks are unconsolidated or not compacted, at least where porosity is to be determined from the sonic log. The less the degree of compaction, the less grain to grain contact occurs in these rocks. Fluid filling the voids of less compacted rocks results in more travel through the fluid and more fluid transit time to the total contribution of time involved (Dresser Atlas, 1975). An increase in transit time results as the fluid supports a lower velocity.

Considering the overburden thickness at the site and the fact that the area has been glaciated, the shale concerned was assumed to be well consolidated and compacted. The range of transit times recorded on the sonic log for this study, 81.5 to 126.5 microseconds per foot, supports this assumption. The Dykersburg shale transit time values are close to the smallest transit times generally reported for shales (see Table 8) indicating a high degree of compaction and consolidation.

SONIC LOG INTERPRETATION

Interpretation of the sonic logs in this study involved assigning transit time values to the particular core intervals tested. The transit times chosen to represent the tested intervals were averaged over a minimum interval of six inches. That is to say, for samples less than six inches long, transit time values were averaged over a six inch interval containing the sample positioned at the center of the six inch interval.

The minimum interval of six inches was chosen to represent the smaller samples tested owing to the sensitivity of the sonic logging system utilized in the study. Various lithologic changes were studied in relation to the sonic log responses and in general, changes were first discernable when the lithologic units were about six inches thick. That is, the influence of beds less than six inches thick was not discernable on the sonic log tracing.

Table 8. Typical average matrix velocities and matrix transit times for various lithologies (Wichmann, 1974).

Formation	V_{ma} ft/sec.	Δt_{ma} μ sec/ft.
Sandstone:		
Unconsolidated	17,000	58.8
	or less	or more
Semi-consolidated	18,000	55.6
Consolidated	19,000	52.6
Limestone	21,000	47.6
Dolomite	23,000	43.5
Shale	6,000	167.0
	to 16,000	to 62.5
Calcite	22,000	45.5
Anhydrite	20,000	50.0
Granite	20,000	50.0
Gypsum	19,000	52.6
Quartz	18,000	55.6
Salt	15,000	66.7

When averaging the transit time values, it was necessary to determine whether the sonic log depth-interval correctly represented the core depth-interval recorded by the driller.

The interval for the St. David's Limestone in the boring C3-116, according to the driller's log description, is located between 875.8 and 877.6 feet. The sonic log indicated that this formation occurs approximately six inches higher in the section than shown on the boring log. The bed boundary depths are located half-way between the high and low readings on the sonic log (Dresser Atlas, 1975). Thus the travel times utilized in determining an average travel time for particular intervals in borehole C3-116 were adjusted approximately six inches higher in the section than indicated by the rock core sample depth measured in the field.

Transit times were determined at the upper and lower boundaries of the interval of interest as well as in the middle for the purpose of averaging. For very large intervals, a somewhat different approach was used for determining the average transit time value associated with the interval of interest.

The system presented in Table 9 indicates that the number of transit times read from the sonic log for these interval lengths include many more intermediate times than for the six inch intervals. The spacings between transit time readings was chosen to yield at least five transit time values to be averaged per interval.

Not all of the RQD intervals presented in Table 2 were assigned transit time values. Where possible, the largest length of core interval was chosen, that represented by eight feet. The basis for determining which RQD interval to use for transit time assignment was decided with respect to lithologic variation and the variation in sonic-log response time.

Table 9. System utilized for assigning transit time values for different RQD intervals.

RQD INTERVAL (FEET)	DEPTH SPACING		NUMBER OF TIME t VALUES PER RQD INTERVAL
	BETWEEN TIME t VALUES (FEET)		
8	1		9
4	1		5
2	0.5		5

Where an eight foot interval represented basically the same lithology with little variation in sonic log response over the eight foot interval, the transit time value was averaged for the eight foot interval instead of combinations of two or four foot intervals.

If many lithologic or sonic response changes occurred in an eight foot interval, a shorter RQD interval was assigned an average transit time. The more changes, the shorter was the interval chosen. Four and two-foot intervals were the shorter intervals utilized in this study as discussed previously.

Where RQD values of 0.0% occurred, two foot intervals were generally chosen owing to the many possibilities that may influence sonic log response time. One response time may occur for the interval if most of the broken pieces of core are slightly shorter in length than 4 inches. Another type of response may occur if most of the broken pieces are for example, about 1 inch in length.

The transit times for the strength test samples and the RQD classification system intervals are presented in Tables 10 and 11, respectively.

ROCK PROPERTIES COMPARED TO SONIC VELOCITY

Rock strength data were compared to sonic log responses to determine how well sonic logging could be used to estimate strength values. Rock strength and RQD values have been provided in Tables 1, 3, 5 and 6 and the corresponding sonic velocities or travel times are supplied in Tables 10 and 11.

STATISTICAL COMPARISON

The Dykersburg Shale which forms the roof rock at the mine was assumed to be lithologically constant in the borings examined, although some variability was noted when the RQD was determined. This simplifying assumption was necessary for the statistical comparison.

Table 10. Strength test samples and corresponding transit times Δt .

Borehole Number	Sample Number	Core Sample Interval (Feet)	$\Delta t \pm 0.2$ (Microseconds/Feet)
C3-104	4-4-1	946.33-946.62	86.5
	4-4-2	947.67-948.0	87.0
	4-4-3	948.5 -948.75	87.3
	4-4-4a	949.08-949.25	87.2
	4-4-4b	949.33-949.5	87.1
	4-4-5	950.08-950.42	86.7
	4-4-6a	950.5 -950.67	86.7
	4-4-6b	950.67-950.83	86.7
	4-4-7	951.08-951.33	86.7
	4-4-8	952.17-952.5	86.6
	4-4-9	952.5 -952.92	86.7
	4-5-1	953.0 -953.25	86.7
	4-5-3	955.17-955.42	88.0
	4-5-3a	955.42-955.67	88.1
	4-5-5a	960.17-960.33	96.5
	4-5-5b	960.33-960.5	97.0
C3-116	6-3-3	893.0 -893.42	85.0
	6-3-4	893.42-893.75	86.5
	6-3-5	894.5 -894.75	87.8
	6-3-7a1	895.25-895.42	87.4
	6-3-7a2	895.42-895.58	85.0
	6-3-7b1	895.67-895.83	84.8
	6-3-7b2	896.0 -896.17	84.8
	6-3-8	896.17-896.42	84.6
	6-3-9	896.42-896.75	84.6
	6-4-1a	898.0 -898.03	84.8
	6-4-1b	898.17-898.33	84.8
	6-4-2a	898.33-898.62	84.7
	6-4-2b1	898.62-898.7	84.6
	6-4-2b2	898.83-898.94	85.0
C3-118	8-6-1a	898.5 -899.0	84.6
	8-6-1b	899.0 -899.5	84.8
	8-6-1c	899.5 -900.0	85.4
	8-6-2	900.5 -901.0	86.6
	8-6-4	901.83-902.33	86.9
C3-120	0-3-2a	749.17-749.25	86.8
	0-3-2b	749.33-749.5	86.7
	0-3-3a	749.67-749.92	86.8
	0-3-3b	749.92-750.08	86.9
	0-3-4	750.08-750.58	86.3
	0-3-5a	750.58-750.83	86.0
	0-3-5b	750.83-751.0	86.1
	0-3-6	751.0 -751.25	86.4
	0-3-7a	751.42-751.67	87.2
	0-3-7b	751.67-751.83	86.9
	0-3-8	751.92-752.42	86.9
	0-3-11	753.25-753.83	86.9
	0-3-12a	754.0 -754.25	86.6
	0-3-12b	754.25-754.5	86.8
	0-3-13	754.5 -755.0	86.0
	0-4-1	756.0 -756.67	89.9
	0-4-2	756.67-757.0	89.8
	0-4-3	757.0 -757.42	89.6
	0-4-4	757.42-757.75	89.2
	0-4-5a	757.75-757.92	88.6
	0-4-5b	758.0 -758.17	88.4
	0-4-6	758.25-758.83	88.5
	0-4-7	759.17-759.5	89.9
	0-4-8	761.17-761.42	89.9
	0-4-9	762.33-762.58	-
C3-125	5-6-3	942.92-943.25	84.8
	5-6-4	945.5 -946.08	84.4

Table 11. RQD (%) and corresponding transit times Δt .

Borehole Number	Core Interval (Feet)	RQD (%)	$\Delta t \pm 0.2$ (Microseconds/Foot)
C3-104	945.0 -953.0	19.3	86.5
	945.0 -951.0	25.7	86.5
	951.0 -953.0	0.0	86.8
	953.0 -955.0	18.0	87.1
	955.0 -957.0	0.0	87.5
	957.0 -960.5	0.0	86.3
C3-116	889.0 -891.0	0.0	88.7
	891.0 -893.0	0.0	87.0
	893.0 -895.0	46.9	86.6
	895.0 -897.0	74.0	85.8
	897.0 -899.0	18.8	85.0
	899.0 -901.0	0.0	86.7
	901.0 -904.0	0.0	90.0
C3-118	898.5 -900.5	88.5	85.2
	900.5 -902.5	55.7	87.1
	902.5 -904.5	0.0	88.6
	904.5 -905.0	0.0	98.7
	905.0 -907.0	0.0	119.1
	907.0 -909.0	0.0	126.5
	909.0 -911.0	0.0	123.4
	911.0 -912.25	28.1	117.1
	912.25 -914.0	0.0	114.6
	914.0 -915.25	0.0	112.6
C3-120	747.0 -749.0	0.0	89.4
	749.0 -751.0	81.3	86.5
	751.0 -755.0	72.9	86.1
	755.0 -757.0	47.4	88.0
	757.0 -759.0	83.3	89.0
	759.0 -761.0	0.0	90.6
C3-125	903.0 -905.0	0.0	81.5
	905.0 -907.0	43.2	83.0
	907.0 -909.0	35.9	84.6
	909.0 -911.0	0.0	83.7
	911.0 -913.0	21.9	83.1
	913.0 -915.0	16.7	83.6
	915.0 -917.0	18.8	84.1
	925.0 -927.0	37.0	82.6
	927.0 -929.0	0.0	83.1
	929.0 -931.0	16.7	83.3
	931.0 -933.0	0.0	83.1
	933.0 -935.0	0.0	83.0
	935.0 -937.0	0.0	84.2
	937.0 -939.0	0.0	85.6
	939.0 -940.5	0.0	85.6
	940.5 -942.5	17.7	84.9
	942.5 -944.5	35.4	84.6
	944.5 -946.5	29.2	85.6
	946.5 -947.5	0.0	86.9

At the outset a comparison of sample depth versus transit time was made. Elkington et al. (1982) indicate that transit time can be influenced by overburden depth, independent of lithology. A plot of depth versus sonic response represented as transit time showed no obvious dependence on depth over the 200 foot interval involved.

In order to determine the variation in the strength data relative to that of the transit time, the mean, standard deviation and mean deviation were computed for the various parameters. This information is provided in Table 12.

Numerous two variable plots were made on strength values versus Δt , the transit time. This yielded plots known as scatter diagrams as a poor correlation tends to yield a wide scatter of data points, whereas good correlation tends to show linear trends in the data with little scatter.

The following plots were made:

1. RQD vs Δt
2. Core length of samples with 0 RQD vs Δt
3. Young's modulus (pulse velocity) vs Δt
4. Tensile strength vs Δt
5. Poisson's ratio (tangent method) vs Δt with different stress levels for Poisson's ratio
6. Poisson's ratio (secant method) vs Δt
7. Young's modulus (tangent method) vs Δt
8. Young's modulus (secant method) vs Δt
9. Unconfined Compressive strength vs Δt

For these nine plots the scatter of data is too great in six of them to show any reasonable level of correlation. Only Young's modulus from the static test (uniaxial compression) and the unconfined compression test plots showed any promise for correlation. This includes plots 7, 8 and 9 listed above.

Table 12. Rock Strength Parameters, RQD, and Sonic Log Response
 \bar{X} , σ , and MD (see text).

		Mean \bar{X}	Standard Deviation σ	Mean Deviation MD
Tensile Strength	G_t (psi)	1055.00	188.03	175.89
Transit Time	Δt (μ sec/ft)	87.50	2.63	1.68
Unconfined Compressive Strength	q_u (psi)	7521.00	1502.55	1157.86
	Δt (μ sec/ft)	86.40	1.47	1.10
Unconfined Compressive Strength (Point Load)	qu_{pl} (psi)	46053.00	52241.06	40340.73
Young's Modulus (Pulse Velocity Test)	E_{pv} (psi) $\times 10^6$	2.95	0.69	0.52
	Δt (μ sec/ft)	87.30	2.40	1.55
Young's Modulus (Tangent Method)	$E_{tan} \times 10^6$ (psi)			
Stress Level:	1000 psi	1.65	0.33	0.25
	3000 psi	1.45	0.19	0.14
	5000 psi	1.34	0.05	0.05
	Δt (μ sec/ft)	86.30	1.22	1.05
Young's Modulus (Secant Method)	$E_{sec} \times 10^6$ (psi)			
Stress Level:	1000 psi	1.60	0.36	0.30
	3000 psi	1.56	0.19	0.16
	5000 psi	1.51	0.14	0.12
	Δt (μ sec/ft)	86.30	1.22	1.05
Poisson's Ratio (Tangent Method)	ν_{tan}			
Stress Level:	1000 psi	0.14	0.05	0.04
	3000 psi	0.18	0.04	0.04
	5000 psi	0.27	0.03	0.03
	Δt (μ sec/ft)	86.00	1.34	1.20
Poisson's Ratio (Secant Method)	ν_{sec}			
Stress Level:	1000 psi	0.11	0.03	0.03
	3000 psi	0.14	0.04	0.03
	5000 psi	0.18	0.04	0.03
	Δt (μ sec/ft)	86.00	1.34	1.20
RQD	RQD (%)	40.50	23.55	19.85
	Δt (μ sec/ft)	86.80	5.94	3.24
Predominant Sample Length (0.0% RQD)	(Inches)	1.50	0.80	1.38
	Δt (μ sec/ft)	93.30	7.82	10.51

For the unconfined compression strength vs Δt the data plot shows an increase in transit time (or a decrease in velocity) with an increase in unconfined compression strength. This is just the opposite of the trend noted in the literature by Carroll (1966). From this it is clear that the transit times do not properly predict the unconfined compression strength.

For the E_{tan} and E_{sec} vs transit time plots the data corresponding to the 3000 psi stress level provide the best correlation. A least squares method of regression was conducted based on work by Davis (1973). The two equations obtained are:

$$E_{tan} = 8.7459 - 0.0846 \Delta t \quad R^2 = 0.439, R = 0.633$$

$$E_{sec} = 11.5672 - 0.1160 \Delta t \quad R^2 = 0.538, R = 0.733$$

E is in units of 10^6 psi.

R^2 is the regression value. An R value of 1 indicates that 100% of the variation in one variable is accounted for by the other value. The R^2 value should be above 0.4 to indicate significant correlation between variables.

Several additional two-variable plots were made to examine the relationship between various strength measurements. These involved:

- 1 RQD vs Young's modulus (secant method)
- 2 RQD vs Young's modulus (tangent method)
- 3 RQD vs Unconfined compression strength
- 4 Laboratory Pulse velocity vs Sonic Log Velocity

For these four plots, numbers 1, 2 and 4 indicated too much scatter to suggest any reasonable level of correlation between them.

For the other plot, RQD vs unconfined compression strength, reasonably good correlation is indicated. As the RQD increases the unconfined compression strength also increases which is the expected relationship for these two parameters.

CONCLUSIONS

1. Rock strength values obtained in the study were judged to be acceptable except those for pulse velocity and point load strength. Young's modulus values determined from pulse velocity were generally higher than modulus values resulting from uniaxial compression testing. Point load tests were completely unrealistic as compared to the unconfined compression values obtained on the shale samples. No further consideration of point load values was included in the study.
2. The sonic logging system used in this study has a dual receiver sonde. Some inherent problems of that system affected the transit time values. Those values determined for the various intervals should be considered as maximum values.
3. For the strength values measured; RQD, unconfined compressive strength, Poisson's ratio, Young's modulus and tensile strength, only E_{tan} and E_{sec} showed statistical significance. The unconfined compression values showed a reverse trend relative to transit time (or wave velocity) than that established in the literature.
4. Correlation between RQD and unconfined compressive strength was indicated. RQD versus Young's modulus showed no significant correlation. RQD can be a useful predictor of roof rock stability and the unconfined compressive strength is also used in this regard. RQD is primarily an indicator of rock mass properties, whereas unconfined compression strength is a rock property. A relationship does exist between the two, however.
5. In this study the sonic logging method did not prove to be a good predictor of roof rock stability as it failed to relate to unconfined compression strength or RQD value which are the tests used for roof stability. This is likely due to the nature of the roof rock (all shale) and the variation

inherent in the sonic logging method as compared to that involving the physical properties of rock.

References Cited

- Broch, E. and Franklin, J.A., 1972, The Point Load Strength Test, *Int. Jour. Rock Mech. Min. Sci.*, vol. 9, pp. 669-697.
- Carroll, R.D., 1966, Rock Properties Interpreted from Sonic Velocity Logs, *J. Soil Mech. Fdns. Div. Am. Soc. Civil Engrs.*, vol. 92, pp. 43-51.
- Davis, J.C., 1973, *Statistics and Data Analysis in Geology*, John Wiley & Sons, New York, 550 p.
- Deere, D.U., 1963, Technical Description of Rock Cores for Engineering Purposes, *Rock Mechanics and Engineering Geology*, vol. 1, no. 1, pp. 17-22.
- Dresser Atlas, 1975, *Log Interpretation Fundamentals*, Dresser Atlas Industries, Inc., pp. 4-1 to 4-9.
- Elkington, P., Stouthamer, P., and Brown, J., 1982, Rock Strength Predictions from Wireline Logs, *Int. J. Rock Mech. Min. Sci. & Geomech. Abstr.*, vol. 19, pp. 91-97.
- Hoek, E. and Brown, E.T., 1980, *Underground Excavations in Rock*, The Institute of Mining and Metallurgy, London, England, 527 p.
- Hummeldorf, R.G., 1984, The Classification and Evaluation of Roof Rocks for an Underground Coal Mine by Sonic Logging, M.S. Thesis, Purdue University, W. Lafayette, IN.
- Jaeger, J. and Cook, N.G.W., 1976, *Fundamentals of Rock Mechanics*, Second Edition, Chapman and Hill, London, England.
- Myung, J.I. and Helander, D.P., 1972, Correlation of Elastic Moduli Dynamically Measured by In-situ and Laboratory Techniques, *Proc. 13th Annual Logging Symposium*, Tulsa, Oklahoma, pp.1-25.
- Pirson, S.J., 1963, *Handbook of Well Log Analysis*, Prentice-Hall, Englewood Cliffs, New Jersey, pp. 221-236.
- Wichmann, P.A., 1974, Log Review 1, Dresser Atlas Industries, Inc., pp. 6-1 to 6-13.

WICK DRAINS

William Pfalzer
Kentucky Department of Transportation

Three Kentucky Highway projects incorporating Wick Drains, to accelerate the consolidation of foundation soils beneath highway embankments, are currently under construction. These projects, as far as the author is aware, are the first applications of Wick Drains in Kentucky; they are certainly the first Wick Drain applications relating to highway construction. This paper discusses, 1) site or project conditions favoring the use of Wick Drains, 2) getting the right information for Wick Drains from the subsurface investigation, 3) design procedures used in determining appropriate spacings of the drains, 4) specifications (KY had no specifications for Wick Drains at the time these projects were initiated), 5) fabric and drainage blanket considerations, 6) installation, and 7) instrumentation to monitor performance of the drains. Of the three Kentucky projects, by far the largest, with over 600,000 linear feet of Wick Drain, is in the greater Louisville area, and is included in the field trip agenda. The project is a section of I-65, between the outer loop and Fern Valley Road interchanges. The embankment is generally under 35 feet high, but as much as 450 feet wide. Including thru-traffic, collector-system, and on-off ramps, the roadway is as much as 12 lanes wide. Depth to bedrock in the area where Wick Drains are used is 25 to 45 feet. Settlement calculations have indicated that, in several areas, 90% consolidation would take more than seven (7) years without drains, but 6 to 9 months with the Wick Drains. If weather conditions and the contractors work schedules permit, it is anticipated that Symposium participants will be able to observe Wick Drain installations on the field trip.

**THE NATURE OF SOME GLACIAL AND MANMADE SEDIMENTARY SEQUENCES AND
THEIR DOWNHOLE LOGGING BY NATURAL GAMMA RAY**

By N. K. Bleuer
Indiana Department of Natural Resources
Division of Geological Survey
Bloomington, IN 47405

Introduction

Downhole logging can establish an all important stratigraphic framework necessary for understanding the three-dimensional distribution of glacial and other unconsolidated materials, including those in manmade settings. Such a framework should be the ultimate background for larger engineering studies or for hydrogeologic studies that involve water movement, such as in planning hazardous-waste disposal or even deep excavation.

Natural gamma-ray logging measures the varying rates of emission of gamma radiation that are a function of the differing mineralogy of materials. The variations typically parallel variations in the bulk grain-size distribution of the materials (sand, gravel, limestone, organic matter log low; clay and shale log high). Unlike electric-logging methods, this technique can be used both in open holes and in plastic- and steel-cased holes of varying diameters. Gamma-ray tools are available in small diameters that allow logging even the 2-inch I.D. casing commonly used in piezometer installations. Further, the method is not affected by water content of the materials of the hole or by minor variations in hole diameter. (Logging is affected, however, by variations in steel casing, such as drill rod or auger joints.) This versatility makes natural gamma-ray logging the most useful single logging technique available for use in glaciated terrain.

Glacial and related sedimentary sequences

Although downhole logging, particularly by gamma-ray, has been used for many years in programs of aquifer definition in the Midwest, its use can go far beyond simple definition. The use of gamma-ray logging in glacial geologic studies in Indiana has shown that "clay"- "clay" contacts and contact phenomena, which are commonly undetected in drilling and sampling but which are readily apparent on gamma-ray logs, may be as significant as the obvious distinctions between clay and granular lithologies. Contacts may be the most important defining properties of stratigraphy and unit geometry (fig. 1), and they may be

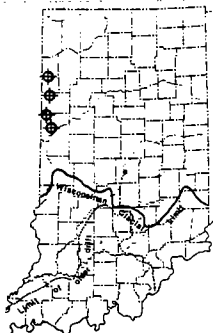
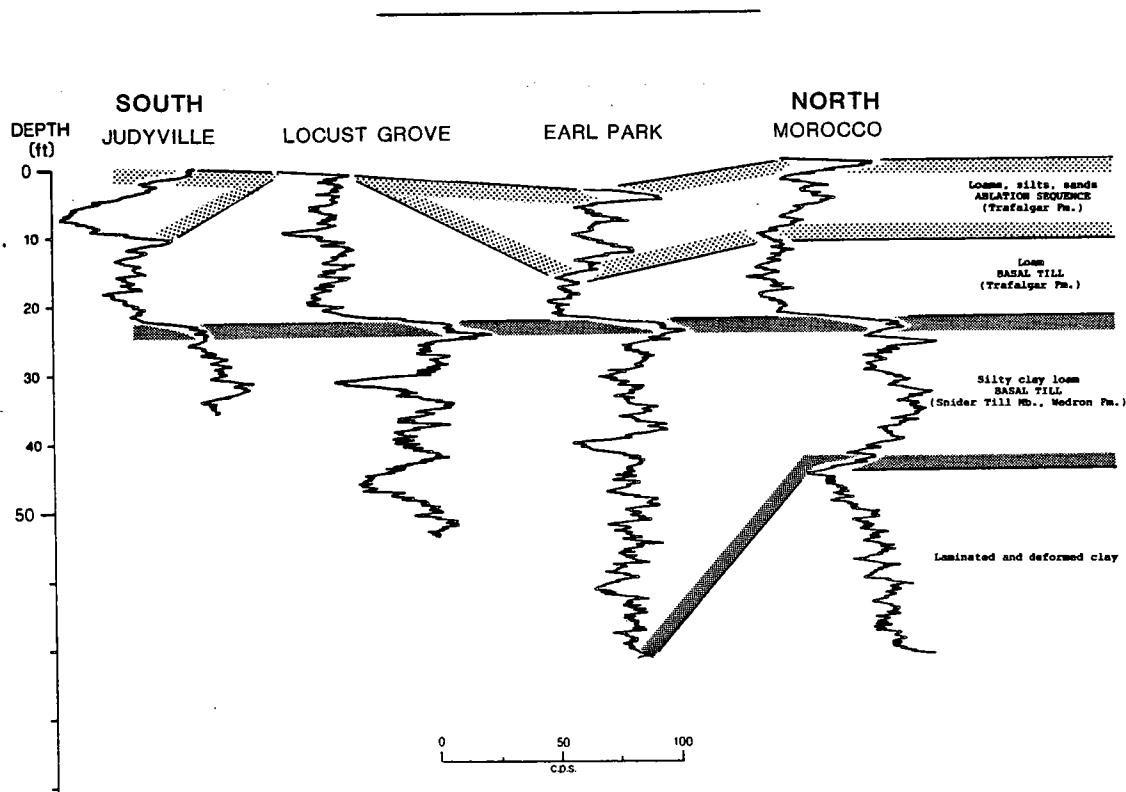


Fig. 1 Regional till-stratigraphic sequences: log of PVC-cased test holes in morainal ridges, west-central Indiana. Note variable character of glacial ablation sequence atop loamy till (Trafalgar Formation) (intermediate count rate, crew-cut form) atop silty clay loam and slightly shaley till (Snider Till Member, Wedron Formation) (high count rate, crew-cut form) (log-datum is top of Snider till; no horizontal scale).

as important as any other characteristic in defining water flow on site.

But beyond this, logging provides the ideal basis for definition of the total sedimentological architecture of specific sites or of large regions. Midwestern glacial deposits are not a heterogeneous morass of debris that they are commonly considered to be. Rather, they commonly consist of recognizable stratigraphic sequences--vertical sequences of deposits that accumulated during the lateral shifting of geologic environments through time. Such sequences include regional till-stratigraphic sequences of overlapping till units, units that are commonly recognizable entities of relatively homogeneous composition and physical properties (figs. 1,2). (See Bleuer and others, 1983; Wickham and Johnson, 1981; and Kemmis, 1981). And they include purely glacigenic sequences of on-site or regional deposition (fig. 2). Such types of sequences together can be conceptualized in a sedimentary model or, for our purposes, in what is termed a glacial "land system model" (Eyles, 1983).

Because the gamma-ray response of till units parallels the physical differences, especially grain size, that are known to differentiate midwestern tills, regional till-stratigraphic sequences of such units can be identified and traced in the subsurface. And just as geophysical logs are the basis for modern petroleum exploration and for the sedimentary models that are the foundation of modern basin analysis (see especially Allen, 1975; Scholle and Spearing, 1982; Galloway and others, 1983; Pirson, 1977; Selley, 1976, 1978), log motif, overall patterns of log response, should aid in identifying glacigenic sequences, which include elements similar to those that have been described from modern fluvial, deltaic, and lacustrine environments as well as from purely glacial environments.

A regional till-stratigraphic sequence is exemplified by the near-surface glacial stratigraphy of west-central Indiana, where tills record deposition from ice sheets of the Huron-Erie Lobe and the Lake Michigan Lobe. A loam-

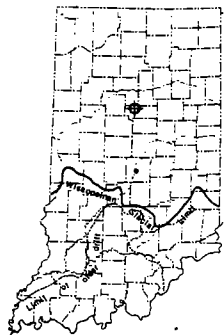
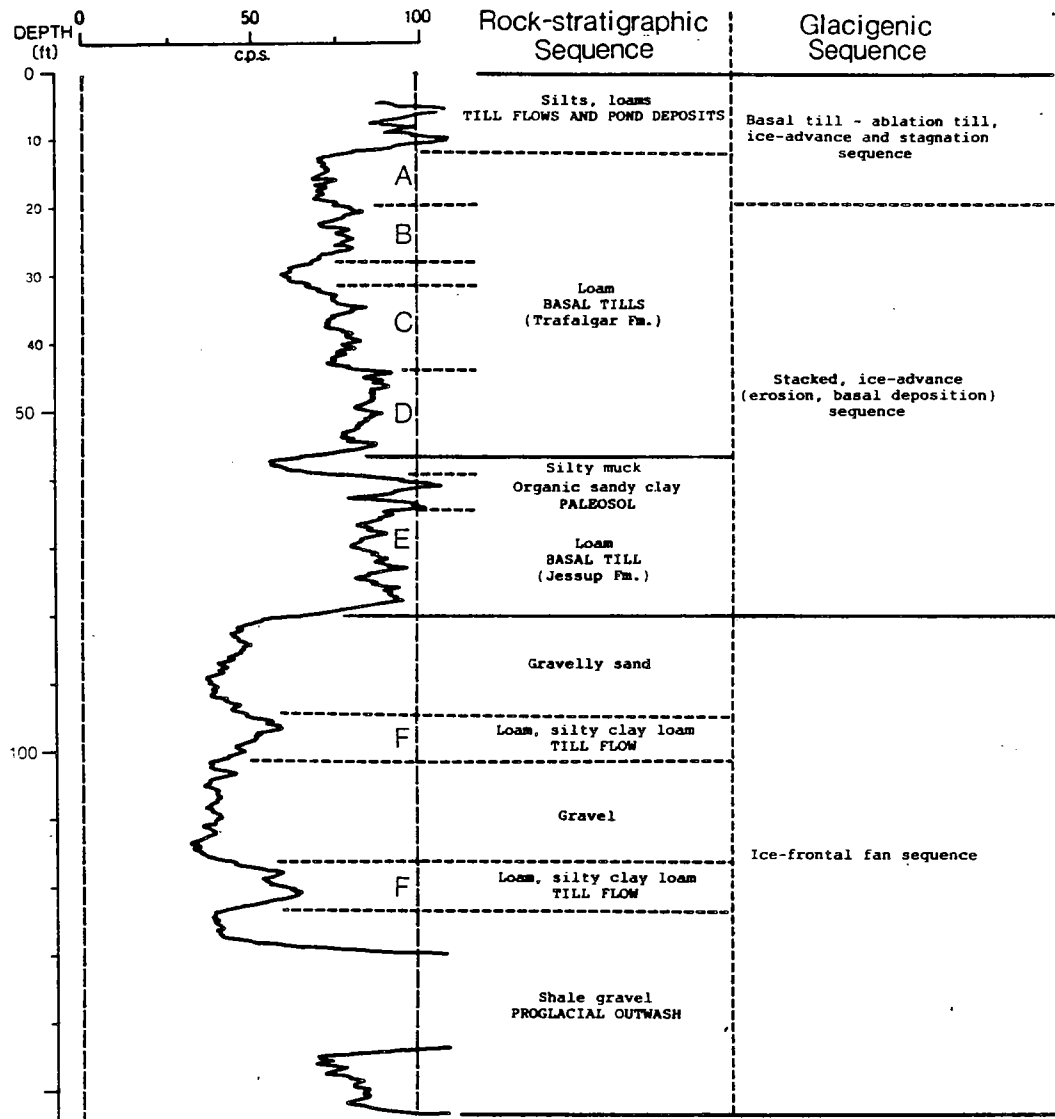


Fig. 2 Regional till-stratigraphic sequences and glacial sequences: log of PVC-cased test hole west of Kokomo, central Indiana. Note upper ablation sequence, multiple loam-textured tills (intermediate count rates, crew-cut form) and clayey paleosol (high count rate) capped by silty muck (low count rate); also nature, of interpreted till flows in outwash, and for basal gravel rich in Devonian black shale (high count rate) (access courtesy of U.S. Geological Survey).

textured till (Trafalgar Formation; Huron-Erie Lobe source) overlies a silty-clay-loam-textured till (Snider Till Member, Wedron Formation; Lake Michigan Lobe source) (fig. 1). Both units, which are interpreted as basal tills, are

relatively compact and slightly overconsolidated. The uppermost part of the Trafalgar is texturally heterogeneous and includes a variety of loamy tills interstratified with silts and sands. This unit, which contains relatively soft materials of high water content and which is normally consolidated, is interpreted as an ablation till.

In contrast, east of the pinchout of the distinctive Snider lithology in central Indiana, several loam-textured basal tills (Trafalgar Formation) can be recognized (fig. 2) on the basis of very subtle grain size and mineralogical differences. And in east-central Indiana loamy tills and older valley-fill lake deposits are capped by a regionally extensive silty-clay-loam-textured till (Lagro Formation).

A significance of such units is that many are present over large areas (figs. 1, 3). The Snider till, for instance, can be traced over much of north-west

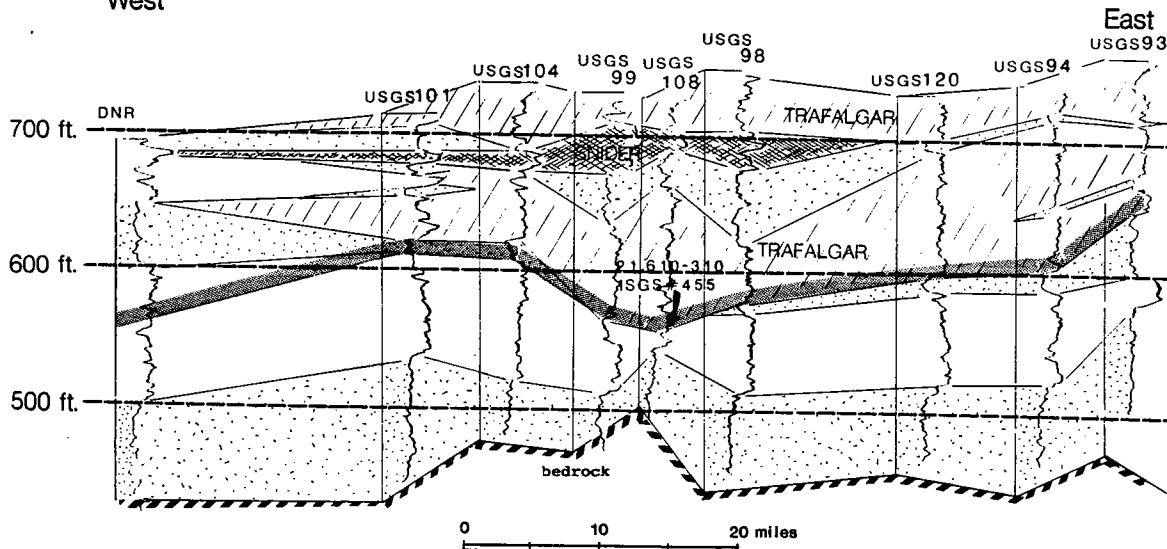
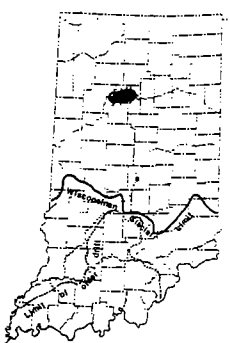


Fig. 3 Regional till-stratigraphic sequences: log cross section of drill-rod cased test holes in the axis of the Mahomet Valley Section (Lafayette Bedrock Valley System, the so-called Teays Valley), north-central Indiana. Note regional distribution of till units, including eastward pinchout of the clayey Snider till between loamy Trafalgar tills (base of the Wisconsin Stage, dark stippled), and, in general, the highly visual record of their internal and mutual relationships overlying the thick basal aquifer (Banner Formation, part equivalent of the Mahomet Sand Member of Illinois) over rock. (access, in part, courtesy of U.S. Geological Survey).



western and west-central Indiana, from great thicknesses within morainal accumulations in the west (fig. 1) to its pinchout in the south and the east (fig. 3). Regionally or on site, the differentiation of such units can be the basis of mapping three-dimensional geometry of the glacial deposits. The position of major aquifers and of significant changes in physical characteristics, including N values and other engineering properties, is most commonly between such units.

A glacial sequence is exemplified by the stratigraphy of deeper deposits south of Lake Michigan (figs. 4, 5). That stratigraphy consists of lake

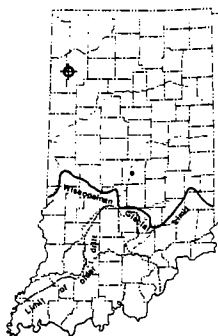
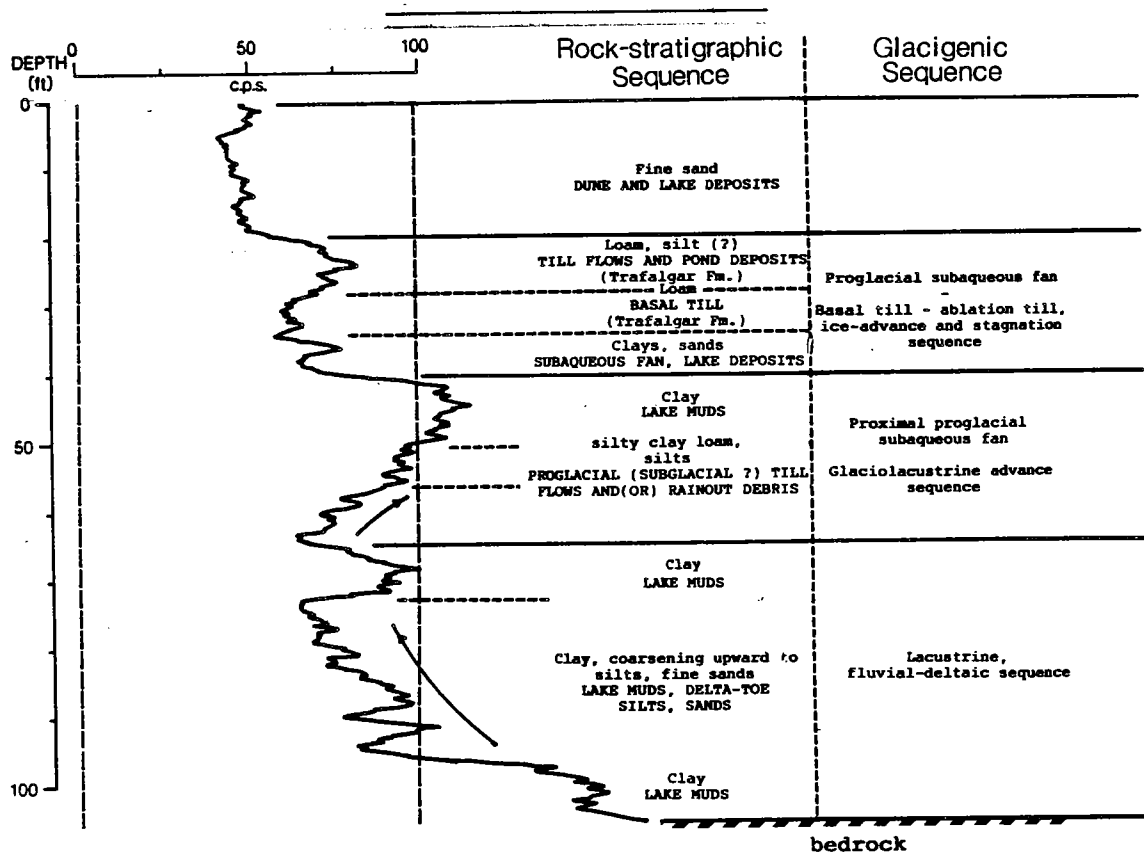


Fig. 4 Glacigenic sequences: log of PVC-cased test hole near Fair Oaks, northwestern Indiana, illustrating a local vertical glacigenic sequence. Note log motif of lake-bottom clays (high count rate, smooth in-out, silt-clay variations), deltaic silts and sands, and ice-derived clayey till flows (facies of the Snider till) associated with retreat of the Lake Michigan Lobe. (access courtesy of Hydrosience Associates, Inc.).

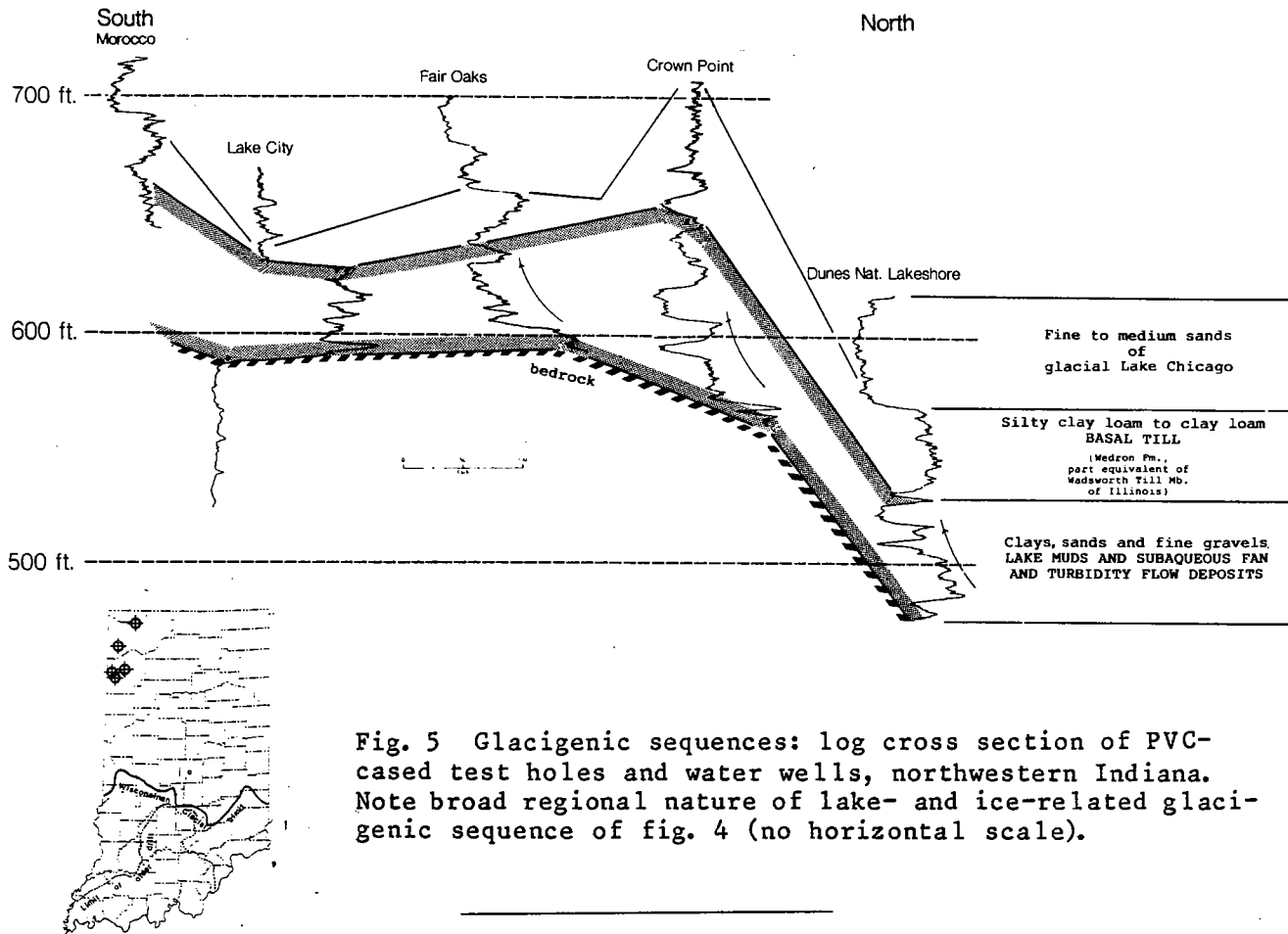


Fig. 5 Glacigenic sequences: log cross section of PVC-cased test holes and water wells, northwestern Indiana. Note broad regional nature of lake- and ice-related glaciogenic sequence of fig. 4 (no horizontal scale).

clays, deltaic sands and silts, and some tills (Snider till) and till-like sediments of sediment-gravity flow and floating-ice rain-out origin. These are soft, normally consolidated sediments with high water content. The deposits are interpreted to be those of an ice front of the Lake Michigan Lobe standing or floating in a large proglacial lake. Those deposits were overridden by ice of both the Huron-Erie Lobe and the Lake Michigan Lobe ice, and as a result the sequence was capped by loamy and clayey tills (Trafalgar Formation and Wedron Formation (equivalent of Wadsworth Till Member of Illinois)). Till units identified in association with this glaciogenic sequence, Snider, Trafalgar, Trafalgar ablation tills, and Wadsworth-equivalent tills are aspects of a regional till-stratigraphic sequence as well as the local glaciogenic sequence.

A similar glaciogenic sequence is exemplified by the stratigraphy of old glacial deposits filling the Marion Valley Section (eastern part of the Lafay-

ette Bedrock Valley System, the so-called Teays Valley) in east-central Indiana (fig. 6). That stratigraphy consists of laminated clays capped by tills. The clays, which are interpreted as deep-water lake deposits, are locally split by thick beds of coarse sand and gravel, which are interpreted as deltaic and subaqueous fan and turbidite deposits that were ultimately derived from the source glacier that blocked and dammed the valley. The various capping till units, including the silty-clay-loam-textured surficial till (Lagro Formation) are, again, components of the regional till-stratigraphic sequence.

A significance of such vertical glacial sequences is that the patterns of vertical change contained within can indicate geologic environment and

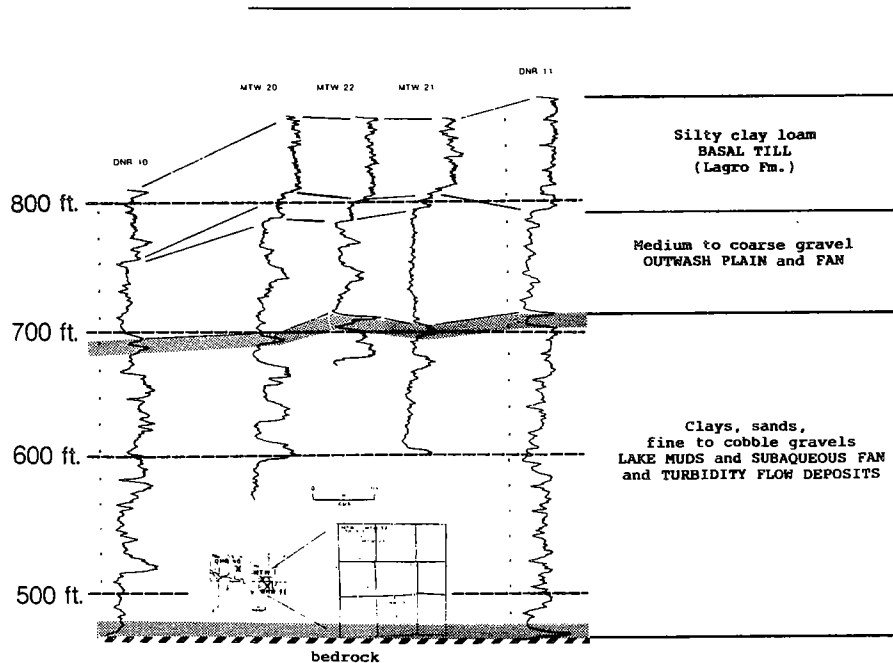


Fig. 6 Glacigenic sequences: log cross section of drill-stem- and PVC-cased test holes in the axis of the Marion valley, east-central Indiana. Note regional background of fine-grained lake sediments with localized coarse-gravel inputs from glacier-fed sources, coarse subaqueous fan and turbidite gravels (low count rate) abruptly interlayered with fine-grained lake sediments (high count rate, smooth in-out, silt-clay variations), also upper clayey till, a regional till-stratigraphic unit (Lagro Formation) and inflections in D.N.R. test holes (x-marked) caused by drill-rod joints at 20-foot intervals (access, in part, courtesy of Stremmel and Hill, Inc., and Howard Consultants, Inc.) (no horizontal scale).



environmental change. Thus, once recognized on site, or suspected from regional knowledge, the log motif of such sequences can provide the background for a predictive depositional model.

Manmade sequences

Manmade structures, such as earthen embankments and dam landfills, and mine-waste piles contain stratigraphic sequences. Sedimentary models can be hypothesized from a knowledge of the construction process, and such models can be used in analysis of failure, in design of remedial measures, and in resource evaluation.

For example, alternating layers of limestone and shale were emplaced in a series of thick interstate-highway fills in southeastern Indiana (fig. 7). The fill materials were derived from adjacent deep cuts through alternating beds of limestone and shale (Maquoketa Group, Late Ordovician age). Continuing subsidence of the roadway appears to be a result of compaction and possibly slide deformation within shale-rich lifts, whose distribution is readily seen in gamma-ray logs.

Within a large landfill in an urban setting of central Indiana, alternating layers of organic-rich and very porous municipal refuse alternate with daily cover material, which was derived from the silty overbank alluvium surrounding the site (fig. 8). The refuse lies immediately atop the virgin alluvium across the site and successively atop outwash gravels with thin interbedded loam-textured tills. Log profiles provide a highly visual record not only of fill geometry and composition but also of some of the critical environmental problems at the site. Examples are: (1) the (manmade) cutout of the silty alluvial floor in one location (a possible location of concentrated leachate leakage) and (2) the thin nature of the dense underlying tills, the aquacludes on which the ultimate hydrologic integrity of the site is based.

And finally, within the gob piles of a strip-mined, orphaned land area of

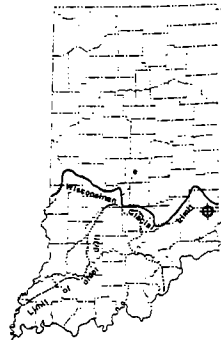
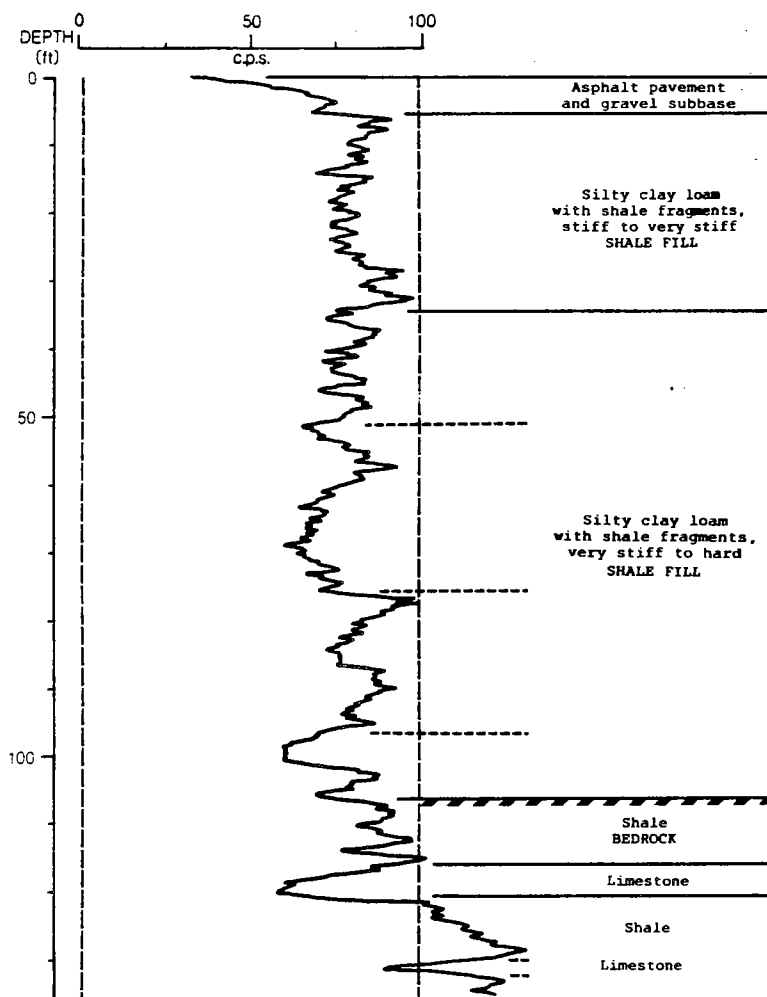


Fig. 7 Manmade sequences: log of aluminum-cased inclinometer hole, eastbound lane of Interstate Highway 74, Dearborn County, southeastern Indiana. Site is centered over an area of continued roadway subsidence. Note log motif of alternating limestone (low count rate) and shale (high count rate) lithologies and zones of large-scale character change (access courtesy of Indiana State Highway Department, Division of Materials and Tests).

western Indiana, downhole gamma-ray logs provide an excellent visual summary of the dumping of mine waste of varying composition (fig. 9). The materials consist of varying proportions of sandstone, shale, clinker, pyrite, rash, coal, and coal slurry. The logs can provide a synthesis of a sequence that is otherwise difficult to sample and somewhat arbitrary in description. Clearly, such logging could also provide a rapid means of characterizing slurry quality (shaliness) for fuel-resource evaluations.

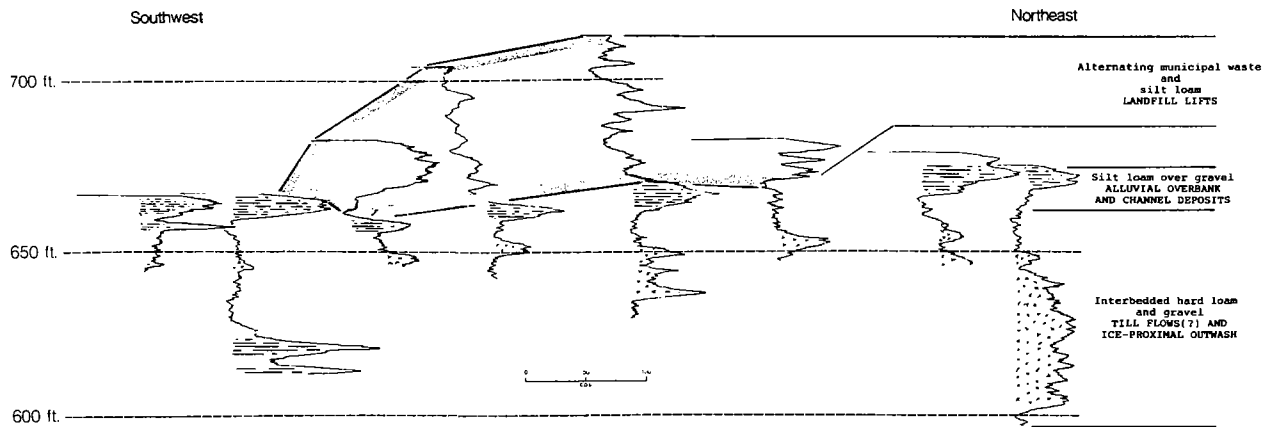


Fig. 8 Manmade sequences: log of PVC-cased piezometers in and beside an area-method municipal landfill, central Indiana. Note log motif of alternating layers of household refuse (low count rates) and silty cover material overlying alluvial overbank silt (the cover source; low count rate) with local cutout, and underlying glacial-fluvial gravels (low count rates) with thin tills (intermediate count rates) (no horizontal scale; approximate total spacing is 3/4 mile) (access courtesy of Wehran Engineering, Inc.).

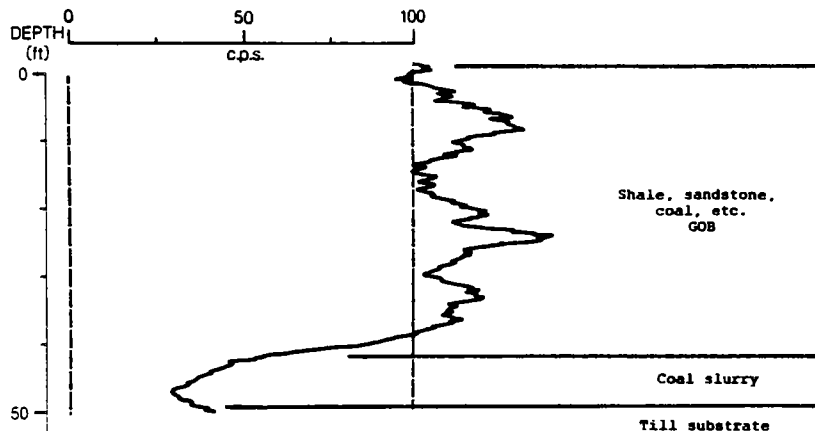


Fig. 9 Manmade sequences: log of PVC-cased piezometer in gob pile of Green Valley Mine reclamation area northwest of Terre Haute, western Indiana. Note log motif of alternating lithologies of mining waste composed of sandstone, coal, rash, clinker (low count rates) and shale (high count rates), overlying coal slurry (low count rate) atop till substrate (access courtesy of Geoscience Associates, Inc.).



Logging in exploration strategy

Advantages of gamma-ray logging in exploration strategy and economics can derive from the use of existing wells or piezometers during preliminary investigations, and from the use of fast and relatively inexpensive rotary-drilled or unsampled hollow-stem augered holes set with temporary casing (fig. 10) to test deep stratigraphy with minimal presence of an on-site professional. The use of logging during preliminary studies can provide a basis for the design of streamlined strategies for selecting sampling intervals, or for selecting successive completion depths of cluster sets with respect to significant contacts and to the overall stratigraphic sequence at a site.

But more basically, concepts of site geometry, including the shape and continuity of aquifers and hydrologic discontinuities, all depend upon there existing a basis for identification of stratigraphic units and for assessing

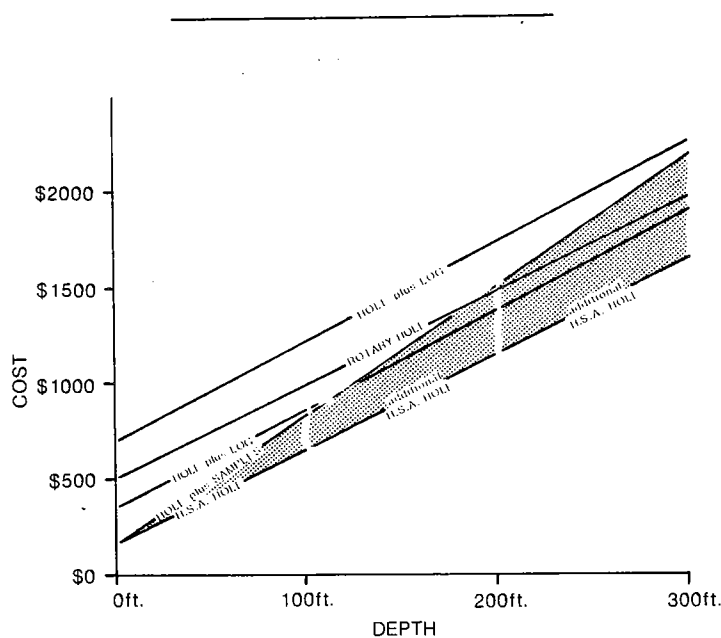


Fig. 10 Graph showing highly generalized cost relationships of holes drilled by rotary and hollow-stem auger methods, with and without logging. Costs include gross estimates of per-foot drilling, rig-time and mobilization, and are based upon assumed availability of local rotary drillers and of logging consultants operating small (non-oil field), slim-line equipment.

the nature of internal variability within those units. Outlining this geometry requires a conceptual model of the sedimentary origins of the units. Log characteristics can provide a primary basis for developing such models regionally and the absolute basis for mapping units locally.

For geologic and economic reasons, logging can (and should) play a major role in exploration strategy in Midwestern glacial materials. Indeed, continuous geophysical logs alone may have far greater value in general exploration than engineering logs (driller's logs plus interval samples) alone. But the two together can complete a total exploration strategy.

Selected bibliography

Allen, D. R., 1975, Identification of sediments--their depositional environment and degree of compaction--from well logs, in Chilingorian, G. U., and Wolf, K. H., eds., Compaction of coarse-grained sediments I, Developments in sedimentology: v. 18a, p. 349-401.

Bleuer, N. K., 1974, Distribution and significance of some ice-disintegration features in west-central Indiana: Indiana Geol. Survey Occasional Paper 8, 11 p

-----, 1975, The Stone Creek section, a historical key to the glacial stratigraphy of west-central Indiana: Indiana Geol. Survey Occasional Paper 11, 9 p.

-----, Melhorn, W. N., and Pavey, R. R., 1983, Interlobate stratigraphy of the Wabash Valley, Indiana: Field Trip Guidebook, 30th Ann. Field Conf., Midwest Friends of the Pleistocene, 135 p.

Chamberlain, A. K., 1984, Surface gamma-ray logs: A correlation tool for frontier areas: Am. Assoc. Petroleum Geologists Bull., v. 68, p. 1040-1043.

Christianson, E. A., 1967, Geology and groundwater resources of the Saskatoon area (73-B), Saskatchewan: Saskatchewan Research Council, Geology Div. Map 7.

-----, ed., 1970, Physical environment of Saskatoon, Canada: National Research Council of Canada Pub. 11378, 68 p.

- Dyke, J. H., Keys, W. S., and Meneley, W. A., 1972, Application of geophysical logging to groundwater studies in southeastern Saskatchewan: Canadian Jour. Earth Sci., v.9, p. 78-94.
- Ehlers, J., and Iwanoff, A., 1983, Geophysical well logging and its stratigraphic interpretation, in Ehlers, J., ed., Glacial deposits in northwest Europe: Balkema, Rotterdam, p. 263-265.
- Eyles, N., 1983, Glacial geology: a landsystems approach; in Eyles, N., ed., Glacial Geology, An introduction for engineers and earth scientists: Pergamon, N.Y., p. 1-18
- , and Menzies, J., 1983, The subglacial landsystem, in Eyles, N., ed., Glacial Geology, An introduction for engineers and earth scientists: Pergamon, N.Y., p. 19-70.
- Eyles, N., and Clark, B. M., 1985, Geophysical well logging and the analysis of subsurface glacial depositional systems: an example from the Lake Ontario and Huron basins (abs.): Geol. Soc. America Abs. with Programs, North-Central Sec. v. 17, p. 287.
- Galloway, W. E., Ewing, T. E., Garrett, C. M., Tyler, N., and Beboit, D. G., 1983, Atlas of major Texas oil reservoirs: Texas Bur. Econ. Geology, Austin, 139 p.
- Greenhouse, J. P., Karrow, P. F., and Farvolden, R. N., 1983, Grant 128 Subsurface Quaternary stratigraphy using borehole geophysics, in Pye, E. G., Geoscience research grant program summary of research 1982-1983: Ontario Geol. Survey Misc. Paper 113, p. 93-95.
- Gold, L. W., ed., 1981, Proceedings of the symposium on processes of glacier erosion and sedimentation: Annals Glaciology, v. 2, p. 176-182.
- Guyod, H., 1966, Interpretation of electric and gamma ray logs in water wells: Log Analyst, v. 65, p. 30-44.
- Jones, P. H., and Skibitzke, H. E., 1956, Subsurface geophysical methods in groundwater hydrology, in Advances In geophysics: Academic Press, N.Y., v.3, p. 241-300.
- Kemmis, T. J., 1981, Importance of regelation process to certain properties of basal tills deposited by the Laurentide ice sheet in Iowa and Illinois, U.S.A., in Gold, L. W., ed., Proceedings of the symposium on processes of glacier erosion and sedimentation: Annals Glaciology, v. 2, p. 147-152.

- Keys, W. S., 1968, Well logging in ground-water hydrology: *Ground Water*, v. 6, no. 1, p. 10-25.
- Keys, W. S., and Brown, R. F., 1973, Role of borehole geophysics in underground waste storage and artificial recharge, in Braunstein, Jules, ed., Second international symposium on underground waste management and artificial recharge, New Orleans, v.1, p. 147-191.
- Keys, W. S., Eggers, D. E., and Taylor, T. A., 1979, Borehole geophysics as applied to the management of radioactive waste -- site selection and monitoring, in Carter, M. W., and others, eds., *Management of Low-level Radioactive Waste*, v. 2, p. 955-980, Pergamon, N.Y.
- Keys, W. S., and MacCary, L. M., 1971, Application of borehole geophysics to water-resources investigations: *Techniques of Water-Resources Investigations of the U.S. Geological Survey*, Book 2, chap. E1, 126 p.
- Montgomery, R. J., Wierman, D. A., Taylor, Robert, and Kock, H. A., 1985, Use of downhole geophysical methods in determining the internal structures of a large landfill, in *Surface and borehole geophysical methods in ground water investigations: Second Nat. Conf., Nat. Water Well Assoc.*, p. 377-386.
- Norris, S. E., 1972, The use of gamma logs in determining the character of unconsolidated sediments and well construction features: *Ground Water*, v. 10, no. 6, p. 14-21.
- Pirson, S. J., 1977, *Geologic well log analysis*: Houston, Gulf Publishing Co., 377 p.
- Read, P. C., 1985, Comparative analyses of surface resistivity surveys and natural-gamma radiation borehole logs in Illinois, in *Surface and borehole geophysical methods in ground water investigations, Second Nat. Conf., Nat. Water Well Assoc.*, p. 215-227.
- Read, P. C., Sargent, M. L., and Gross, D. L., 1983, Use of natural-gamma logging for characterization of bottom sediment in the Mississippi River: *Geol. Soc. America Abs. with Programs*, v. 15, p. 668.
- Rutter, N. W., and Wyder, J. E., 1965, Application of borehole stratigraphic techniques in areas of mountain glacial drift in Alberta, Canada: *Canada Geol. Survey Paper* 69-35, 16 p.
- Scholle, P. A., and Spearing, D., eds., 1982, *Sandstone depositional environments*: *Am. Assoc. Petroleum Geologists Mem.* 31, 410 p.

Selley, R. C., 1976, Subsurface environmental analysis of North Sea sediments: Am. Assoc. Petroleum Geologists Bull, v. 60, p. 184-195.

-----, 1978, Ancient sedimentary environments: Cornell Univ. Press, Ithaca, 287 p.

Taylor, T. A., and Dey, J. A., 1985, Bibliography of borehole geophysics applied to ground-water hydrology: U. S. Geological Survey Circular 426, 62 p.

Wickham, S. S., and Johnson, W. H., 1981, The Tiskilwa Till, a regional view of its origin and depositional processes, in Gold, L. W., ed., Proceedings of the symposium on processes of glacier erosion and sedimentation: Annals Glaciology, v. 2 p. 176-182.

Laboratory Testing as an Aid in the Design of Cable Anchor Systems
for Rock Reinforcement

DAVID A. LIENHART, Supervisory Geologist

TERRY E. STRANSKY, Staff Geologist

U. S. Army Corps of Engineers, Ohio River Division, Geotechnical Laboratory
5851 Mariemont Ave., Cincinnati, OH 45227

ABSTRACT

The design of cable anchor systems, whether for dam tie-down projects or rock-slope reinforcement, requires, among other things, a knowledge of the bond strength (both ultimate and residual) between the grout used to set the cable anchor and the rock into which the anchor is to be set.

Quite often, field tests of anchor systems, owing to costs, time constraints or geologic factors such as rock inhomogeneity, are impractical. In such cases, past experience with similar material or standard laboratory grout-on-rock tests, performed in direct shear equipment, are employed to determine bond strengths. The former may grossly mis-estimate the necessary parameters and the latter usually determines bond strength parameters in a direction parallel to bedding surfaces or discontinuities, when what is actually required are those parameters normal or oblique to the bedding surfaces or other discontinuities.

Two laboratory tests, a push-out cylindrical shear and a direct pull-out test were performed on rock core from several localities, and

a comparison is presented. Limitations and factors affecting test results, as well as the applicability of these results in the determination of anchor length are discussed.

INTRODUCTION

The design of rock anchoring systems requires a knowledge of the anticipated bond shear strengths between the grout used to embed the anchor and the surrounding rock into which the grout and anchor are emplaced. Several methods for determining this strength are in general use today. These include past experience or "rule-of-thumb" design; the use of generalized bond strength values provided by manufacturers of anchors and embedding materials; field tests of actually emplaced anchors; and laboratory-scale tests designed specifically to test the bond strength by using cylinders of rock into which cables or threaded steel rods are emplaced (pull out shear) or grout masses into which a piece of rock core is emplaced (push-out shear).

In the following sections we present an analysis and evaluation of two of these laboratory-scale tests. The push-out shear test has been in use for a number of years, particularly by manufacturers of anchors and embedding materials, and also by this laboratory.

Recently, however, we have developed a pull-out type test which can be performed on the same equipment used to run direct-shear type grout-on-rock bond strength tests, provided a suitable holder is used.

Our preliminary data from this type of test on several sedimentary materials, and a comparison of bond strength values with those obtained from the conventional push-out test, indicate significant differences in anticipated bond strengths. The likely explanation for these differences appears to be the differences in deformation behavior as evidenced by a comparison of Poisson's Ratio values for these sedimentary

materials and the accompanying grout embedding material.

Calculation of Required Anchor Length

Determination of necessary anchor lengths is site specific, depending on local geologic conditions, consequences of anchor failure, extent of allowable deformation etc.

The anchorage length may be calculated using the following formula (Seegmiller, 1982):

$$l_a = \frac{U_m F_a}{\pi d \tau_b}$$

where l_a = anchor length

U_m = maximum anchor force

F_a = safety factor against anchorage failure

d = diameter of borehole

τ_b = grout-rock bond strength (ultimate)

The factor τ_b , grout-rock bond strength, is that item with which this paper concerns itself.

For structures overlying horizontally stratified rock, anchorage lengths are dependent upon both expected uplift forces (for example, those due to seepage) and weight of overburden and existing structures. It is necessary in this case to determine bond strengths for each lithologic unit, sum the bond strengths, and calculate anchor lengths using appropriate safety factors (see Figure 1).

Push-Out Cylindrical Shear Test

The push-out cylindrical shear test, though in existence for a number of years, is not a very widely known or often used test, its use being predominantly confined to manufacturers of rock anchors.

The test essentially consists of pushing a sample of rock core through a steel cylinder, the annulus between the core and the cylinder being filled with grout (see Figure 2 for typical test set-up). The rock is loaded at a predetermined, constant rate (either constant load or constant deformation rate) at least until failure of the grout-rock bond, but preferably until the shear stress stabilizes. The assumption is made that the transfer of force to the rock occurs at the grout-rock interface and that the shear stresses are transmitted uniformly. Knowing the height(h) and the diameter(d) of the sample, the bond strengths (ultimate and residual) may be calculated by:

$$\text{Shear Strength} = \frac{\text{Load (lbs.)}}{\pi dh}$$

If deformation readings parallel to the loading direction are obtained, the stress-strain loading curve for the sample may also be obtained.

We recognize that the assumption of uniformly transmitted shear stresses may not be valid. In addition, several other factors need to be considered in the evaluation of the results obtained with this test. First, because of the relative stiffness of the metal cylinder, lateral expansion of both the concrete annulus and the rock core is restricted, resulting perhaps in stronger bonds than may actually be expected.

Secondly, our experience has been that, quite often, the supposed bond failure is caused not by transmitted shear stresses, but by radial cracking of the grout annulus due to tensile forces, followed by failure of the grout-rock bond. The tensile forces are caused by

the differential in Poisson's Ratio between the rock cylinder and concrete annulus.

Additionally, if the stress-strain curves are desired, problems arise when plastic, easily deformable materials such as clay shales are tested. In such cases, observed deformations are those due to the compression and corresponding increase in diametral strain of the sample itself, not from deformation of the grout-rock contact.

Manufacturers of anchoring systems frequently quote "typical" values of "ultimate" bond strengths for different rock types. As can be seen from Tables 1 and 2, results obtained on the same general rock type may be widely variable. Consequently, if one takes "typical" values, estimates of anchor length using safety factor criteria may be unnecessarily conservative, or not conservative enough.

Direct Pull-Out Test

The test apparatus for this type of test, as developed by the authors, is shown in Figure 3. The test consists of grouting either a wire cable or a threaded bar into a hole drilled in a piece of rock core, allowing the grout to cure, and then literally attempting to pull the grout plug out of the core at a predetermined rate.

Several problems were encountered during the development of this test. At low grout strengths (grout cured for only a relatively short period of time) it was found to be easy to pull out the plug with few problems. However, as the bond between the grout plug and the rock was

allowed to develop strength, splitting tensile failure of the rock occurred prior to actual bond failure due to the dilation of the grout plug as compressional forces were applied. Thus, in many cases, the only statement one could make was that the bond strength exceeded a certain value.

It was thus determined that, in order to obtain meaningful data, it would be necessary to confine the piece of rock core in which the grout rock was embedded.

Secondary Factors Affecting Cylindrical Shear Test Results

Avenues for Further Study

Several factors affecting the validity of the results obtained from these tests need to be considered: the eccentricity of the load, the roughness of both the anchor surface and the borehole wall in the rock, the effect of the grout strength on the grout-rock bond, the effect of confinement of the sample and the orientation of the cable embedment with respect to bedding or other planar features in the rock.

The present direct pull-out apparatus appears to preclude all but the most minimal eccentric loads due to the alignment of the worm gear providing the shearing load and the tension load-cell providing the force readings. Eccentric loading for the push-out shear test may be overcome by the use of swivel platens on a universal testing machine.

The effect of borehole and anchor surface roughness on test

results has not as yet been studied.. It is to be expected that their effects on ultimate stress values will be minimal, but may be significant with respect to residual stress values. In the latter case, asperities within the borehole must be overridden before a limiting residual stress is obtained.

The effect of confinement of the sample on test results has been shown to be critical. Without sample confinement, which mimics the confinement of the grouted anchor in the rock mass, tensile failure of the rock often precedes or precludes actual failure of the grout-rock bond.

The effect of grout strength on the strength of the grout-rock bond has been examined only briefly during the course of our testing program. Results indicate little or no effect on bond strengths. It appears however, that the use of expansive-type grouts may promote better bonds.

In both the push-out shear and the direct pull-out tests the direction of cable embedment is normal to the planar features in the rock. Unfortunately, this is not truly reflective of embedments in the field, which are usually at some angle approaching 45° in order to mobilize shear strength along rock mass discontinuities. If the rock material were homogeneous and isotropic this would not matter since material properties in all direction would be the same, but significant differences in obtained values may occur if this is not the case. We have not as yet studied this aspect of this test; however, the

problem is more one of logistics than an insurmountable hurdle. We propose in the future to obtain, by redrilling at various orientations, cores in which the planar features are oriented at more realistic angles to the cable embedment direction.

Comparison of Pull-Out and Push-Out Shear Test Results

As can be seen in Tables 2 and 3, data obtained from these tests is not comparable. In fact, values obtained using the pull-out shear test are consistently (with one exception) on the order of 1.5 - 3 times that obtained using the push-out shear test.

What this means in terms of design parameters, is that using values obtained from push-out shear tests, when one considers that safety factors are already built into the design calculations, will result in unnecessarily conservative anchoring systems, if Poisson's Ratio for the rock is lower than that for the grout.

The explanation for the discrepancy in data obtained from the two tests lies in the differences in deformation behavior between the rock and the grout, particularly as evidenced by markedly different Poisson's Ratio values (Table 4). In the push-out test of, say, shale embedded in grout, the shale gives a falsely high value due to its deformation and diametral expansion in the much stiffer grout. The opposite is true, however, for a well-cemented quartz sandstone. Its Poisson's Ratio value is less than that for the grout and the result is analogous to a rod punching through wet sand.

The pull-out test, however, is the antithesis of the push-out test. In attempting to pull the grout plug from a confined sandstone specimen, the grout, with its higher Poisson's Ratio will deform diametrically and the increased friction will produce a higher bond strength. A grout plug embedded in a material with a higher Poisson's Ratio than itself, however, will act like the "rod punching through wet sand".

CONCLUSIONS

It is evident from this study that the Poisson's Ratio of the rock sample and of the grout must be considered in designing a test for grout-rock bond strength. This investigation has shown that the previously often-used push-out test produces grout-rock bond strengths one-and-a-half to three times too low for rock with Poisson's Ratios of 0.10 to 0.15, and bond strengths almost two times too high for rock where the Poisson's Ratio is about 0.30. The pull-out test eliminates this production of erroneous data and gives the designer an improved analysis from which he may work.

ACKNOWLEDGEMENT

The authors wish to thank Messrs. Robert Stadler and Charles Canning for their comments and suggestions after review of the first draft of this paper. We also would like to thank Ms. Deborah Bender for her patience and diligence in typing the drafts and final manuscript.

REFERENCES

- Seegmiller, B. L., 1982, Rock Reinforcement Design for Surface Mine Bench Instabilities: Mining Engineering, Vol. 34, pp. 1567-1575.
- Stransky, T., 1981, Emsworth Lock & Dam: Results of Laboratory Testing of 6" Rock Core: U. S. Army Engineers, Ohio River Division Laboratory Open-File Report #103/81.609P, unpagged.
- Stransky, T., 1983, Montgomery Lock & Dam: Results of Push-Out (Cylindrical) Shear Tests of 6" Sandstone Core: U. S. Army Engineers Open-File Report #103/82.629P, unpagged.
- Stransky, T., 1983, Mill Creek Channel Improvement, Section 2: U. S. Army Engineers Open-File Report #103/84.603L, unpagged.
- Stransky, T., 1984 (in progress), Dashiels Lock & Dam: Results of Laboratory Testing of Rock Core: U. S. Army Engineers Open-File Report #103/84.604P, unpagged.
- VSL Corporation, 1971, Prestressed Rock and Soil Anchors, p. 15.

Table 1. Push-Out Shear Test, Ultimate Bond Strengths, PSI
(VCL Rock Anchors, Inc.)

Rock Type/Description	Bond Strength *
Sandstone, Friable, poorly lithified	53
Sandstone, well-cemented	325
Sandstone, chalky	411
Serpentine, slightly weathered, slickensided	225
Basalt, moderately weathered	560
Limestone, tertiary	400

*Note: "Typical" values may actually vary quite widely. Even rock which appears to be isotropic and homogeneous will vary both laterally and vertically; therefore, use of "typical" values is NOT recommended.

Table 2. Ultimate Bond Strengths, (Ohio River Division Laboratories)

Rock Type/Description	Push-Out Test	Pull-Out Test
Clay Shale (Kope Fm)	40-152	--
Clay Shale (Formation not known)	225-285	--
Limestone (Formation not known)	312-466	--
Siltstone (Conemaugh Fm)	245-593	624-982
Sandstone (Conemaugh Fm)	295-485	863-978
Shaly Siltstone	864-798	290

Table 3. Comparison of Push-Out and Pull-Out Shear Test Results on
Rock from Conemaugh Formation

Rock Type	Push-Out Shear Strength, PSI	Pull-Out Shear Strength, PSI
Sandstone	481	863
Sandstone	485	978
Sandstone	296	878
Siltstone	490	982
Siltstone	487	624
Shaly Siltstone	593	290*
*partial separation along shale layers.		

Table 4.

Poisson's Ratio	Rock Type
0.104 - 0.156	Sandstone
0.1 - 0.15**	Siltstone
0.224 - 0.312	Shaly Siltstone
0.175	Grout
**typical values.	

Problem: From the thickness and ultimate bond strength (determined from the pull-out test) of each lithologic unit, determine the bonding force for a 4" diameter hole in each unit.

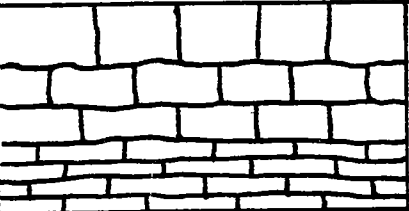


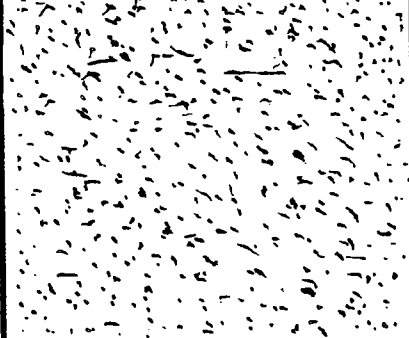
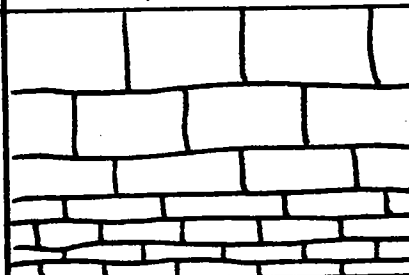

Thickness of Rock Unit	Stratigraphic Section	Lithology	Ultimate Bond Strength (PSI)	Answer: Bond for 4" Diameter Hole
8.5'		Limestone A	750	961,327 lbs.
9.7'		Shale A	225	329,113 lbs.
2.0'		Coal	180	54,286 lbs.
14.8'		Sandstone	825	1,841,224 lbs.
10.4'		Limestone B	780	1,223,260 lbs.
8.0'		Shale B	290	349,847 lbs.

Figure 1. Illustration of manner in which bond strengths may be calculated for various lithologic units and then summed to determine anchor length.

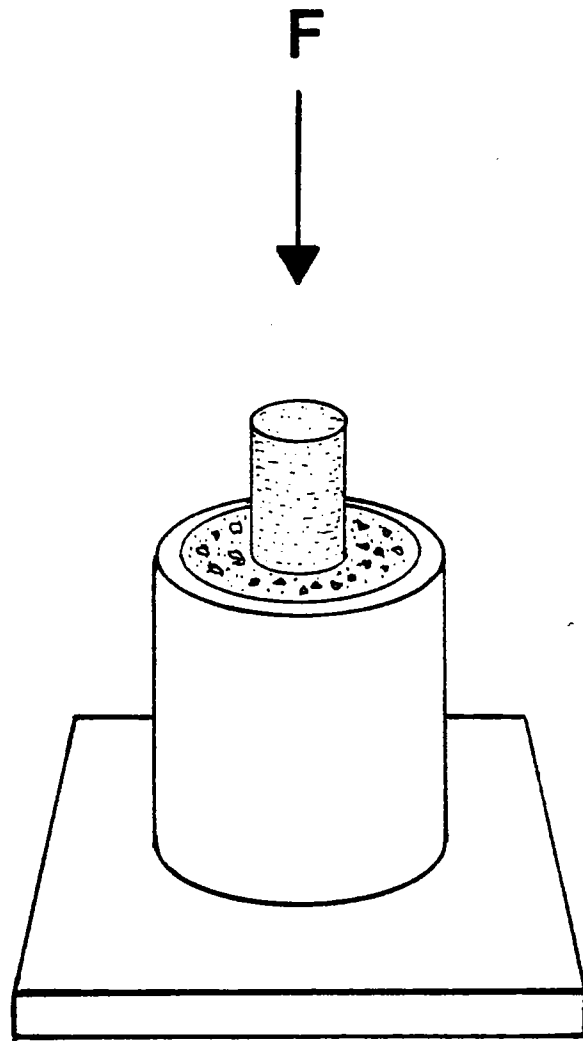


Figure 2. Schematic of the push-out test configuration.

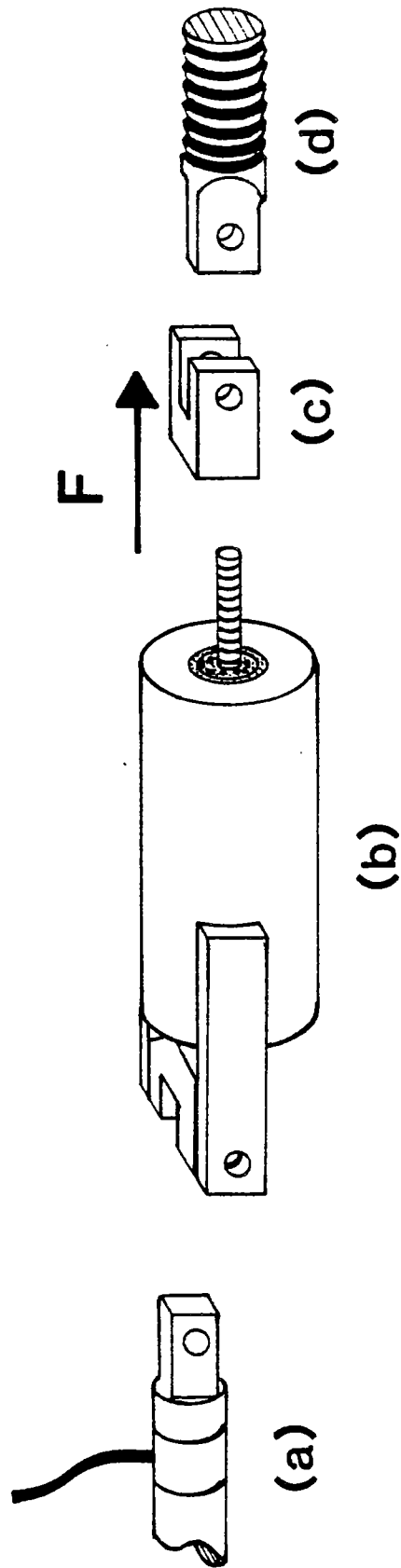


Figure 3. Schematic (exploded view) of the pull-out test configuration; (a) tension load cell, (b) sample holder, (c) nut, and (d) screw jack.

PREDICTING SETTLEMENTS WITHIN COMPACTED EMBANKMENTS

by

S. O. Nwabuokey and
C. W. Lovell

School of Civil Engineering
Purdue University
West Lafayette, Indiana

ABSTRACT

Compaction is an essential step in the construction of fills. Compaction causes densification by a reduction of air voids due to changes in the relative positions of soil aggregates and/or soil grains. This induces a compactive prestress in the soil, which represents the fraction of the compaction energy/pressure which is effectively transmitted to the soil matrix through plastic deformation. The ensuing amount of plastic deformation depends on the duration of application of the compaction energy/pressure and the constraint posed by the induced pore fluid (water and air) pressures.

With the increasing demand for higher embankments, the need arises to produce definite and predetermined compressibility and settlement responses within embankments for both the short and long term periods.

The initial vertical strains within a compacted embankment are those due to self weight. The magnitude of these movements is highly dependent upon the values of prestress established by the compaction process; however, they occur as rapidly as the embankment can be built. The major vertical strains will probably occur as the fill becomes wetter and softens in service. The material in the upper portion of the embankment will often swell under low confinement and the net movement is an appropriate summing of these events with the compressions that occur deeper in the fill.

By testing a series of samples, using a procedure that involves one dimensional compression testing in three stages, with a range of confinements which match those which will be imposed by the prototype embankment, representative vertical strains are defined. The integration of these strains over the fill height produces the prediction of movement within the embankment.

INTRODUCTION

Compaction has long been recognized as the most economical mechanical procedure for improving the compressibility, shear strength and permeability characteristics of a soil. The improvement of these characteristics is usually effected by specifying suitable placement compaction conditions, such as water content, dry density, compaction effort and type of compaction equipment, so as to ensure adequate short and long term performances.

Excavation, transportation, dumping and spreading in the field (or degradation in the laboratory) before compaction, substantially obscures the geologic preconsolidation stresses. Compaction causes densification by reduction of air voids due to a change in the relative positions of the soil aggregates and/or grains. This induces a compactive prestress in the soil, which though analagous to preconsolidation stress, represents the fraction of the compaction energy which is effectively transmitted to the soil matrix due to plastic deformation. The ensuing amount of plastic deformation depends on the duration of application of the compaction energy/pressure and the constraint posed by the induced pore fluid (water and air) pressures.

With the increasing demand for higher fills/embankments, in which the soil within defined layers is at different "overconsolidation ratios", due to the as-compacted prestress, the need arises to produce definite and predetermined compressibility and shear strength responses in these soil structures.

The compressibility and shear strength characteristics of a compacted material are influenced by the compaction water content, compaction energy/pressure and the mode of compaction. These characteristics are modified during the service life of the fill/embankment due to the unavoidable changes in the environmental conditions.

Thus, for an engineer to quantitatively predict and control the compressibility characteristics of a compacted fill/embankment, both for the short and long term periods, an explicit knowledge of the magnitudes of the as-compacted prestresses are essential.

EXPERIMENTAL APPARATUS AND PROCEDURE

The soil utilized for this study was obtained from an excavation alongside the relocated US Highway (30) at about 4.831 Km (3 miles) from Zulu in Allen County in northeastern Indiana. The excavation lies within the southern limits of the Lake Maumee plain, consisting of lacustrine deposits, formed during the period of Wisconsin glaciation. These are generally greater than

9.0 m (230 ft) in thickness. The underlying bedrock is believed to be from the Silurian period.

The soil is a brown and gray mottled medium stiff clay. The index properties and classification test results for the clay soil are given in Table 1.

RESULTS, DISCUSSION, AND ANALYSIS OF RESULTS

Compaction

The impact (dynamic) compaction energy mode was used for this study to investigate the variation of the compressibility characteristics of a compacted soil, with the primary compaction independent variables (molding water content and compaction energy). The relationships between dry density and water content for the lacustrine clay compacted at the three energy levels considered for this study, "15-blow" (low energy) Proctor, Standard Proctor {AASHTO (1978), designation T99}, and Modified Proctor {AASHTO (1978), designation T180} are given in Figure 1.

As-Compacted Prestress

The as-compacted prestress can be a very useful parameter in the design of embankments/fills, since the compressibility behavior of the soil mass will be different at embankment/fill confining pressures above or below this value.

The as-compacted prestress represents the fraction of the compaction energy which is effectively transmitted to the soil matrix due to plastic deformation and represents the stress level beyond which significant particle and/or aggregate orientation occurs.

The as-compacted prestress values are presented in Figure 2 as a function of water content for the various nominal impact energy levels used in this study. Observe from Figure 2 the dependence of the as-compacted prestress on the compaction water content and energies, respectively. The following general conclusions can be made with respect to the prestressing capacity of the soil.

1. Dry of optimum water content:-
 - a. At a given impact compaction energy level, the as-compacted prestress decreases with increasing water content level.
 - b. As the impact compaction energy increases, the value of as-compacted prestress also increases significantly.

TABLE 1

Index Properties and Classification of Soil

Category	Properties and Classification
Liquid Limit (%)	47.
Plastic Limit (%)	20.
Plastic Index (%)	27.
Specific Gravity	2.75
Clay Fraction (< 2 μ m)%	33.
Skempton's Activity	0.82
Unified Soil Classification	CL
ASSHTO Soil Classification	A-7-6

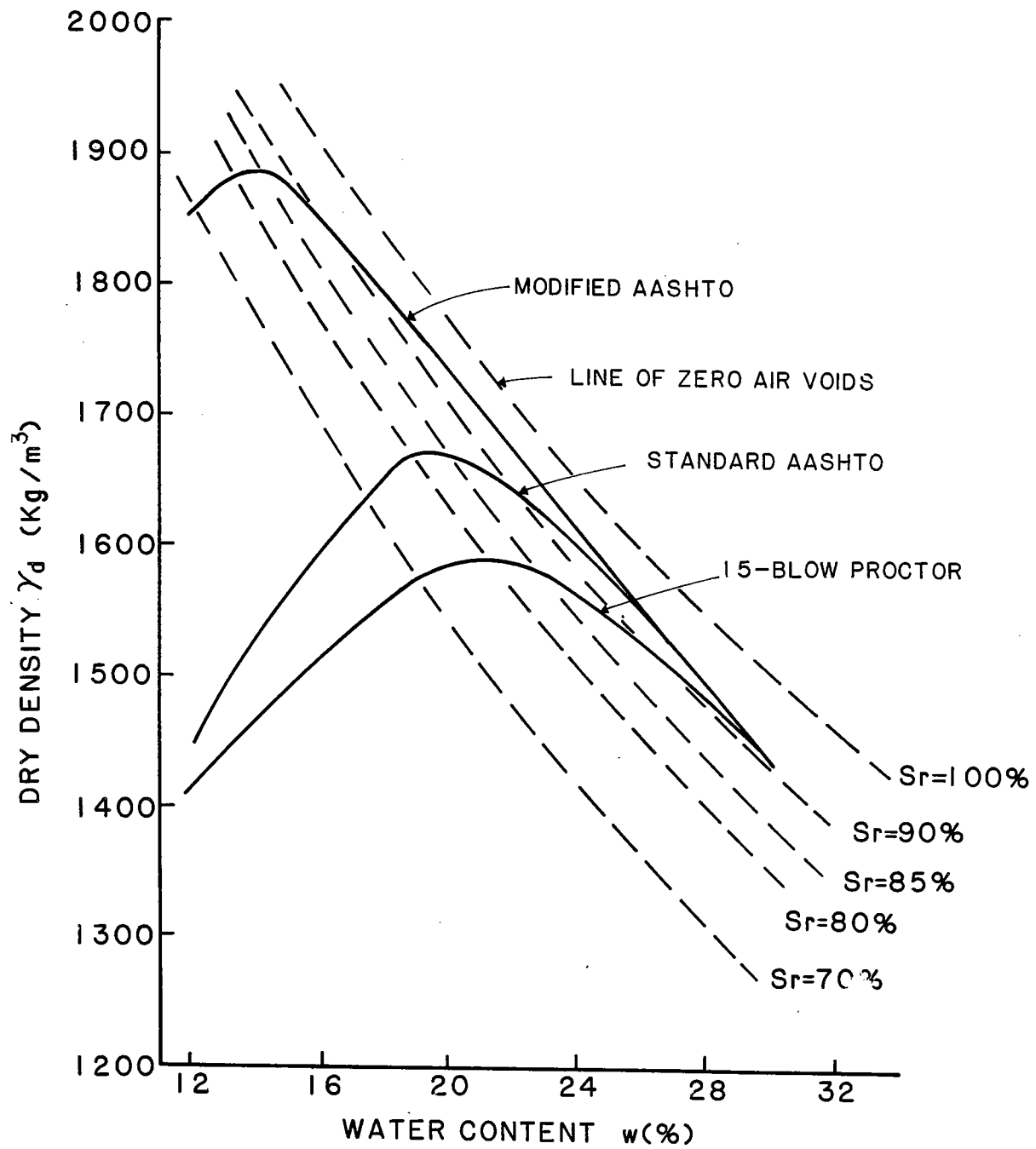


Figure 1 Dry Density vs. Moisture Content
For The Lacustine Clay.

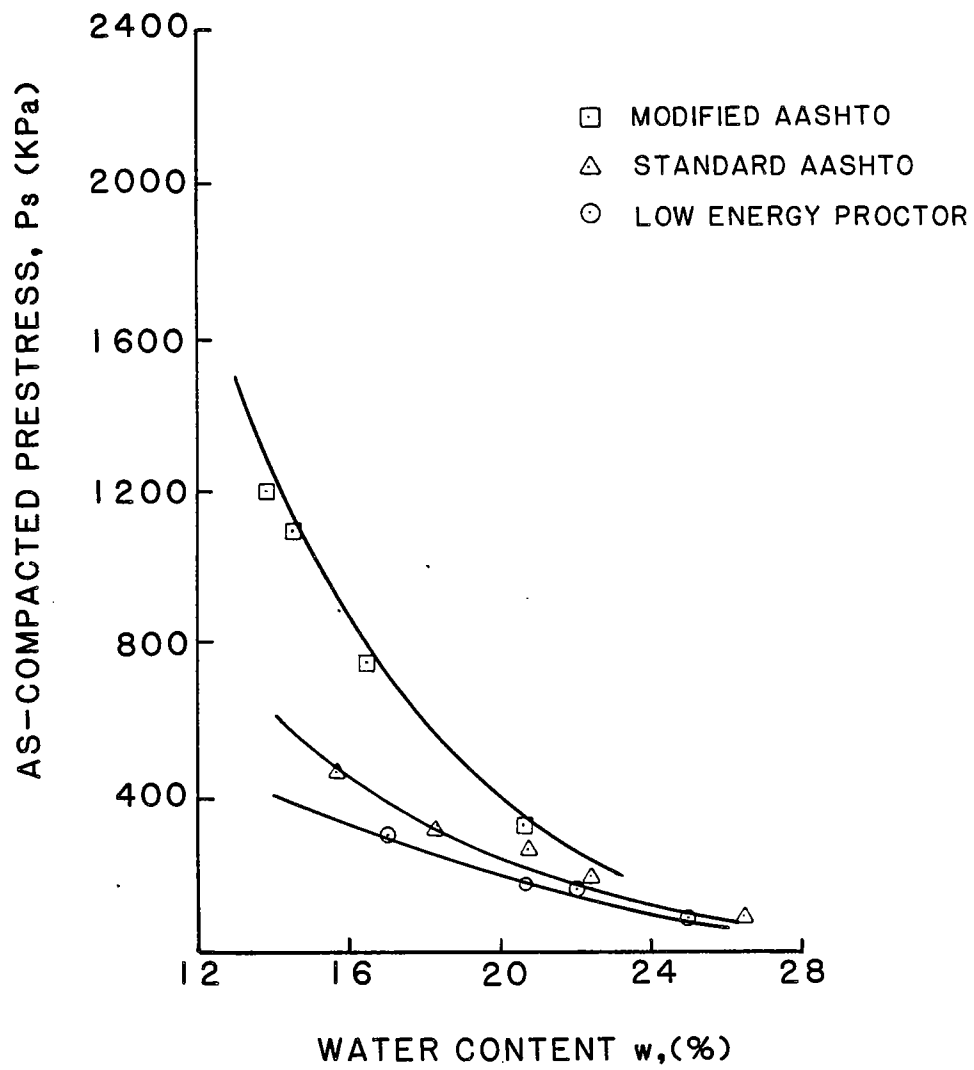


Figure 2. As-Compacted Prestress vs. Water Content

2. Wet of optimum water content:-

- a. At a given impact compaction energy level, the as-compacted prestress decreases, though at a smaller rate than the dry side samples, with increase in water content.
- b. As the impact energy increases, the magnitude of as-compacted prestress also increases at a lower rate than the dry side compacted soil.
- c. At very high water contents, 26% and greater, the magnitude of the as-compacted prestress is virtually unchanged for the various energy levels.

Saturated Compressibility

The effects of saturation due to changes in the environmental conditions were approximated by loading compacted soil samples to different levels of confining pressures and then saturating them in an oedometer by a back pressure process.

A coding procedure was adopted for identifying the various samples tested. L, S, and M represent the low energy Proctor, Standard AASHTO, and Modified AASHTO compaction energies respectively. D, O, and W refer to the water content conditions of dry of optimum, optimum, and wet of optimum respectively. The numbers 1, 2, and 3 immediately following the letters D, O, and W are used to differentiate between samples of identical initial conditions, while the subsequent numbers refer to the levels of confining pressure. The last number is followed by a number which shows the magnitude of the confining pressure.

Volume Changes Due to Saturation

Volume changes in a compacted embankment/fill have been considered for both the short and long term conditions. The former represents the effects resulting from the self weight of the embankment/fill, and as shown earlier, its magnitude depends on the values of the as-compacted prestress established by the compaction process. It will, in general, occur as rapidly as the embankment is constructed. During the service life of the embankment/fill the unavoidable changes in environmental conditions may lead to a near saturation condition. This will cause a volume increase or decrease in the soil mass, with attendant changes in the compacted soil void ratio, degree of saturation, and the as-compacted prestress.

These behaviors have been approximated in this study by incrementally loading the compacted samples in an oedometer to different load levels, simulating embankment confining stresses, and then saturating them by a back pressure process. The ensuing one dimensional volume changes ($\frac{\Delta V}{V_0}$) were measured.

The general trend is one in which the swelling tendencies decrease with increasing as-compacted void ratio. Also, the compacted soil samples exhibit increasing swelling tendencies with decreasing void ratio. Similar behavior was reported by Abeyesekera (1978), DiBernardo (1979) and Lin (1981) from their studies on compacted shale, laboratory kneading compacted high plastic clay, and field compacted high plastic clay, respectively.

The volume change behavior of a compacted soil subjected to a confining pressure and exposed to the influence of water can be visualized as the resultant effect of several processes. Consequently, the nature of the volume changes, swelling or compression, will depend on the initial compaction water content, void ratio, as-compacted prestress and the magnitude of the applied confining pressure.

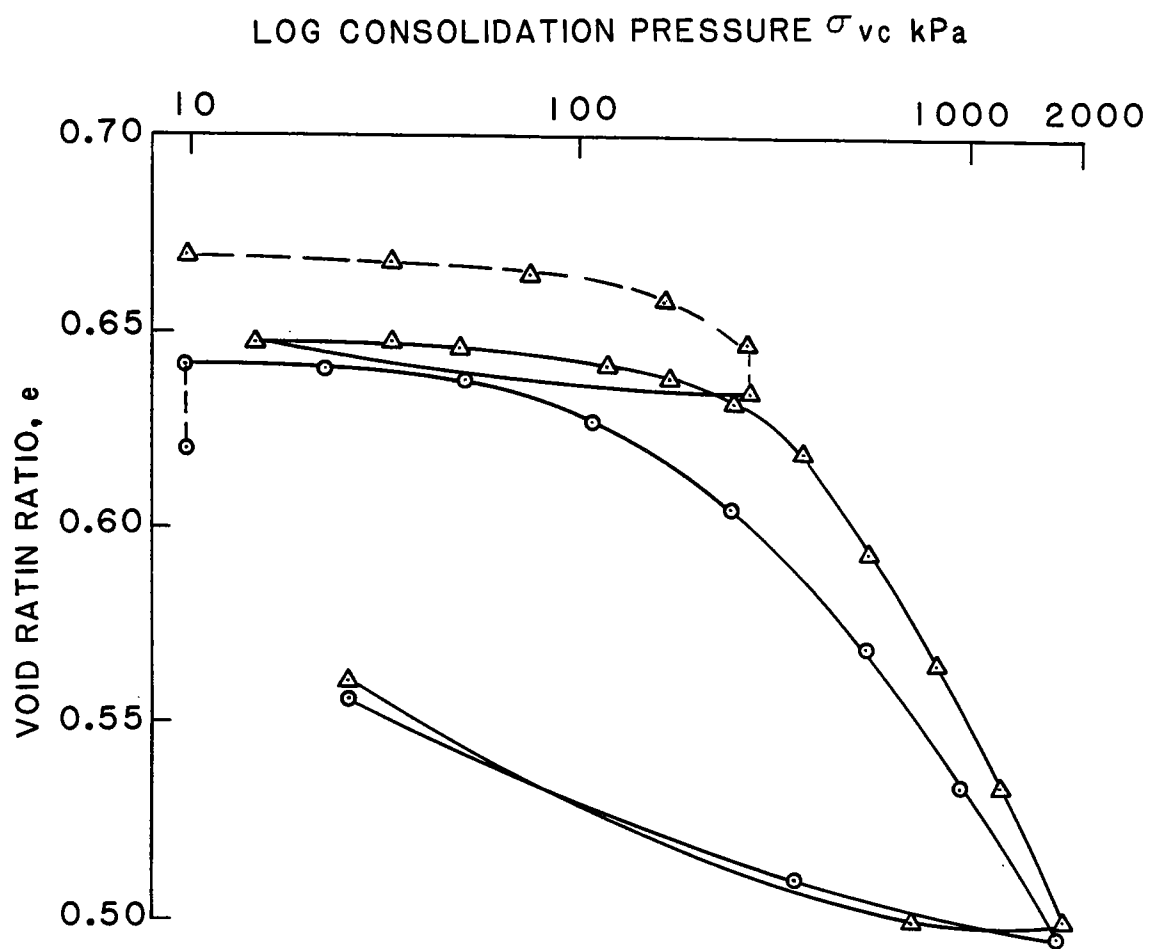
At low confining pressure levels (less than 60kPa) dry of optimum, optimum, and even wet of optimum samples exhibit a swelling behavior when saturated. The swelling pressures from the hydrating clay minerals, and the reduction in the effective stresses due to saturation must have exceeded the combined effects of the softening of the clay aggregates and the confining pressures. Hence, the observed volume increases. The compression tendencies observed at confining pressures greater than 140 kPa, can be attributed to the combined effects of the softening of the clay aggregates, reduction in the magnitude of the as-compacted prestress, and the confining pressure, which were sufficient to overcome the swelling tendencies of the compacted soil samples resulting from the hydration of the clay minerals and reduction in the effective stress in the soil samples.

As illustrated in Figure 3, it is possible to obtain three aspects of compressibility from a single oedometer sample, viz., as compacted compressibility, vertical deformation upon saturation (swell or settlement), and saturated compressibility.

Statistical Analysis

Regression analysis is a formal means of expressing the variation of a dependent variable with independent variables, and the scattering of observations around the curve representing the statistical relationship. Consequently, regression analysis has become an essential tool in research, and is used for the interpretation of multifactor data with a view to describing, controlling, and predicting the behavior of the process of interest.

The Statistical Package for the Social Sciences (SPSS, Nie et al., 1975), part of the software library at Purdue University, provided the programs which were utilized in the linear regression analysis. Detailed discussion regarding the theory of multiple regression analysis can be found in Draper and Smith (1981).



SPECIMEN No AND SYMBOL	INITIAL VOID RATIO e	CONFINING STRESS, σ_{vc} kPa	INITIAL WATER CONTENT $w(\%)$	INITIAL DEGREE OF SATURATION $S_r(\%)$
S011-10.0 ○—○	0.6215	10.0	20.04	88.68
S014-276.2 △—△	0.6697	276.2	20.04	82.29

Figure 3. Effect Of Confining Pressure On The Compressibility Behavior Of Standard ASSHTO Compacted Optimum Samples.

Prediction Model For As-Compacted Prestress

The basic independent variables utilized for the prediction equation for the dependent variable, as-compacted prestress, σ_s , are compaction energy and water content. The regression equation obtained by using the appropriate combinations of the above indicated basic compaction variables is given below:-

$$\begin{aligned}\sigma_s = & -45.9398 + 131337.66 \frac{\sqrt{\bar{E}}}{w^2} - 18982.205 \frac{\sqrt{\bar{E}}}{w} \\ & + 1023.6757 \sqrt{\bar{E}} - 17.0117w \sqrt{\bar{E}} \\ & - 0.12497 \times 10^{-4} w^2 \bar{E}^2\end{aligned}\quad (1)$$

where E = compaction energy in Kg-m
 w = compaction water content in percent

The coefficient of multiple determination for the above relationship is 0.997. From equation (1), for a given compaction energy level, the as-compacted prestress decreases with increase in water content. Also, at a given water content, the as-compacted prestress increases with compaction energy, particularly for the dry-of-optimum water content compacted samples. The prediction model given in equation (1) is valid within the compaction water content and energy level limits of the samples tested.

Prediction Model for Volume Change Due to Consolidation and Saturation

The effects of saturation due to changes in the environmental conditions were approximated by loading compacted samples to different levels of confining pressures and then saturating them in an oedometer by a back-pressure process. The percent one dimensional volumetric strains ($\frac{\Delta V}{V_o}$)% were measured.

The independent variables employed in the development of the prediction equation for the one dimensional volumetric strains in percent are:- (1) as-compacted void ratio (e), (2) compaction water content (w), (3) confining pressure (σ_o), and (4) as-compacted prestress (σ_s).

$$\frac{\Delta V}{V_o}(\%) = -0.7595 + 0.3094 \times 10^{-3} w^2 \sqrt{\sigma_o}$$

$$\begin{aligned}
 & - 0.2242 \times 10^{-2} e_o \sigma_s - 0.7839 \times 10^{-6} w \sigma_o^2 \\
 & - 0.1223 \times 10^{-2} \frac{\sigma_o^2}{w^2} + 1.8653 \frac{\sigma_o}{w^2}
 \end{aligned} \tag{2}$$

where

$$\begin{aligned}
 \left(\frac{\Delta V}{V_o} \right) \% &= \text{percent volumetric strain} \\
 w &= \text{compaction water content} \\
 \sigma_o &= \text{confining pressure in kPa} \\
 e_o &= \text{as-compacted void ratio} \\
 \sigma_s &= \text{as-compacted prestress in kPa}
 \end{aligned}$$

The coefficient of multiple determination for the above prediction equation is 0.8437. For the prediction model, a positive value of percent volumetric strain indicates compression while a negative value represents swelling.

At a given water content and void ratio, the compacted samples exhibit increasing compressive tendencies with increase in confining pressure applied during saturation. Also, at a given void ratio and confining pressure during saturation, the compacted samples show increasing compressive behavior with increase in water content.

Application of Results

The quantitative prediction and control of the overall performance of a compacted fill/embankment requires an adequate knowledge of the compressibility characteristics of the compacted material within the short and long term periods. It is also necessary that the engineer ascertain the appropriate initial compaction conditions that will yield the desired overall performance of the compacted material.

Based on the findings of this study, procedures which will enable the engineer to predict the compressibility of a compacted fill/embankment both for the short and long term periods are outlined.

For the short term period, the initial vertical strains experienced by a compacted fill/embankment are those due to self weight. The magnitudes of these settlements are highly dependent upon the values of the as-compacted prestress established by the compaction process. They, however, occur as rapidly as the fill/embankment is constructed. This has been simulated in this study, by loading compacted samples in an oedometer at a load increment ratio (LIR) of 0.5 until the as-compacted prestresses and "compression indices" were well defined.

Under long term conditions, the fill/embankment will become wetter and soften in service due to the unavoidable changes in environmental conditions. This has been approximated in this study by loading the compacted samples at a load increment ratio (LIR) of 0.5 until the desired confining pressures were attained. The soil samples were then saturated by a back-pressure saturation process, unloaded and reloaded at a load increment ratio of 0.5 until the saturated prestresses and compression indices were well defined. The ensuing volume changes under the influence of the vertical confining pressures during the saturation process were measured.

A procedure for the estimation of the compressibility characteristics of a compacted embankment due to self weight and the effects due to changes in environmental conditions is illustrated below by an example.

Given, a wide embankment, 10.0m high, constructed of the clay used in this study, in 0.25m thick lifts and compacted to a water content (w) and dry density (γ_d) of 20.04% and 1648.0Kg/m³ ($e = 0.67$), respectively. The specific gravity of the soil solids is 2.75. Estimate the settlement of the embankment due to self weight and saturation in service.

A schematic vertical section through the embankment is shown in Figure 4a. Also indicated are some of the symbols used in the solution of the problem given above. Let γ_d = dry weight, and wet unit weight $\gamma_m = \gamma_d(1 + w)$; then, the embankment pressure at any depth, z_i , is:

$$\sigma_{ozi} = \gamma_d(1 + w)z_i = \gamma_m z_i \quad (3)$$

where

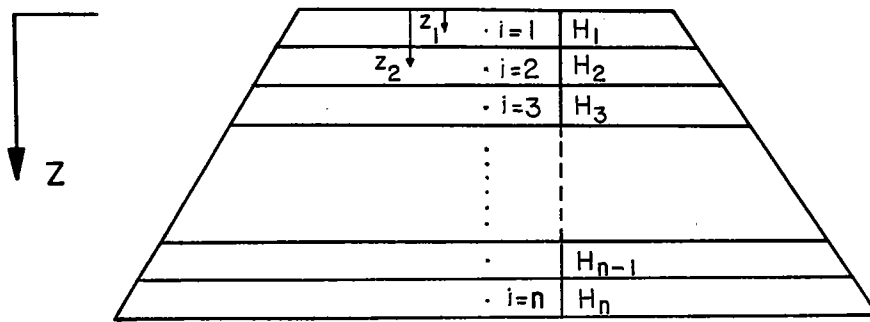
$$\begin{aligned} \sigma_{ozi} &= \text{embankment pressure at depth } z_i \text{ in kPa} \\ \gamma_d &= \text{dry density in Kg/m}^3 \\ w &= \text{compaction water content in percent} \\ z_i &= \text{depth at center of embankment in meters} \\ \gamma_m &= \text{wet density in Kg/m}^3 \end{aligned}$$

Using the oedometer test results, the vertical strain at the center of layer, i , thickness, H_i , corresponding to an embankment pressure σ_{ozi} is:

$$\epsilon_{vi} = \frac{\Delta H_i}{H_i} \quad (4)$$

$$H_i \epsilon_{vi} = \Delta H_i \quad (5)$$

a)



Vertical Section Through A Typical Embankment

b)

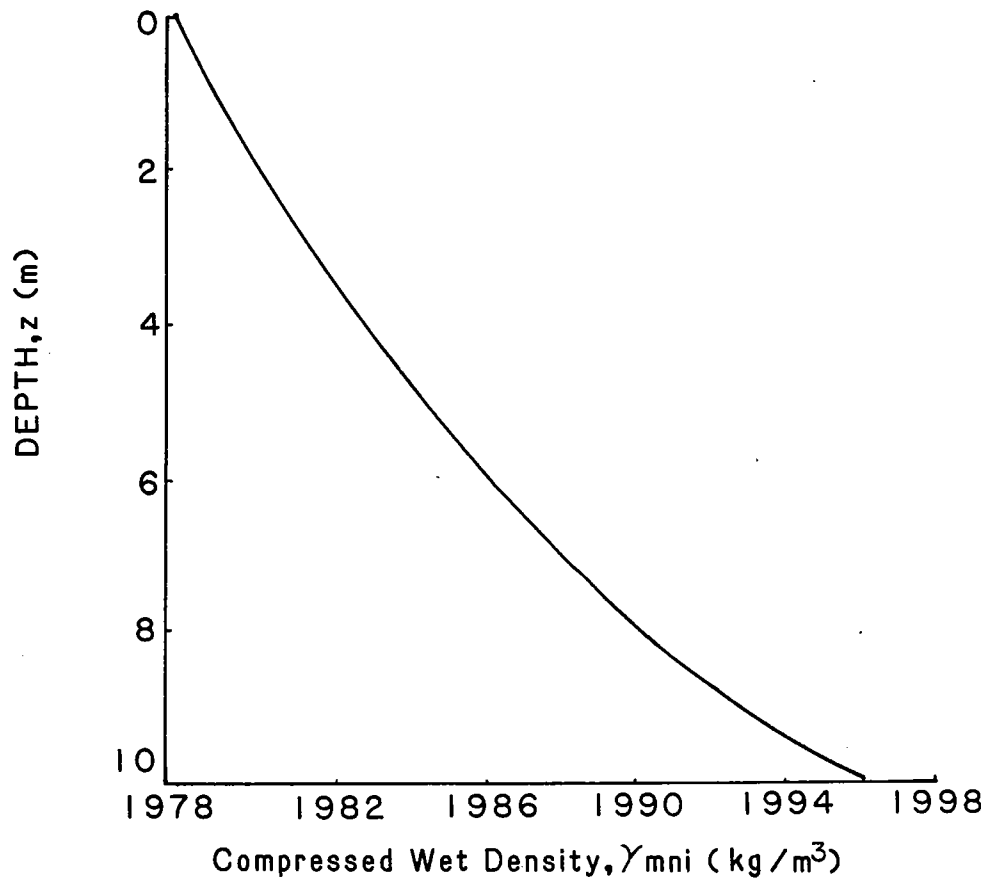


Figure 4. Section Through An Embankment And Variation Of Compressed Wet Density γ_{mni} With Depth.

where

- ϵ_{vi} = one dimensional vertical strain due
self weight for layer, i
 ΔH_i = one dimensional deformation of layer, i,
in meters
 H_i = thickness of soil layer, i, in meters

Thus, the deformation of the embankment due to overburden stresses is:

$$\delta_o = \sum_{i=1}^n \Delta H_i = \sum_{i=1}^n H_i \epsilon_{vi} \quad (6)$$

where

- δ = embankment settlement in meters
 ΔH_i^o = one dimensional deformation in layer, i,
in meters
 H_i = thickness of soil layer, i, in meters
 ϵ_{vi} = vertical strain for layer, i
 n = number of soil layers

Settlement due to self weight occurs about as rapidly as the fill is constructed. If there is need to control the magnitude of the settlement due to self weight, the as-compacted prestress should be as large as possible, with due consideration to subsequent side effects on compressibility and strength characteristics, once the material becomes saturated in service. The variation of compressed wet density within the embankment is shown in Figure 4b.

Determination of the vertical strain due to saturation $(\frac{\Delta H_{si}}{H_i})$, is accomplished by substituting the as-compacted void ratio, as-compacted water content, and the appropriate vertical fill pressure in equation (2). In the one dimensional process, $(\frac{\Delta V}{V})\% = \epsilon_{vsi}$. For very small embankment deformations (due to self weight), and for conditions in which the embankment is saturated (no buoyancy effect), the appropriate vertical fill pressure (σ_{onzi}) can be approximated by the use of the saturated unit weight corresponding to the as-compacted void ratio (e_o), given by:

$$\sigma_{onzi} = \gamma_{sat} z_i \quad (7)$$

where

$$\gamma_{sat} = \frac{G_s \gamma_w + \gamma_w e_o}{1 + e_o} \quad (8)$$

where

- σ_{onzi} = embankment pressure at any depth, z_i ,
 using saturated density in kPa
 γ_{sat} = saturated density in Kg/m³
 z_i = depth from top of embankment to the
 center of layer, i
 γ_w = density of water in Kg/m³
 e_o = as-compacted void ratio
 G_s = specific gravity of soil solids

However, for a saturated embankment in which a submerged condition exists, the submerged unit weight of the fill material should be used. Thus, since

$$\frac{\Delta H_{si}}{H_i} = \epsilon_{vsi} \quad (9)$$

settlement of the fill due to saturation is given by

$$\sum_{i=1}^n \Delta H_{si} = \sum_{i=1}^n H_i \epsilon_{vsi} \quad (10)$$

where

- ΔH_{si} = change in height of soil layer, H_i ,
 due to saturation (in meters)
 ϵ_{vsi} = one dimensional vertical strain due
 to saturation
 H_i = thickness of soil layer, i , in meters
 n = number of soil layers

On the other hand, if the deformation (δ_o) determined from equation (6) is large, then new embankment overburden stresses must be computed, to account for the effect of the added compacted soil required to give the desired embankment height. Details are given in Nwabuokei (1984).

The numerical solution for an example embankment problem is given in Table 2. For an embankment 10 meters in height, the predicted settlement under self weight is 3.5cm; additional settlement when saturated is 2.0cm. The variations of settlement due to saturation with depth are given in Figure 5.

TABLE 2

Example Solution for Settlements within an Embankment

$$H = 10.0\text{m}; H_1 = H_2 = H_n = 1.0;$$

$$\gamma_d = 1648.0 \text{ kg/m}^3; \text{ and } w = 20.04\%$$

Layer No.	Depth z_i (m)	Embankment Pressure σ_{ozi} (kPa)	Vertical Strain ϵ_{vi} (Figure 5)	Settlement Due to Self Weight (m)	Depth z_j (m)	Saturated Unit Weight γ_j (kg/m^3)	Embankment Pressure σ_{satj} kPa	Vertical Strain Due to Saturation	Settlement Due to Saturation (m)
i or j	j	(m)	(kPa)	(m)	(m)	(kg/m^3)	kPa	ϵ_{vsi}	(m)
1	0.5	9.703	0.000098	0.000098	0.0350	2047.9	0.3516	-0.013987	-0.000490
2	1.5	29.11	0.00050	0.00050	0.5345	2048.8	10.7515	-0.007874	-0.007874
3	2.5	48.52	0.0015	0.0015	1.5347	2049.3	30.8464	-0.003423	-0.003422
4	3.5	67.92	0.0020	0.0020	2.5338	2050.3	50.9346	-0.000719	-0.000718
5	4.5	87.33	0.0030	0.0030	3.5319	2050.8	71.3902	0.001278	0.001276
6	5.5	106.73	0.0035	0.0035	4.5529	2051.9	91.4637	0.002801	0.002792
7	6.5	126.14	0.0045	0.0045	5.5262	2052.4	111.5298	0.004027	0.004013
8	7.5	145.55	0.0055	0.0055	6.5222	2053.5	131.5886	0.005035	0.005013
9	8.5	164.96	0.0065	0.0065	7.5172	2054.5	151.6376	0.005874	0.005840
10	9.5	184.36	0.0080	0.0080	8.5122	2055.6	171.6768	0.006575	0.006532
11					9.5040	2057.2	191.7038	0.007163	0.007106

$$\sum_{i=1}^n \Delta H_i$$

$$= 0.0351 \text{ m}$$

$$= 3.51 \text{ cm}$$

$$\sum \Delta H_{sj}$$

$$= 0.020\text{m}$$

$$= 2.0\text{cm}$$

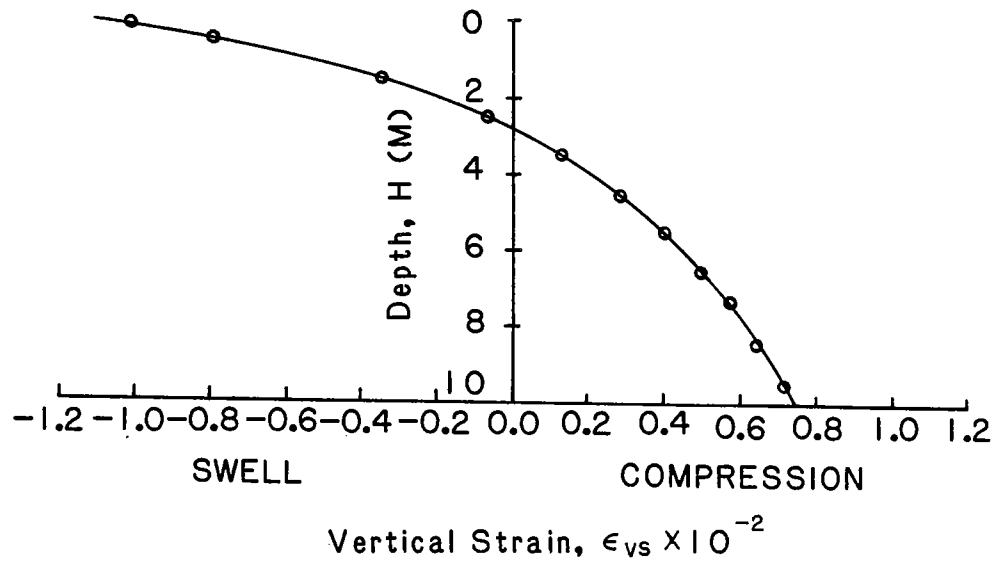


Figure 5. Variation Of Vertical Strain Due To Saturation.

CONCLUSIONS

The effects of compaction variables on the short and long term compressibility characteristics of a laboratory impact compacted lacustrine clay from Allen County in northeastern Indiana, have been investigated and examined critically in this study.

The results obtained from this study allow the following conclusions to be drawn:-

1. The as-compacted prestress (σ_s), a total stress parameter, is dependent on the compaction water content (w) and compaction energy (E). The as-compacted prestress decreases with compaction water content for a given compaction energy level. Also, at a constant compaction water content, particularly for dry-of-optimum compacted soils, the as-compacted prestress increases with compaction energy.
2. At low confining pressures, dry-of-optimum, optimum and even wet-of-optimum samples exhibit a volume increase (swelling) upon saturation. This is attributable to swelling pressure from the hydrating clay minerals, and the reduction in the effective stresses within the samples due to saturation. These effects must have exceeded the combined effect of the softening of the clay aggregates and confining pressures. On the other hand, at high confining pressures, the compacted samples exhibited a compressive behavior upon saturation. This is attributable to the combined effects of the softening of the clay aggregates, reduction in the magnitude of the as-compacted prestress, and the confining pressures. These were sufficient to overcome the swelling tendencies from the compacted samples due to the hydrating clay minerals and the reduction in the effective stresses within the samples.
3. From the statistical analysis, one dimensional percent volumetric strain ($\frac{\Delta V}{V_0} \times 100$) due to saturation is a function of compaction water content (w), confining pressure (σ_c), as-compacted prestress (σ_s), and as-compacted void ratio (e_0) [equation (2)]. The compacted samples exhibit increasing compressive tendencies with increasing confining pressure at a given compaction water content and as-compacted void ratio. Also, at a given void ratio and confining pressure during saturation, the compacted samples show increasing compressive tendencies with increasing water content.
4. A systematic procedure for the evaluation of settlements, for the short and long term periods, within an embankment is proposed and this has been illustrated with an example.

REFERENCES

1. Abeyesekera, R. A. (1978). "Stress-Deformation and Strength Characteristics of a Compacted Shale", Ph.D. Thesis, Purdue University, West Lafayette, Indiana, May, 420 pp. (Also, Joint Highway Research Project Report No. 77-24).
2. DiBernardo, A. (1979). "The Effect of Laboratory Compaction on the Compressibility of a Compacted Highly Plastic Clay", MSCE Thesis, Purdue University, West Lafayette, Indiana, May, 187 pp. (Also, Joint Highway Research Project Report No. 79-3).
3. Draper, N. R. and Smith, H. (1981). "Applied Regression Analysis", John Wiley and Sons, N.Y., 407 pp.
4. Lin, P. S. (1981). "Compressibility of Field Compacted Clay", Ph.D. Thesis, Purdue University, West Lafayette, Indiana, 153 pp. (Also, Joint Highway Research Project Report No. 81-4).
5. Nie, N. H., Hull, C. H., Jenkins, J. G., Steinbrenner, K. and Bent, D. H. (1975). "Statistical Package for Social Sciences", 2nd Ed., McGraw-Hill Book Company, N.Y., 675 pp.
6. Nwabukei, S. O. (1984). "Compressibility and Shear Strength Characteristics of Impact Compacted Lacustrine Clay", Ph.D. Thesis, Purdue University, West Lafayette, Indiana, Dec., 542 pp. (Also, Joint Highway Research Project Report No. 85-6).

THE EFFECTS OF SAMPLE DISTURBANCE ON THE STRESS-
DEFORMATION BEHAVIOR OF SOFT SANDSTONES

by

Robert C. Bachus
School of Civil Engineering
Georgia Institute of Technology
Atlanta, Georgia .

A Paper Presented at the
36th Highway Geology Symposium
Clarksville, Indiana .

May, 1985

THE EFFECTS OF SAMPLE DISTURBANCE ON THE STRESS-
DEFORMATION BEHAVIOR OF SOFT SANDSTONE

by

Robert C. Bachus⁽¹⁾

INTRODUCTION

Soft rocks are often characterized by extreme difficulties in obtaining intact and competent samples which are suitable for conventional laboratory testing. During the sampling operation, disturbance imparted to the specimen may severely alter both the structure and competence of the retrieved sample. In the most severe instance this sample may bear little or no resemblance to the undisturbed intact rock mass. In dealing with soil or rock formations which are subject to alterations upon sampling, it is incumbent upon the geotechnical engineer to evaluate the effects of sample disturbance on the laboratory determined engineering design parameters. The purpose of this paper is to report the results of one such investigation.

Data for this report were obtained by sampling and subsequently testing the recovered samples from weakly cemented sand deposits exposed along the bluffs overlooking the Pacific Ocean south of San Francisco. Samples were obtained by conventional hammered-in split spoon samples and pushed-in Shelby tubes. Additional field samples were obtained via a Pitcher barrel sampler and block sampling at the bluff face. In order to fully understand the behavior of these weakly cemented natural soils, selected results of a laboratory test program using artificially cemented sand are presented. The data from this study indicate that no conventional sampling procedure is successful in supplying specimens that, when tested, yield results similar to those obtained from testing the block samples. Furthermore, in-situ testing techniques, particularly using the self-boring pressuremeter, appear to offer significant promise to evaluating representative engineering design parameters.

TEST SITE

The primary field test site was located on the bluffs of the city of Pacifica located approximately 10 miles (16 km) south of San Francisco as shown in Figure 1. The materials at the site are actually part of an elevated marine terrace of Middle Pleistocene age. Loose dune sands of Holocene age overlie these deposits. Instability of the 65-400 ft. (20-120 m) high, 50°-70° soil/rock slopes in this area during earthquakes has been reported by the USGS (Youd and Hoose, 1978). Locally the slopes are approximately 100 ft. (30 m) in height and are near vertical as shown in Figure 2. Of primary concern are the very weakly cemented sands in the upper 60 ft. (18 m) of the deposit because of their sampling difficulty.

⁽¹⁾

Assistant Professor, School of Civil Engineering, Georgia Institute of Technology, Atlanta, Georgia.

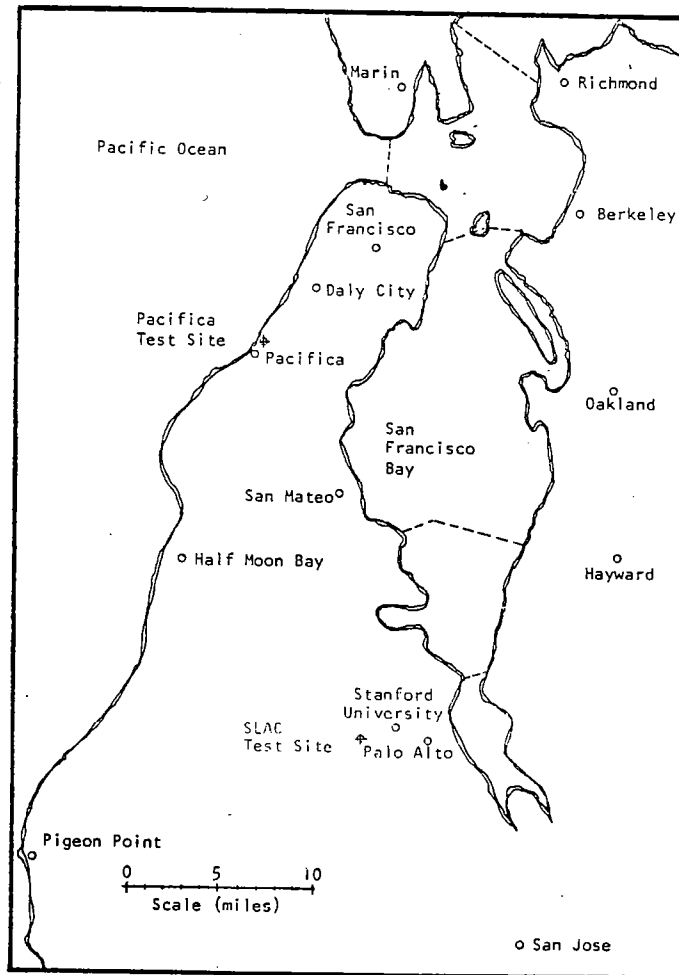


FIG. 1. PLAN VIEW OF SAN FRANCISCO PENINSULA INDICATING THE LOCATION OF LIGHTLY CEMENTED SAND DEPOSITS.

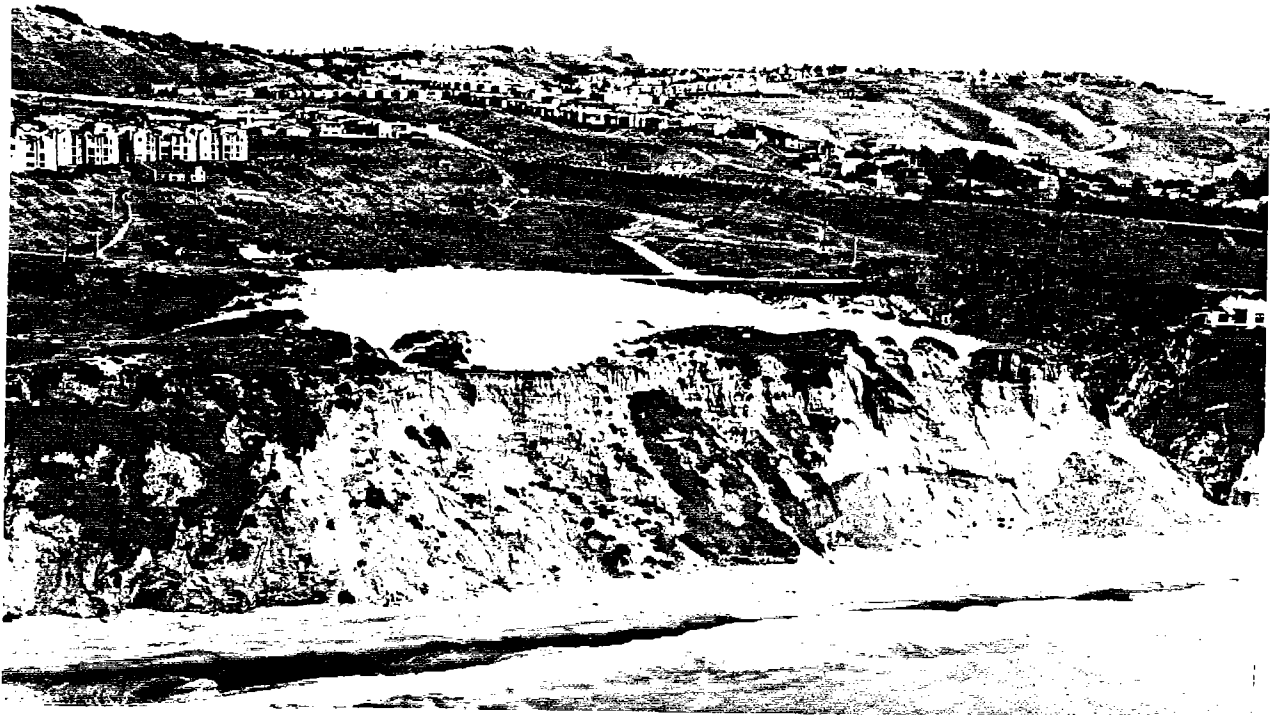


FIG. 2. AERIAL VIEW OF THE PACIFICA TEST SITE.

The weakly cemented sands at the Pacifica site are cross-bedded and composed of rounded to subrounded particles of relatively uniform grain size. The d_{50} grain diameter is .008 in. (0.2 mm) with only 5 percent passing the No. 200 sieve. Cementation occurs at the points of grain contact and is primarily iron oxide. Due to the nature of the cementing agent and the relative sparsity of the grain contacts, the mass is relatively weak and extremely brittle. Although the material will stand in unsupported bluff or trench faces, it is easily hand carved and will yield under very slight fingertip pressure. Details of the geology can be found in Bachus, 1982 and Bachus, et al., 1981.

BLOCK SAMPLE AND ARTIFICIALLY CEMENTED SAND TEST RESULTS

Prior to a discussion of the effects of sampling-induced disturbance on conventional laboratory test results, it is necessary to understand the behavior of undisturbed samples of cemented sand. Two distinct approaches were taken in establishing this understanding. These were careful block sampling of the naturally cemented bluff material and the formation and testing of artificially cemented sand samples under laboratory control. Block samples were hand carved from the bluff face at elevations where later attempts to obtain conventional samples would be made. Blocks could easily be formed by light scraping of the surface with a rock hammer. They were subsequently wrapped and cushioned for immediate transfer to the lab for trimming and testing. Despite this care nearly 50 percent of the blocks crumbled, generally along old apparent bedding planes, during the trimming/handling operation. Typical stress-strain curves for the block samples that were successfully trimmed are presented in Figure 3. Although there are slight inconsistencies in volumetric strain response, the data are generally consistent. In all cases there is a rapid increase to a peak strength followed by a strain-softening response to a somewhat constant stress level. The degree of strain-softening is a function of confining pressure, diminishing as confinement increases. In order to better understand these results and prior to a discussion of the strength and modulus characteristics of the block samples, the artificially cemented sand results are presented.

The artificially cemented sand investigation was actually being conducted simultaneously with the block sampling program and was undertaken to study the behavior of lightly or weakly cemented soils. Although the details of the program are beyond the scope of this paper, a brief description of the preparation procedure follows. Samples of Monterrey No. 0 sands were premixed with either 0, 2, or 4 percent portland cement and 8 percent water. Following thorough mixing the material was rodded into plexiglas cylindrical sample jackets and moisture cured for 14 days. The samples were subsequently removed from the jackets and subjected to laboratory testing. For details of this procedure the reader is directed to Sitar (1979).

The effects of cementation on the triaxial compression axial stress - axial strain - volumetric strain behavior is clearly shown in Figure 4. These results are for the uncemented and 4 percent cement specimens; the 2 percent sample results were consistently intermediate the plotted values and are omitted here simply for clarity. The following general observations regarding the effects of cementation are noted (Clough, et al., 1981).

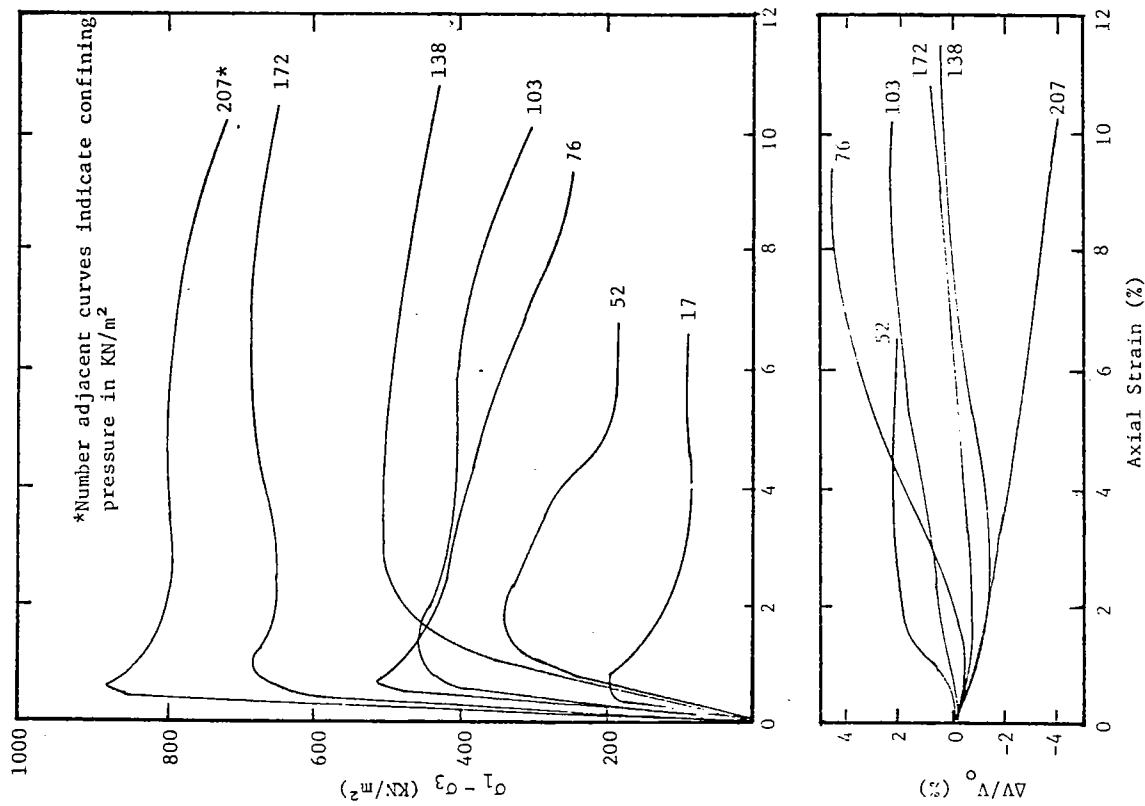


FIG. 3. STRESS-STRAIN PLOTS FOR CONSOLIDATED DRAINED TRIAXIAL COMPRESSION TESTS CONDUCTED ON BLOCK SAMPLES FROM PACIFICA.

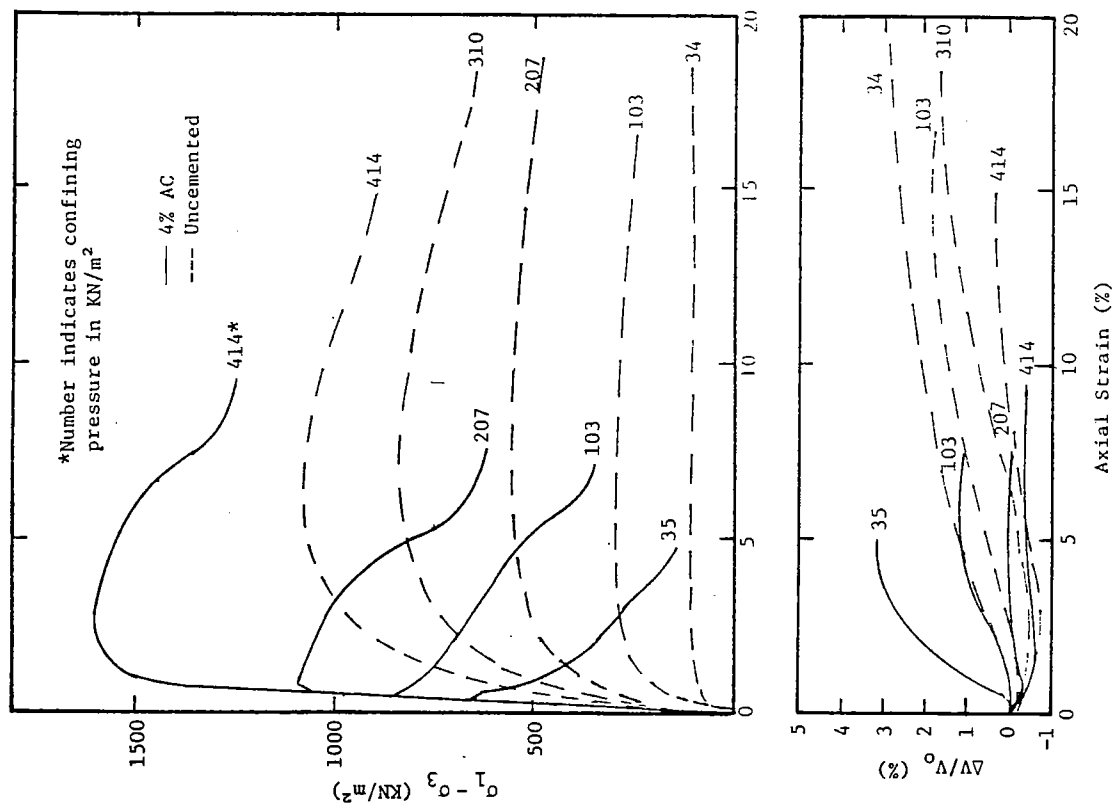


FIG. 4. TYPICAL STRESS STRAIN PLOTS FOR CONSOLIDATED DRAINED TRIAXIAL COMPRESSION TESTS CONDUCTED ON 4% ARTIFICIALLY CEMENTED AND UNCEMENTED SAND.

1. Small amounts of cementation significantly enhance the peak strength but do little to alter the post-peak or residual strength.
2. Cementation induces a very brittle response where the peak strength is mobilized at very low axial strain.
3. At the stress levels tested the initial tangent modulus was significantly affected by cementation. In contrast to the uncemented sand response, however, this modulus was not significantly affected by confining pressure.
4. In general, the amount of total volumetric strain is not consistent at various amounts of cement but the rate of volumetric strain is consistently faster and occurs at lower strain levels as the degree of cementation increases.
5. The brittle characteristics of cemented soils are a function of confining pressure. At low confining pressure, frictional resistance is low and thus cementation is the primary contributor to strength; brittle characteristics prevail. As the confining pressure increases the frictional resistance is enhanced while the cementation effects remain relatively unchanged, thus the material tends to behave as its uncemented and ductile counterpart. It is conceivable that at very high confining pressure the effect of light cementation on strength properties would be minimal.

These characteristics, based on wholly intact and completely undisturbed weakly cemented sand specimens, serve as a benchmark for comparing both block and conventionally obtained samples.

Comparing the results of the two test programs yields several interesting observations. Based on the data presented in the previous Figures 3 and 4, the block samples results clearly show cemented sand characteristics although not as pronounced as the depicted 4 percent sand results. Comparison of the strength envelopes is shown in Figure 5. The Mohr-Coulomb failure criterion adequately fits the data. At constant relative density the primary effect of cementation is on the cohesion intercept which varies directly with the degree of cementation; the frictional response is apparently not affected by cementation. The frictional strength, in turn, varies directly with relative density while the cohesion is just slightly affected. The block sample results are closely bounded by the results of the artificially cemented sand and, although the tests were not conducted, the behavior of the block samples was similar to the expected behavior of 2 percent cemented dense sand specimens.

Figure 6 presents the initial tangent modulus versus confining pressure variation for both artificially cemented and naturally cemented sands. These data are normalized by the atmospheric pressure, p_a , and the terms K and n are defined by the equation

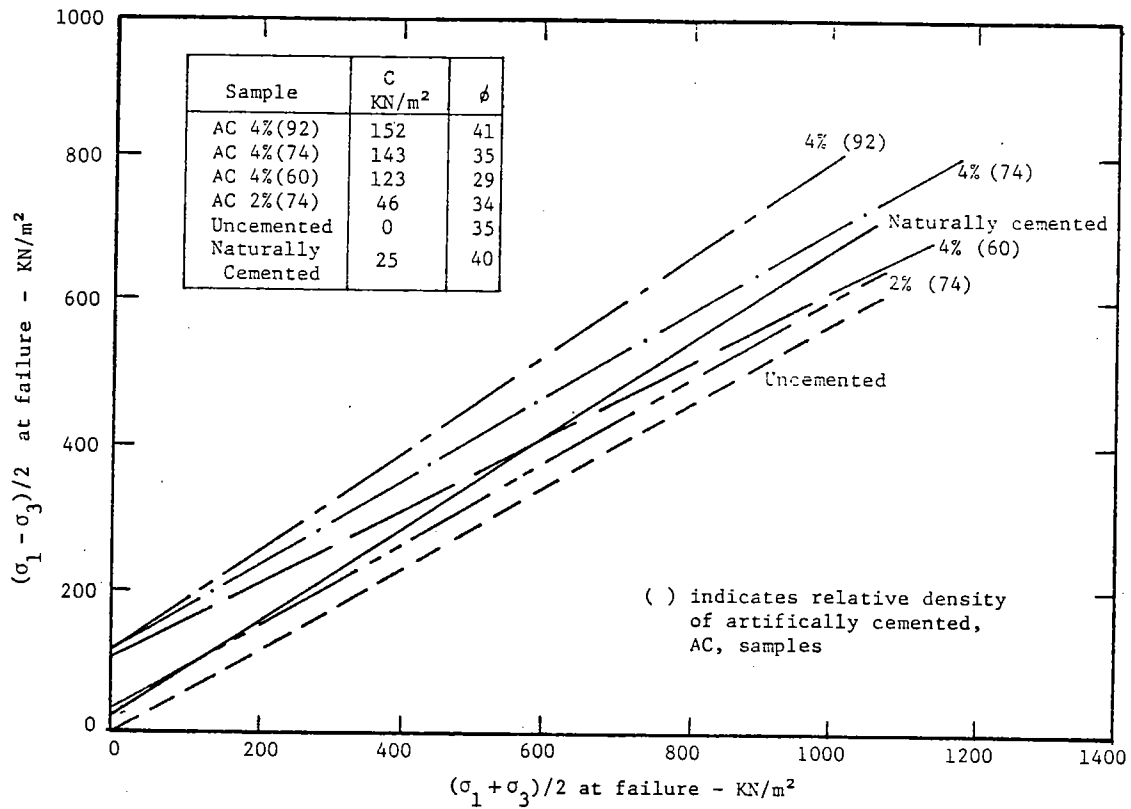


FIG. 5. PEAK STRENGTH VALUES FOR ARTIFICIALLY CEMENTED SAND, UNCEMENTED SAND AND BLOCK SAMPLES.

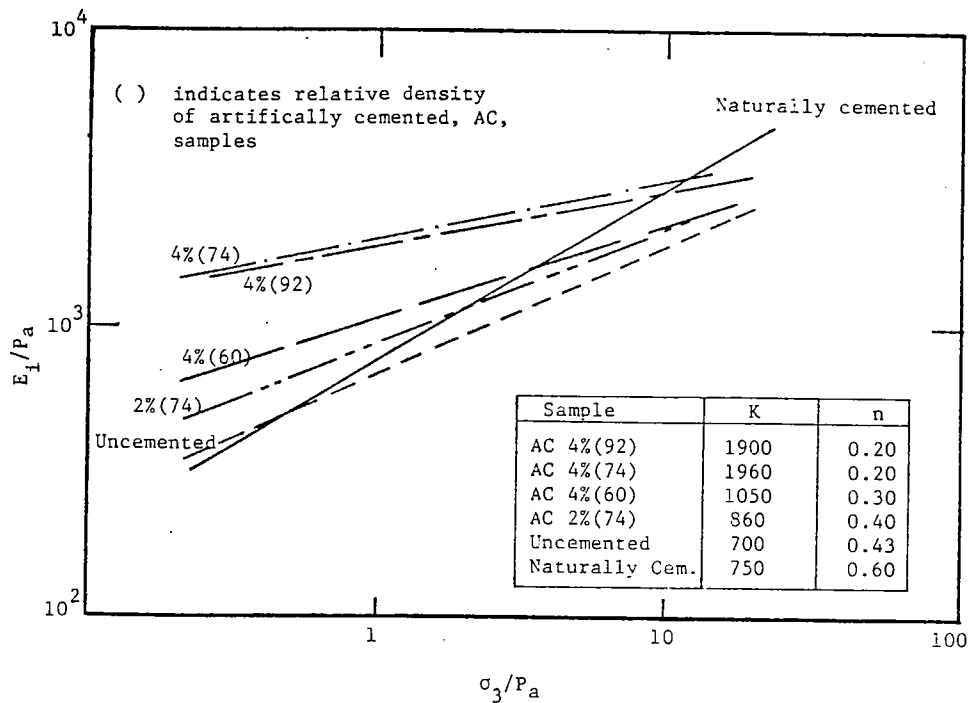


FIGURE 6. VARIATION OF INITIAL TANGENT MODULUS WITH CONFINING PRESSURE FOR ARTIFICIALLY CEMENTED SAMPLES AND BLOCK SAMPLES.

$$E_i = K p_a \left(\frac{\sigma_3}{p_a} \right)^n$$

where K is the modulus at $\frac{\sigma_3}{p_a} = 1$ and n represents the rate of modulus

increase as confining pressures are increased. The data shown in Figure 6 indicate that, with particular reference to the artificially cemented sand results, as the degree of cementation increases the modulus increases, yet the rate of modulus increase diminishes. A similar modulus/modulus rate relationship is generally detected as the relative density increases, although these results are somewhat inconsistent. The naturally cemented sand block sample results are again bounded by the artificially cemented results. These data, however, suggest a larger dependence on confining pressure for the natural samples relative to the laboratory-prepared specimens.

The results of the block sample and artificially cemented sample testing programs are consistent and establish the fundamental characteristics of cemented sand behavior. These materials are true $c-\phi$ materials, the cohesion originating due to the slight cementation at the grain to grain contacts. This cohesion significantly affects the initial and small strain response of the material. Both strength and modulus are enhanced. The cementation is however brittle and tolerates little grain slippage. Upon yielding of this bonding the frictional resistance of the material controls behavior. The material response due to friction depends largely upon the confining pressure. Therefore, at low confining pressures the frictional resistance is quite low and the cementation controls the material response. A small amount of cementation significantly increases both initial modulus and peak strength. The post-peak response is due primarily to grain to grain friction. As confinement levels increase, the frictional response increases while the effect of cementation is essentially constant. The net result is still an enhanced stiffness and peak strength relative uncemented materials, but the effects of cementation are gradually masked by friction. Eventually, the effect of cohesion could be completely neglected due to high frictional resistance.

Although these tests establish fundamental behavior, there remains two additional items that are important yet fall outside the scope of this project. The post-peak response noted in the stress-strain curves shown earlier was taken directly from the lab test data for strength and deformation. No attempt to actually quantify actual strain or account for the strain of a prescribed failure mode was attempted. The second point concerns the results presented on the figures and the fact that these samples were tested at a limited range of confining pressures. No attempt to increase the confining pressure to initiate yielding of the cementing bonds upon consolidation was made. Based on the conclusions made in the previous paragraph, it is likely that both the failure envelope and normalized plot of E_i versus σ_3 would gradually deviate from the shown linear response and tend towards the response of the uncemented material.

CONVENTIONAL SAMPLING AND TESTING OF LIGHTLY CEMENTED SANDS

Subsequent the block sampling program along the bluff face a drill rig was maneuvered as close to the slope crest as safely possible in order to obtain conventional split spoon, Shelby tube and Pitcher barrel samples.

Drilling support was provided by the USGS using a mobile B-50 rig. Sampling was conducted through hollow stem augers using a downhole SPT hammer for the split spoon samples and using a pushed 2.9 in. (73 mm) diameter Shelby tube.

At two elevations a Pitcher barrel sampler was employed. This sampler was developed for sampling stiff or alternating stiff/soft soil deposits and consists of a conventional Shelby tube enclosed within a rotating coring barrel. The Shelby tube extends from the front of the core barrel and although it is not allowed to rotate, it is held in the extended position by a large spring. As the sampler is advanced into the subsurface soils a conventional Shelby tube sample is obtained. If the sampled soil resists penetration by the spring supported Shelby tube, the spring will compress and the sample tube will retract to the face of the core barrel. The coring operation removes the harder material while allowing a central core of the material to enter the Shelby tube. If upon coring the material a softer deposit is encountered, the spring will advance the Shelby tube into this deposit and the coring operation will again be used to simply clear the cuttings from the large diameter hole. The intent of this operation is to provide a continuous undisturbed Shelby tube sample of the stratified or stiff material that would normally be extremely difficult to sample.

The split spoon samples were extruded in the field, placed in a plastic bag to preserve the field water content, and carefully transported to the lab for testing. The Shelby tube and Pitcher barrel samples were capped in the field and returned to the lab for extrusion and testing. Most of these samples were extruded by pushing the samples from the Shelby tube, however, selected Shelby tubes were longitudinally split using an end mill in hopes of minimizing the effects of extrusion disturbance.

Once extruded, all samples were trimmed and prepared for laboratory testing. At a minimum, water contents were obtained and in cases where samples could be trimmed unit weight, void ratio and degree of saturation determinations were made. The trimmed specimens were then subjected to either consolidated drained triaxial compression or Brazilian tension tests in order to establish the strength-deformation characteristics of the material.

TEST RESULTS ON CONVENTIONALLY OBTAINED SAMPLES

The first and most dramatic result was strictly observational; the conventionally obtained samples simply did not look like the materials obtained during block sampling. Much of the recovered material crumbled upon laboratory extrusion. Although this disruption was generally confined to certain segments of selected tubes, there were tubes that yielded no intact material suitable for testing. Apparently the sampling procedure so disrupted the material that the sensitive grain to grain contact bonds were broken, thus reducing the previously cemented mass to individual sand grains. Portions of each tube were collected for water content determination. For the samples that could be extruded and trimmed for testing, unit weight evaluations were conducted in addition to the water contents. Results of this early phase of testing indicated four significant observations, albeit based on limited data (Clough and Bachus, 1982).

Calculated water contents ranged from 11-20% which were considerably higher than the 5% typical for the block samples. This difference is presumed due to the location of the block samples on the exposed bluff face rather than inherent material differences. Regardless of the sampling procedure, however, no specimens drier than 14% water content remained intact during the extrusion procedure. Thus, there appears to be a threshold water content that precludes conventional sampling. Coupled with the water content is the observation that some of the material at water contents >14% appeared to contain slightly more fines than the drier specimens. This could not be quantified due to the small sample size but is offered as an additional factor in consideration of the ability to sample these soils. A third observation concerns the unit weight of the trimmed samples. Again, based on somewhat limited data, the dry unit weight varied as follows: split spoon > Shelby tube \approx Pitcher barrel > block samples. Finally, the Pitcher barrel and Shelby tube samples extruded by longitudinally splitting the Shelby tube were of poor quality, consisting of little more than fragments of cemented sand in an uncemented sand matrix. These observations and simple quantitative test results all support a rather troublesome conclusion. While attempting to obtain conventional samples of weakly cemented sands, the sensitive cementing bonds are broken and the samples remolded during either the sampling or extrusion process. The water and fines content potentially interact to determine whether the remolded specimen remains intact and capable of trimming and testing.

To quantify these disturbance effects the trimmed samples were subjected to consolidated-drained triaxial compression tests in the lab. Presentation of the results of the 18 test series is too extensive for this paper, but can be found in Bachus, et al., 1981. Typical stress-strain curves are, however, presented in Figure 7. These results are representative of the complete study and clearly show that sample disturbance dominates the behavior of cemented sands. Discussion of these test results, in terms of both initial stiffness behavior and ultimate strength characteristics, are presented in the subsequent paragraphs.

Most notable in the results presented in Figure 7 are the shapes of the stress-strain curves, particularly the initial modulus and strain to peak failure. Shelby tube sample results indicate a mechanism and response similar to the block samples. The response is, however, softer and subsequently results in higher failure strains. In the particular case shown, the post-peak strength was higher for the Shelby tube sample when compared to block sample results at equivalent confining pressures. The strain softening response was completely absent for the majority of split spoon samples; the strain to failure was considerably higher and the modulus lower than either the block or Shelby tube results. Indeed, the entire mechanism appears to be different for these samples. Strain to first failure for the typical results was shown in Figure 7. Analysis of the complete set of results indicated that this range of data was relatively small and tended to be representative of the sampling technique as tabulated on the same plot. Coupled with strain to first failure is the initial tangent modulus. The results of the entire triaxial test series is presented in Figure 8 which again utilized the normalized E_1 vs. σ_3 coordinates of Figure 6. For striking comparison the block sample results from the earlier figure are superimposed in Figure 8. The softer response

Sampling Technique	σ_3 (kN/m ²)	ϵ_f	Avg. ϵ_f for all tests
Block Sample	121	.6%	2.0%
Shelby Tube	121	3.5%	3.6%
Split Spoon	242	12.0%	10.7%

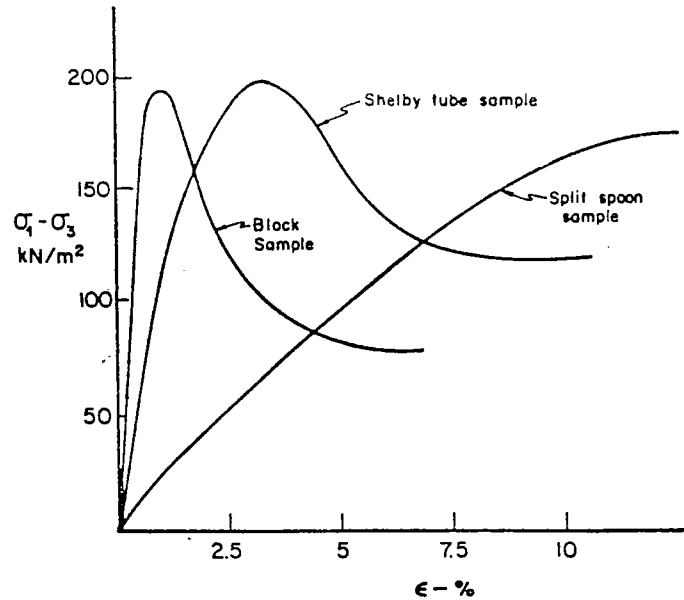


FIG. 7. TYPICAL STRESS-STRAIN RESPONSE OF DIFFERENT SAMPLES OBTAINED AT THE PACIFICA SITE.

as the degree of sample disturbance increases is demonstrated. Once again the initial visual observation that the conventional samples did not "look" like the block samples is reinforced by the lab tests. Sampling imparts disturbance that disrupts the sensitive grain to grain contact bonds which in turn leads to a different material, one of a less brittle stress-strain loading response.

A final view of the conventionally obtained sample test results is from a perspective of ultimate strength. The summary Mohr-Coulomb failure envelopes are presented in Figure 9. The average values of c and ϕ are plotted on this graph but actually represent a wide range of data which are also tabulated on the plot. Unfortunately, unlike the preceeding results, there are few consistent points in these data to differentiate the results. The conventional samples are generally weaker than the block samples, but are exceedingly variable. Notably, the more disturbed split spoon samples are generally stronger than the Shelby tube samples. Apparently the effects of sample disturbance are not as noticeable when considering ultimate strength behavior. The remolding effects on Shelby tube samples are to substantially reduce strength due to the breaking of the inter-particle bonds during sampling. However, this remolding and subsequent increased densification of the split spoon samples increases strength relative the Shelby tube results. The cohesion parameter is presumably

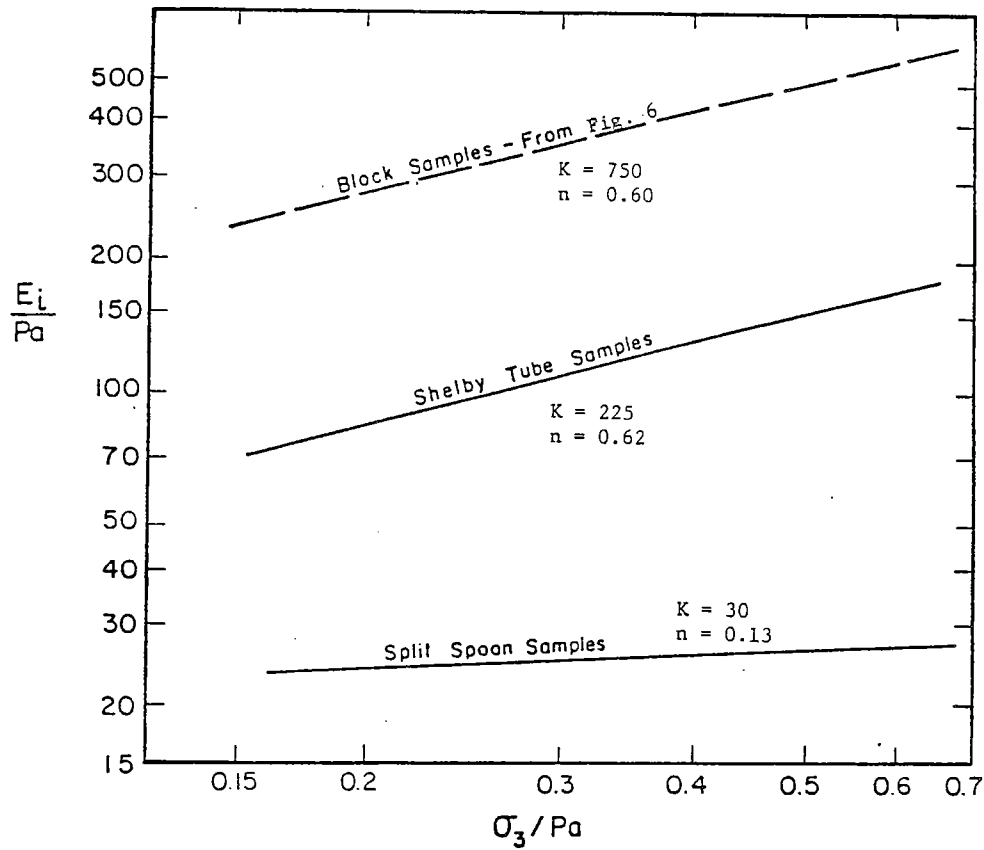


FIG. 8. VARIATION OF INITIAL TANGENT MODULUS WITH CONFINING PRESSURE FOR DIFFERENT SAMPLES OBTAINED AT THE PACIFICA SITE.

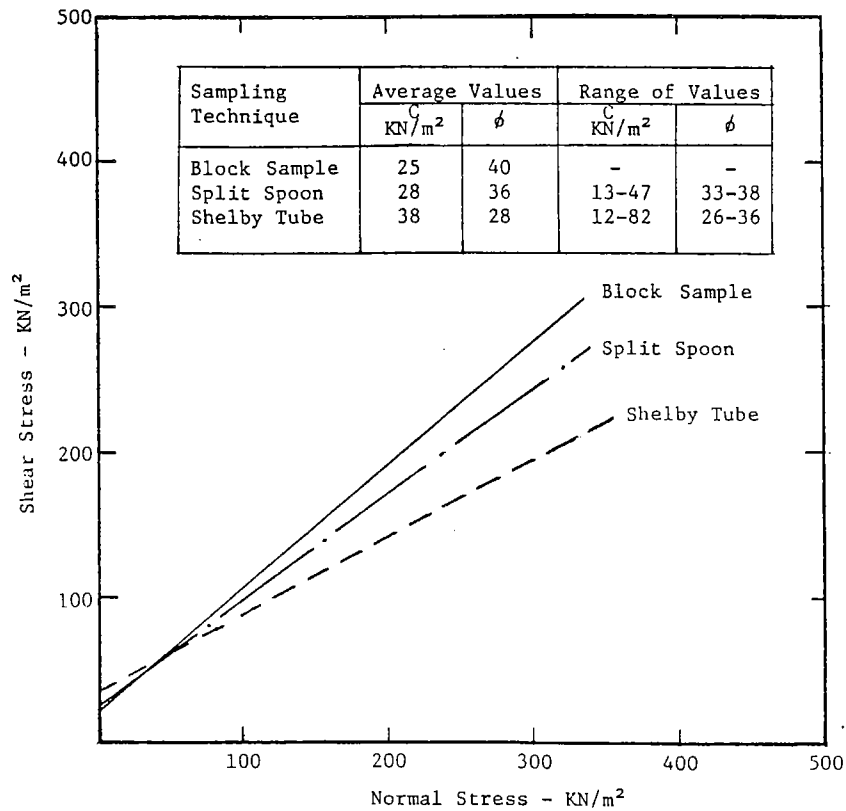


FIG. 9. AVERAGE MOHR-COULOMB FAILURE ENVELOPES FOR BLOCK, SPLIT SPOON, AND SHELBY TUBE SAMPLES.

due to capillary tension in the specimens as the true cementation was apparently destroyed during sampling. As a net result, the strength characteristics are poor indicators of sample disturbance.

ALTERNATIVES TO CONVENTIONAL SAMPLING

It has been shown that the disturbance effects induced during the sampling of weakly cemented sand deposits significantly alters the stress-deformation response of the recovered specimens. Given the realization that the sampling operation itself may destroy the samples, the geotechnical engineer is in a quandary as to how to best solve this problem. Block sampling, while convenient at the Pacifica site, is often cost-prohibitive, particularly for deep soil/rock deposits. In-situ test offers hope to the dilemma. The highlights of three in-situ testing programs will be presented subsequently, however, for details the reader is directed to Bachus, et al., 1981 or Bachus, 1982.

Standard penetration tests (SPT) were conducted during the split spoon sampling operation. Blow counts ranged from 23-100. Observation of the recovered "sand" sample would potentially indicate this a suitable technique for determining the relative density and consistency of the subsurface soil. The consistency of results may, in fact, represent consistency in the degree of cementation and blow counts themselves may reflect the strength of the cementing bond between sand grains and not necessarily reflect the in-situ soil density. The concept of relative density in cemented soils and how it relates to behavior requires further study. To their credit, however, the blow counts are relatively high and do indicate a medium to very dense sand. Visual observation of the samples and calculation of unit weight would indicate that the SPT results are in themselves unusually high and thus serve as indicators of unusual material or behavior.

Dutch cone penetrometer tests (CPT) were also attempted at the site. Testing was aborted at a depth of just 10 ft. (3 m) due to excessive vertical reaction, itself an indicator of competent subsurface soils. Further, the sleeve friction was quite low relative the tip bearing, a characteristic of dense or cemented sand behavior (Sanglerat, 1972). Although initial results were encouraging, the requirement for large reaction forces may preclude use of the CPT in conventional geotechnical testing programs.

Self-boring pressuremeter tests (SBPM) were conducted at the Pacifica site with encouraging results. Conventional pressuremeter testing was conducted at the SLAC test site (refer to Figure 1) which also served as a trial section for the self-boring work. The details of this study are beyond the scope of this paper but has been addressed in the previously referenced work as well as in a recent presentation by Bachus, 1985. In short, the SBPM program was successful in yielding result for both initial modulus and ultimate strength which closely compared to the block sample test results. Additionally, values of in-situ lateral earth pressures were measured and found to be reasonable, based on the test depth and position relative the bluff face. Although the results are encouraging, the self-boring procedure is slow and requires operator experience to successfully conduct a test program.

CONCLUSION

Weakly cemented sands or soft sandstones are widely distributed and pose significant problems in engineering practice. These problems are compounded by the fact that the material is easily disrupted upon application of light finger-tip pressure. Lab tests on this material, when sampled by careful block sampling procedures, revealed that cementation has a very important influence on behavior and that the behavior is controlled by a combination of interparticle contact bonds and intergranular friction. At low confining pressures the cohesion dominated and a stiff, brittle response resulted. As the degree of confinement increased, the friction played a more dominant role and at higher pressures could essentially mask the effects of cementation. After the cementation bonds were disrupted the post peak response approached the behavior of uncemented sand. This behavior was shown to be identical to that of laboratory-prepared artificially cemented sand.

Conventional split spoon and Shelby tube sampling both imparted irrecoverable degrees of disturbance which appeared to disrupt the sensitive interparticle bonds during the sampling operation. The recovered specimens were denser than their block sampled counterparts. Pitcher barrel samples at this site were unexpectedly quite poor and showed signs of extreme disturbance due to disruption of the cementing bonds. The in-situ water content and possibly the fines content appear to affect the ability of the disrupted and remolded specimen to remain intact upon extrusion. Lab testing results indicate that the recovered conventional samples were much more ductile than the block samples as characterized by lower modulus, higher strain to failure, and general lack of strain softening characteristics. The ultimate strength characteristics were surprisingly similar. It is felt, however, that these strength similarities are somewhat coincidental and agree for completely different reasons. Block sample strengths arise from an undisrupted interparticle bond and friction while the conventional sample strength arises from frictional behavior on a denser uncemented material and possibly capillary tension due to incomplete saturation.

In-situ standard penetration, cone penetrometer and pressuremeter tests offer potential in characterizing these materials. SPT results yield higher than expected blow counts when compared to the recovered sample unit weights. This in itself may be indicative of cementation but is difficult to quantify. CPT results yield very high tip bearing relative to side friction, indicative of either dense or cemented sands. To complete a study of this type however, a large cone rig or anchored drill rig is required to supply large vertical reactions. Conventional pressuremeter and self-boring pressuremeter tests offer promise in characterizing cemented sands. The PM must be capable of inflation to sufficient pressures to induce failure in the soil without over-inflating and rupturing the membrane. The SBPM results were the most encouraging and compared extremely well to block sample results for both strength and modulus.

ACKNOWLEDGEMENTS

The author was supported at Stanford University for the duration of this project. Financial support as well as drilling support was supplied by the USGS, grant contract 19763. The support of both these is gratefully acknowledged.

REFERENCES CITED

- Bachus, R. C., "An Investigation of the Strength Deformation Response of Naturally Occurring Lightly Cemented Sands", PhD Thesis, Stanford University, 1982.
- Bachus, R.C., "The Use of the Pressuremeter to Evaluate the Strength-Deformation Characteristics of Soft Rocks", Proceedings, 26th U.S. Symposium on Rock Mechanics, Rapid City, S.D., 1985.
- Bachus, R.C., Clough, G.W., Sitar, N., Nader, S.R., Crosby, J., and Kaboli, P., "Behavior of Weakly Cemented Soil Slopes Under Static and Seismic Loading Conditions", Vol. II, Report 52, John Blume Earthquake Engineering Center, July, 1981, 247 pp.
- Clough, G.W., and R. C. Bachus, "An Investigation of Sampling Disturbance in Weakly Cemented Sands", Engineering Foundation Conference on Updating Subsurface Sampling and In-Situ Testing, Santa Barbara, CA., 1982.
- Clough, G.W., N. Sitar, R.C. Bachus, and N. Shafii-Rad, "Cemented Sands Under Static Loading", Journal of the Geotechnical Engineering Division, ASCE, Vol. 107, No. GT6, 1981.
- Sanglerat, G., "The Penetrometer and Soil Exploration", Elsevier Publishing Co., 1st ed., 1972.
- Sitar, N., "Behavior of Slopes in Weakly Cemented Soils Under Static and Dynamic Loading", PhD Thesis, Stanford University, 1979.
- Youd, T.L., and S. N. Hoose, "Historic Ground Failures in Northern California Triggered by Earthquakes", United States Geological Survey, Professional Paper No. 993, 1978.

MOMENT-DRIVEN DEFORMATION IN ROCK SLOPES

Alberto S. Nieto and Peter K. Matthews
Dept. of Geology, University of Illinois, Urbana-Champaign, IL

ABSTRACT

Factors of safety for translational failures in rock slopes (e.g. slumps or glides) are derived from sum-of-forces equilibrium equations, whereas such factors for moment-driven deformation (e.g. toppling) need be derived from sum-of-moments equilibrium equations. Two modes of moment-driven deformation are discussed: "toe kicking" and deep-seated toppling. Results of physical models of these two modes of deformation suggest that they are kinematically possible. Numerical models suggest that the forces involved in moment-driven deformation are less than those in translational failures assuming similar strength parameters. Therefore, remedial measures planned assuming a translational failure mode when one is actually in the presence of a moment-driven failure may lead to overconservative and unduly expensive procedures.

INTRODUCTION

A majority of rock-slope failures involve translational movements over a sliding surface. Many of these failures result in large deformations of the rock masses affected, large velocities and catastrophic consequences. Figure 1 shows an example of one such failure. The stability of rock slopes with respect to translational movements can be evaluated by limit equilibrium methods. The assumption is generally made the equilibrium is satisfied if

$$\sum F_x = 0 \quad (1)$$

$$\sum F_y = 0 \quad (2)$$

The third equilibrium condition,

$$\sum M_o = 0 \quad (3)$$

is generally not considered. There are, however, field situations in which tall, prismatic bodies of rock can become unstable because of force moments (Figure 2). The importance of moments, as cause for slope deformation and failure, has been recognized relatively recently in rock-slope engineering. Toppling of blocks and prisms has been discussed by Muller (1971), Goodman and Bray (1976), and others. Toppling is in fact one form of moment-driven deformation. Figure 3 is a free-body diagram of one such prism ("columns" in two dimensions) showing the weight vector and the external forces. The clockwise rotational tendency of the prism is due simply to the location of line of action of the weight vector, W , with respect to the base of the column. This clockwise rotation creates displacements

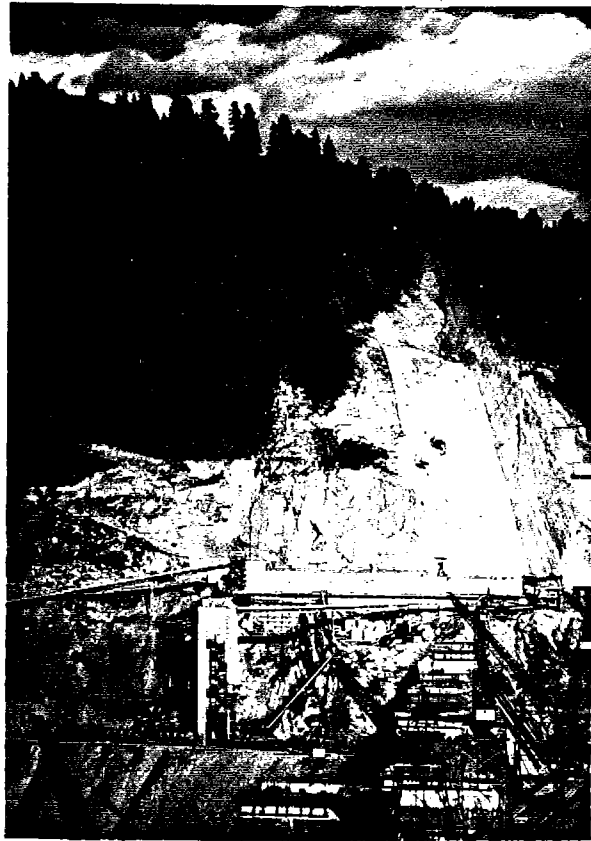


FIGURE 1. LEFT ABUTMENT OF LIBBY DAM, LIBBY, MONTANA, AFTER WEDGE FAILURE (TRANSLATIONAL) AND CLEAN-UP OPERATION. COURTESY OF BILL HERB.



FIGURE 2. INCIPIENT TOPPLING FAILURE IN STEEPLY DIPPING SEDI-MENTARY ROCKS ALONG CENTRAL HIGHWAY; PERU; 125 KM EAST OF LIMA.

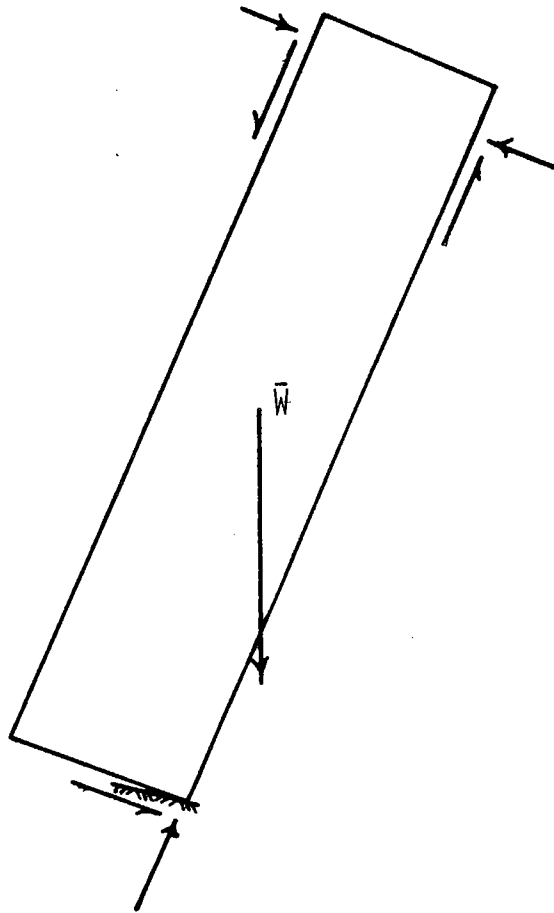


FIGURE 3. FREE-BODY DIAGRAM OF TALL ROCK COLUMN WITH OVERTURNING TENDENCY.

to the right in the upper right-hand corner and to the left in the lower left-hand corner. If a slope lies to the right of the column, the overturning tendency results in toppling, but if the slope lies to the left, that tendency results in a kicking out of the toe to the slope, analogous to the sliding of a ladder leaning on a wall.

OCCURRENCE OF TOPPLING

Of the two types of moment-driven deformation described above, as far as we can determine, only toppling has been described in the literature. Toppling can take place in any type of rock mass containing steeply dipping discontinuities. However, most of the field descriptions come from sedimentary and metamorphic terrains where bedding and foliation discontinuities provide the boundary planes for the toppling prisms or columns (De Freitas and Watters, 1973; Goodman and Bray, 1976; Wyllie and Wood, 1982). The senior author has worked on a toppling failure in igneous rocks at a large open-pit mine in western Canada in which the steeply dipping discontinuities are believed to be a series of shear fractures caused by the emplacement of an intrusive body. Figure 4 shows the field situation and the stress system responsible for the fracture sets. Note that one set is better developed and possesses a closer spacing than the other set. The role of the gently dipping fracture set is very important and will be discussed later. We believe that the two sets of fractures shown in Figure 4 are not uncommon in igneous and high-grade metamorphic complexes.

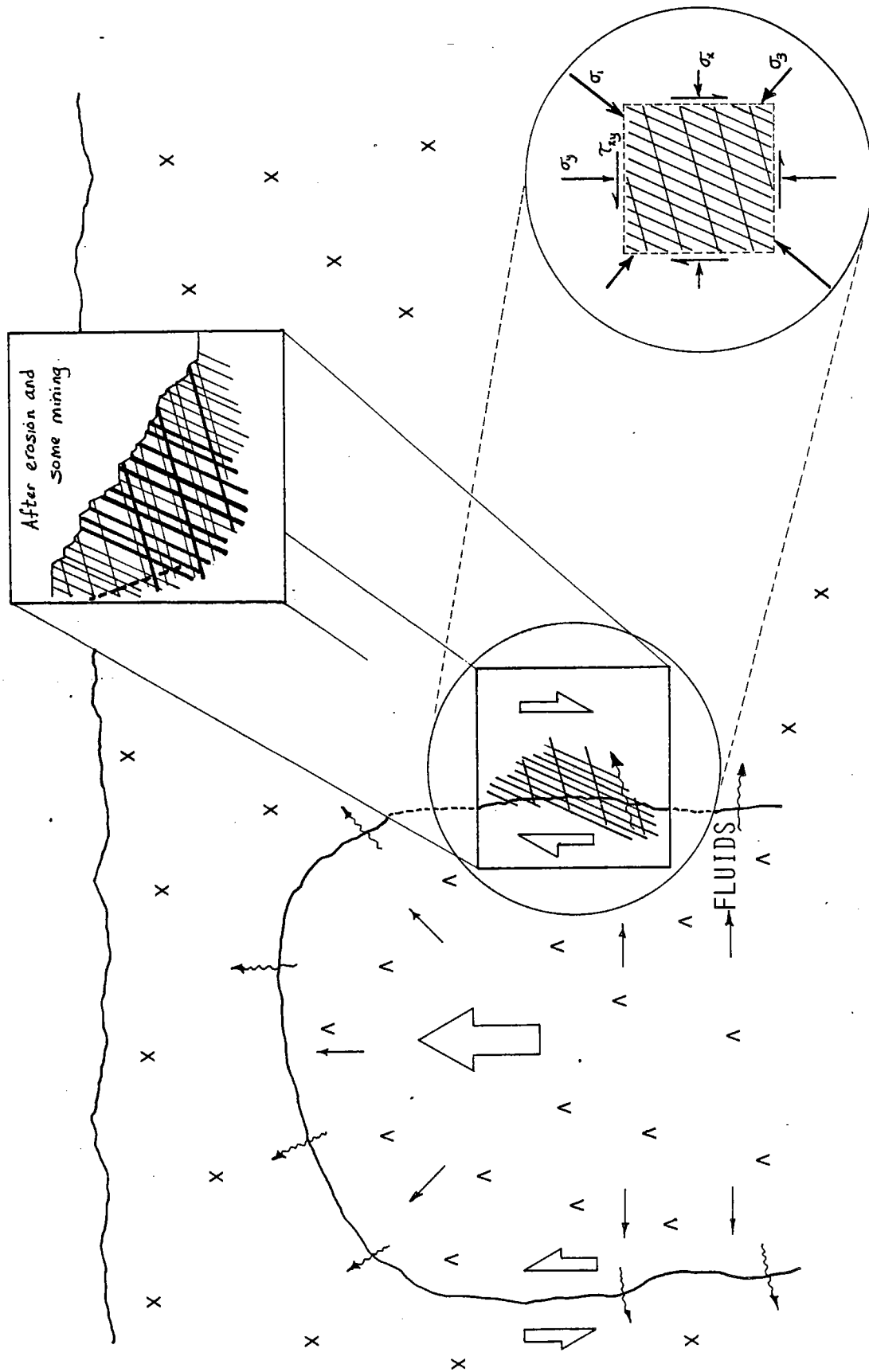


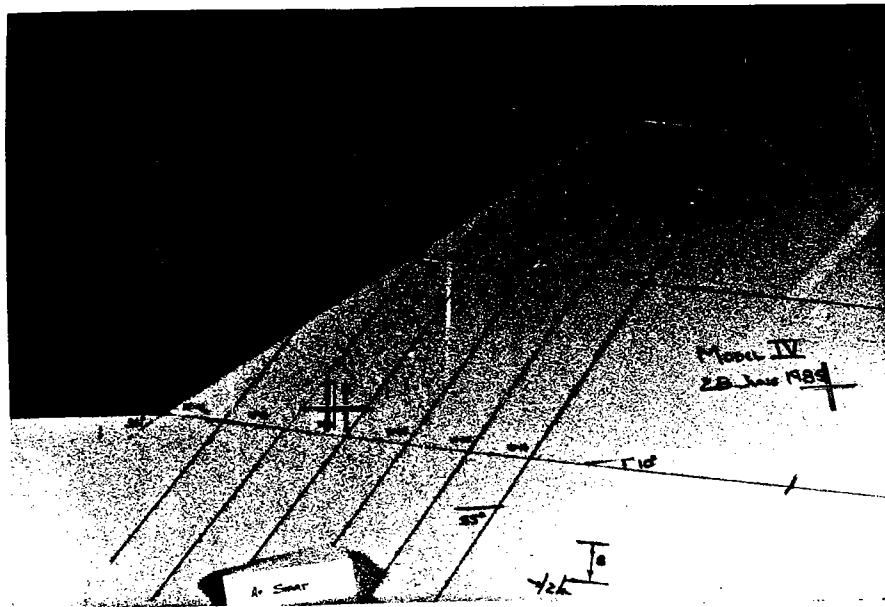
FIGURE 4. FIELD RELATIONS FOR CONJUGATE SETS OF SHEAR DISCONTINUITIES NEAR AN INTRUSIVE CONTACT; ACCOMPANYING STRESS SYSTEM AND MINE SLOPE SUSCEPTIBLE TO TOPPLING.

Furthermore, these discontinuities can have very low shear strengths because of their shear origin and the hydrothermal alterations that they often undergo. Many of these complexes are sites for important mining developments and the attendant highway and mine rock cuts thus can be susceptible to toppling.

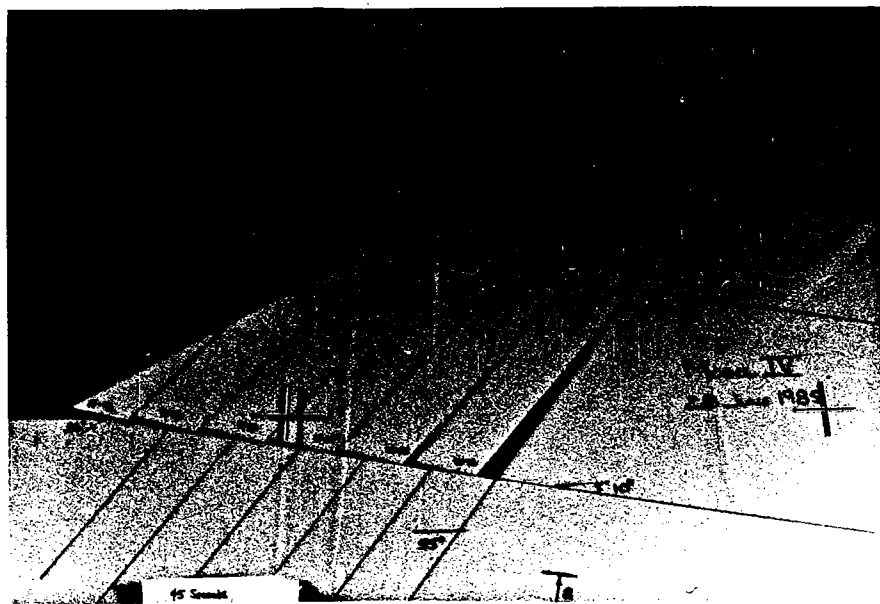
Toe kicking as such has not been recognized in the literature as a mode of slope deformation. This may be so because the attitude of the discontinuities that give rise to toe kicking have been traditionally considered kinematically incompatible with block sliding or because the observed deformation has been ascribed to instability of bilinear wedges.

STUDIES OF MOMENT-DRIVEN SLOPE DEFORMATION.

In the last two years, we have conducted physical-model and analytic studies of moment-driven deformation of slopes. Figures 5 and 6 are photographs of model slopes deformed on a base-friction table at the Engineering Geology Laboratory of the University of Illinois, Urbana-Champaign. The slope elements were cut from three-quarter inch extruded styrofoam with masking and Scotch tapes was adhered to the sides of the columns and wedges to simulate the low friction of the discontinuities. The models were then placed on a table with a 51-inch wide sanding belt which upon turning dragged the models in the direction of movement thus simulating the pull of gravity. The deformation trends are then observed after a certain time.

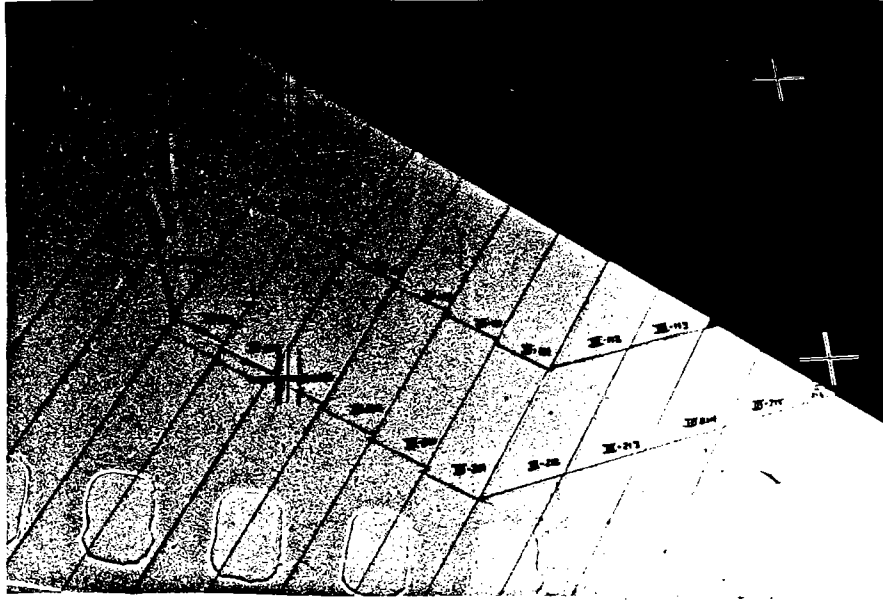


(A)

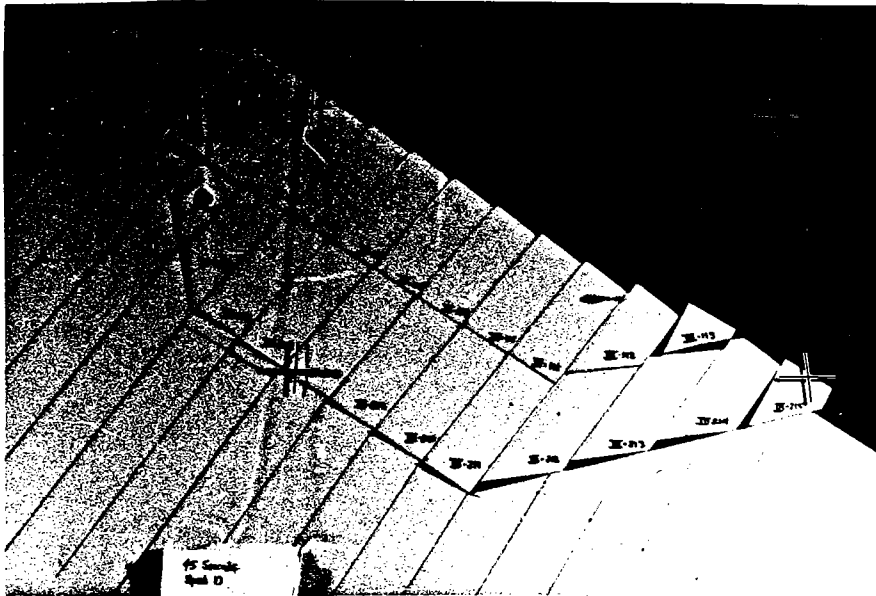


(B)

FIGURE 5. BASE-FRICTION MODEL OF A SLOPE DEFORMING BY TOE-KICKING: (A) INITIAL CONDITIONS; (B) AFTER CONSIDERABLE DEFORMATION. DISTANCE BETWEEN FIDUCIAL MARKS, HORIZONTAL: 18 IN., VERTICAL: 12 IN.



(A)



(B)

FIGURE 6. BASE-FRICTION MODEL OF DEEP TOPPLING FAILURE AT AN OPEN PIT MINE IN WESTERN CANADA; (A) INITIAL CONDITIONS; (B) AFTER CONSIDERABLE DEFORMATION. DISTANCE BETWEEN FIDUCIAL MARKS; HORIZONTAL: 18 IN. VERTICAL: 12 IN.

Figure 5 is an example of toe kicking and shows the clockwise rotation of the prisms and pyramids and the displacement to the left of the lower left-hand corner of these slope elements. The observation of the surface deformation alone would normally induce one to analyze such a slope failure by means of a bilinear wedge. The wedge would be divided into active and passive sections by a line from the point of intersection of the two discontinuities forming the kinematic boundaries to the surface. A factor of safety equal to unity would be assumed and the strength parameters would be back-calculated. The remedial work then would be based on the results of this bilinear wedge analysis. However, Figure 5b shows that the deformation is much more complex than that resulting from the simple interaction of active and passive sections. In fact, at this point we do not know what is the relation between the factor of safety for a bilinear wedge and the actual factor of safety of this slope, or if the slope would fail catastrophically or if it would simply deform as shown and would eventually become stable.

Figure 6 shows the model of slope in an important open pit mine in western Canada (see above); this slope has sustained a large amount of deep toppling deformation which has led to extensive surface disruption, to the extent that no permanent access roads can be maintained on it. The essential elements of this slope failure, as shown in Figure

6a, are: (1) a set of deeply dipping discontinuities or toppling discontinuities (TD's) and, (2) a set of gently dipping discontinuities (BD's, for basal discontinuities). The latter can be considered to be a conjugate set to the TD's (see Figure 4). Only portions of two members of this second set are shown for the sake of simplicity; in reality, the BD's occur throughout the slope but are not as well as developed or as closely spaced as the TD's. The other elements of the slope failure are: (3) a toppling base (TB), shown in Figure 6 at a stepped surface, and (4) a head discontinuity (HD), dipping steeply in the same direction as the slope. The toppling base is a virtual (nonexistent) discontinuity; it is formed by a series of preexisting nonsystematic joints perpendicular to the TD's or perhaps by tension joints induced by the toppling of the columns. The head discontinuity is not essential to the deformation mechanism. It can be a steeply dipping joint as shown in Figure 6, a tension crack, or it may not exist at all. In this last case the toppling base extends beyond the crest of the slope until it intercepts the ground slope. The rock is a granodiorite of medium to high strength and the significant discontinuities (TD's, BD's, and HD's) have soil-like fillings with residual strengths as low as $\phi_r = 8^\circ$, $c = 0$. The toppling base probably has the high peak strength of tension joints.

Kinematically the model is divided into three sections (Figure 7): A passive wedge at the toe, a deep toppling section in the middle, and an active wedge, if an HD or a tension crack exists near the crest of the slope. The stability of the entire slope is controlled by the stability of the passive wedge; no toppling displacements are possible if the passive wedge does not move. The driving forces trying to displace the passive wedge are a combination of toppling forces and active wedge forces.

This model of slope deformation by deep toppling has rather unusual characteristics. First, the surficial deformation features have all of the characteristics of those of a slump failure: Tension cracks and a head scarp develop near the crest, shear fractures with obsequent (upslope-facing) scarps develop in the middle portion and the toe section bulges. However, observation of the potential sliding surface in the model shows that all of that surface deformation has taken place without any shear displacements along the toppling base. If an HD existed the interaction between the toppling section and the passive wedge would still be the same as shown in Figure 5a.

The factor of safety of the model can be calculated by limiting equilibrium methods and is defined in terms of the factor of safety of the passive wedge. The equilibrium condition for the toppling section can be computed using the

Goodman-Bray method. The toppling forces are assumed to be transmitted at the top of the prisms because the prisms separate along their lower portions as they rotate on a stepped base. (See e.g. Goodman and Bray, 1976, Figure 4; Willey and Wood, 1982, Figure 1). The factor of safety with respect to toppling for the slope in Figure 7 is very close to unity for the values of strength given and a water table very close to the ground surface. By contrast, the factor of safety along the potential sliding surface is considerably greater than one.

It should be emphasized that a catastrophic failure may not take place in spite of the large deformation that accompanies toppling. Indeed, toppling slopes become stable after some deformation. After a certain amount of rotation the openings between columns close and further rotation is possible only under dilatant conditions; this creates a need for shear displacement along the toppling base which in turn increases stability. The stage of deformation shown in Figure 6b is very advanced and was chosen for demonstration purposes only. In fact, this stage is well beyond the closure of the openings between the toppling prisms and the onset of dilatant behavior. If the length of the columns in the toppling section of Figure 6b is assumed to be 100 feet, then the surface displacements in the mid-portion of the slope are approximately 10 feet.

There should be, at least in theory, some engineering situations in which the deformation of the slope and the surface

disruption, including tumbling blocks, does not create unsafe conditions and is therefore acceptable knowing that the slope will eventually stabilize itself. In other cases, deformation cannot be tolerated and remedial work would have to be undertaken. However, the remedial work will have to be planned knowing that one is in the presence of a moment-driven type of failure (toppling) and not a regular slump. The driving forces involved in the latter are much larger if one assumes that the potential sliding surface for the slump has similar strengths as the critical discontinuities of the toppling model. Therefore such an assumption would be unduly overconservative.

The presence of BD's (shallow in-dipping discontinuities) is very significant because it allows toppling to develop under conditions that the standard (Goodman-Bray) model does not. The standard toppling geometry considers a toppling base roughly perpendicular to the toppling discontinuities as shown in Figure 7. That base creates columns that are not slender enough for toppling. In fact, the slope in Figure 7 is quite stable against toppling if the standard geometry is considered. The BD's, however, allow for a much deeper toppling base and therefore more slender columns, so that toppling tendencies are much greater. We believe that the two sets of discontinuities essential to the model (TD's and BD's) are not uncommon and that some of the slope movements that may have been ascribed to slumping in the past might be really toppling movements as described here.

CONCLUSIONS

The overturning moments of tall columns of rock that are formed by a set of steeply dipping discontinuities, when combined with a set of gently dipping ones, can induce rock-slope deformation. Two modes of deformation are recognized: toe kicking and deep toppling.

Moment-driven deformation can lead to a large amount of surface disruption but not necessarily to catastrophic results. Our poor understanding of moment-driven deformation and the similarity in surface features resulting from moment-driven deformation and slumping may account for the lack of recognition of these processes in the literature.

A model of toppling failure was presented which extends toppling to greater depths than the standard (Goodman-Bray) model. It consists of a passive wedge, a central toppling section and, in some cases, an active wedge.

REFERENCES CITED

- De Freitas, M. H. and Watters, R.J., 1973, Some field examples of toppling failures, *Geotechnique*, v. 23, n. 4, pp. 495-514.
- Goodman, R. E. and Bray, J. W., 1976, Toppling of rock slopes, *Proc. Spec. Conf. Rock Engineering for Foundations and Slopes*, Boulder, CO, ASCE, v. 2.
- Muller, L., 1968, New considerations of the Vajont slide, *Felsmechanik und Ingenieurgeologie*, v. 6, n. 1, pp. 1-91.
- Wyllie, D. C. and Wood, D. F., 1982, Stabilization of toppling rock slope failure, *Proc. 33rd. Annual Highway Geology Symposium*, Denver, CO., pp. 103-115.

36th ANNUAL
HIGHWAY GEOLOGY SYMPOSIUM
FIELD TRIP
MAY 14, 1985

BUILDING ON AND WITH SEDIMENTARY BEDROCK

Field Trip Leaders

Earl M. Wright
Kentucky Department of Highways

Richard T. Wilson
Kentucky Department of Highways

ACKNOWLEDGEMENTS

We are indebted to Roy Kepferle, Eastern Kentucky University for his discussion and comments relating to the geological formations encountered on this field trip. Jackson Graham and Don Ackerman with Traylor Brothers have graciously given us permission to visit their construction activities as well as providing technical information and assistance. For this we thank them for their time and efforts.

Expression of gratitude is extended to Tom Anderson with Schnabel Company and Don Ashfield with Geotechniques for providing specifications, comments and discussions of their areas of expertise. The Indiana Department of Highways personnel will provide traffic control while Rick Hockett will explain the D-cracking problems encountered by their department and review a geological rock cut section.

We wish to thank the following personnel from the Louisville District: Steve Hoefler, Charles McLaughlin, Bernie Roach and Barry Sanders for their time and assistance in making this trip possible.

A great deal of effort has been made by personnel of the Geotechnical Staff. Henry Mathis, Bill Pfalzer, Doug Smith and Ed Munson for providing case histories and comments for concepts that are encountered on this field trip. Our appreciation is expressed to Everett Gray and Mike Blevins for providing logistical support, Jami Salisbury and Terry Gash for graphics and Kim Sheets for secretarial work.

Last but not least, we wish to acknowledge Terry West and the publication staff of Purdue University.

INTRODUCTION

On behalf of the National Steering Committee, the sponsors of this 36th Annual Highway Geology Symposium welcome you to Kentucky and Indiana.

You are invited to participate in a field trip that traverses the outer bluegrass region of Kentucky and portions of southern Indiana (Figure 1). While the buses are in route, a commentary on the Geological Formations and associated geotechnical engineering problems will be provided. The lithologic divisions on new USGS maps are shown in a correlation chart, (Figure 2) to help clarify the "Old" and "New" geological nomenclature.

The primary emphasis of this field trip is directed to geotechnical engineering practices of building highways on and with sedimentary rocks. The field trip will provide a review of different concepts utilized in slope stabilization. Visits to construction sites in the Louisville area are subject to last minute adjustments, however, we intend to observe a tunneling operation and wick drain installations.

We hope the field trip will be of interest and benefit all participants. Safety vests and hard hats will be available and participants are encouraged to exercise safety precautions at all times. Questions and discussions are certainly welcome, however, your cooperation in maintaining the time schedule will be appreciated.

Earl Wright
Richard Wilson

TABLE OF CONTENTS

	PAGE
Acknowledgements	I
Introduction	1
Guide Map for Field Trip	2
Formation Correlation Chart	3
Field Trip Road Log	4
Special Illustrations and Comments	14-31
Stop #1 Wick Drain Installation and Use by Bill Pfalzer	14
Stop #2 Rapid Tunnel Excavation by Don Ackerman	17
Stop #3 Mill Creek Embankment Corrections by Doug Smith	22
Stop #4 Horizontal Drains for Landslide Stabilization by Ed Munson	26
Stop #5 Slide Retainment - Tiedback Wall by Tom Anderson	28
Stop #6 Maintenance Correction by Henry Mathis	29
Stop #7 D-Cracking Pavement and Rock Cut Section on U.S. 421 in Indiana by Rick Hockett	31
References	34

GUIDE MAP FOR FIELD TRIP

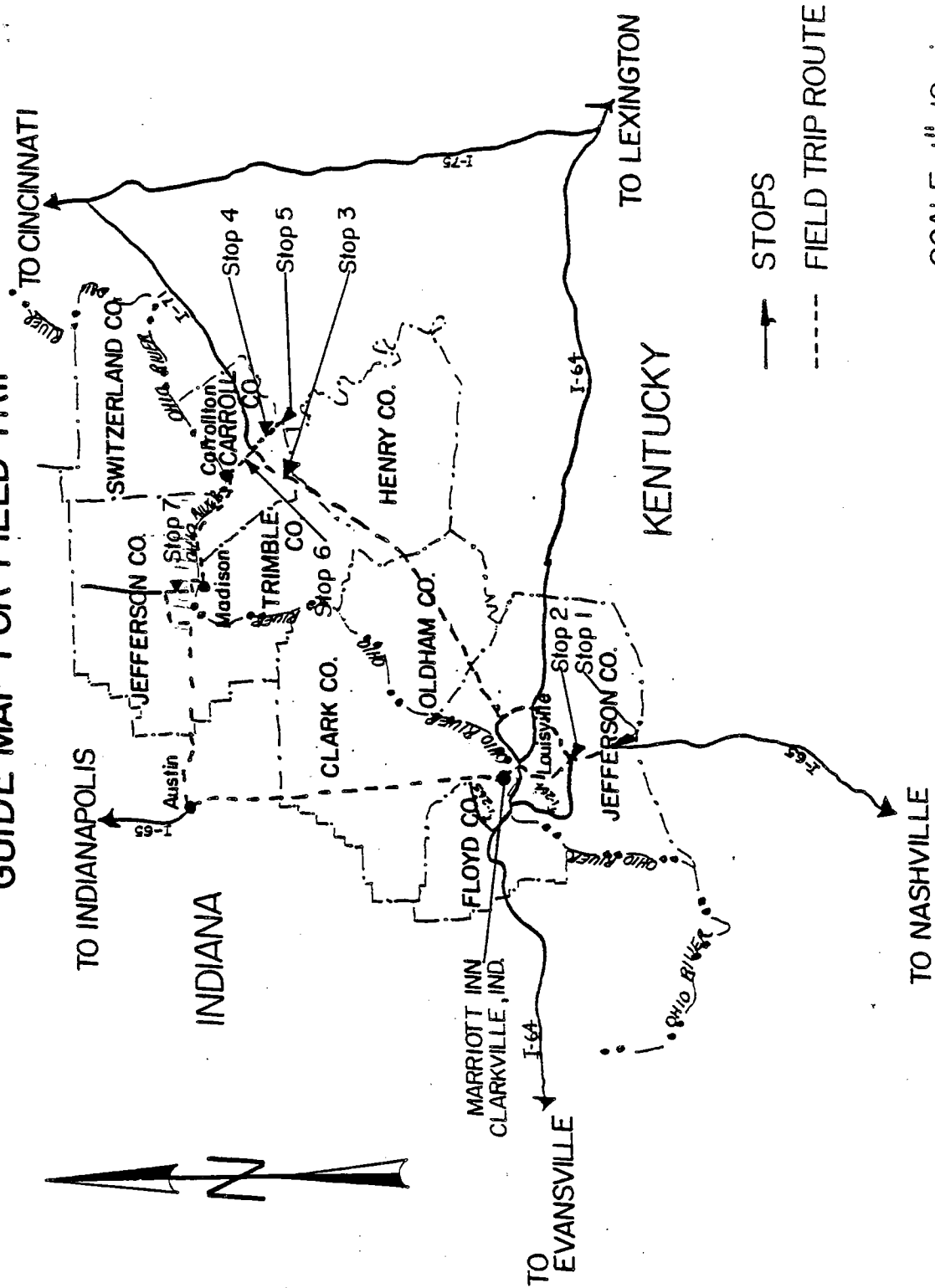


FIGURE 1

FORMATION CORRELATION CHART

System	Series	Formation & Member	Nomenclature Of Earlier Works	Thickness
Devonian	Upper & Middle Devonian	New Albany Shale	New Albany Shale	30'+
	Middle & Lower Devonian	Sellersburg Limestone	Sellersburg Limestone	3- 15'
		Jeffersonville Limestone	Jeffersonville Limestone	20- 27'
Silurian	Middle Silurian	Louisville Limestone	Louisville Limestone	40- 80'
		Waldron Shale	Waldron Shale	8- 15'
		Laurel Dolomite	Laurel Dolomite	47- 54'
		Osgood Formation	Osgood Formation	13- 19'
	Lower Silurian	Brassfield Formation	Brassfield Limestone	1- 7'
Ordovician	Upper Ordovician	Drakes Formation Saluda Dolomite Member	Richmond Saluda Limestone	40- 48'
		Bardstown Member	Liberty	35- 44'
		Rowland Member	Waynesville	0- 35'
		Bull Fork Formation	Arnheim	87-175'
		Grant Lake Limestone	Maysville Bellevue	55-100'
		Fairview Formation	Fairview	85-100'
	Middle Ordovician	Kope Formation	Eden	160'+

FIGURE 2

FIELD TRIP ROAD LOG
Tuesday, May 14, 1985

Mileage

0.0 Begin Trip. Marriott Inn Parking Lot. Buses will load at 7:45 AM and depart promptly at 8:00 AM proceeding south on I-65 to the Fern Valley Interchange.

11.1 Stop #1 (20 Minutes): I-65 Over Northern Ditch.

 The purpose of the stop is to observe embankment construction techniques in an unstable area. Wick drains are being installed by Geotechniques American from Bay St. Louis, Mississippi. The wick drains provide a method of expediting construction by decreasing consolidation time requirements. Bill Pfalzer of the Geotechnical Engineering Branch will be available for questions. For additional comments and information, refer to page 14.

 Return to I-65 and proceed north to I-264 (Watterson Expressway Interchange).

14.0 Stop #2 (30 Minutes): I-65/Ramp to Westbound I-264.

 This stop is to observe tunnel excavations in the Louisville Limestone. At this time both standard drilling and blasting and rapid tunnel excavation (mole) are being utilized to complete a storm sewer system under the I-264 interchange.

Due to the extremely high volume of traffic, E. H. Hughes elected to build the storm sewer system under this 100 million dollar interchange by tunneling rather than open trench. Traylor Brothers of Evansville, Indiana has been contracted to construct 5000 ft. of storm sewer tunnels. Approximately 3800 ft. of tunnel will be built using 115 in. and 86 in. hard rock tunnel boring machines (mole). In addition 1200 ft. will be constructed using the traditional drill and shoot method. Mr. Don Ackerman or Jackson Graham with Traylor Brothers will be available for comments. Refer to page 17. Anyone desiring a close up view of the underground production work area, a short tour, is possible, at your own risk.

Proceed east on I-264 to I-71 north.

17.8 The Corporate Headquarters for Kentucky Fried Chicken is located on the right side of the Watterson Expressway.

25.7 MP 22 of I-264. A Formation contact of the Sellersburg/Jeffersonville Limestone (Devonian) and Louisville Limestone (Silurian) is exposed. The Devonian limestones vary from 35-50 ft. in thickness. The coral Halysites aids in identifying the Louisville Limestone.

26.5 I-264/I-71 Interchange. A rock contact between the Jeffersonville and Louisville outcrops in the cut section. These limestones are used as a source for agriculture, industry and road construction purposes. At this time quarry operations are not permitted within the city of Louisville.

28.3 MP 7 of I-71. Rock outcrop of the Jeffersonville Limestone.

32.6 Oldham/Jefferson County Line.

33.3 MP 12. This roadway cut exposes contacts between Silurian Formations of Louisville Limestone, Waldron Shale and the Laurel Dolomite. The Waldron Shale is plastic when wet and degrades rapidly, and is generally unstable for roadway construction.

34.6 I-71. Rest Stop (20 Minutes).

Exposed at this stop is the Laurel Dolomite (Silurian). The Laurel Dolomite is composed of two types, the upper portion is micrograined to very fine crystalline and evenly bedded. The lower portion is more massive and is a common source of roadway aggregates.

At the east end of the cut the Laurel contacts shale of the Osgood Formation (Silurian). The Osgood, like the Waldron, is unstable in both embankments and cut sections.

- 35.3 MP 14. Note the solution features in the Laurel Dolomite with the overlying Waldron Shale forming a gentle slope.
- 36.3 MP 15. Outcrops of the Louisville Limestone (Silurian), Waldron Shale (Silurian) and the Laurel Dolomite are visible. The Waldron and Osgood Shales are impermeable and provide particularly good locations for farm ponds.
- 39.6 Upper Ordovician. Outcrops of the Saluda Dolomite Member, which is the upper member of the Drakes Formation, are visible for the next five miles. The deeper I-71 cuts in the Saluda were made on a 1:20 slope in the late 60's. These cuts are now showing signs of differential weathering between the more durable upper Saluda and the less durable lower Saluda. The upper portion of the Saluda are generally in layers 1/4 in. to 1 in. thick and on exposed surfaces may show color banding. The lower part of the Saluda is a dolomitic mudstone characterized by a blocky prismatic appearance.
- 40.3 Notice the large ant hills on left side of the road.
- 43.2 Ky. 53 overpass. Two members of the Drakes Formation (Upper Ordovician) are exposed in this cut section, (the Saluda Dolomite Member and the Bardstown Member). The Bardstown consist primarily of limestone with interbedded shale. Whole and broken fossils consisting of brachiopods, bryozoans, and horn corals are abundant in the larger granular limestone.

44.6 Contact between the Laurel Dolomite and Osgood is exposed.

46.1 Henry/Oldham County Line.

For the next 4.5 miles the Saluda Dolomite forms the ridge tops in moderately rolling uplands. The underlying Bardstown is exposed in the more dissected topography or deeper road cuts along I-71.

51.1 Just south of Fallen Timber Creek. In the cut section on the right side, the fine-grained argillaceous limestone blocks lying in the ditch are from the Rowland Member of the Drakes Formation. The underlying limestone and shale are part of the Bull Fork Formation which is fossiliferous. The fauna includes brachiopods, bryozoans, trilobite fragments, pelecypods and cephalopods.

58.2 In 1968 8 inches of continuously reinforced concrete pavement over 6 in. dense graded aggregate base was used on I-71 beginning at Ky. 55 and extending approximately 7 miles to the Kentucky River. After only 4 or 5 years of service the pavement deteriorated and required extensive maintenance. The worst sections were removed and replaced with full depth bituminous concrete. In 1982 a contract was let to remove the concrete pavement and replace it with bituminous concrete. Due to serious traffic control problems the decision was made to change the contract and overlay the pavement with 7 inches of bituminous concrete in lieu of removal and replacement.

59.4 Henry/Trimble County Line.

59.8 The Grant Lake Limestone is exposed on a rubbly 1:1 slope. The formation is thin to medium bedded argillaceous limestone with minor calcareous shale. Small sinkholes are present where the limestone is dominate.

60.1 Trimble/Carroll County Line.

61.0 Bridge over Mill Creek. The contact between the Grant Lake Limestone and the Fairview Formation is visible in the upper 1/3 of the cut.

The Fairview Formation is producing the large limestone slabs on the slope. The interbedded calcareous shale has a bluish gray lumpy appearance. Rock fences were installed to prevent the slabs from falling on the highway. This was the first of three rock fences along this section of the highway.

62.3 MP 41. A very distinct contact between the Fairview and Kope Formations is exposed in the cut section on the left. The Fairview consists of 75-80 percent limestone where the Kope has only a 15-30 percent limestone content. The calcareous shales disintegrate rapidly and contributes to unstable cut and embankment slopes. The Kentucky Department of Highways is in the process of adopting specifications for compaction of shale embankments.

Rugged topography consisting of narrow sharp ridges and V-shaped valleys are the rule in the Kope. The Kope erodes easily and the remaining slope is generally littered with limestone slabs.

64.3 Exit 43, turn right on Mill Creek Road.

67.7 Stop #3 (20 Minutes): I-71/Mill Creek Bridge Abutments.

This stop provides an example of correcting embankment failures on stream crossings without disturbing the existing structures or creek location. The original embankment was constructed on a 2:1 slope with material consisting of limestone slabs and soil like shale derived from the Fairview and placed on the Kope Formation.

The crib walls enable the slopes to be flattened to 3:1 utilizing limestone backfill material. Doug Smith with the Geotechnical Engineering Branch will be available for questions. Refer to page 22.

Return to Exit 43 and continue north on I-71.

72.8 Exit 44, turn right and follow Ky. 227 to General Butler State Park picnic area.

North of this exit on Interstate 71 for 33 miles (MP 45 thru 78) there are 67 shale embankment failures presently being investigated by the Geotechnical Engineering Branch.

75.3 Lunch Stop (1 Hour): General Butler State Park.

76.6 Turn right on Ky. 227 and proceed south.

78.4 Stop #4 (20 Minutes): Ky. 227 South of I-71.

Illustrates a method of stabilizing a hillside by dewatering. Horizontal drains were used to lower the water table in the embankment under the highway and railroad. Check valves were utilized in the ends of drains to prevent water from re-entering the slopes during high water. Ed Munson will be available for questions and comments. Refer to drawing on page 26.

Continue south on Ky. 277. At Worthville, reverse direction and head north on Ky. 227 toward Carrollton.

80.9 Stop #5 (25 Minutes): Ky. 227 South of I-71.

A tiedback wall illustrates a different method of slope stabilization by retainment.

A permanently anchored wall was constructed (13,865 sq. ft.) for a lump sum price of \$416,700. This is equivalent to a unit price of \$31.12/sq. ft. of wall face. Tom Anderson with Schnabel Foundation Company will offer comments and answer questions. Refer to drawing on page 28.

Continue north on Ky. 227.

76.4 Stop #6 (20 Minutes): Ky. 227 North of I-71.

This slide is an example of correction techniques applied by maintenance forces in stabilizing Ky. 227 which is being subjected to erosion by the Kentucky River. Henry Mathis, Geotechnical Engineering Branch Manager will discuss the project. Refer to page 29.

Continue north on Ky. 227.

88.8 Turn left onto US 42 in Carrollton.

91.2 The first wick drains installed in Kentucky are under the approach embankments for the Little Kentucky River Bridge. The intended purpose of the drains was to eliminate lateral squeeze on the bridge piling by reducing consolidation time. The piles are not driven until most of the consolidation has occurred. Approximately 900 wicks, averaging 34 ft. long, were installed at a price of \$2.10/ft. This is an experimental project and the Division of Research is currently monitoring consolidation rates, lateral movement, and pore pressures.

91.5 Turn right onto Ky. 36 and traverse the Ohio River flood plain to Milton, Kentucky.

96.9 Left side. Martin Marietta has a sand and gravel operation which supplies a large amount of materials used in this vicinity.

- 101.8 Turn right onto US 421. Cross the Ohio River bridge and proceed to the Riverside Park area in Madison, Indiana.
- 103.4 Rest Stop (20 Minutes): Madison, Indiana, Riverside Park.
Proceed north on US 421.
- 106.8 Stop #7 (30 Minutes): US 421 North of Madison, Indiana.
The principal subject of discussion at this stop is disintegration-cracking (D-cracking) of concrete pavement. An opportunity to collect fossils from the roadway cut section is also available for interested participants. Rick Hockett with the Indiana Department of Highways will provide comments.
Refer to page 31.
Continue north on US 421.
- 107.7 Turn left on IND 62. Proceed to IND 256.
- 114.2 Turn right on IND 256 and enjoy the beautiful Indiana farm land.
- 134.1 Enter I-65 south and return to Marriott Inn.
- 166.8 Exit 1. Right onto Stansifer.
- 167.3 Marriott Inn. End of Trip.

STOP #1: WICK DRAIN INSTALLATION AND USE
by
Bill Pfalzer

Wick drains have been used on three Kentucky highway projects to accelerate the consolidation of clay foundation soils. As the foundation soils are loaded, settlement and an accompanying displacement of water commences. Because the clays have very low permeabilities, water is displaced very slowly; and because water is essentially incompressible, it initially carries the load (in the form of excess pore water pressure). As the water is slowly displaced, the load is transferred onto the soil structure itself causing settlement (consolidation).

The consolidation process may take months, or even years, to be 90 percent complete. Where it has been desirable to accelerate settlement rates, vertical drains have often been used. These drains shorten consolidation time by shortening the distance water must travel through low permeability clays to reach a drain. Sand drains, formed by augering through the clay and backfilling with sand, have been largely replaced in recent years by wick drains which are generally easier and less expensive to install.

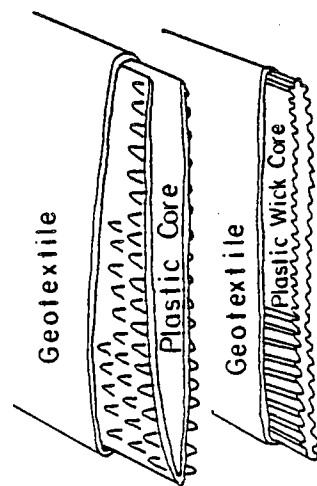
Wick drains typically consist of a plastic strip which contains grooves or projections permitting water to flow along the length of the wick (Figure 3-A). These plastic cores are wrapped in a geotextile, which allows water to pass, but prevents fines from clogging the grooves. The wicks are pushed into the ground by a hollow mandrel. Installation is similar enough

to the operation of a sewing machine that the equipment used to install the wicks is referred to as a sticher (Figure 3-B). At the base of the mandrel, the wick is wrapped around a rod which remains in the ground and prevents the wick from being pulled out as the mandrel is withdrawn (Figure 3-C).

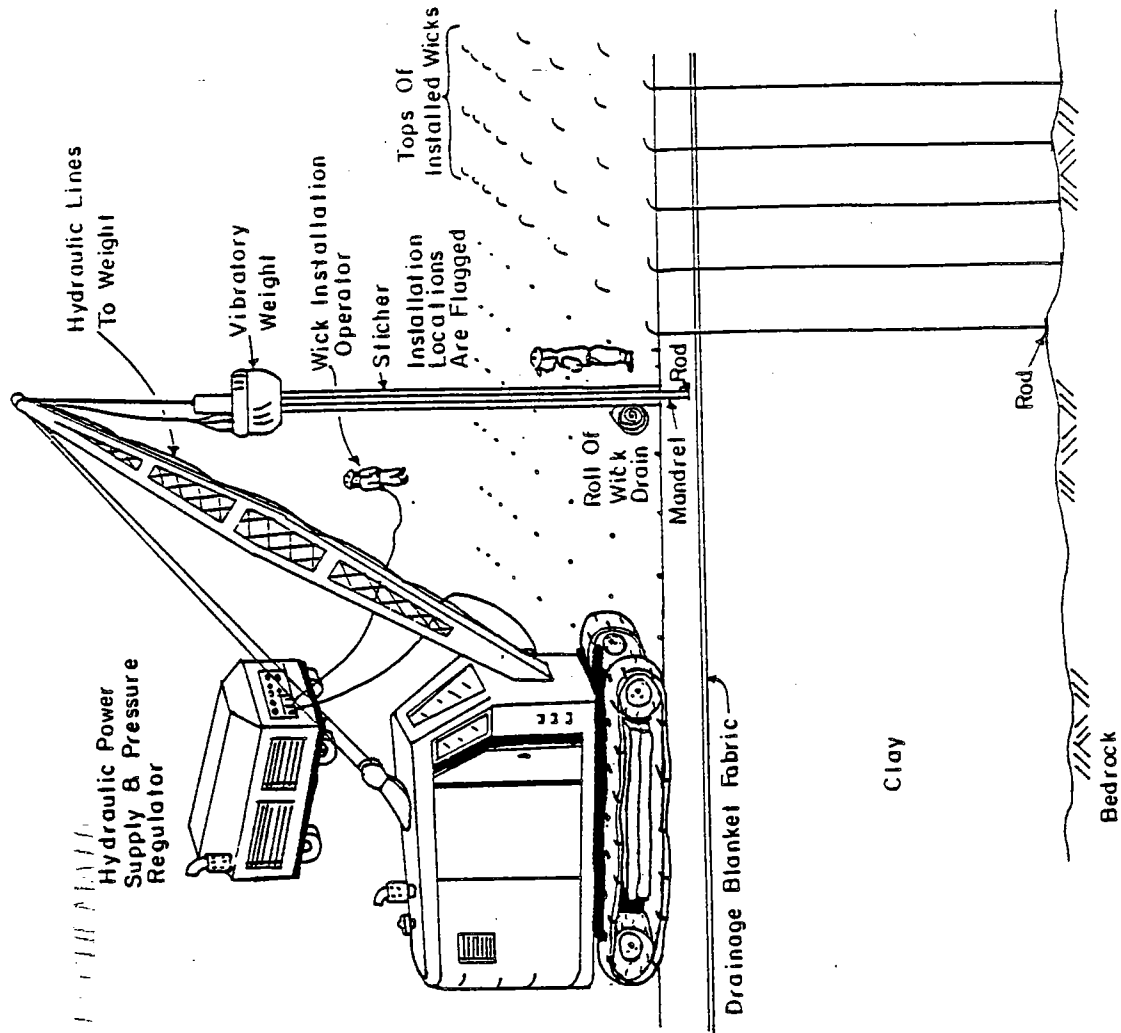
The wick drains on this project extend 20 to 30 ft. below the drainage blanket and are spaced on 6 ft. centers. There are approximately 620,000 ft. of wick drains to be installed at a bid price of \$0.60 per ft. The drains reduced the predicted time for 90 percent consolidation from approximately 5 years to 4 months.

TYPICAL WICK DRAIN TYPES

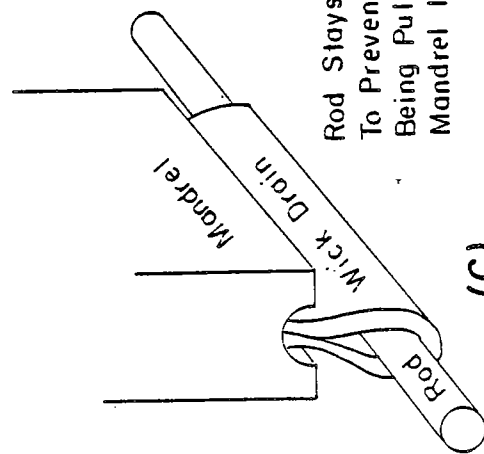
(A)



(B)



(C)



Rod Stays In Ground To Prevent Wick From Being Pulled Out As Mandrel Is Withdrawn.

FIGURE 3 - WICK DRAIN SCHEMATICS

STOP #2: RAPID TUNNEL EXCAVATION
by
Don Ackerman

Introduction . . .

Traylor Brothers, Inc. of Evansville, Indiana has been contracted by E. H. Hughes to complete all the underground work on the I-65/I-264 (Watterson Expressway) interchange. The work consists of tunneling approximately 3800 linear feet with a mining machine and 1200 linear feet by the traditional drill and shoot method (Figure 4). Following the tunneling operation, reinforced concrete pipe will be installed and grouted. The grout is injected in 10 inch diameter holes on 100 foot spacings. After the pipe has been installed, manhole structures will be built by E. H. Hughes Construction Company.

Tunneling Operations . . .

The Jarva Mark 6-0702 Tunnel Boring Machine (TBM) is designed to bore a nominal 86 inch tunnel in hard rock (Figure 5). The Mark 6 consists of the working section of the TBM and an ancillary power trailer. The power trailer supplies electric and hydraulic power to the boring machine and provides other necessary backup services. The operator's control station is also mounted on the power trailer. The working section of the TBM consists of two primary assemblies; a clamping section and a cutting section.

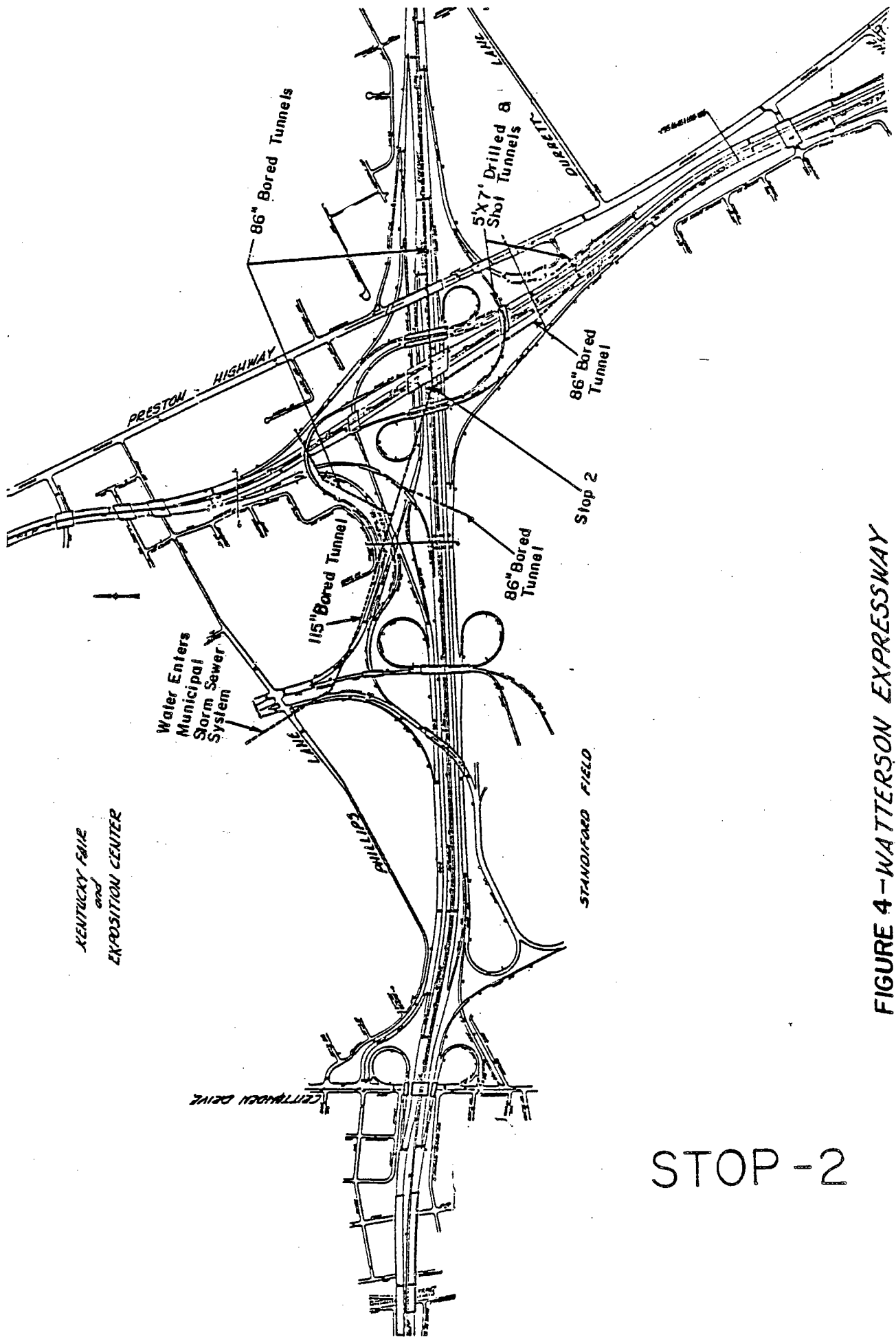
Penetration rates depend mostly on the type and compressive strength of the rock. In this area, rock strengths which we are encountering are ranging from 12,000 to 20,000 psi. The machine is capable of mining 12 feet per hour or about a penetration rate of 2 1/4 in. to 2 1/2 in. per minute under ideal situations.

Muck is loaded out by using two conveyors. The first, called the machine conveyor, is mounted on top of the bearing housing and main body and extends from the back of the cutterwheel to a point behind the drive motor. From the hopper the machine conveyor is loaded, then the muck is loaded onto a trailing conveyor mounted on the power sled. From this point the muck is loaded into muck cars or any other method the owner may find suitable.

In determining whether to drill and shoot or use a mole depends mostly on the length of the required tunnel. On distances less than 200-300 feet a mole would prove impractical due to the length of time it takes to set up the mole. But, on long distances a mining machine is the most economical method because of its high production rates. A mining machine can advance approximately three to four times as fast as drilling and shooting.

Mining Machine Specifications ...

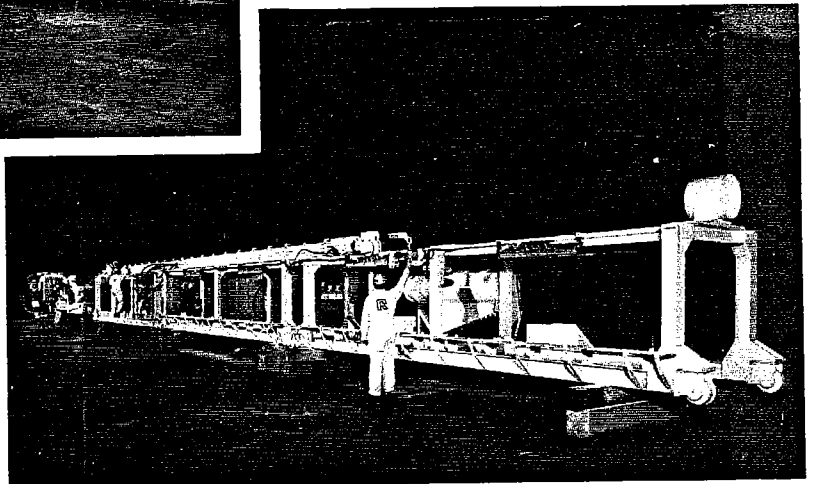
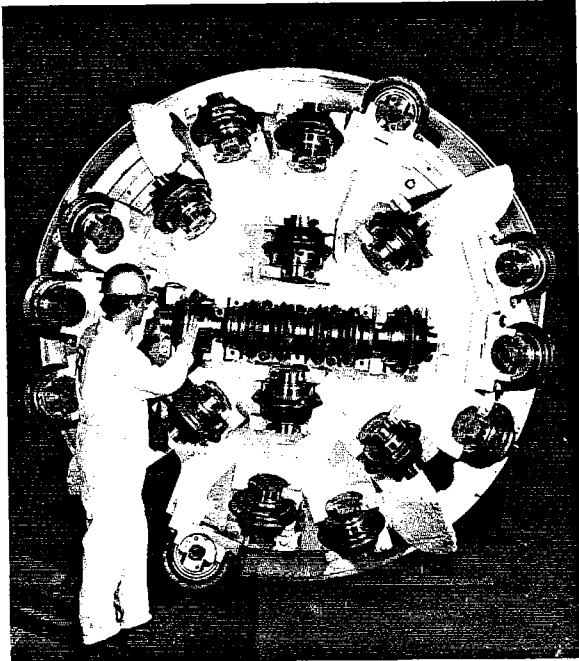
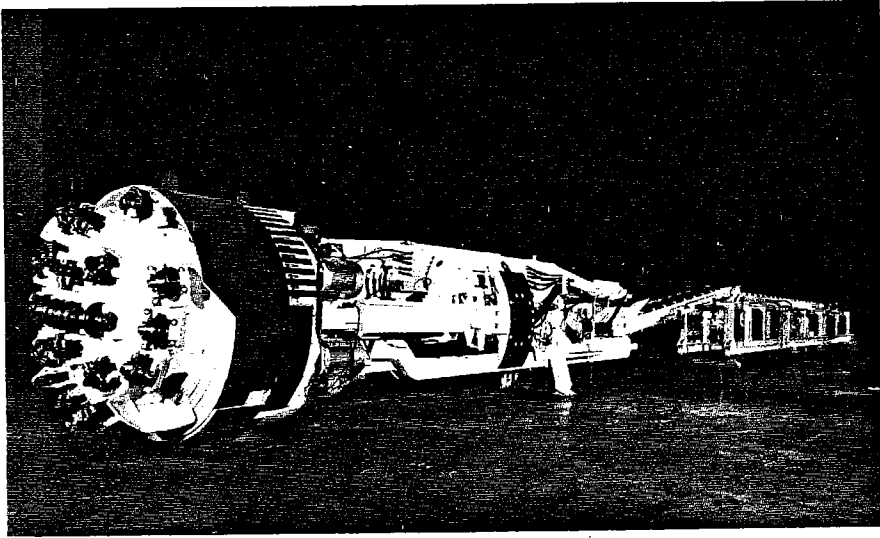
Type	Jarva Mark VI-0702 Hard Rock Tunnel Boring Machine
Bore Diameter	86 in.
Drive Horsepower	200 hp
Maximum Hydraulic System Pressure	2500 psi
Cutterhead Thrust	422,000 @ 2500 psi
Cutterhead Speed	12.4 rpm
Cutterhead Torque	84,700 16-ft.
Cutter Stroke	4.0 ft.
Cutter Configuration	1 - 12 in. multiple disc center cutter 6 - 12 in. single disc inside cutter 4 - 12 in. single disc gage cutter <hr/> 11 TOTAL
Anchor Force	1,134,000 lb. @ 2500 psi
Drive Motor	200 hp, 1780 rpm, 460 vac, 3 ph, 60H
Hydraulic Pump Motors	15 hp, 1800 rpm, 460 vac, 3 ph, 60H
Conveyor Pump Motor	15 hp, 1800 rpm, 460 vac, 3 ph, 60H
Total Power Consumption	250 KVA, 4160/480 vac, Transformer Used
Muck Handling Capacity	65 tons/hr. @ 20 ft./hr. R.O.P.
Machine Weight	Approximately 37 tons
Power Trailer Weight	Approximately 10 tons



STOP-2

FIGURE 4-WATTERSON EXPRESSWAY
I-264 @ I-65

TUNNELING OPERATIONS -----



**HARD ROCK ROTARY MACHINE
DIAMETER 9 ft 6 in. (2,8 m)**

FIGURE 5- Hard rock tunnel boring machine ("Mole")

STOP #3: MILL CREEK EMBANKMENT CORRECTIONS
by
Doug Smith

The project is located in southern Carroll County where I-71 crosses Mill Creek and Mill Creek Road. Construction of I-71 was completed in 1967. Numerous problems were encountered on construction, one of which was water flowing from the existing formation. The water appeared to be a main factor contributing to the failure. A French drain was installed on the south approach in 1969 after movement was noticed, however, future movement prevented the drain from operating.

By the spring of 1973 the south approach had failed and moved toward Mill Creek leaving the pile cap of the eastbound lane exposed. The north approach showed signs of movement, however, no failure had developed. Signs of stress were visible in both structures. It was at this time the Geotechnical Engineering Branch was requested to investigate the slide and determine possible solutions to stabilize the approach embankments.

In this area, the troublesome shales of the Kope and Fairview Formations are encountered. The difficulty of compacting the materials obtained from these formations is known as a primary cause of slope instability. Flaggy limestone slabs interfere with the compactive efforts of construction equipment, and prevent the shale from being broken down by the compaction operations. Subsequently water in the voids causes the large pieces of shale to slake. This process leads to continual settlements and long term (creep) slope failures.

The south approach consists of a side hill embankment approximately 55 feet in height measured from the toe to the shoulder. The failure was a sliding wedge along the rock disintegration zone according to the slope inclinometer data. The presence of water along the failure, and the loss of shear strength in the embankment due to the slaking of the soil like shales, were the causes of the landslide.

The north approach consists of a full embankment approximately 56 feet in height with 2 to 1 side slopes. According to the slope inclinometer data the failure was circular through the embankment tangent to the rock disintegration zone. This failure was due to the loss of shear strength in the embankment.

Slope inclinometer data and field observations were used to determine the critical failure surface which approximates the existing distress. Shear strength parameters were then back calculated using an effective stress analysis assuming the factor of safety of 1.0. Using these assumptions the strength parameters at failure were as follows:

$$\bar{\phi} = 20^{\circ}$$

$$\bar{c} = 0 \text{ psf}$$

$$\gamma = 125 \text{ pcf}$$

The following alternate corrections were considered:

1. Extend the bridge and flatten the slopes.
2. Construct a culvert for Mill Creek and flatten the slopes for the existing bridge.
3. Stabilize the abutments by retaining walls using the "Root Pile" system.
4. Construct retaining walls at the toe of the embankments and flatten the slopes.

The Department decided to use the crib wall and slope flatten concept for correction (Figure 6). Construction on the project began in the fall of 1978 and was completed in 1979 for a total cost of \$478,593. The price per square foot of wall face was \$22.35 not including the backfill. There was 25,776 tons of granular backfill material at a unit cost of \$8.36/ton.

This project has been monitored since completion by the Geotechnical Engineering Branch with slope inclinometers and tiltplates. As of April 23, 1985 no significant movement has been detected.

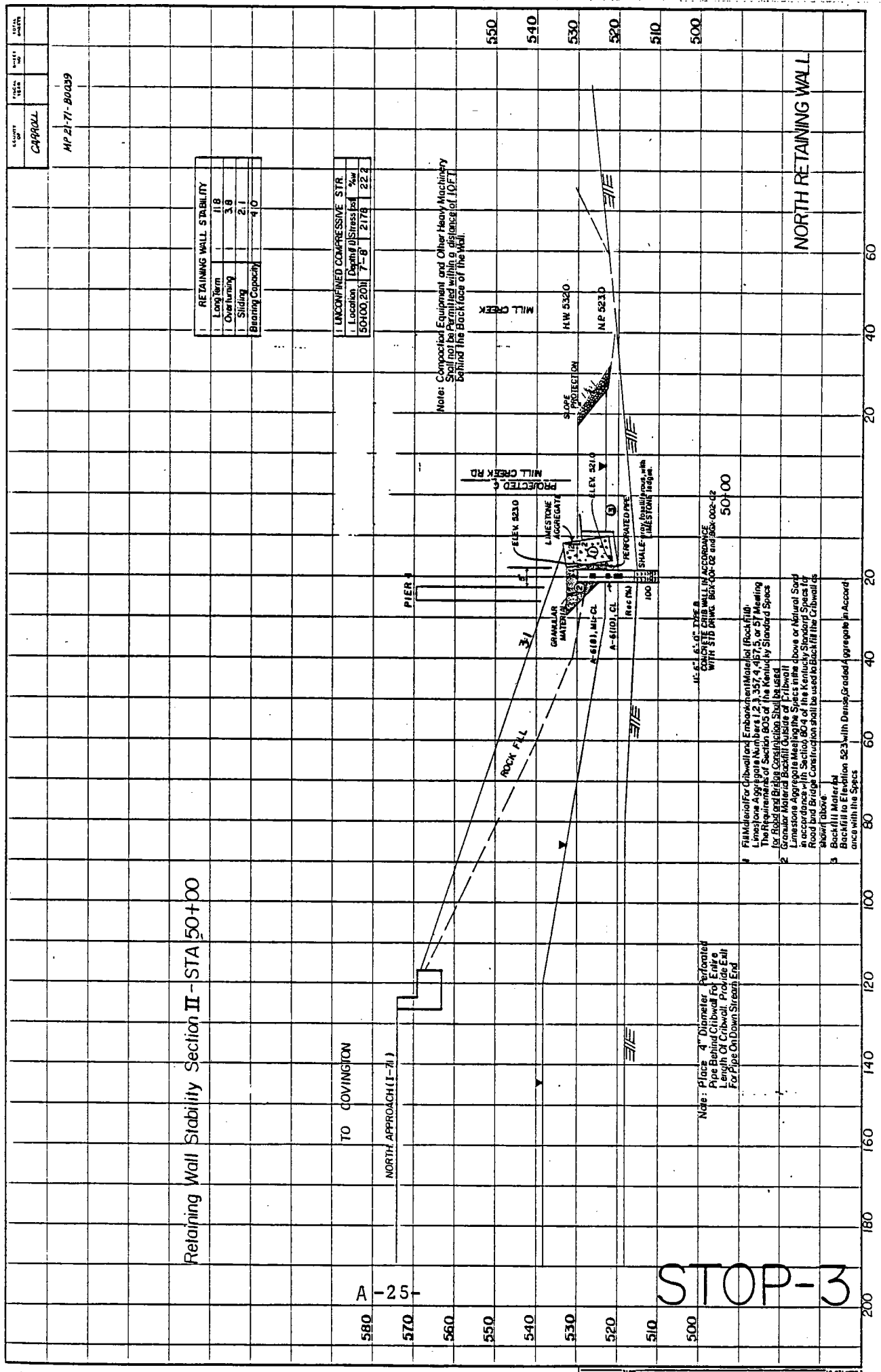


FIGURE 6 - MILL CREEK EMBANKMENT CORRECTION

STOP #4
HORIZONTAL DRAINS FOR LANDSLIDE STABILIZATION
by
Ed Munson

The landslide correction on Ky. 227 was accomplished using horizontal drains and removing a three to five foot layer of asphalt paving from the roadway section (Figure 7). This slide and the slide at the next stop were let together as a Federally funded project in November 1983 for a total of \$1,071,900. Horizontal drains were installed at the contract unit price of \$8.20 per foot. A total of 10,250 linear feet of drains were installed for at a cost of \$84,050.

Water levels have dropped between 10 to 20 feet in the embankment since the drains were installed.

CARROLL
EHRS 4-6(9)
SP21-72-9C1

Note: The correction consists of installing horizontal drains under the roadway to lower the water level within the slopes. The drains were drilled back from the edge of the river to a point under the left ditch, a distance 250 ft.

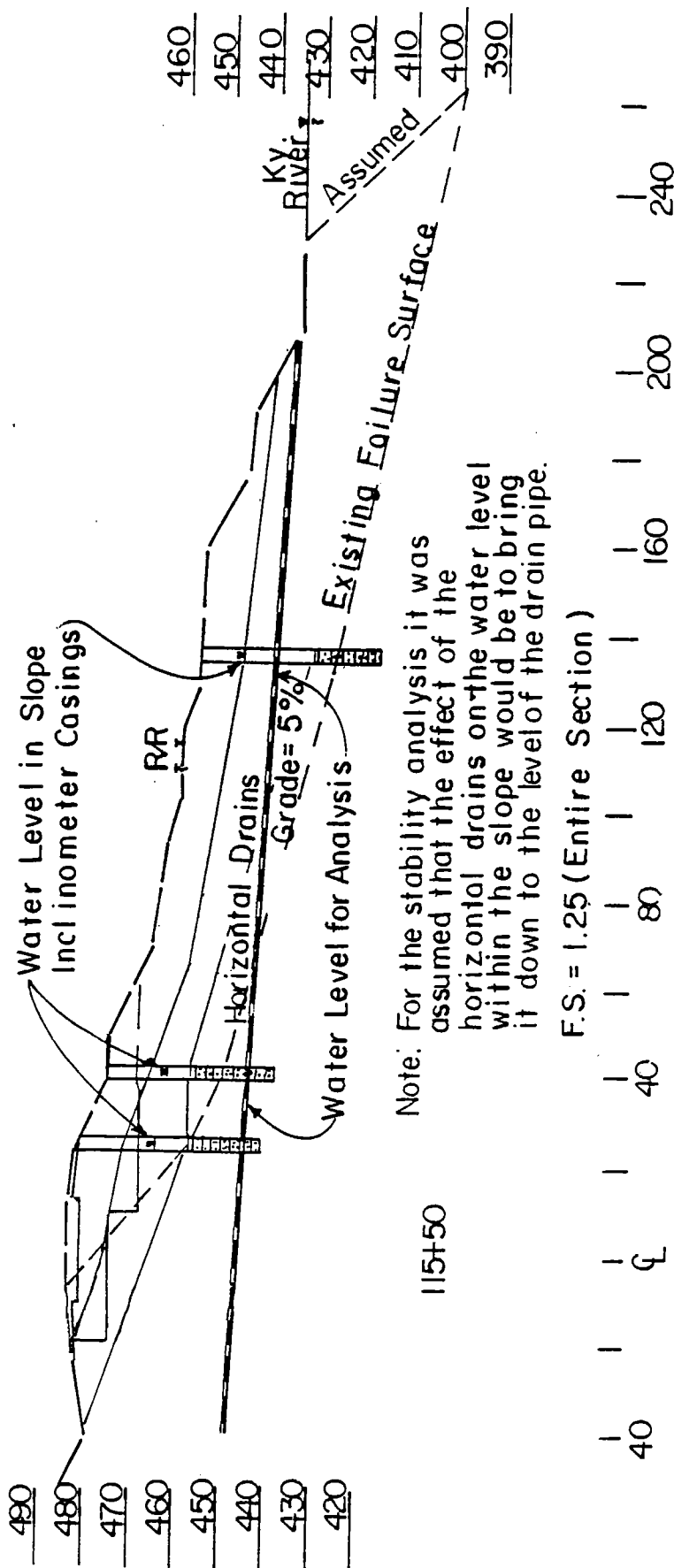
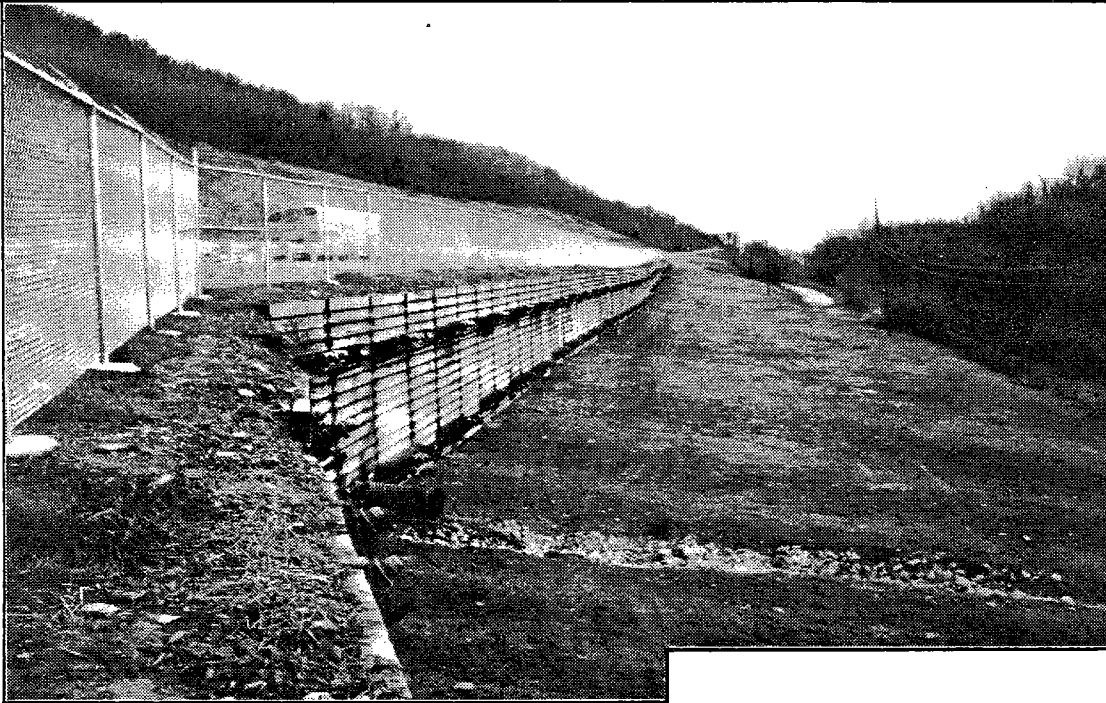


FIGURE 7 - HORIZONTAL DRAINS FOR LANDSLIDE STABILIZATION

FIGURE 8
Slide Retainment — Tiedback Wall
by Tom Anderson



TIEDBACK SLIDE CONTROL WALL
Kentucky Route 227

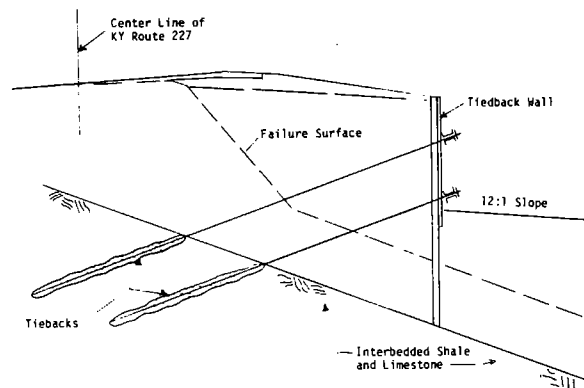
A 1,000-foot-long, fifteen-foot-high Tiedback Wall stabilized an overburden/fill slide on the downhill side of the roadway. The driven H-piles of the Tiedback Wall are supported by two rows of corrosion-protected rock tiebacks anchored in the interbedded shales and limestones of the Kope/Eden Formation. A prefabricated drainage system was installed behind pressure-treated lagging.

This Tiedback Wall was built from the top down, which provided early stabilization of the slope. Highway traffic was not disrupted during construction of this landslide control wall.

General Contractor: Ohio Valley Paving
Carrollton, Ohio

Owner: Kentucky Department of
Highways
Frankfort, Kentucky

Tiedback Wall Contractor: Schnabel Foundation Company
Cary, Illinois



**TIEDBACK WALL STABILIZES
HIGHWAY LANDSLIDE**

STOP #6: MAINTENANCE CORRECTION
by
Henry Mathis

Rapid drawdown and erosion by the Kentucky River caused several landslides on Ky. 227 near Carrollton. Department of Highways Maintenance Forces attempted to correct the landslides by end dumping limestone rock over the river bank for slope protection. As the failures continued to progress, three gabion retaining walls bearing on railroad rail piling were constructed by the Maintenance Forces. Lightweight aggregate (cinders and slag) was used as backfill material (Figure 9).

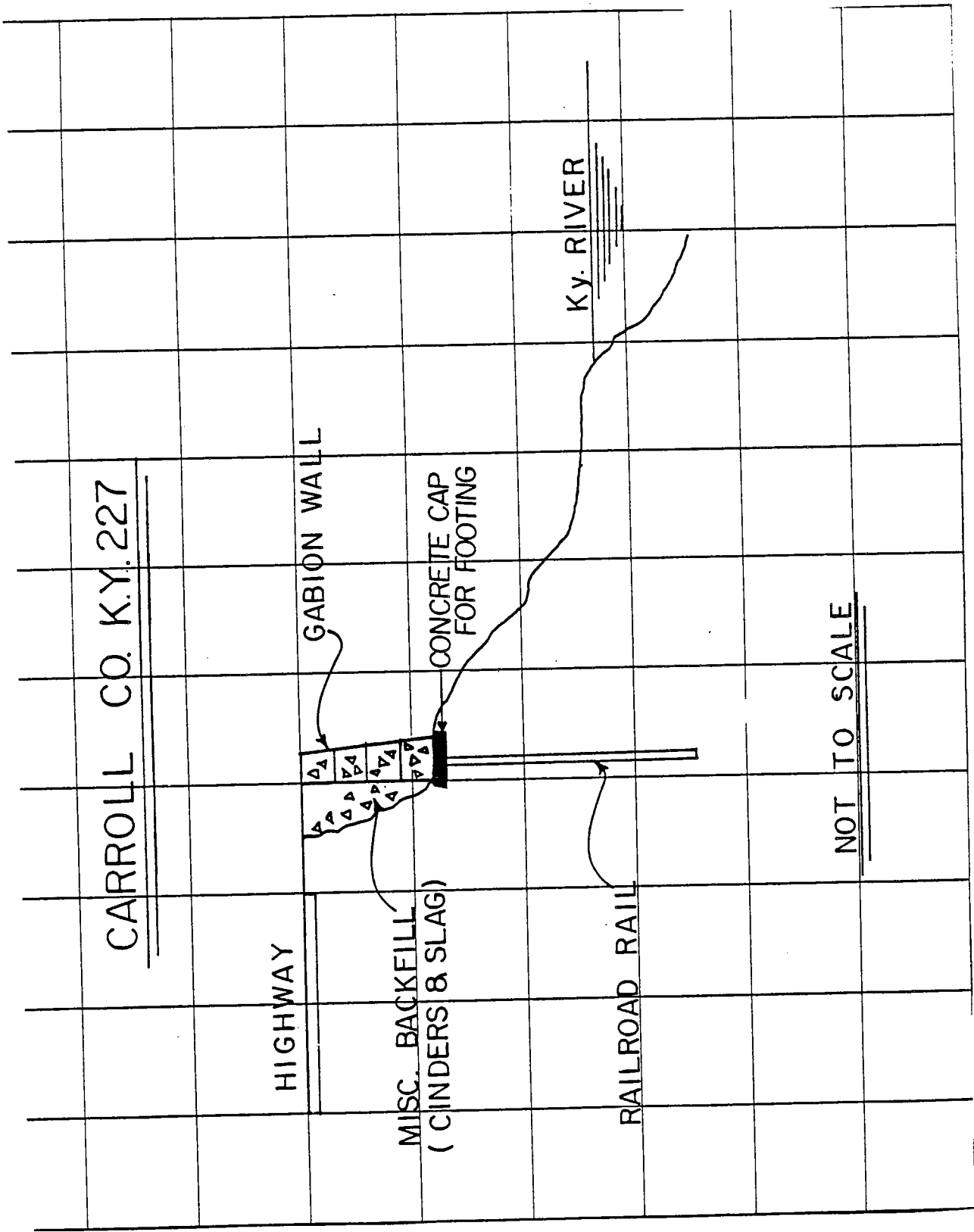


FIGURE 9 - MAINTENANCE CORRECTION

STOP #7: D-CRACKING PAVEMENT AND ROCK
CUT SECTION ON US 421 IN INDIANA

by
Rick Hockett

Rocks exposed in this cut are Silurian and Ordovician age
(Figure 10).

<u>System</u>	<u>Formation</u>	<u>Member</u>
Silurian	Salamonie	Laurel
Silurian	Salamonie	Osgood
Silurian	Brassfield	
Ordovician	Saluda	
Ordovician	Dillsboro	

The Dillsboro Formation at this locality contains an abundant and varied fauna characteristic of the famed Cincinnati Series. Participants will have an opportunity to collect from the lowermost shale unit in this road cut.

The Portland cement concrete pavement at this location is in the beginning stages of D-cracking. D-cracking (for disintegration-cracking) is present in many, if not most, concrete pavements in Indiana. This pavement distress is typically characterized by fine cracks which develop parallel to the joints and slab edges, and progress by parallel development towards the center of the slab. D-cracking is caused by a combination of freeze-thaw cycling, saturated pavement, and aggregates with a susceptible pore structure.

Recent research conducted at Purdue University has defined the offending pore size distributions, using mercury intrusion porosimetry. The Indiana Department of Highways has acquired the necessary equipment to perform these tests and is currently developing a specification for Portland cement concrete aggregates based on pore size distribution.

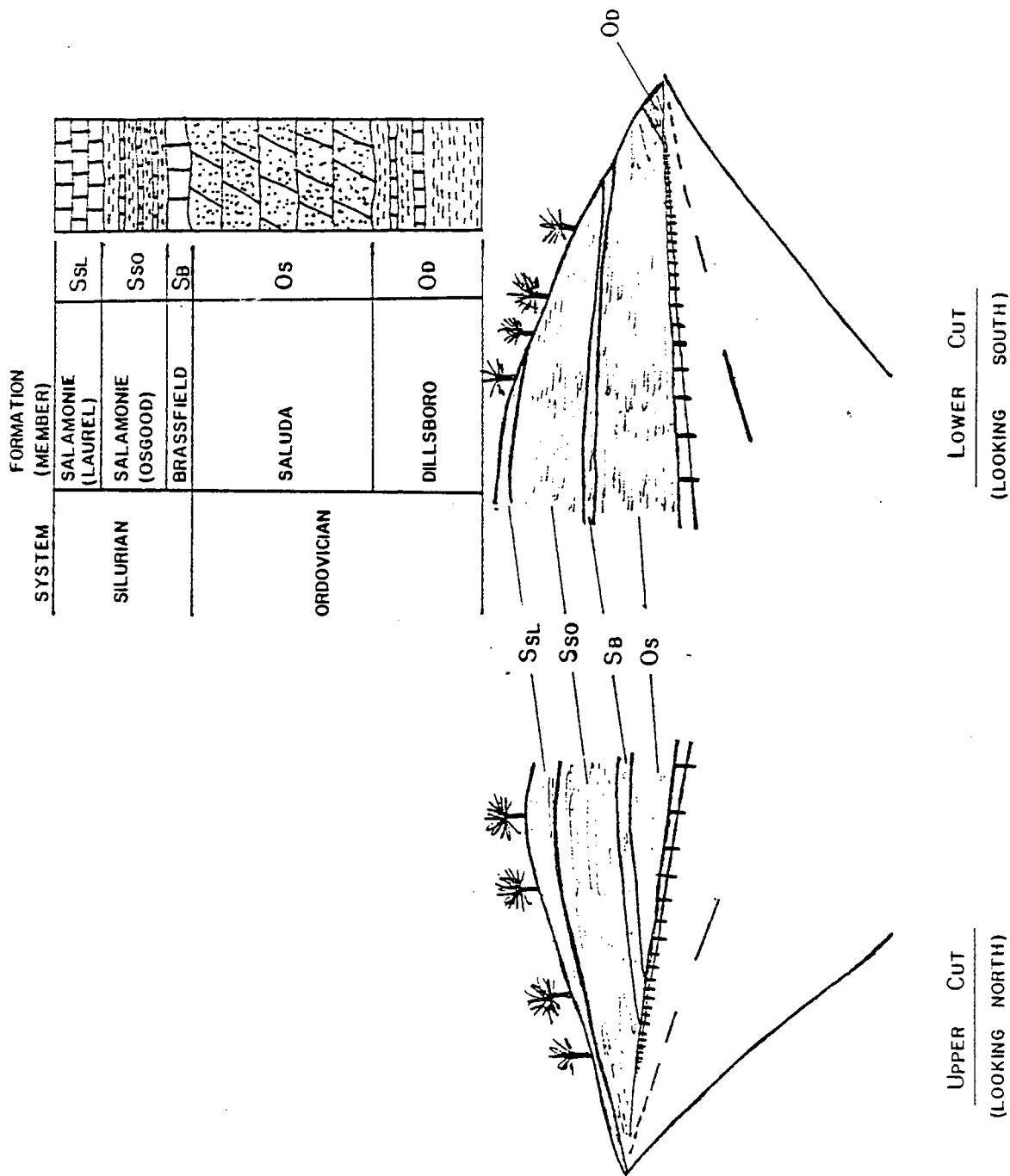


FIGURE-10
Geologic Section of a Highway Cut on US-421

REFERENCES

- Hall, F.R., and Palmquist, Jr., W.N., 1960, Availability of Ground Water in Carroll, Gallatin, Henry, Owen, and Trimble Counties, Kentucky: U.S. Geological Survey Hydrologic Investigation Atlas H.A.-23, scale 1:125,000.
- Kepferle, R.C., 1974, Geologic Map of the Louisville East Quadrangle, Jefferson County, Kentucky: U.S. Geological Survey Quadrangle Map GQ-1203, scale 1:24,000.
- Kepferle, R.C., 1974, Geologic Map of part of the Jeffersonville, New Albany and Charlestown Quadrangles, Kentucky-Indiana: U.S. Geological Survey Quadrangle Map GQ-1211, scale 1:24,000.
- Kepferle, R.C., 1976, Geologic Map of the Crestwood Quadrangle, North-Central Kentucky: U.S. Geological Survey Quadrangle Map GQ-1342, scale 1:24,000.
- Kepferle, R.C., Wigley, P.B., and Hawke, B.R., 1971, Geologic Map of the Anchorage Quadrangle, Jefferson and Oldham Counties, Kentucky: U.S. Geological Survey Quadrangle Map GQ-906, scale 1:24,000.
- Luft, S.J., 1977, Geologic Map of the Smithfield Quadrangle, North-Central Kentucky: U.S. Geological Survey Quadrangle Map GQ-1371, scale 1:24,000.
- Moore, F.B., Kepferle, R.C., and Peterson, W.L., 1972, Geological Map of the Jeffersontown Quadrangle, Jefferson County, Kentucky: U.S. Geological Survey Quadrangle Map GQ-999, scale 1:24,000.
- Palmquist, Jr., W.N., and Hall, F.R., 1960, Availability of Ground Water in Bullitt, Jefferson and Oldham Counties, Kentucky: U.S. Geological Survey Hydrologic Investigations Atlas H.A.-22, scale 1:125,000.
- Peterson, W.L., Moore, S.L., Palmer, J.E., and Smith, J.H., 1971, Geologic Map of part of the LaGrange Quadrangle, Oldham County, Kentucky: U.S. Geological Survey Quadrangle Map GQ-901, scale 1:24,000.

Swadley, W.C., 1973, Geologic Map of parts of the Vevay South and Vevay North Quadrangle, North-Central Kentucky: U.S. Geological Survey Quadrangle Map GQ-1123, scale 1:24,000.

Swadley, W.C., 1976, Geologic Map of part of the Carrollton Quadrangle, Carroll and Trimble Counties, Kentucky: U.S. Geological Survey Quadrangle Map GQ-1281, scale 1:24,000.

Swadley, W.C., and Gibbons, A.B., 1976, Geologic Map of the Campbellsburg Quadrangle, North-Central Kentucky: U.S. Geological Survey Quadrangle Map GQ-1364, scale 1:24,000.

LIST OF REGISTRANTS

HIGHWAY GEOLOGY SYMPOSIUM
Clarksville, Indiana
May, 1985

Thomas C. Anderson
Schnabel Foundation Co.
210 Cleveland St.
Cary, IL 60013
(312) 639-8900

Michael Blevins
Kentucky Trans. Cabinet
Div. of Materials
940 Inverness Rd.
Frankfort, KY 40601
(502) 564-3160

Joseph E. Armstrong
Montana Dept. of Highways
454 West Lawrence
Helena, MT 59601
(406) 444-6280

Daniel G. Bradfield
Indiana Dept. of Highways
105 Pine
Hebron, IN 46341
(219) 362-6125 (ext. 71)

Associated Pile & Fitting Corp.
262 Futherford Blvd.
Clifton, NJ 07014
(201) 773-8400
Representative:
Richard L. McKillip
Route No. 2
Cadiz, KY 42211
(502) 522-3972

Vernon L. Bump
S.D.D.O.T. - Foundations & Geology
S.D. Dept. Transportation
Pierre, SD 57501
(605) 773-3401

Jack L. Conway
Kentucky Trans. Cabinet
Div. of Materials
Frankfort, KY 40601
(502) 564-2374

Robert C. Bachus
Georgia Inst. of Technology
School of Civil Engr.
Atlanta, GA 30332

Prof. John H. Cleveland
Indiana State University
2411 N. 9th
Terre Haute, IN 47804
(812) 232-6311 (ext. 2444)

Ed Belknap
Colorado Dept. of Highways
3035 So. Harrison St.
Denver, CO 80210
(303) 757-9750

Zvi Dagan
Hilfiker Retaining Walls
P.O. Drawer L
Eureka, CA 95501
(707) 443-5091

William D. Bingham
NC Dept. of Transportation
Raleigh, NC 27611
(919) 733-6911

Robert C. Deen
Univ. of Kentucky
533 South Limestone
Lexington, KY 40506-0043
(606) 257-4513

Everett Gray
Kentucky Trans. Cabinet
Div. of Materials
Frankfort, KY 40601
(502) 564-3160

Jaqat S. Dhamrait
Illinois Dept. of Trans.
126 East Ash Street
Springfield, IL 62706
(217) 782-7207

Santo Dovi
Evergreen Systems Inc.
P.O. Box 345
King's Park, NY 11754
(516) 368-4000

Joe Drumheller
GeoSystems Inc.
207 East Holly Avenue
Sterling, VA 22170

Leo A. Legatski, President
Elastizell Corp. of America
P.O. Box 1462
Ann Arbor, MI 48106
(313) 761-6900

Henry Erhardt
Sprague and Henwood, Ind.
P.O. Box 446
Scranton, PA 18501
(717) 344-8506

Charles B. Gover
Puerto Rico Highway Authority
Soils Engr. Office
G.P.O. Box 3909
San Juan, PR 00936
(809) 753-1155

Don Grabner
The Reinforced Earth Co.
10400 W. Higgins Road
Rosemont, IL 60018
(312) 824-6630

Richard B. Hockett
Indiana Dept. of Highways
100 N. Senate Avenue
Indianapolis, IN 46204
(312) 232-5280

Henry Gray
Indiana Geological Survey
Dept. of Natural Resources
611 North Walnut Grove
Bloomington, IN 47401

Milton M. Greenbaum
Milton M. Greenbaum Assoc.
994 Longfield Avenue
Louisville, KY 40215
(502) 361-8447

Sandor R. Greenbaum
Milton M. Greenbaum Assoc.
994 Longfield Avenue
Louisville, KY 40215
(502) 361-8447

Richard L. Hall
Schnabel Foundation Co.
4720 Montgomery Ln, Ste. 300
Bethesda, MD 20814
(301) 657-3063

Neil F. Hawks
Transportation Res. Board
2101 Constituion Ave. NW
Washington, D.C. 20418
(202) 334-2956

Harold Hilfiker
Hilfiker Retaining Walls
P.O. Drawer L
Eureka, CA 95501
(707) 443-5091

Bill Lovell
Civil Engineering Dept.
Purdue University
2918 Linda Lane
West Lafayette, IN 47906
(317) 494-5034

Harry Ludowise
Federal Highway Admin.
6308 N.E. 12th Avenue
Vancouver, WA 98665
(206) 696-7738

Jeff Hynes
Colorado Geological Survey
4340 E. Louisiana
Denver, CO 80210

Charles T. Janik
Pennsylvania Dept. of Trans.
309 Glenn Road
Camp Hill, PA 17011

Jeffrey Jensen
Jensen Drilling Co.
230 Cusick Road
Alcoa, TN 37701

Richard Johnson
Atec Associates, Inc.
1846 Cargo Court
Louisville, KY 40299
(502) 491-9523

Jerome B. Kenkel
The H.C. Nutting Co.
4120 Airport Road
Cincinnati, OH 45226
(513) 321-5816

Myrna M. Killey
Illinois State Geol. Survey
615 East Peabody Drive
Champaign, IL 61820
(217) 344-1481 (ext. 273)

Alberto S. Nieto
1301 W. Green
205 N. #B
Univ. of Illinois
Urbana, IL 61801

Alan s. Ortiz
Golder Associates, Inc.
3772 Pleasantdale rd.
Suite 165
Atlanta, GA 30340
(404) 496-1893

Henry Mathis
Kentucky Dept. of Highways
451 Monticello Blvd.
Lexington, KY 40503
(502) 564-3160

Willard McCasland
Oklahoma Dept. of Trans.
321 Sahoma Terrace
Edmond, OK 73034
(405) 521-2677

Cary A. McGuire
Indiana Dept. of Natural Res.
614 State Office Bldg.
Indianapolis, IN 46204
(317) 232-4150

Harry Moore
Tennessee Dept. of Trans.
P.O. Box 58
Knoxville, TN 37901

William E. Munson
Kentucky Trans. Cabinet
Div. of Materials
Wilkinson Blvd.
Frankfort, KY 40622
(502) 564-2374

Bill Knorr
Mobile Drilling Co.
3807 Madison Avenue
Indianapolis, IN 46227
(317) 787-6371

Larry R. Rhodes
Rhodes and Associates, Inc.
2627 Regency Road
Lexington, KY 40503
(606) 278-9465

David N. Richardson
Univ. of Missouri-Rolla
Butler-Carlton Hall
Rolla, MO 65401
(314) 341-4487

William J. Pfalzer
Kentucky Trans. Cabinet
Div. of Materials
1081 Paxton Road
Lawrenceburg, KY 40342
(502) 564-2374

Bob Pickard
Illinois Dept. of Trans.
700 East Norris Drive
Ottawa, IL 61350
(815) 434-6131

James F. Quinlan
National Park Service
Mammoth Cave National Park
Box 8
Mammoth Cave, KY 42259

R. Bruce Reeves
Lang Tendons, Inc.
3623 Charnbridge Rd.
Fairfax, VA 22030
(703) 591-4928

The Reinforced Earth Co.
Rosslyn Center
1700 N. Moore St.
Arlington, VA 22209-1960
(703) 527-3434

Berke L. Thompson
W. Virginia Dept. of Highways
312 Michigan Ave.
Charleston, WV 25311

Sam I. Thornton
E340 Univ. of Arkansas
Fayetteville, AR 72701
(501) 575-6024

John Tyree
School of Civil Engr.
Grissom Hall
Purdue University
West Lafayette, IN 47907

David E. Weatherby
Schnabel Foundation Co.
4720 Montgomery Lane
Bethesda, MD 20814
(301) 657-3063

Charlie Riggs
Central Mine Equipment Co.
6200 North Broadway
St. Louis, MO 63147
(314) 381-5900

Nick Schmitt
Law Engr. Testing Co.
5006 Volney Ct.
Louisville, KY 40291

Robert T. Semones
Kentucky Trans. Cabinet
Div. of Materials
Frankfort, KY 40601
(502) 564-2379

W.R. Sullivan
The Reinforced Earth Co.
Suite 9
4100 Executive Park Drive
Cincinnati, OH 45241
(513) 563-7786

Richard W. Thomas
Tenech Engineering
515 Park Avenue
Louisville, KY 40208-2387
(502) 636-3565

Douglas W. Witt
Howard K. Bell, Cons. Engineers
P.O. Box 546
Lexington, KY 40585
(606) 278-5412

Earl M. Wright
Kentucky Dept. of Highways
Frankfort, KY 40622
(502) 564-3160

Edward J. Zeigler
Rummel, Klepper & Kahl
1035 N. Calvert St.
Baltimore, MD 21202
(301) 685-3105

Roderick L. Zeller, Jr.
Wehr Constructors, Inc.
2517 Plantside Drive
Louisville, KY 40299
(502) 491-9250

Terry West
Dept. of Earth & Atmos. Sci.
Purdue University
West Lafayette, IN 47907
(317) 494-3296

Richard Wetzer
Sprague and Henwood, Inc.
P.O. Box 446
Scranton, PA 18501
(717) 344-8506

William A. Wisner
Florida Dept. of Trans.
P.O. Box 1029
Gainesville, FL 32602
(904) 372-5304

Paul Owens
IDOH
State Office Bldg.
100 N. Senate
Indianapolis, IN 46204

Richard T. Wilson
Kentucky Trans. Cabinet
Div. of Materials
Frankfort, KY 40601
(502) 564-3160